國立臺灣大學工學院環境工程學研究所

博士論文

Graduate Institute of Environmental Engineering

College of Engineering

National Taiwan University

Doctoral Dissertation

環境中新穎全氟化合物的探測與發現 –
以半導體業廢水為例

Detection and Discovery of Novel Perfluoroalkyl and Polyfluoroalkyl Substances (PFAS) in the Environment – A Case Study of Semiconductor Wastewater

陳怡如

Yi-Ju Chen

指導教授：林郁真 博士

Advisor: Angela Yu-Chen Lin, Ph.D.

中華民國 113 年 7 月

July, 2024

doi:10.6342/NTU202402180

國立臺灣大學碩(博)士學位論文
口試委員會審定書
MASTER'S THESIS(DOCTORAL DISSERTATION) ACCEPTANCE CERTIFICATE
NATIONAL TAIWAN UNIVERSITY

環境中新穎全氟化合物的探測與發現－以半導體業廢水為例

Detection and Discovery of Novel Perfluoroalkyl and Polyfluoroalkyl Substances (PFAS) in the Environment–A Case Study of Semiconductor Wastewater

本論文係 陳怡如 (姓名) D02541005 （學號）在國立臺灣大學 環境工程學研究所 (系/所/學位學程)完成之碩(博)士學位論文，於民國 113 年 7 月 11 日承下列考試委員審查通過及口試及格，特此證明。

The undersigned, appointed by the Department / Graduate Institute of Environmental Engineering on 11 (date) July (month) 2024 (year) have examined a Master's Thesis (Doctoral Dissertation) entitled above presented by Yi-Ju Chen (name) D02541005 (student ID) candidate and hereby certify that it is worthy of acceptance.

口試委員 Oral examination committee:

林郁真
（指導教授 Advisor）

何國榮　林逸彬　侯嘉洪

陳宇揚　于昌平　駱尚廉

系（所、學位學程）主管 Director: 席行正

致謝

在職念博士班這段漫長時光，育兒生活與繁忙的工作讓我放慢了修業的腳步，感謝大家的幫助，我才能夠走到最後。特別感謝我的指導教授林郁真特聘教授，在我因論文審查意見感到徬徨無助時，您提供了許多寶貴建議，培養了我的專業能力，使我有信心回應期刊編審的問題。林教授如同我的精神支柱，給予我安心穩定的力量。在我因時間不足而想放棄學位時，您堅定地帶領我前行，最終我才能如期完成學位。衷心感謝林教授的悉心教導與溫暖關懷。

感謝博士論文指導小組：于昌平教授、吳先琪教授、林正芳教授、林逸彬教授、侯嘉洪教授、康佩群教授、駱尚廉教授，以及所外的陳家揚教授和何國榮教授。感謝您們提供許多寶貴的建議與指導，提點論文研究方向，並時時勉勵我，一路幫我加油打氣，感恩教授們的提攜與指導。

感謝實驗室同窗楊政憲同學，您總是熱心助人並提供寶貴建議，是我的貴人。也感謝實驗室的Hank學長、明皓學長、明季同學、宥翔、婉寧，還有實驗室的學弟妹們的幫忙，您們是我強大的後援，謝謝您們。

謝謝我的學長與前同事王仁得先生，您在化學化工領域的專業知識令我深感敬佩，這篇論文的產生深受您的啟發，感謝您在研究過程中的指導。感謝我的同事姿惠、仕麟、欣穎，以及長官同仁的幫助，讓我能在公餘時間進修。最後，特別感謝我的先生，除了精神上的支持與分擔許多家事，還提供我許多業界訊息與產業脈動資訊，還要謝謝我的兩位女兒，總是把時間留給我，讓我能夠專心寫論文，並且願意聽我分享研究上酸甜苦辣，有您們真好。謝謝我孩子的保姆，在我需要的時候總是挺身而出，謝謝您的神救援。

最後，我要感謝我自己，堅持到最後，勇敢追求真理與環境正義，相信自己的直覺，相信自己做得到。

doi:10.6342/NTU202402180

中文摘要

全氟與多氟烷基物質（Per- and polyfluoroalkyl substances, PFAS）是含有 CF_2 或 CF_3 結構的人造物質，化合物種類多達上萬種，因其穩定性和特殊的物理化學性質，廣泛應用於工業和民生用品。然而，多數 PFAS 具有持久性、生物累積性和毒性，斯德哥爾摩公約已將全氟辛烷磺酸（Perfluorooctane sulfonate, PFOS）等長鏈 PFAS 列為持久性有機污染物並禁止使用，工業現已轉向使用新型 PFAS 替代長鏈 PFAS。本研究旨在使用液相層析高解析質譜儀開發無需使用標準品的新型非目標物鑑定方法，用以辨識新興 PFAS 及其環境降解產物，藉由掌握 PFAS 獨特的質譜碎片資訊，我們建立了質譜碎片掃描和中性丟失掃描模式，首次運用 $[SO_2NC_2H_4O]^-$ 碎片掃描具磺醯胺乙醇結構的 PFAS 及中性損失 CH_2CO_2 掃描具磺醯胺乙酸結構的 PFAS。配製一個品管樣品具有 11 類亞種共 39 種 PFAS 的混合標準品，運用本次開發出來的非目標物鑑定方法，可成功鑑定出混合標準品樣品中 36 種 PFAS，鑑別率達 92%。由於半導體產業表示 PFAS 對於製程的良率至關重要，雖然宣稱已停用 PFOS，但其替代物質的資訊仍然有限。我們透過開發之新型鑑定方法，調查了半導體業廢水和其污水處理廠放流水，從採集 5 家半導體廠的 10 個廢水樣品中，我們成功鑑定了 83 種 PFAS，涵蓋 12 類亞群，其中有 30 種是首次被鑑定之結構，在這些半導體廢水中的主要 PFAS 化合物是全氟丁烷磺醯胺衍生物，包括全氟丁烷磺醯胺乙醇（Perfluorobutane sulfonamidoethanol, FBSE）、全氟丁烷磺醯胺（Perfluorobutane sulfonamdie, FBSA）和全氟丁烷磺醯胺二乙醇（Perfluorobutane sulfonamido diethanol, FBSEE diol），其最高廢水濃度

分別為482 μg/L、141 μg/L與83.5 μg/L。此外，在樣品中還篩測出三種超短鏈全氟烷基酸（Perfluoroalkyl acids, PFAAs），濃度介於0.004 μg/L到19.9 μg/L之間。半導體業廢水經三個污水處理廠處理後，發現全氟丁烷磺醯胺乙酸（Perfluorobutane sulfonamido acetic acid, FBSAA）系列在放流水濃度顯著提高（65%-82%），顯示生物處理將FBSE轉化為FBSAA。本研究亦對FBSEE diol的中間代謝物進行辨識，藉由實驗室的模擬試驗反應，提出了一種新的FBSEE diol代謝途徑。綜整半導體廢水與放流水中PFAS種類與濃度，全氟丁烷磺醯胺衍生物占90%（1934 μg/L），而過去常獲得關注的全氟烷基酸類僅占10%（205 μg/L），表明新興全氟丁烷磺醯胺衍生物可能成為半導體行業的新趨勢與替代品，並通過污水處理廠之生物降解機制轉化成FBSAA而排入環境。

關鍵字：全氟與多氟烷基物質，半導體業，全氟丁烷磺醯胺，全氟丁烷磺醯胺乙醇，全氟丁烷磺醯胺乙酸，降解產物，前驅物

ABSTRACT

Per- and polyfluoroalkyl substances (PFAS) are synthetic compounds with at least one perfluorinated methyl ($–CF_3$) or methylene group ($–CF_2–$), comprising over ten thousand types. Their stability and unique properties make them widely used in industrial and consumer products. However, many PFAS are persistent, bioaccumulative, and toxic. The Stockholm Convention has banned long-chain PFAS like perfluorooctane sulfonate (PFOS) as persistent organic pollutants, prompting industries to adopt new PFAS alternatives. This study aimed to develop a novel nontarget approach to identify emerging PFAS and their environmental degradation products by liquid chromatography coupled to high-resolution mass spectrometry. A distinct fragment- based approach has been established to identify the hydrophobic and hydrophilic features of acidic and neutral fluorosurfactants through fragments and neutral losses, including those outside the homologous series. This method introduces the sulfonamido ethanol fragment $[SO_2NC_2H_4O]^-$ and the neutral loss of CH_2CO_2 as novel indicator. In a mixture of PFAS standards, 92% (36 out of 39 compounds across 11 classes) were detectable using the fragment-based nontarget procedure. This demonstrates the method's effectiveness in identifying the hydrophobic and hydrophilic properties of various fluorosurfactants. The semiconductor industry has claimed that

PFOS has been eliminated from semiconductor production; however, information about the use of alternative compounds remains limited. Ten sewage samples from 5 semiconductor plants were analyzed with target and nontarget analysis. Among the 83 identified PFAS spanning 12 subclasses, 30 were identified for the first time. The dominant identified PFAS compounds were C4 sulfonamido derivatives, including perfluorobutane sulfonamido ethanol (FBSE), perfluorobutane sulfonamide (FBSA), and perfluorobutane sulfonamido diethanol (FBSEE diol), with maximum concentrations of 482 μg/L, 141 μg/L, and 83.5 μg/L in sewage, respectively. Subsequently, three ultrashort chain perfluoroalkyl acids (PFAAs) were identified in samples, ranging from 0.004 to 19.9 μg/L. Three effluent samples from the associated industrial wastewater treatment plants (WWTPs) were further analyzed. This finding, that the C4 sulfonamido acetic acid series constitutes a significant portion (65%−82%) of effluents from WWTP3 and WWTP4, emphasizes the conversion of fluorinated alcohols to fluorinated acids during aerobic treatment. The identification of the intermediate metabolites of FBSEE diol, further supported by our laboratory batch studies, prompts the proposal of a novel metabolic pathway for FBSEE diol. The total amount of perfluorobutane sulfonamido derivatives reached 1934 μg/L (90%), while that of PFAAs, which have typically received attention, was only 205 μg/L (10%). This suggests that perfluorobutane sulfonamido derivatives are emerging as a new trend in

doi:10.6342/NTU202402180

fluorosurfactants used in the semiconductor industry, serving as PFAS precursors and contributing to the release of their metabolites into the environment.

Keywords: Per- and polyfluoroalkyl substances, PFAS, Semiconductor industry, Perfluorobutane sulfonamide, Perfluorobutane sulfonamido ethanol, Perfluorobutane sulfonamido acetic acid, Metabolites, Precursors

CONTENT

doi:10.6342/NTU202402180

doi:10.6342/NTU202402180

List of Figures

doi:10.6342/NTU202402180

doi:10.6342/NTU202402180

doi:10.6342/NTU202402180

List of Tables

doi:10.6342/NTU202402180

List of Abbreviations and Symbols

AFFF	Aqueous film forming foam
ARCs	Anti-reflective coatings
BARCs	Bottom anti-reflective coating
BHF	Buffered hydrofluoric acid
BOE	Buffered Oxide Etch
CL	Confidence level
6:2 Cl-PFESA	9-chlorohexadecafluoro-3-oxanonane-1-sulfonate; 9Cl-PF3ONS; F-53B
9Cl-PF3ONS	9-chlorohexadecafluoro-3-oxanonane-1-sulfonate; 6:2 Cl-PFESA; F-53B
DiPAPs	Di-Substituted polyfluorinated phosphate esters
d$_5$-N-EtFOSAA	N-ethyl-d$_5$-perfluoro-1-octanesulfonamidoacetic acid
d$_3$-N-MeFOSAA	N-methyl-d$_3$-perfluoro-1-octanesulfonamidoacetic acid
DUV	Deep ultraviolet

EPA	Environmental Protection Agency
EtFOSE	N-ethyl perfluorooctanesulfonamidoethanol
EtFOSAA	N-ethylperfluoro-1-octanesulfonamidoacetic acid
FASAs	Perfluoroalkane sulfonamides
FASAAs	Perfluoroalkane sulfonamide acetic acids
FASEs	Perfluoroalkane sulfonamide ethanols
FBSA	Perfluorobutylsulfonamide; Perfluorobutane sulfonamide
FBSAA	N-perfluorobutanesulfonyl glycine; perfluorobutane sulfonamido acetic acid
FBSE	Perfluorobutane sulfonamido ethanol; 1,2,2,3,3,4,4,4-Nonafluoro-N-(2-hydroxyethyl)-1-butanesulfonamide
FBSEE diacid	Perfluorobutane sulfonamido diacid
FBSEE diol	Perfluorobutane sulfonamido diethanol; N,N-Bis(2-hydroxyethyl) perfluorobutanesulfonamide
FBSEE mono-ol monoacid	N-(2-hydroxyethyl) perfluoroalkane sulfonamido acetic acids
FOSA	Perfluoro-1-octanesulfonamide
FTAs	Fluorotelomer acrylates
FTCAs	Fluorotelomer carboxylic acids
FTOHs	Fluorotelomer alcohols
FTSAs	Fluorotelomer sulfonic acids
FTUCAs	Fluorotelomer unsaturated carboxylic acids
n:2 FTSAs	n:2 fluorotelomer sulfonic acids
4:2 FTSA	1H,1H,2H,2H-perfluoro-1-hexanesulfonate
6:2 FTSA	1H,1H,2H,2H-perfluoro-1-octanesulfonate
8:2 FTSA	1H,1H,2H,2H-perfluoro-1-decanesulfonate

HR-MS	High resolution mass spectrometry
LOQ	Limits limit of quantification
MDL	Method detection limit
MeFBSA	N-methyl perfluorobutane sulfonamide; N-(Methyl) nonafluorobutanesulfonamide
MeFBSE	N-methyl perfluorobutane sulfonamido ethanol; Nonafluoro-N-(2-hydroxyethyl)-N-methyl-1-butanesulfonamide
MeFBSAA	N-methyl perfluorobutane sulfonamido acetic acid; Perfluorobutanesulfonylamide(N-methyl)acetate; N-Methyl-N-[(1,1,2,2,3,3,4,4,4-nonafluorobutyl)sulfonyl] glycine
MeFOSAA	N-methylperfluoro-1-octanesulfonamidoacetic acid
M8FOSA	Perfluoro-1-[$^{13}C_8$] octanesulfonamide
M2-4:2FTSA	1H,1H,2H,2H-perfluoro-1-[1,2-$^{13}C_2$] hexanesulfonate
M2-6:2FTSA	1H,1H,2H,2H-perfluoro-1-[1,2-$^{13}C_2$] octanesulfonate
M2-8:2FTSA	1H,1H,2H,2H-perfluoro-1-[1,2-$^{13}C_2$] decanesulfonate
MPFBA	Perfluoro-n-[$^{13}C_4$]butanoic acid
M3PFBS	Perfluoro-1-[2,3,4-$^{13}C_3$] butanesulfonate
M6PFDA	Perfluoro-n-[1,2,3,4,5,6-$^{13}C_6$] decanoic acid
MPFDoA	Perfluoro-n-[1,2-$^{13}C_2$] dodecanoic acid
M4PFHpA	Perfluoro-n-[1,2,3,4-$^{13}C_4$] heptanoic acid
M5PFHxA	Perfluoro-n-[1,2,3,4,6-$^{13}C_5$] hexanoic acid
M3PFHxS	Sodium perfluoro-1-[1,2,3-$^{13}C_3$] hexanesulfonate
M9PFNA	Perfluoro-n-[$^{13}C_9$]nonanoic acid
M8PFOA	Perfluoro-n-[$^{13}C_8$]octanoic acid
M8PFOS	Sodium perfluoro-1-[$^{13}C_8$] octanesulfonate

doi:10.6342/NTU202402180

M5PFPeA	Perfluoro-n-[$^{13}C_5$]pentanoic acid
M7PFUdA	Perfluoro-n-[1,2,3,4,5,6,7-$^{13}C_7$] undecanoic acid
M2PFTeDA	Perfluoro-n-[1,2-$^{13}C_2$] tetradecanoic acid
MRM	Multiple reaction monitoring
OECD	Organization for Economic Co-operation and Development
PAGs	Photo-acid generators
PAPs	Mono-Substituted polyfluorinated phosphate esters
PBSF	Perfluorobutane sulfonyl fluoride
PFAAs	Perfluoroalkyl acids
PFAS	Perfluoroalkyl and polyfluoroalkyl substances
PFBA	Perfluoro-n-butanoic acid
PFBS	Perfluoro-1-butanesulfonate
PFBSi	Perfluorobutanes ulfinic acid
PFCAs	Perfluoroalkyl carboxylic acids
PFdiCA	Perfluoroalkyl dioic acids
PFDA	Perfluoro-n-decanoic acid
PFDoA	Perfluoro-n-dodecanoic acid
PFDS	Perfluoro-1-decanesulfonate
PFECAs	Per- and polyfluoroalkyl ether acids
PFHpA	Perfluoro-n-heptanoic acid
PFHpS	Perfluoro-1-heptanesulfonate
PFHxA	Perfluoro-n-hexanoic acid
PFHxS	Perfluorohexanesulfonate
PFNA	Perfluoro-n-nonanoic acid
PFNS	Perfluoro-1-nonanesulfonate

PFOA	Perfluorooctanoic acid
PFOSF	Perfluorooctane sulfonyl fluoride
PFOS	Perfluorooctane sulfonate
PFPAs	Perfluoroalkyl phosphonates
PFPeA	Perfluoro-n-pentanoic acid
PFPeS	Perfluoro-1-pentanesulfonate
PFPiAs	Perfluoroalkyl phosphinates
PFPrA	Pentafluoropropionic acid
PFSAs	Perfluoroalkane sulfonic acids
PFTrDA	Perfluoro-n-tridecanoic acid
PFTeDA	Perfluoro-n-tetradecanoic acid
PFUdA	Perfluoro-n-undecanoic acid
PHxSF	Perfluorohexane sulfonyl fluoride
POSF	Perfluorooctane sulfonyl fluoride
REACH	Registration, Evaluation, Authorization, and Restriction of Chemicals
RT	Retention time
SPE	Solid phase extraction
TARCs	Top anti-reflective coating
TFA	Trifluoroacetic acid
TFMS	Trifluoromethanesulfonic acid
UPLC	Ultrahigh performance liquid chromatography
WWTP	Wastewater treatment plant
WSC	World Semiconductor Council

1. Introduction

1.1. Background

Perfluoroalkyl and polyfluoroalkyl substances (PFAS) are a diverse class of chemicals that have been produced and widely used in industrial and commercial applications including in coatings for paper, cookware, carpets, textiles and leathers, or used as lubricants, surfactants and firefighting foams since 1950.[1,2] PFAS have an aliphatic carbon backbone in which hydrogen atoms have been completely (prefix: per-) or partially (prefix: poly-) replaced by fluorine. The perfluoroalkyl ($C_nF_{2n+1}^-$) moiety provides hydrophobic and lipophobic properties.[3] The Organization for Economic Co-operation and Development (OECD) expanded the scope of fluorochemicals in its 2021 revision of the PFAS definition, classifying PFAS as fluorinated substances with at least one fully fluorinated methyl ($-CF_3-$) or methylene ($-CF_2-$) carbon atom.[4] The carbon-fluorine bonds are very difficult to break and resistant to physical, chemical, and biological degradation. These properties make PFAS extremely thermally and chemically stable. For numerical uses, one end of PFAS is functionalized to polar groups, such as carboxylic acid, sulfonic acid, or sulfonamide, which can make them highly polar and chemically unique. Perfluoroalkyl carboxylic acids (PFCAs) with 7 or more perfluorinated carbons and perfluoroalkane sulfonic acids (PFSAs) with 6 or more perfluorinated carbons are considered to be ‘long-chain’ PFAS.[3] PFAS, with fluorine-substituted aliphatic carbon backbones, exhibit stability, low refractive index, and hydrophobic/oleophobic properties,[3,5] making them valuable for surfactants and coatings.[6] PFAS characterized by their functional groups and their structures are summarized in **Table 1**.

Table 1 Groups and structures of PFAS

Group	Abbreviations	Structure
Perfluoroalkyl carboxylic acids	PFCAs	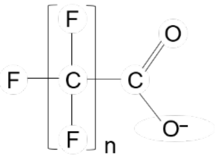
Perfluoroalkane sulfonic acids	PFSAs	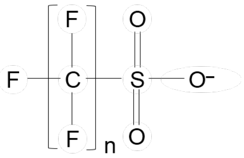
Fluorotelomer carboxylic acids	FTCAs	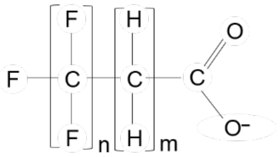
Fluorotelomer sulfonic acids	FTSAs	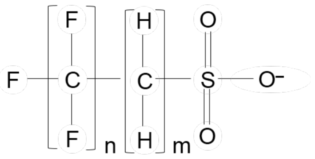
Fluorotelomer unsaturated carboxylic acids	FTUCAs	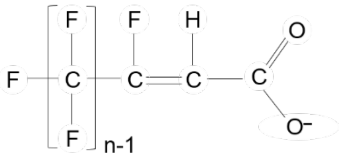
Perfluoroalkane sulfonamides	FASAs	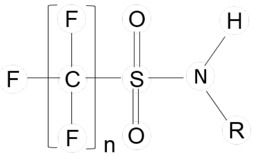 R=H, Me, Et

Group	Abbreviations	Structure
Perfluoroalkyl sulfonamide ethanols	FASEs	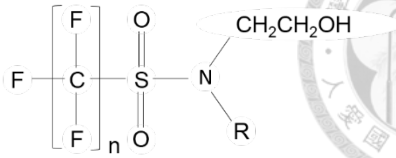 R=Me, Et
Perfluoroalkyl sulfonamido acetic acids	FASAAs	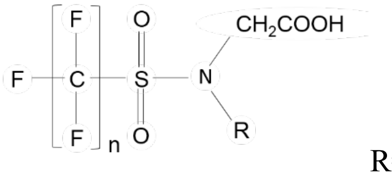 R=H, Me, Et
Fluorotelomer alcohols	FTOHs	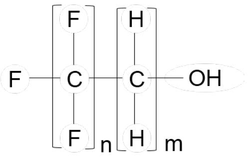
Perfluoroalkyl phosphonates	PFPA	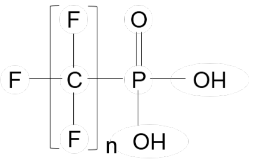
Perfluoroalkyl phosphinates	PFPiA	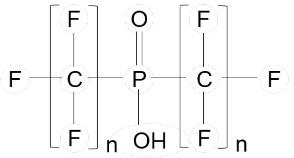
Mono-substituted polyfluorinated phosphate esters	PAP	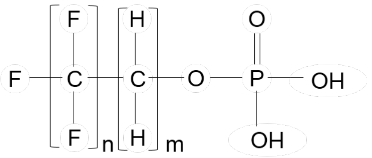
Di-substituted polyfluorinated phosphate esters	diPAP	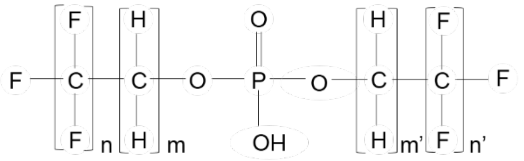

Based on Glüge et al.'s analysis[7] of the SPIN database[8], **Figure 1** illustrates PFAS usage in Sweden, Finland, Norway, and Denmark from 2000 to 2017. It emphasizes a significant role of PFAS in plastic and rubber manufacturing, the electronics industry, and coatings and paints. These three sectors consumed over 3000 tonnes of PFAS collectively. Additionally, approximately 1500 tonnes were used in construction and as lubricants, with another 1200 tonnes in the chemical industry. Non-polymeric PFAS usage in Nordic countries totaled 6300 tonnes, with 90% comprised of 1H-pentafluoroethane, a hydrofluorocarbon and greenhouse gas. The majority of the remaining non-polymeric PFAS, over 70% (470 tonnes), was utilized in flame retardants and extinguishing agents. Polymers were primarily used in plastic and rubber manufacturing, coatings and paints, lubricants, and the chemical industry.

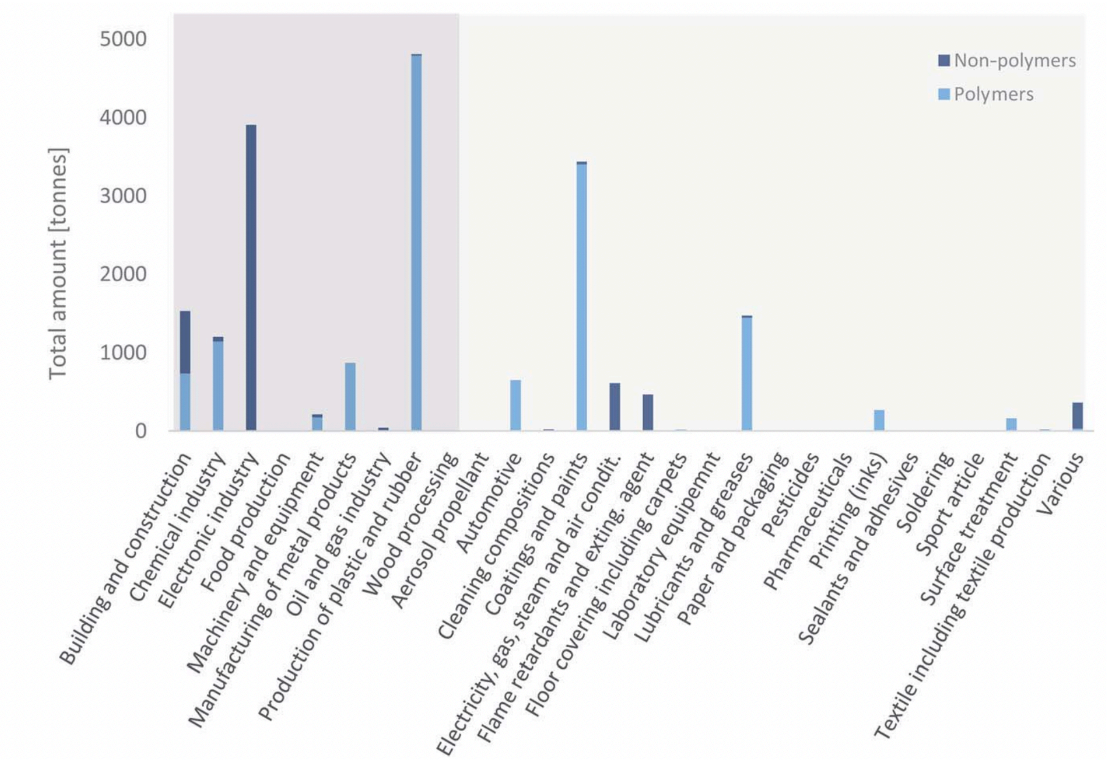

Figure 1 The database[8] reports PFAS usage in Sweden, Finland, Norway, and Denmark from 2000 to 2017. Dark backgrounds in the data indicate industrial branches, while light grey backgrounds represent other use categories.[7]

In 2000, a major U.S. manufacturer (3M Company) proclaimed a voluntary phase-out of perfluorooctane sulfonate (PFOS) and PFOS-related products as well as other long-chain PFAS including perfluorooctanoic acid (PFOA) and perfluorohexane sulfonate (PFHxS). The aroused concerns were based on the analytical results showed these persistent compounds could be detected at low levels in the environment and in humans.[3,9] In 2006, the United States Environmental Protection Agency (USEPA) announced a Product Stewardship agreement with 8 global manufacturing companies who pledged to reduce PFOA emissions and product content by 95% in 2010 and work towards its disappearance by 2015.[3,10] Under the Toxic Substances Control Act (TSCA) Section 8(a)(7), USEPA mandates reporting regulations for PFAS in 2023, requiring manufacturers and processors to submit detailed information on PFAS substance usage from 2011 to 2022, covering identification, applications, quantities, environmental impacts, and health effects.[11]The European Union (EU) has progressively regulated PFOS, PFOA, and PFHxS along with their salts and related compounds through a series of amendments to Regulation (EU) 2019/1021,Regulation (EU) 2020/784, and Regulation (EU)2023/1608, effective from 2019 to 2023. PFOS, its salt, and its precursor, were listed as a persistent organic pollutant (Annex B) by the Stockholm Convention in 2009. PFHxS including its salts and over one hundred PFHxS-related compounds, defined as structures containing C_6F_{13} capable of degrading into PFHxS,[12]

doi:10.6342/NTU202402180

have been listed in the Stockholm Convention to restrict and eliminate their use since 2022.

Historically, numerous manufactures used long chain PFCAs and PFSAs in their production process.[13,14] Since 2000 there has been an on-going industrial transition to replace long-chain PFCAs and PFSAs with shorter-chain PFCAs, PFSAs, and other types of (non)fluorinated alternatives.[15] Nowadays, information on these substitutions including their chemical identities, has not been published or made easily accessible to the public. Wang et al. have arouse three points need to be intensified: (i) “developing accurate analytical techniques for alternatives that can be used for further laboratory testing and field monitoring of these chemicals”; (ii) “developing more sophisticated study designs and data analysis for environmental fate, toxicity and bioaccumulation studies to facilitate up-to-date regulatory decisions”; and (iii) “developing a new industrial ecology where the latest scientific findings can be readily implemented in the product design phase to develop materials with similar function, but with negligible hazardous properties”.[15,16]

In recent years, the semiconductor industry has represented approximately 13-15% of Taiwan's gross domestic product (GDP).[17] Between 2018 and 2022, Taiwan's semiconductor industry saw substantial growth, with its output nearly doubling from \$87.0 billion to \$162.5 billion, as indicated in **Table 2**. Manufacturing accounted for

doi:10.6342/NTU202402180

the largest portion of Taiwan's semiconductor output in 2022, representing 60 percent. Design followed as the second largest segment, comprising 25 percent.[17]

Table 2 Taiwan semiconductor industry segment outputs, 2018–2022, in billions and percentages.[17,18]

Segment	2018	2019	2020	2021	2022
Design	21.3	22.4	29.0	43.5	41.4
Manufacturing, including:	49.3	47.7	61.9	79.8	98.1
Foundry	42.7	42.5	55.4	69.5	90.2
Memory and other	6.7	5.2	6.5	10.3	7.9
Packaging	11.4	11.2	12.8	15.6	15.7
Testing	4.9	5.0	5.8	7.3	7.3
Total industry output	87.0	86.4	109.6	146.1	162.5

In the semiconductor industry, IC manufacturing involves a key process of photolithography that transfers specific patterns onto a wafer, enabling the fabrication of microchips with extremely small patterns,[19] which is illustrated in **Figure 2**. The processes of constructing these circuits layer by layer on a silicon wafer substrate, which involve the significant use of PFAS.[6,20,21,22] PFAS serve as essential components, such as photo-acid generators (PAGs), photosensitizers, anti-reflective coatings (ARCs), etching solutions and rinse surfactants.[6,7,20] These functionalities will be further explored in detail in the subsequent literature review. PFOS served as a surfactant in buffered hydrofluoric acid (BHF) for etching silica dioxide,[22] acting as a PAG[5] and contributing to the low refractive index in ARCs,[23] while perfluorooctanoic acid (PFOA) was reported as a PAG in photoresist.[5] PFOS was found to be the dominant constituent in photolithographic wastewater (12.6 mg/L) and in semiconductor effluents (up to 0.13 mg/L).[13] PFOS was declared eliminated from semiconductor manufacturing by the World Semiconductor Council (WSC) in 2017, and there is a commitment to phase out PFOA and related substances by 2025.[24] The industry has shifted toward primarily using short-chain PFAS-containing materials[23,24] and non-PFAS surfactants, such as silicone-based ones.[5] Despite this transition, literature on the discovery and investigation of alternative compounds remains limited, which makes the semiconductor industry a potentially essential but unexplored source of nontarget PFAS.[25,26] Previous studies identified ultrashort and short per and polyfluoroalkyl acids (PFAAs) in wastewater from electronic fabrication facilities,[26,27] suggesting the adoption of shorter chain structures for some PFAS alternatives.[25] Prior nontarget analysis disclosed per- and polyfluoroalkyl ether acids (PFECAs) in electronic wastewater, linked to fluorotelomer-based acrylate polymers in photoresists.[26] While PFAAs typically receive attention,[26,27] neutral and slightly acidic PFAS, such as perfluoroalkane sulfonamide (FASAs) and perfluoroalkane sulfonamido substances, remain underexplored and warrant further investigation.

doi:10.6342/NTU202402180

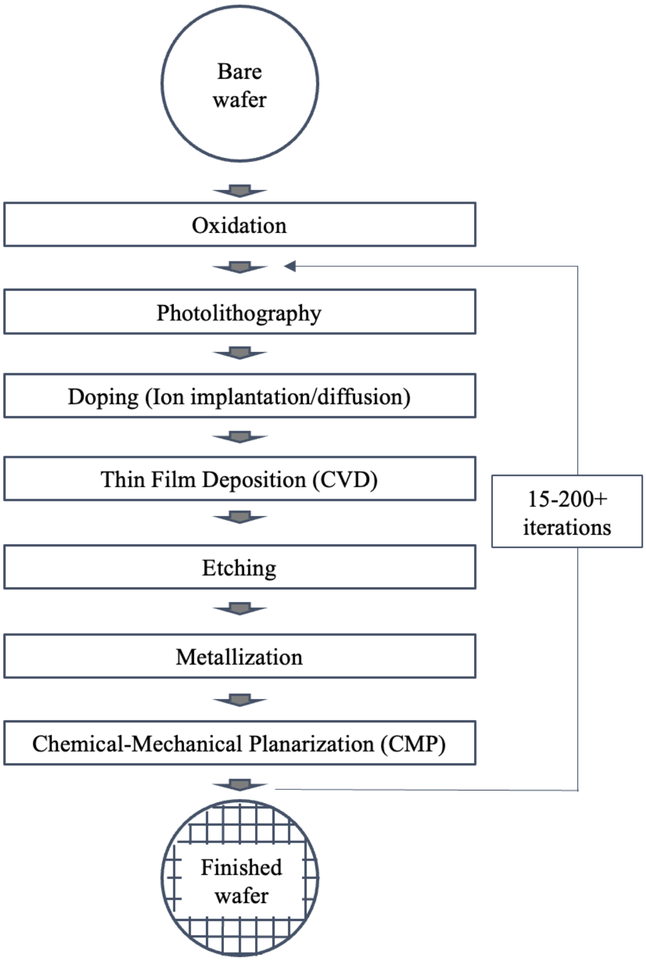

Figure 2 Overall process flow diagram of semiconductor manufacturing (OECD, 2010)[28]

To comprehend the unknown sources of PFAS, high-resolution mass spectrometry (HRMS) has been used in several fields for suspect and nontarget screening of PFAS. The workflow of nontarget identification, including mass defect identification,[29,] homologous pattern recognition,[30] characteristic in-source fragment identification,[31] characteristic fragment ion flagging,[32] and fragment mass difference measurements,[33] is critical for discovering PFAS. Mass defect and homologous patterns are powerful tools in finding undiscovered PFAS in fluorochemical factories,[34] landfills,[35] municipal

doi:10.6342/NTU202402180

WWTPs,[36] and organic waste products[37] due to the presence of a series of homologous substances. However, industrial chemicals are functionalized diversely and uniquely; thus, homologs with similar structures are less likely to occur in industrial manufacturing. Some substances are problematic to identify via homologous patterns when the series contains only two homologs in wastewater from the electronics industry.[26] Thus, a versatile fragment-based approach is anticipated to excel in discerning functionally distinct PFAS, including those outside conventional homologous series.

This study aimed to develop a nontarget approach to discover PFAS substitutions in semiconductor manufacturing. Thus, a novel approach based on fragment and neutral loss screening of the hydrophilic and hydrophobic features of fluorosurfactants with high-resolution mass spectrometry has been established to simultaneously investigate acidic and neutral PFAS. Chemicals used in industrial processes exhibit diverse and precise functionalizations, leading to various reactions such as hydration, oxidation, and deamination in complex sewage mixtures.[38, 39] This distinctive method led to the discovery of numerous PFAS compounds that do not fit within homologous series. In this study, ten sewage samples from five semiconductor plants and three effluents from their associated wastewater treatment plants (WWTPs) were analyzed to identify PFAS-related byproducts, transformation products from oxidation, and diverse reaction

doi:10.6342/NTU202402180

products from semiconductor manufacturing Prior research has explored the environmental presence, toxicity, and transformation of PFAAs precursors,[26,40,16] but there is a limited focus on the metabolic pathways involved in their biotransformation.[38,41] Therefore, this study contributes to the field by identifying PFAS precursors in semiconductor manufacturing and their transformation products during WWTP procedures. Notably, we introduce a novel aspect by proposing the metabolic pathway of fluorinated diol.

1.2. Hypothesis

Hypothesis 1 A 'fragment-based approach' serves as a solution for the challenging identification of certain substances containing only two homologs via the conventional homologous patterns approach.

Hypothesis 2 In semiconductor supply chains without substitutes for PFAS, alternatives may include short-chain PFAS, modified perfluorinated chains, or altered functional headgroups.

Hypothesis 3 PFAS precursors can transform into 'degradation products' during wastewater treatment, then enter the environment.

1.3. Objectives

This study aims to develop and apply an analytical method for detecting and identifying emerging PFAS and their degradation products in the environment. Due to the vast number of PFAS species (>10,000) and the scarcity of commercial standards, acquiring authentic standards for emerging PFAS has been challenging. Therefore, a detection technique "independent of authentic standards" is required. HRMS allows for the target analysis of PFAS with predictable molecular formulas and enables non-target analysis by collecting all m/z peaks and specific MS2 fragments. A versatile fragment-based approach using HRMS is expected to excel in discerning functionally distinct

doi:10.6342/NTU202402180

PFAS through fragment and neutral loss scanning modes, including those outside conventional homologous series. Given the critical role of specific PFAS in semiconductor manufacturing and the limited non-PFAS substitutes for chip production,[5,6] PFAS are inevitably present in semiconductor discharge. Thus, sewage samples from semiconductor plants were collected as a case study to identify emerging PFAS using this novel approach. Additionally, PFAS precursors and their transformation products in effluents during wastewater treatment procedures were studied and the metabolic pathway was further verified. The specific objectives of this study are as follows:

1. **Develop a novel fragment-based approach for nontarget analysis of PFAS.**
2. **Investigate emerging PFAS in sewage samples from semiconductor plants.**
3. **Identify degradation products of PFAS precursors in WWTP effluent samples and propose a metabolic pathway.**

1.4. Dissertation overview

This dissertation is presented in six chapters. **Chapter 1** introduction of this thesis providing the background, motivation, hypotheses and framework. **Chapter 2** is the literature review of this work. **Chapter 3** describes the experimental methods, and lists

doi:10.6342/NTU202402180

the required chemicals/materials. **Chapter 4** gives the experimental results and discussion of this study. **Chapter 5** summarizes the major results of this dissertation in conclusion section, and shows the environmental implications and suggestions. The references supporting this work are located in **Chapter 6**.

The content of this dissertation has been publishing in Environmental Science and Technology 2024, 58, 3, 1648–1658 under the title of " Emerging Perfluorobutane Sulfonamido Derivatives as a New Trend of Surfactants Used in the Semiconductor Industry" and Sustainable Environment Research 2024, 34, 14 under the title of " Comprehensive Nontargeted Analysis of Fluorosurfactant Byproducts and Reaction Products in Wastewater from Semiconductor Manufacturing"

doi:10.6342/NTU202402180

2. Literature Review

2.1. Alternatives to Long-chain PFAS

According to Decision SC-9/4, PFOS, its salts, and its precursor PFOSF were revised in Part III of Annex B to the Stockholm Convention, detailing updated exemptions and acceptable uses. These include the use of insect baits containing sulfluramid (CAS No. 4151-50-2) to control leaf-cutting ants, approved solely for agricultural purposes. Exemptions also apply to PFOS in closed-loop metal plating systems, particularly hard-metal plating, and its use in fire-fighting foam for suppressing liquid fuel vapor and extinguishing Class B fires, in both mobile and fixed systems. These amendments took effect in December, 2020.[23]

PFOA, its salts, and related compounds are tightly regulated under Annex A, mandating their removal. Nevertheless, specific exemptions allow for their utilization across a range of applications, such as semiconductor manufacturing, medical devices, firefighting foam production, high-voltage transmission cables, fluororubber, and industrial sealants, among others. These exemptions grant extended usage until 2025-2036, depending on the specific activity.[42]

For the safety of the environment and human health, it is crucial to consider potential fluorinated alternatives to long-chain PFAS in industries such as semiconductor, textiles, food packaging, and metal plating industry. Here, we summarize publicly accessible information on the production and use of fluorinated alternatives in these various industrial sectors.

2.2. Surface Treatment of Textile, Leather and Carpets

Fluorinated finishes are a technology known to deliver durable and effective oil and water repellence and stain and oil release properties. Historically, fluorinated polymers based on PFOS electrochemical fluorination chemistry have been used. In addition, fluorotelomer-based polymers have also been produced.[43] In 2006, the European Parliament and the Council of the European Union jointly published the Directive on the Restriction of Sale and Use of PFOS (2006/122/EC), and prohibits the sale of substances containing PFOS as ingredient or elements in amount of or above 0.005% (50 ppm) of total mass or concentration, or finished or semi-finished products or parts and components containing PFOS in amount of or above 0.1% (1000 ppm) of total mass or concentration. The Directive became effective from the date of publication, and the member countries shall implement related restrictions from June 27, 2008.[44]

According to Stockholm convention, PFOS, its salt, and its precursor cannot be produced or used anymore in specific industries in 2015. For examples, Substances based on acrylate, methacrylate, adipate and urethane polymers of N-ethyl perfluorooctanesulfonamidoethanol (EtFOSE) can no longer be used in this application.[45] According to the survey of Wang et.al.,[15] since 2003, 3M has commercialized a series of surface treatment products such as Scotchguard PM-3622

doi:10.6342/NTU202402180

(CAS No. 949581-65-1), PM-490 (CAS No. 940891-99-6) and PM-930 (CAS No. 923298-12-8) containing C4 ($C_4F_9SO_2$) side-chain fluorinated polymers[46] to replace PFOS based chemicals. Some producers in China and Italy have initiated the production of perfluorohexane sulfonyl fluoride (PHxSF, $C_6F_{13}SO_2F$)-based derivatives as alternatives in surface treatment products, but these can degrade into PFHxS in the environment [11] and are thus considered as long-chain PFSA precursors.[11]

Other fluorotelomer manufacturers have developed products based on highly purified fluorotelomer raw materials (mostly 6:2), including copolymers derived from 6:2 fluorotelomers and organosiloxane (Unidyne ® TG-5521 developed by Daikin and Dow-Corning (Dow Corning, 2007)).[15] According to the survey of 14 samples of textile by Nortic,[43] fluorotelomer alcohols (FTOHs) were found in eight of the 14 samples. The highest concentration of FTOHs was 464 $\mu g/m^2$. Test results showed that some manufacturers are already using C6 telomer alcohols (i.e. 352 $\mu g/m^2$ of 6:2 FTOH). Long-chain C10 telomers were also used in the products (10:2 around 200 $\mu g/m^2$). Next to the FTOHs, fluorotelomer acrylates (FTAs), also known as polyfluorinated acrylates, were also detected in some samples (8:2 and 6:2). These acrylates are intermediates in the production of fluorinated polymers. Like the C8 telomers, they can be converted into PFOA through oxidation.[43]

2.3. Food Packaging

In terms of oil and water repellency, it is well recognized in the paper industry that phosphate-based fluorinated surfactants provide good oil repellency but have limited water repellency.[43] Acrylate polymers with fluorinated side chains derived from sulfonamido alcohols and fluorotelomer alcohols are the most widely used polymers because they deliver oil, grease, and water repellence.[43] Fluorinated surfactants have been evaluated for paper uses since the early 1960s. From 1974 until 2002, 3M Company produced phosphate diesters (SAmPAP, e.g., FC 807, CAS No. 30381-98-7, based on EtFOSE) and perfluorooctane sulfonyl fluoride (POSF) -based side-chain fluorinated polymers (e.g., CAS No. 92265-81-1) which were used commonly in food contact materials. SAmPAPs have only recently been detected in environmental samples as mono- and di-esters (SAmPAP and diSAmPAP respectively) and they are also potential Perfluorooctane sulfonate (PFOS) precursors. After 3M Company ceased its production of SAmPAP,[47] there is no evidence that from perfluorobutane sulfonyl fluoride (PBSF) -based derivatives are used as alternatives.[15] PAPs/diPAPs were then substituted for SAmPAPs and used in food-contact paper products and as levelling and wetting agents.[14]

U.S. Food and Drug Administration (FDA) has subsequently amended the food

doi:10.6342/NTU202402180

additive regulation [11] that these food additive containing extended perfluoroalkyl chains ≥ eight carbons in length and as such are long-chain PFAS are no longer authorized. Since then, major manufacturers, in conjunction with global regulators, have agreed to discontinue the manufacture of "long-chain"-based fluorinated products and move to "short-chain"-based fluorinated products.[45] Nowadays fluorotelomer manufacturers have developed products based on 6:2 fluorotelomers to replace their earlier products (both side-chain fluorinated polymers and diPAPs) that were based on longer-chain fluorotelomer derivatives.[48]

doi:10.6342/NTU202402180

2.4. Metal (chromium) Plating

Fluorinated surfactants are able to lower the surface tension in chrome acid baths used for chrome plating by forming a thin foamy layer on the surface of the chrome bath. This mist suppressant layer dramatically reduces the formation of chromium-(VI) aerosols, which are well-known as carcinogenic, sensitizing and dangerous for the environment.[49] The challenges to this application are to have a surfactant that are stable in the presence of hot chromic acid and can resist decomposition during the electrolysis as well. Under these demanding conditions perfluorinated surfactants such as PFOS is stable and maintains its activity under a long period.[43]

Historically, salts of PFOS have been used as wetting agents and mist-suppressing agents in decorative plating and non-decorative hard plating. In Europe, salts of 6:2 fluorotelomer sulfonic acid (6:2 FTSA) are applied as alternatives to PFOS. However, due to its slightly higher surface tension compared to PFOS,[15] 6:2 FTS cannot thoroughly substitute for PFOS, especially in the process of non-decorative hard plating. Tetraethylammonium perfluorobutyl sulfonate ($N(Et)_4$ -PFBS CAS No. 25628-08-4) is also registered for metal plating under Registration, Evaluation, Authorization, and Restriction of Chemicals (REACH) with a production volume of 1–10 tonnes per annum[50] to replace PFOS. In China, several producers have used F-53 (salts of

doi:10.6342/NTU202402180

$C_6F_{13}OCF_2CF_2SO_3H$, CAS No. 754925-54-7) and F-53B (Cl-$C_6F_{12}OCF_2CF_2SO_3K$, CAS No. 73606-19-6, also named as 6:2 Cl-PFESA).[15]

2.5. Semiconductor industry

In the semiconductor industry supply chain, the design of integrated circuits (ICs) constitutes the upstream sector, the manufacturing of ICs is the midstream sector, and the packaging and testing of ICs form the downstream sector. Photolithography is a process that transfers specific patterns onto a wafer. It can create incredibly small patterns, even down to a few tens of nanometers in size, to fabricate billions of transistors and interconnected wiring in microchips. The process of constructing these circuits layer by layer on a silicon wafer substrate, involving the use of PFAS, follows standard procedures in a semiconductor fab. **Figure 3** illustrates the mid-stream semiconductor supply chain in IC manufacturing and highlights the roles of PFAS.[6,19,20]

- **Oxidation**- Diffusing O_2 or H_2O vapor into a silicon wafer to create a protective SiO_2 layer on the wafer surface.
- **Photoresist application and exposure**- A photoresist polymer is coated onto a wafer and then baked to form a solid film. The coated wafer is exposed through a patterned photomask using specific wavelength light. Reflectivity can be an issue

during this exposure, so an ARC helps absorb light and reduce reflections. If applied after the photoresist, it is called a top anti-reflective coating (TARC), and if applied before, it is a bottom anti-reflective coating (BARC).

- **Development**- Following exposure, the coated wafer proceeds to development, where exposed regions dissolve while others create a protective coating, resulting in a patterned photoresist.
- **Etching**- It can be performed in a wet process using acids, bases, or liquid solvents in a tank or in a dry process using various plasma-forming gases in a vacuum chamber.
- **Assembly, test and packaging**- A semiconductor package protects semiconductor devices from the environment, connects them to printed circuit boards (PCBs), and involves wafer inspection, dicing, packaging in materials such as plastic, ceramic, or metal, and shipping for product integration.

doi:10.6342/NTU202402180

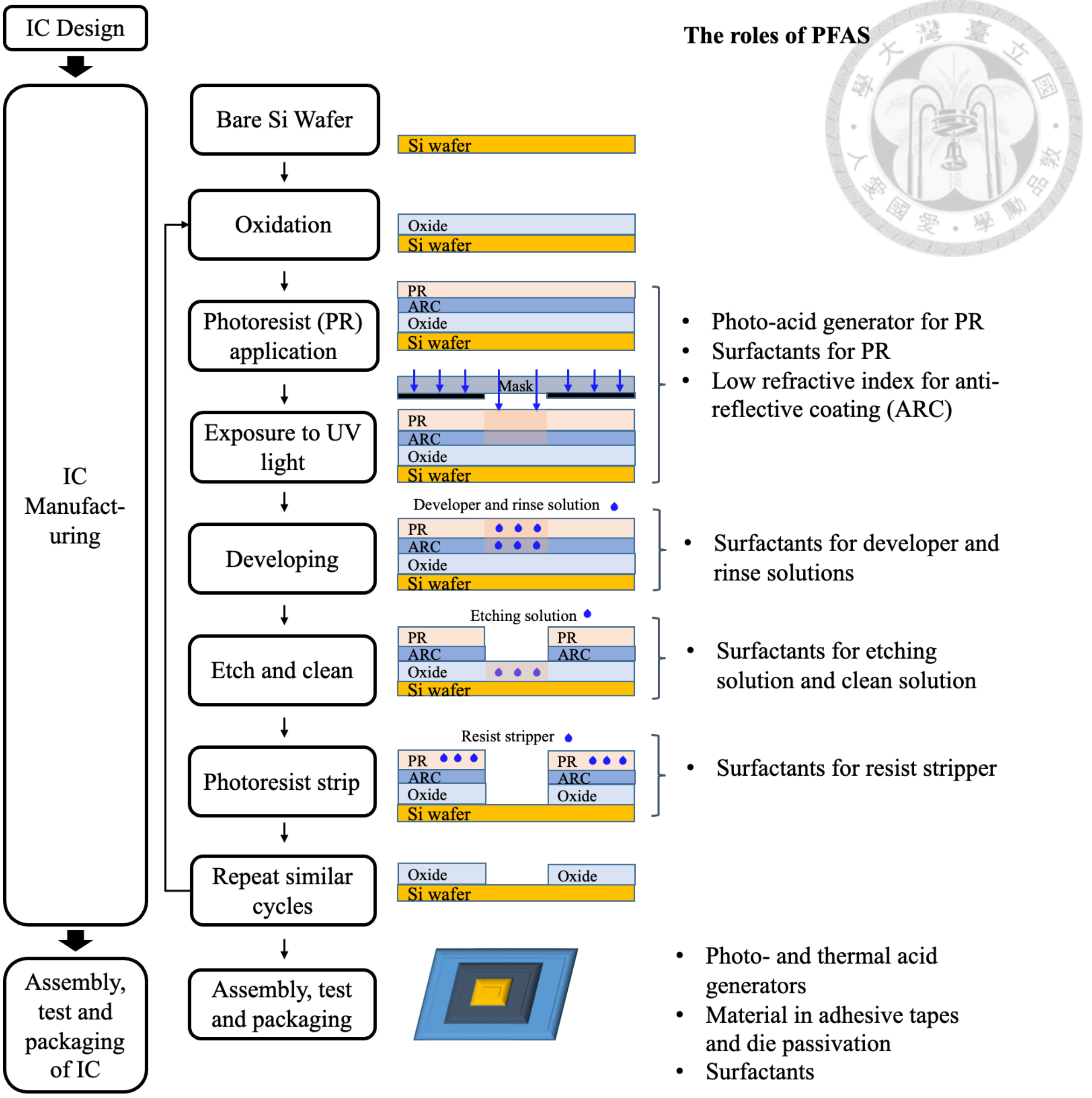

Figure 3 Illustration of the semiconductor supply chain of IC manufacturing and the roles of PFAS

2.5.1. PFAS Used in Photoresists

PFAS plays a pivotal role in the realm of photolithography, particularly in the formulation of photoresists. Here's an introduction of the application of PFAS in photoresists.

1. Certain deep ultraviolet (DUV) photoresists require DUV-sensitive PFAS-containing **PAGs** to provide the necessary strong acidity.
2. DUV photoresists typically contain small amounts of PFAS compounds as **photosensitive agents** to increase the photosensitivity of photoresist.
3. Some formulations of DUV photoresists also include PFAS-containing **surfactants** to improve surface coating uniformity and reduce line collapse.

2.5.1.1.Photo-acid generator (PAG) in Photoresists

In semiconductor, development of smaller features on the surface of a silicon wafer are enabled by photoresists which are light sensitive polymer coating on the silicon wafer. Light exposure changes the solubility of the photoresist enabling to develop (etch) the small circuit features. Photoresists require the use of PAGs to increase their sensitivity to allow etching images smaller than the wavelength of visible light. PAGs are essential in semiconductor photolithography and the patterning performance of PAGs depends on their ability to interact with photons and dissociate to form catalytic photoacids. Typical polar ionic PAGs consist of a photosensitive cation and an acidic counter-ion which releases when exposed to light (**Figure 4**). Historically, the photo-acid generator was PFOS or a PFOS-related substance. The PFOS or PFOS-

doi:10.6342/NTU202402180

related substance concentration was in the range of 0.02wt% to 0.1wt% for photoresists.[45] The industry aimed to replace longer-chain PFAS materials with shorter-chain alternatives, such as four-carbon (C4) or single-carbon (C1) PAG anions, for example, perfluorobutane sulfonate (PFBS). However, the prospect of fully eliminating PFAS-containing materials from PAGs remains uncertain. Studies comparing non-PFAS PAGs in krypton fluoride (KrF) photoresists have shown that non-PFAS alternatives fall short in critical properties such as photospeed, diffusivity, transparency at exposure wavelengths, solubility, and temperature stability. Currently, no available or experimental replacement molecules match the performance of existing PFAS PAGs, especially for 193-nm PAGs, which require very strong acids. There are concerns that finding suitable non-PFAS solutions for some applications may be chemically impossible.[20]

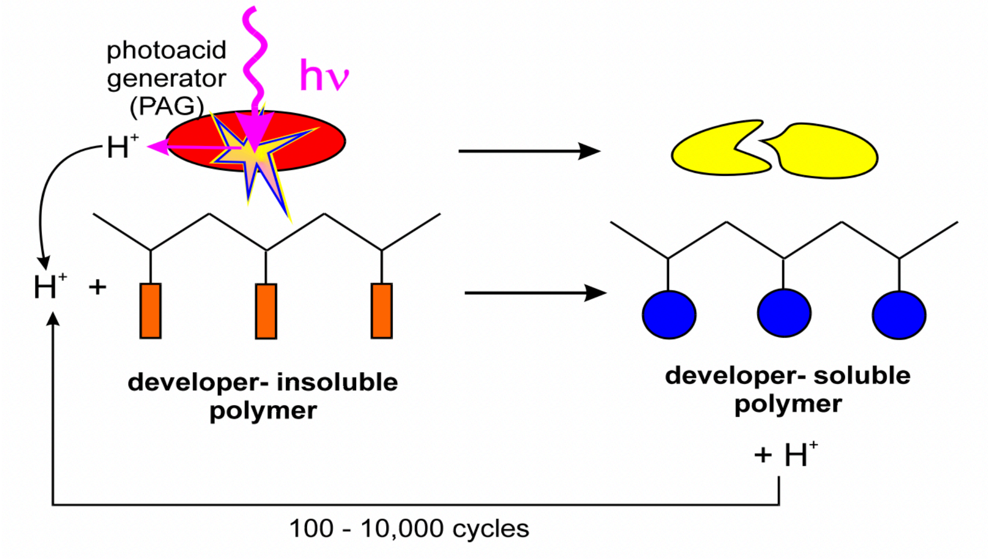

Figure 4 Basic scheme of photoresists: The solubility of a polymer (photoresists)

changes during a dark reaction due to the action of a photoacid catalyst formed from the photolysis of a PAG.[20]

2.5.1.2.Photosensitizer in Photoresists

Photosensitive agents, crucial components in photoresist formulations, are often based on PFAS-free chemistry to ensure optimal photosensitivity. However, in some cases, particularly in DUV photoresists, DUV-sensitive PFAS-containing PAGs are required to provide the necessary strong acidity for the lithographic process. These DUV photoresists typically contain small amounts of PFAS compounds as photosensitive agents (<1% wt) to increase the photosensitivity of the photoresist.[6, 7]

2.5.1.3.Surfactants in Photoresists

PFAS serves as a surfactant in photoresists, ensuring even distribution of the resist material, enhancing pattern clarity, reducing defects, and preventing line collapse. Specifically, these molecules are highly effective at protecting photoresists during immersion lithography while not swelling the photoresist. They form extremely effective surfactants compared to quaternary amines, carboxylates and sulfonates. [6]

2.5.2. Anti-reflective Coatings (ARCs)

ARCs are often used to help reduce blurred images. Two types of ARCs are used: TARCs, applied after the photoresist, and BARCs, applied before the photoresist.

doi:10.6342/NTU202402180

Typically, the concentration of PFOS and/or PFOS-related substances in ARC formulations is around 0.1 wt%.[45]

2.5.3. Developer Rinse Solution

Developer rinsing solutions in photolithography often contain PFAS-containing surfactants. These surfactants serve crucial roles in the development process by effectively reducing the surface tension between adjacent patterned features, thereby preventing toppling or tipping of the pattern. Efforts to replace some PFAS surfactants with silicon-based alternatives and remove PFAS from aqueous developer solutions have been ongoing for over seven years, according to research by the PFAS Alliance in 2022.[6] However, a universally applicable alternative solution is currently lacking, particularly in cutting-edge technologies where PFAS-containing surfactants significantly enhance performance at scales of 3 nanometers or below. Thus, comprehensive conversion may not be feasible for all applications due to material specificity.

2.5.4. Etching Agent for Semiconductor

BHF, or Buffered Oxide Etch (BOE), is an aqueous etchant used in semiconductor fabrication to selectively etch silicon dioxide and silicon nitride~~,~~ as well as for stripping photoresist (the removal of photoresist and BARC from a wafer surface). It consists of hydrofluoric acid and ammonium fluoride, with proportions adjusted for specific etching needs. Surfactants are sometimes added to improve wetting, penetration, and mass transport. Key factors necessitating the use of fluorinated surfactants include: [7, 22]

- **Resistance to Decomposition**: Fluorinated surfactants must withstand chemically reactive conditions (acidic, basic, oxidizing, or reducing) due to the exceptionally strong carbon-fluorine bonds.
- **Low Surface Tension**: These surfactants achieve very low aqueous surface tensions much lower than hydrocarbonsand other materials, due to their low polarizability, high molecular surface area, and the unique conformation of their perfluorocarbon tail groups.
- **Stability at Low pH**: Fluoroalkyl acid surfactants have near-zero acid dissociation constants (pKa), ensuring their headgroups remain ionized and hydrophilic even at very low pH levels.
- **Activity in Nonaqueous Media**: Surfactants with perfluorinated tail groups are both oleophobic and hydrophobic, maintaining surface activity in nonaqueous environments.
- **Low refractive index**: The properties of fluoroalkyl chain provides the ability to reduce the reflection of the etching solution:

Previously, PFOS was used as a surfactant but has been replaced with

doi:10.6342/NTU202402180

alternatives.[45] According to information provided by the World Semiconductor Council,[24] non PFOS-based surfactants such as short-chain perfluoroalkyl sulfonates are alternatives in use.

doi:10.6342/NTU202402180

2.6. Pretreatment for Concentration of Environmental Samples

Solid phase extraction (SPE) is used widely as the sample preparation technology for environmental samples. SPE is a process to concentrate and purify samples for analysis. The principle of SPE is similar to that of liquid-liquid extraction (LLE). It involves partitioning between a liquid (sample matrix or solvent with analytes) and a solid sorbent phase (**Figure 5**). First, the suitable solid sorbent will be selected and conditioned the sorbent using an appropriate solvent to make them able to interact with the sample. Then pull the matrix to flow through the solid sorbent using gravity or a pump. During this step, the analytes as well as some matrix components are retained and thus concentrated on the SPE packing material and some interferences which could not be retained would be flushed. Successively, the analytes and interferences separation could be obtained by selective washing or selective elution. Selective washing is accomplished when the target analytes and the impurities are retained on the sorbent bed: the impurities will be rinsed through with wash solutions but weak enough to leave the analytes behind. Differently, selective elution consists in the elution of the adsorbed compounds of interest by a solvent that leaves the strongly retained impurities behind. Finally, the elution would be collected, dried under a gentle stream of N_2 and analyzed.[51]

doi:10.6342/NTU202402180

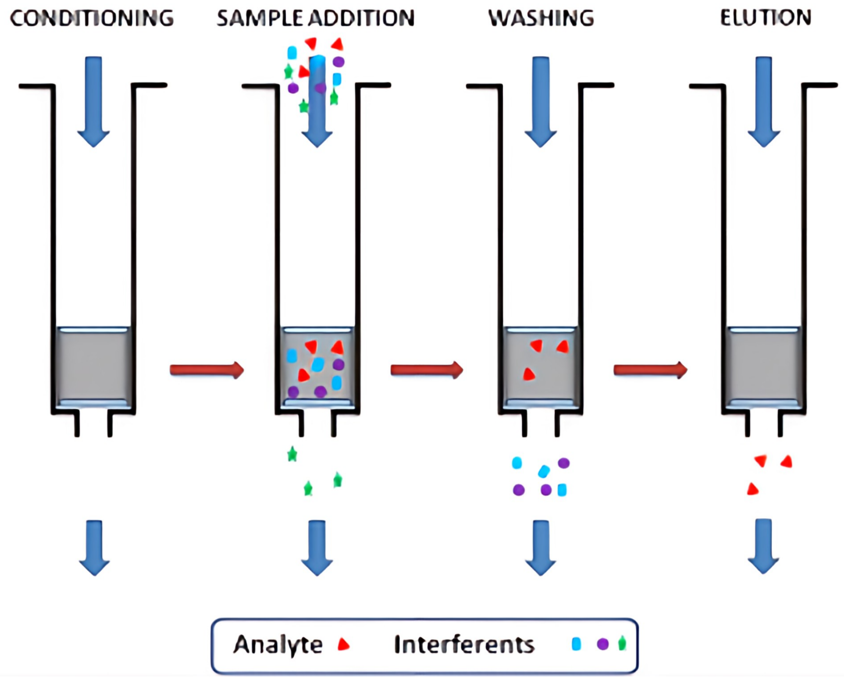

Figure 5 Schematic representation of SPE procedure[51]

PFAS such as PFOS or PFOA are very strong acid. To extract strong acid from the matrix, the stationary of SPE is usually chosen to be anion exchange sorbents (**Figure 6**). Anion exchange sorbents are derivatized with positively charged functional groups that interact and retain negatively charged anions, such as PFOS and PFOA. Oasis WAX (Waters company) is a mixed-mode sorbent that combines weak anion exchange and reversed-phase characteristics. According to the pKa ± 2 rule, Oasis WAX contains secondary/tertiary amines with a pKa of 6,[52] making them fully positively charged at pH values below 4 and completely uncharged at pH values above 8 (**Figure 7**). Thus, the capture strategy for these compounds involves conducting the loading and washing steps at a pH below 4, specifically adjusted to 3 in this study. Weakly acidic PFAS, such as 6:2 FTSA, probably stayed unionized at pH 3, and, along with neutral PFAS compounds, are retained by the reversed-phase sorbent. Conversely, this approach means that compounds with a positive charge could not be adsorbed during the loading step and were consequently removed in the pretreatment process. Elution was carried out with MeOH at a neutral pH to release neutral PFAS compounds, such as FASAs. Subsequently, the sorbent becomes uncharged at a high pH achieved through elution with a solution of 2% NH_4OH in MeOH. Once the charge is neutralized, the electrostatic interaction between the analyte and the stationary phase no longer exists and the analyte will elute from the cartridge resulting in the release of negatively charged chemicals such as strong acids.

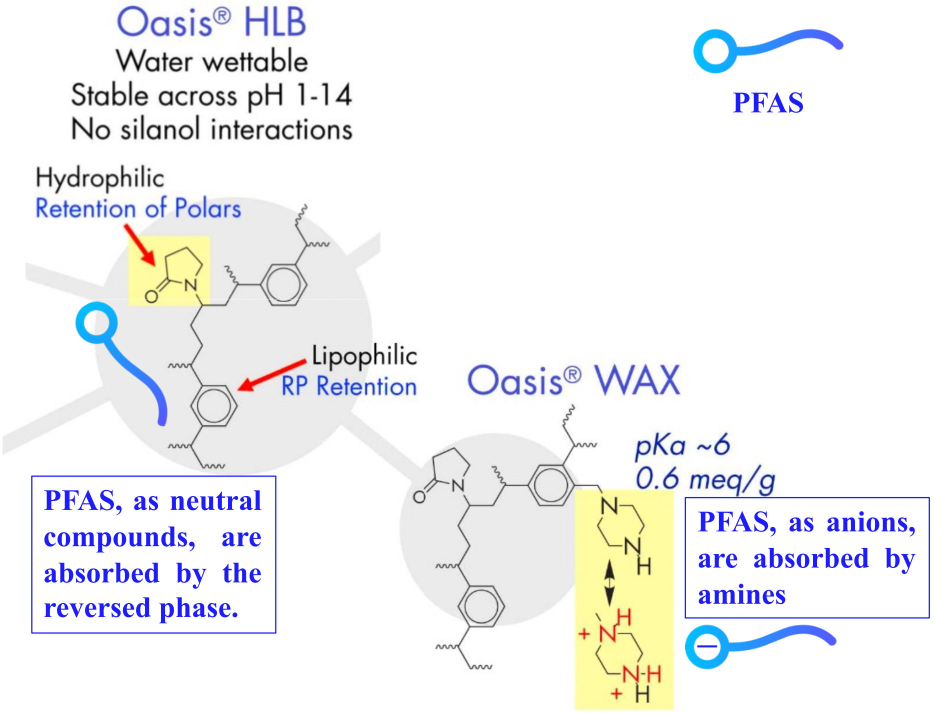

Figure 6 SPE absorbent serves as a weak anion exchanger with a reversed phase for the absorption of PFAS[52]

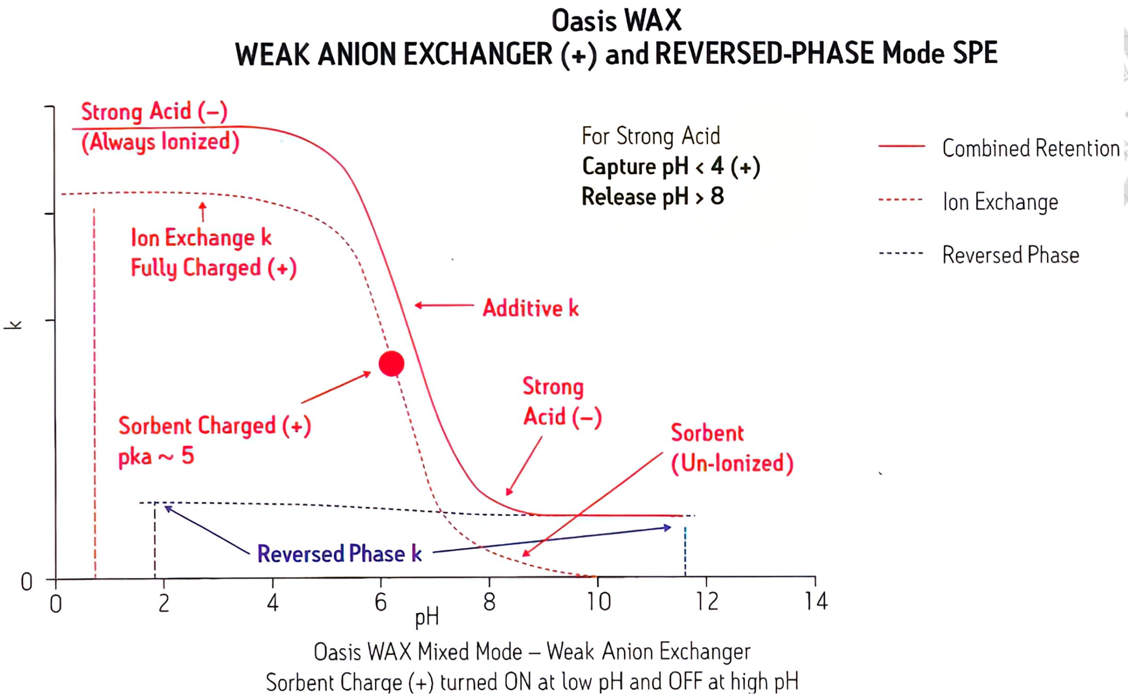

Figure 7 SPE absorbent as weak anion exchanger with reversed phase[52]

2.7. Detection and Discovery of PFAS and Their Alternative

The increased availability of HRMS in chemical analysis has dramatically improved the detection and identification of compounds in environmental samples. HRMS makes the characterization of unknown compounds possible based on the inherent combination of high spectral resolving power (RP) (i.e., RP ≥ 10,000) and high mass accuracy (i.e., ≤ 5 parts-per-million (ppm)). [31,53] This enables the assignment of molecular formulas to observed m/z peaks (exact mass), for example, by using quadrupole time-of- flight mass spectrometry (QTOF-MS). In highly complex matrices, high mass resolving power (RP ≥ 100,000) can provide additional discovery power by further baseline resolving the features in mass spectra, allowing minor analytes to be uncovered and thus their chemical formulas to also be predicted. Technologies that are capable of HRMS include orbitrap (Orbitrap-MS) and Fourier-transform ion cyclotron resonance (FTICR-MS).[31]

Schymanski et al. provided three main approaches towards substance identification in HR-MS analysis which are summarized here with some additional nuances:[54] (i) target screening involves a reference standard measured in-house under the same analytical conditions such that retention time (RT), HRMS and, where possible, (HR-)MS/MS information is available for identification and confirmation. (ii) suspect-target screening is performed when prior information (from various sources, discussed in greater detail below) indicates that a given structure may be present in the sample. Thus, while no reference standard is available, the exact mass and isotope pattern calculated from the molecular formula and plus/minus the expected adduct(s) of the suspect substance can be used to screen for this substance in the sample. (iii) non-target screening involves all remaining components detected in a sample where no prior information is available. As no structural information is available in advance, a full non-target identification starting from the exact mass, isotope, adduct and fragmentation information needs to be performed.

Figure 8 illustrates the confidence levels (CLs) for identifying small molecules using HRMS and outlines the minimum data requirements for each level, as provided by Schymanski et al.[55] Level 1 (Confirmed structure) relies on reference standards, requiring MS, MS^2, RT, and reference standards. Level 2 (Probable structure) can be identified via library spectrum match or diagnostic evidence, requiring MS, MS^2, and either library MS^2 or experimental data. Level 3 (Tentative candidates) involves potential structures, substituents, or classes, needing MS, MS^2, and experimental data. Level 4 (Unequivocal molecular formula) requires MS isotope/adduct data to determine the exact molecular formula. Level 5 (Exact mass) simply requires MS to identify the exact mass of interest. The note emphasizes that MS^2 can denote any form of MS

doi:10.6342/NTU202402180

fragmentation.

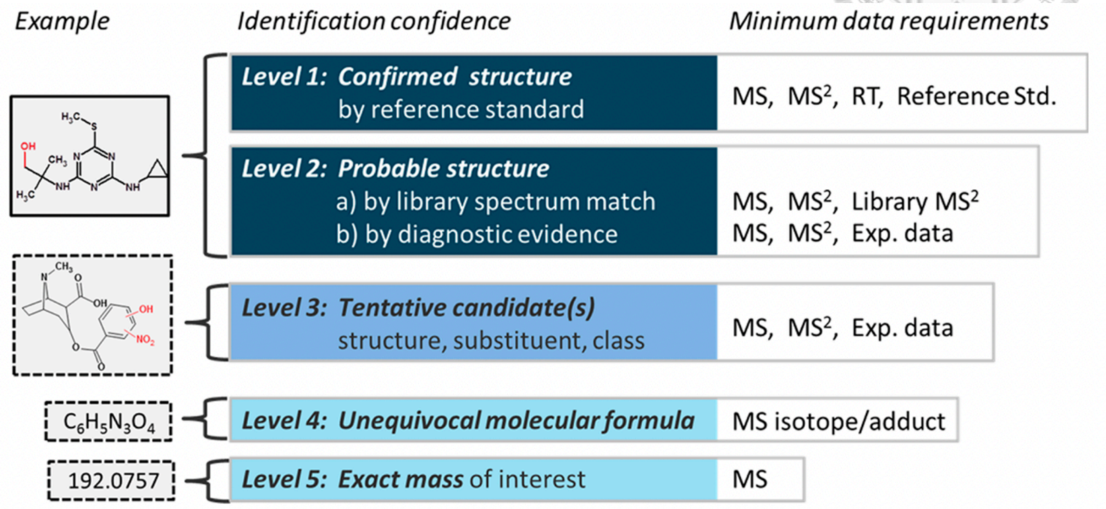

Figure 8 Matrix of identification approach versus identification confidence[55]

Nowadays, CLs are adapted from the upgraded classification by Charbonnet et al.,[56] which clarify and contextualize the previous guidelines by Schymanski et al.[55] This study categorizes identification confidence from Level 1a to Level 5b based on criteria such as accurate mass, mass defect, isotopic pattern match, consistent RT, and evidence from homologous series and MS² fragments. Level 1a represents the highest confidence, confirmed by a reference standard, while Level 1b indicates PFAS isomers, differing in substitution positions, branching, or unsaturated bonds within their fluorinated tails, are nearly indistinguishable by MS2 fragmentation alone. Levels 2a to 2c involve probable identification based on a library spectrum match (Level 2a), diagnostic fragmentation evidence (Level 2b), and diagnostic homologue evidence

doi:10.6342/NTU202402180

(Level 2c). Levels 3a to 3d include positional isomer candidates (Level 3a), fragmentation-based candidates (Level 3b), circumstantial candidates with fragmentation evidence (Level 3c), and circumstantial candidates with homologue evidence (Level 3d). These levels rely on evidence from fragmentation patterns and homologous series, with some reliance on in silico data for structural elucidation. Level 4 provides unequivocal molecular formulas, while Levels 5a and 5b are the lowest CLs, based on exact mass matches with suspect lists or homologous series. This classification system standardizes the communication of PFAS identification confidence via HRMS, ensuring clarity and consistency in reporting. Notably, CL is determined by the number of MS2 fragments, with a single fragment corresponding to CL3, while two or more fragments are classified as CL2 or above. According to this classification, suspect screening, which belongs to one confidence level of nontarget analysis, depends on the availability of the MS2 library. In databases equipped with an MS2 library, the matching is classified as CL2a. In databases that provide only 'formula' information without MS2 libraries, identification relying on formula matching (isotope pattern matching, MS1) is classified as CL4. Therefore, based on the updated scope of identification, we have divided our analysis into two aspects: target analysis and nontarget analysis.

doi:10.6342/NTU202402180

2.7.1. Nontarget Screening of PFAS and Their Alternative

PFAS are synthetic chemicals of significant concern due to their persistence and potential health impacts. Most studies have focused on a few legacy and alternative PFAS using targeted measurement methods, which capture only a small fraction of these compounds. Therefore, advanced analytical techniques are crucial for identifying both known and emerging PFAS. Nontarget analysis using ultra-high-performance liquid chromatography (UHPLC) coupled with HRMS has emerged as a powerful tool for detecting and identifying PFAS in various environmental samples.

2.7.1.1.Homologous Series and Mass Defect Analysis

One of the key strategies for nontarget screening of PFAS is the use of homologous series and mass defect analysis. Homologous series recognition helps identify PFAS compounds with repeating perfluorinated units, while mass defect analysis leverages the unique mass differences to distinguish PFAS from other substances. These approaches enhance the reliability and confidence in identifying PFAS in collaboration with the compound’s RT in chromatography.

A study focuses on conducting target and nontarget analysis of PFAS in wastewater from electronics fabrication facilities in the United States, employing a homologous screening approach.[26] The analysis identified 41 homologous series of

doi:10.6342/NTU202402180

PFAS, totaling 133 homologues, and proposed structures for 15 series, including six newly identified ones. Notably, the study identified per- and polyfluoroalkyl ether acids (PFECAs) in electronics fabrication facilities using a homologous-based approach linked to fluorotelomer-based acrylate polymers used in photoresists. Challenges were encountered in identifying substances based on homologous patterns, particularly in instances where series contained only two homologs.

PFAS in 47 organic waste products (OWP) applied in French agricultural fields were characterized, including both historical and recent materials.[37] Enhanced extraction methods and homologue-based nontargeted analysis with Kendrick mass defect filtering, along with target/suspect-target screening, were employed. This approach detected 160 PFAS across 42 classes. Agricultural wastes like pig slurry, poultry manure, and dairy cattle manure showed low PFAS levels (median $\sum 46$PFAS: 0.66 μg/kg dry matter), while higher concentrations were found in urban and industrial wastes, paper mill sludge, sewage sludge, and residual household waste composts (median $\sum_{46}$PFAS: 220 μg/kg). Historical municipal biosolids and composts (1976–1998) were contaminated with PFOS, EtFOSAA, and PFOS precursors. Contemporary urban OWP (2009–2017) were dominated by zwitterionic fluorotelomers, comprising on average 55% of $\sum_{160}$PFAS (up to 97%). This study underscores urban sludges and composts as significant reservoirs of zwitterionic and cationic PFAS, shedding light on their contributions to agricultural environments.

Suspect and nontarget screening of PFAS in wastewater from a fluorochemical manufacturing park employed quadrupole time-of-flight tandem mass spectrometry.[34] Potential PFAS homologues were identified based on mass differences of CF_2 (49.99681 Da) or CH_2CF_2 (64.01246 Da), common in industrial PFAS synthesis. A total of 90 PFASs across 15 classes were detected, including 12 legacy, 41 known, and 37 new PFAS. Wastewater treatment showed limited removal efficiency, with only one PFAS class significantly reduced (fold change < 1/6), while four classes increased (fold change > 6), potentially indicating precursor transformation.

2.7.1.2.Fragment-Based Screening

Fragment-based screening is another critical aspect for the nontarget screening of PFAS. This technique involves analyzing the fragmentation patterns of PFAS in MS2 spectra to provide additional structural information. By investigating these fragmentation patterns, researchers can corroborate the identities of PFAS compounds.

Yanna Liu et al.[31] developed an analytical approach to discover and identify emerging PFAS by in-source fragmentation flagging scans designed to yield marker fragment ions including $[C_2F_5]^-$ (m/z 118.992), $[C_3F_7]^-$ (m/z 168.988), $[SO_4H]^-$ (m/z 96.959), and $[Cl]^-$ (m/z 34.9). For flagged PFAS, plausible empirical formulas were

doi:10.6342/NTU202402180

generated from accurate masses, isotopic patterns, and fragment ions. In the next step, another injection was made to collect high resolution MS2 spectra of suspect PFAS ions, allowing further confirmation of empirical formulas while also enabling preliminary structural characterization. 36 new PFAS in an industrial wastewater were discovered and of these, 26 were confidently assigned to 3 new PFAS classes that have not previously been reported in the environment: polyfluorinated sulfates ($[C_nF_{n+3}H_{n-2}SO_4]^-$; n = 5, 7, 9, 11, 13, and 15), chlorine substituted perfluorocarboxylates ($[ClC_nF_{2n}CO_2]^-$; n = 4 − 11), and hydro substituted perfluorocarboxylates ($[HC_nF_{2n}CO_2]^-$; n = 5 − 16).

PFAS were discovered using non-targeted screening with Fragment Ion Flagging (FIF), enabling identification at trace levels. Traditional techniques like homologous series detection proved ineffective, while fragment-based mass spectrometry provided a successful alternative. This study analyzed ion fragmentation spectra for characteristic fragments ($[C_nF_{2n+1}]^-$, $[C_nF_{2n-1}]^-$, $[C_nF_{2n-3}]^-$, $[C_nF_{2n-7}]^-$, $[C_nF_{2n-11}]^-$, and $[C_nF_{2n+1}O]^-$), identified novel PFAS in surface water.[32] By matching these fragments to their precursor ions based on RT, 40 PFAS were tentatively identified in four surface water samples from the Netherlands, including four newly discovered species not previously documented. Eight of these PFAS, identified through FIF, do not belong to any homologous series, underscoring the limitations of traditional non-targeted PFAS screening methods based on the homologous screening.

In the context of landfill leachates and groundwater, non-target analysis using HRMS has been instrumental in detecting and identifying novel PFAS.[35] Characteristic fragments utilized for various classes of PFAS in negative ESI are documented in the literature, such as $[C_nF2_{n+1}]^-$ for PFCA, FSO_3^-, SO_3^- and $[C_nF_{2n+1}]^-$ for PFSA, $[C_nF_{2n+1}]^-$ and $[C_nF_{2n-1}]^-$ for H-PFCA, $[C_nF_{2n-1}]^-$ for H-PFSA, $[C_nF_{2n+1}O]^-$ for 1:n PFECA, and $C_{n+3}H_5NO_4F_{2n+1}S^-$ for N-methyl FASAAs, NO_2S^- for FASA, [CnF2n-1]$^-$ and $[C_nOF_{2n-1}]^-$ for H-PFESA, FSO_3^-, FSO_2^- and $[C_nOF_{2n}Cl]^-$ for Cl-PFESA, FSO_3^- and $[C_nF_{2n+1}]^-$ for PFASi, etc. A total of 651 PFAS were identified, including 17 legacy and 637 emerging PFAS, highlighting their occurrence in both raw and treated leachate as well as groundwater.

2.7.2. Knowledge Gap for Current Nontarget Approach of PFAS

Based on the literature review for the nontarget approach of HRMS, several knowledge gaps emerge in the field of PFAS analysis. Identifying substances via homologous patterns is challenging when a series contains only two homologs. Industrial chemicals are often functionalized diversely and uniquely, making homologs with similar structures less likely to occur in industrial manufacturing. Additionally, current approaches primarily utilize fragment-based screening focused on designing fluoroalkyl chain fragments, such as $C_nF_{2n+1}^-$ and $C_nF_{2n+1}O^-$, with limited exploration of PFAS with polar functional groups at the opposite end, such as carboxylic acid (COOH). Moreover, while PFAAs typically receive attention, neutral and slightly acidic PFAS such as FASAs and perfluoroalkane sulfonamido substances remain underexplored. The development of characteristic fragments designed based on the fragments of neutral PFAS is also rare in current research. Our study aimed to develop a distinct fragment-based approach to identify the hydrophobic and hydrophilic features of acidic and neutral fluorosurfactants through fragments and neutral losses, including those outside homologous series.

doi:10.6342/NTU202402180

3. Experimental Section

3.1. Sample Collection

Ten sewage (wastewater) samples (nos. 184-187, no. 190, no. 191, nos. 194-197) from semiconductor plants and three effluent samples (WWTP3, WWTP4, WWTP5) from the three industrial WWTPs were collected in November 2020 and January 2021, respectively (**Figure 9**). Sewage samples were obtained as grab samples from sewage pipelines with flowing wastewater, while effluent samples were collected as grab samples from the discharge points of the WWTPs. The factory's fabrication area for certain processes, such as photolithography, was not accessible due to strict proprietary confidentiality protocols. Instead, we collected sewage downstream of the factory before it entered the main wastewater pipe. Therefore, the sewage specifically belongs to each factory's wastewater. The effluents were collected from the discharge points of the wastewater treatment plants where the activated sludge process was utilized in all of the studied WWTPs. The maximum discharge capacities of the sewage and effluents are provided in **Table 3**. Notably, our initial experimental design aimed to discover novel PFAS compounds used in the semiconductor industry and to investigate PFAS in the effluents of these industrial WWTPs; hence, influent samples were not included in our collection. The samples were stored in 1 L polypropylene bottles and shipped to the laboratory at 4 °C prior to analysis.

Sewage (wastewater) and effluent samples from the same sampling points were recollected in August 2023 to verify the impact of centrifugation pretreatment for target analysis. Since our initial design did not include collecting influent samples, recycled sludge (15,900 mg/L) from WWTP4 was collected for the degradation experiment of FBSEE diol in activated sludge, aimed at understanding the biotransformation of PFAS precursors into metabolites during wastewater treatment.

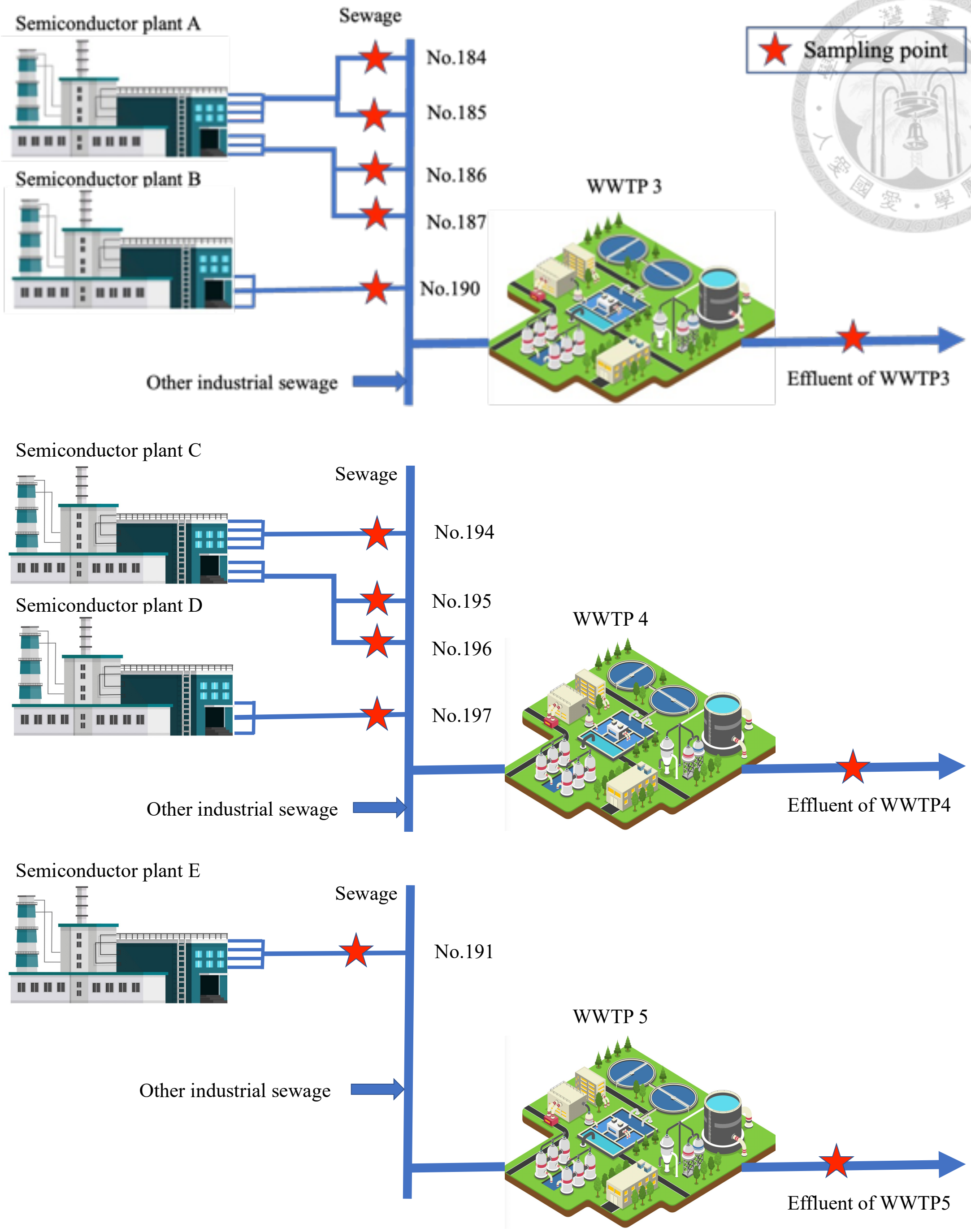

Figure 9 Illustration of samples nos. 184-187, nos. 190-191, and nos. 194-197 from pipes in semiconductor plants and samples WWTP3, WWTP4, and WWTP5 from individual WWTPs.

Table 3 Sampling points and their maximum discharge capacity

Plant	Sampling point (Sample name)	Feature	Maximum discharge capacity (m^3/day, CMD)
Plant A	no. 184	Sewage	4,200
Plant A	no. 185	Sewage	4,200
Plant A	no. 186	Sewage	3,475
Plant A	no. 187	Sewage	3,475
Plant B	no. 190	Sewage	9,654
Plant C	no. 194	Sewage	9,519
Plant C	no. 195	Sewage	4,691
Plant C	no. 196	Sewage	4,691
Plant D	no. 197	Sewage	29,955
Plant E	no. 191	Sewage	15,753
WWTP 3	WWTP 3	Effluent	16,542
WWTP 4	WWTP 4	Effluent	145,000
WWTP 5	WWTP 5	Effluent	24,000

For calculation for the combination of multiple sewage samples from semiconductor plants, the concentration of each sewage was multiplied by the maximum capacity and then divided by the total maximum capacity to determine the concentration to the sewage in the plant.

3.2. Materials

The authentic reference standards for the 25 target PFAS analytes and mixtures of isotopically labeled standards as internal standards (ISs) were purchased from Wellington Laboratories (Guelph, Ontario, Canada), as shown in **Table 4** and **Table 5**. Meanwhile, twenty-five PFAS listed in Table 4 were also used to establish each diverse headgroup pattern of PFAS, including the fragmentation and neutral loss values identified in PFAS screening. Eleven authentic standards were subsequently purchased for the confirmation of identified PFAS via nontarget analysis are listed in **Table 6**.

SPE cartridges (WAX, 150 mg, 6 c.c.) were purchased from Waters Company (USA). Methanol (LC/MS grade) were purchased from Merck (Darmstadt, Germany). Formic acid (ACS reagent grade) and ammonium hydroxide solution (NH_4OH, 28-30%, LC/MS grade) were purchased from Honeywell Fluka. Ammonium acetate (LC/MS grade) was purchased from Fluka. De-ionized water (DI water) (ELGA, 0.22 μm filtered, 18.2 $M\Omega \cdot cm^{-1}$) was used for chemical analysis. Plastic PP vials (0.7 mL) were purchased from Macherey-Nagel GmbH (Germany) and PE screw caps were purchased from Waters (USA).

doi:10.6342/NTU202402180

Table 4 List of 25 target PFAS standards with their concentrations, solvent, and supplier

No.	Compound	Abbreviation	Concentration (µg/L)
1	Perfluoro-n-butanoic acid	PFBA	2000
2	Perfluoro-n-pentanoic acid	PFPeA	2000
3	Perfluoro-n-hexanoic acid	PFHxA	2000
4	Perfluoro-n-heptanoic acid	PFHpA	2000
5	Perfluoro-n-octanoic acid	PFOA	2000
6	Perfluoro-n-nonanoic acid	PFNA	2000
7	Perfluoro-n-decanoic acid	PFDA	2000
8	Perfluoro-n-undecanoic acid	PFUdA	2000
9	Perfluoro-n-dodecanoic acid	PFDoA	2000
10	Perfluoro-n-tridecanoic acid	PFTrDA	2000
11	Perfluoro-n-tetradecanoic acid	PFTeDA	2000
12	Perfluoro-1-octanesulfonamide	FOSA	2000
13	N-methylperfluoro-1-octanesulfonamidoacetic acid	MeFOSAA	2000
14	N-ethylperfluoro-1-octanesulfonamidoacetic acid	EtFOSAA	2000
15	Potassium perfluoro-1-butanesulfonate	L-PFBS	1770 (as the anion)
16	Sodium perfluoro-1-pentanesulfonate	L-PFPeS	1880 (as the anion)
17	Potassium perfluorohexanesulfonate	PFHxSK: linear isomer	1480 (as the anion)
		PFHxSK: ∑ branched isomers	344(as the anion)
18	Sodium perfluoro-1-heptanesulfonate	L-PFHpS	1900 (as the anion)
19	Potassium perfluorooctanesulfonate	PFOSK: linear isomer	1460 (as the anion)
		PFOSK: ∑	391(as the anion)

No.	Compound	Abbreviation	Concentration (µg/L)
		branched isomers	
20	Sodium perfluoro-1-nonanesulfonate	L-PFNS	1920 (as the anion)
21	Sodium perfluoro-1-decanesulfonate	L-PFDS	1930 (as the anion)
22	Sodium 1H,1H,2H,2H-perfluoro-1-hexanesulfonate	4:2 FTSA	1870 (as the anion)
23	Sodium 1H,1H,2H,2H-perfluoro-1-octanesulfonate	6:2 FTSA	1900 (as the anion)
24	Sodium 1H,1H,2H,2H-perfluoro-1-decanesulfonate	8:2 FTSA	1920 (as the anion)
25	Potassium 9-chlorohexadecafluoro-3-oxanonane-1-sulfonate	9Cl-PF3ONS	46600 (as the anion)

doi:10.6342/NTU202402180

Table 5 List of 19 isotope labelled internal standards (ISs) with their concentrations, solvent, and supplier

No.	Compound	Abbreviation	Concentration (μg/L)
1	Perfluoro-n-[$^{13}C_4$]butanoic acid	MPFBA	1000
2	Perfluoro-n-[$^{13}C_5$]pentanoic acid	M5PFPeA	1000
3	Perfluoro-n-[1,2,3,4,6-$^{13}C_5$] hexanoic acid	M5PFHxA	1000
4	Perfluoro-n-[1,2,3,4-$^{13}C_4$] heptanoic acid	M4PFHpA	1000
5	Perfluoro-n-[$^{13}C_8$]octanoic acid	M8PFOA	1000
6	Perfluoro-n-[$^{13}C_9$]nonanoic acid	M9PFNA	1000
7	Perfluoro-n-[1,2,3,4,5,6-$^{13}C_6$] decanoic acid	M6PFDA	1000
8	Perfluoro-n-[1,2,3,4,5,6,7-$^{13}C_7$] undecanoic acid	M7PFUdA	1000
9	Perfluoro-n-[1,2-$^{13}C_2$] dodecanoic acid	MPFDoA	1000
10	Perfluoro-n-[1,2-$^{13}C_2$] tetradecanoic acid	M2PFTeDA	1000
11	Perfluoro-1-[$^{13}C_8$] octanesulfonamide	M8FOSA	1000
12	N-methyl-d_3-perfluoro-1-octanesulfonamidoacetic acid	d_3-N-MeFOSAA	1000
13	N-ethyl-d_5-perfluoro-1-octanesulfonamidoacetic acid	d_5-N-EtFOSAA	1000
14	Sodium perfluoro-1-[2,3,4-$^{13}C_3$] butanesulfonate	M3PFBS	929 (as the anion)
15	Sodium perfluoro-1-[1,2,3-$^{13}C_3$] hexanesulfonate	M3PFHxS	946 (as the anion)
16	Sodium perfluoro-1-[$^{13}C_8$] octanesulfonate	M8PFOS	957 (as the anion)
17	Sodium 1H,1H,2H,2H-perfluoro-1-[1,2-$^{13}C_2$] hexanesulfonate	M2-4:2FTSA	935 (as the anion)
18	Sodium 1H,1H,2H,2H-perfluoro-1-[1,2-$^{13}C_2$] octanesulfonate	M2-6:2FTSA	949 (as the anion)
19	Sodium 1H,1H,2H,2H-perfluoro-1-[1,2-$^{13}C_2$] decanesulfonate	M2-8:2FTSA	958 (as the anion)

Table 6 List of 11 authentic standards utilized to confirm the identified PFAS

No.	Compound	Abbreviation	Purity	Supplier
1	Trifluoroacetic acid	TFA	99.5%	Alfa Aesar
2	Pentafluoropropionic acid	PFPrA	99.4%	Sigma Aldrich
3	Trifluoromethanesulfonic acid	TFMS	99.7%	Thermo Fisher
4	Perfluorobutanesulfinic acid	PFBSi	100%	Synquest Laboratories, USA
5	Perfluorobutylsulfonamide	FBSA	98.4%	Toronto Research Chemicals, Canada
6	1,2,2,3,3,4,4,4-Nonafluoro-N-(2-hydroxyethyl)-1-butanesulfonamide	FBSE	98%	Toronto Research Chemicals, Canada
7	N,N-Bis(2-hydroxyethyl) perfluorobutanesulfonamide	FBSEE diol	98%	Synquest Laboratories, USA
8	N-perfluorobutanesulfonyl glycine	FBSAA	50 mg/L	Chiron AS
9	N-(Methyl) nonafluorobutanesulfonamide	MeFBSA	97%	A2B Chem LLC
10	Nonafluoro-N-(2-hydroxyethyl)-N-methyl-1-butanesulfonamide	MeFBSE	97%	Toronto Research Chemicals
11	Perfluorobutanesulfonylamide(N-methyl)acetate; (N-Methyl-N-[(1,1,2,2,3,3,4,4,4-nonafluorobutyl)sulfonyl] glycine)	MeFBSAA	97%	APOLLO scientific supporting discovery

doi:10.6342/NTU202402180

3.3. Target Analysis

3.3.1. Pretreatment

For the target PFAS analysis, an approach of direct injection analysis was conducted (**Table 7**). A 1500 μL of each sample was centrifuged at 8000 rpm for 15 min, and 792 μL of supernatant was withdrawn and spiked with 8 μL of a 10 μg/L ISs solution (19 isotopic labelled internal standards were listed in Table 5) as pretreatment. The pretreated samples were stored at −20 °C before analysis.

3.3.2. Instrumental Setup

A 300 μL injection was made into an Agilent 1290 UPHLC binary pump system equipped with a 2.1 × 100 mm column (ACQUITY UPLC HSS T3, 1.8 μm) that was interfaced to an Agilent 6495 triple quadrupole mass spectrometer (LC-MS/MS as LC-QqQ) with a negative electrospray ionization (ESI) source. The LC was modified to reduce the background PFAS by setting a delay column of 3.0 × 50 mm (Poroshell 120, EC-C18, 2.7 μm) between the binary pump and the autosampler. Details on the LC gradient program and other method settings are shown in **Table 7**. Analyses are conducted by LC-MS/MS in the multiple reaction monitoring (MRM) mode and the MRM transitions of analytes and ISs are given in Table 8.

doi:10.6342/NTU202402180

Table 7 Details on the LC–MS/MS (Agilent 6495 triple quadruple, QqQ) instrumental method for target analysis

LC system	Agilent 1290 Infinity II UHPLC system		
Separation column	ACQUITY UPLC HSS T3, 1.8 µm, 2.1 mm × 100 mm		
Delay column	Poroshell 120 EC-C18, 2.7 µm, 3.0 mm × 50 mm		
Column oven Temperature	35 °C		
Mobile phases	A: 5mM ammonia acetate in H_2O B: 5mM ammonia acetate in MeOH		
Flow rate	0.4 mL/min		
Chromatographic gradient	Time (min)	A (%)	B (%)
	0	98	2
	0.25	60	40
	12.0	0	100
	15.0	0	100
	16.5	98	2
	20.5	98	2
Injection volume	300 µL		
Source parameter	Mode	Electrospray (ESI)	
	Polarity	Negative	
	Gas Temp (°C)	290	
	Gas Flow (l/min)	18	
	Nebulizer (psi)	35	
	Sheath Gas Heater	400	
	Sheath Gas Flow	12	
	Capillary (V)	4000	
	Neg High Pressure RF	90	
	Neg Low Pressure RF	60	
MS setting	Dynamic MRM (cycle time 700 ms)		

doi:10.6342/NTU202402180

Table 8 MRM transitions of 25 target PFAS and the internal standards with CE values

Type	Target	MRM 1 of Target[1]	CE	MRM 2 of Target[1]	CE	Internal standard	MRM of ISTD	CE
PFCAs	PFBA	213.0 -> 169.0	8	None[2]		M4PFBA	217.1 -> 172.0	9
	PFPeA	263.0 -> 219.0	5	263.0 -> 69	40	M5PFPeA	268.0 -> 223.0	5
	PFHxA	313.0 -> 268.9	5	313.0 -> 119	21	M5PFHxA	318.0 -> 273.0	5
	PFHpA	363.0 -> 319.0	9	363.0 -> 169	17	M4PFHpA	367.0 -> 322.0	9
	PFOA	413.0 -> 368.9	6	413.0 -> 168.9	15	M8PFOA	421.0 -> 376.0	9
	PFNA	463.0 -> 419.0	5	463.0 -> 169	21	M9PFNA	472.0 -> 427.0	5
	PFDA	513.0 -> 468.9	9	513.0 -> 268.8	17	M9PFNA	472.0 -> 427.0	5
	PFUdA	563.0 -> 518.7	9	563.0 -> 268.9	16	M7PFUdA	570.0 -> 525.0	9
	PFDoA	613.1 -> 568.7	9	613.1 -> 319	21	MPFDoA	615.0 -> 570.0	9
	PFTrDA	663.0 -> 618.8	9	663.0 -> 168.9	29	M2PFTeDA	715.0 -> 670.0	9
	PFTeDA	713.0 -> 668.8	9	713.0 -> 169	30	M2PFTeDA	715.0 -> 670.0	9
PFSAs	PFBS	299.1 -> 80.1	33	299.1 -> 99	40	M3PFBS	302.0 -> 99.0	33
	PFPeS	348.9 -> 79.9	40	348.9 -> 98.9	40	M3PFBS	302.0 -> 99.0	33
	PFHxS	399.0 -> 79.9	41	399.0 -> 98.8	37	M3PFHxS	402.0 -> 99.0	37
	PFHpS	449.0 -> 80.0	41	449.0 -> 99	57	M3PFHxS	402.0 -> 99.0	37
	PFOS	499.0 -> 79.9	50	499.0 -> 98.9	53	M8PFOS	507.0 -> 99.0	53
	PFNS	548.9 -> 98.9	48	548.9 -> 79.9	76	M8PFOS	507.0 -> 99.0	53
	PFDS	599.0 -> 79.9	50	599.0 -> 98.9	50	MPFDoA	615.0 -> 570.0	9
Fluorotelomer	4:2 FTS	327.0 -> 306.9	20	327.0 -> 80.9	36	M2-4:2FTS	329.0 -> 81.0	36
	6:2 FTS	427.0 -> 406.8	25	427.0 -> 81.0	49	M2-6:2FTS	429.0 -> 81.0	49

Type	Target	MRM 1 of Target[1]	CE	MRM 2 of Target[1]	CE	Internal standard	MRM of ISTD	CE
	8:2 FTS	527.1 -> 506.9	29	527.1 -> 79.9	49	M2-8:2FTS	529.0 -> 81.0	49
Ether PFSA	6:2 Cl PFAES	530.9 -> 350.9	20	530.9 -> 83	40	M8PFOS	507.0 -> 99.0	53
FASA	FOSA	498.0 -> 78.1	45	498.0 -> 169	30	M8FOSA	506.0 -> 78.0	30
N-alkyl FASAAs	MeFOSAA	570.0 -> 418.9	20	570.0 -> 482.9	16	d_3-N-MeOFSAA	573.0 -> 419.0	20
	EtFOSAA	584.0 -> 418.9	20	584.0 -> 525.9	20	d_3-N-MeOFSAA	573.0 -> 419.0	20
						M6PFDA[3]	519.0 -> 474.0	9
						d_5-N-EtFOSAA[3]	589.0 -> 419.0	20

[1] MRM1 transitions were used for quantification, MRM2 transition were used for qualification.

[2] Only one MRM transition of 213.0 →169.0 for PFBA, which was used for quantification.

[3] M6FDAS and d_5-N-EtFOSAA were used for the verification of centrifugation-induced losses in hydrophobic PFAS

3.3.3. Quantitation of Target Analysis

Calibration- The method calibrates and quantifies PFAS analytes using isotopically labeled standards. Quantification was conducted using MRM transitions for the analytes and internal standards, as detailed in **Table 8**. Each PFAS analyte was quantified using MRM1 as the primary quantification ion and MRM2 as the confirmation ion. A weighted linear regression analysis (1/x) of the calibration curve with a minimum of five concentration levels (10-2000 ng/L) was carried out for the quantitation of 25 target PFAS using LC–QqQ. The associated internal standards, as shown in Table 8, enabled quantification through isotope dilution with mass-labeled internal standards,

$$y=a*x+b \qquad \text{(Eq 1)}$$

where y represents the ratio of the response of the MRM1 transition of the target PFAS (A_T) to the response of the MRM transition of the internal standard (A_{IS}), and x represents the ratio of the concentration of the target (C_T) to the concentration of the internal standard (C_{IS}) ($y = \frac{A_T}{A_{IS}},\ x = \frac{C_T}{C_{IS}}$).

Quantitative Calculation of Samples The measured values C_T were then multiplied dilution factor to obtain final concentration of the samples.

$$\text{Concentration (ng/L)} = C_T*DF1*DF2 \qquad \text{(Eq 2)}$$

DF1= 800/792=1.01. The sample preparation involved taking 792 µL of the sample and

doi:10.6342/NTU202402180

adding 8 μL of the internal standard, resulting in a dilution factor of 1.01 (800/792).

DF2= Dilution factor. If no dilution was performed, then DF=1

Quantitative Calculation of the Plant with Multiple Sewage samples

To calculate semiconductor plants with multiple sewages (Plant A, C, D), the concentration of each sewage was multiplied by the maximum capacity and then divided by the total maximum capacity to determine the concentration to the sewage in the plant. For instance, the concentrations of samples no. 184, no. 185, no. 186 and no. 187 were individually multiplied by their corresponding wastewater maximum capacity as detailed in Table 3 and then normalized by the total flow capacity to obtain the final concentration for semiconductor plant A.

3.3.4. QA/QC of Target Analysis

One method blank, one quality control sample, one duplicate sample, and one spike sample were included in each batch (maximum 10 samples per batch). For verifying centrifugation-induced losses in hydrophobic PFAS, we analyzed 8 sewage samples (from plants A, B, C, D, E) and 3 effluent samples (from WWTP3, WWTP4, WWTP5) in August 2023. To evaluate the impact of centrifugation on hydrophobic losses, eleven samples were fortified with internal standards (ISs) at a concentration of 5 ng/L before and after centrifugation.

doi:10.6342/NTU202402180

3.4. Nontarget Analysis

3.4.1. Pretreatment

For nontarget analysis, a SPE cartridge (Oasis WAX) featuring a weak anion-exchange and reversed-phased sorbent was applied to concentrate water samples. After thoroughly shaking the sample bottles, 200 mL of water was withdrawn and adjusted to pH<3 with formic acid before loading. The cartridge was subsequently preconditioned with 6 mL 2% NH_4OH in methanol, 6 mL methanol, and 6 mL water. Then, the cartridge was soaked with 3 mL 0.1% formic acid in water, which then flowed through the cartridge. Before the cartridge dried, water sample was loaded and then the cartridge was washed with 3 mL 0.1% formic acid in water and 3 mL pure water. The cartridge was then dried for 15 min. The WAX cartridge was then eluted with 6 mL methanol for neutral PFAS and 6 mL 2% NH_4OH in methanol for acidic PFAS. Neutral PFAS was frequently lost during the methanol wash of the WAX cartridge.[57,58] To investigate neutral PFAS, the cartridge was eluted with 6 mL methanol for neutral PFAS, followed by elution with 6 mL 2% NH_4OH in methanol for acidic PFAS. The eluent was combined and concentrated to near dryness under nitrogen in a water bath at 50 °C. The extract was then reconstituted with 500 μL methanol and filtered through a 0.22 μm nylon filter. The extract was added to DI water at a methanol/water ratio of 3:7 (vol/vol) and then stored at -20 °C before the Q-Exactive MS analysis (High resolution mass spectrometry, HRMS). Method blanks were included in each batch and were treated in the same way as the samples.

3.4.2. Instrumental Setup

A 50-100 µL extract was injected into a Thermo Scientific UltiMate 3000 RS UPHLC binary pump system equipped with a 2.1 × 100 mm column (ACQUITY UPLC HSS T3 1.8 µm) that was interfaced to a negative electrospray ionization source coupled with a Q Exactive hybrid mass spectrometer (LC–QE), a high resolution mass spectrometry (HRMS). Mass spectrometric analysis was performed in full MS/data-dependent MS2 mode. Full scan analysis from m/z 77-1155 followed by the top 20 data-dependent MS2 scans with fragmentation energy applied. A dynamic exclusion list was used, ensuring that precursor ions reappearing within 10 seconds would not be fragmented to observe additional MS2 spectra. Details on the LC gradient program and mass spectrometry settings are shown in **Table 9**.

doi:10.6342/NTU202402180

Table 9 Details on the LC–MS/MS (Thermo Q Exactive, QE) instrumental method for nontarget analysis

LC–MS/MS system	Thermo Scientific Dionex UltiMate 3000		
Autosampler	Thermo Scientific Accela autosampler		
Separation column	ACQUITY UPLC HSS T3, 1.8 µm, 2.1 mm × 100 mm		
Column oven Temperature	30 °C		
Mobile phases	A: 5mM ammonia acetate in H_2O B: 5mM ammonia acetate in MeOH		
Flow rate	0.3 mL/min		
Chromatographic gradient for nontarget analysis	Time (min)	A (%)	B (%)
	0	98	2
	1.0	65	35
	24.0	50	50
	88.0	20	80
	89.0	0	100
	96.0	0	100
	98.0	98	2
	103.0	98	2
Chromatographic gradient for quantitative and semi-quantitative analysis	Time (min)	A (%)	B (%)
	0	98	2
	1.0	65	35
	10.0	50	50
	25.0	20	80
	26.5	0	100
	30.5	0	100
	32.0	98	2
	36.0	98	2
Injection volume	50-100 µL for nontarget analysis 20 µL for quantitative and semi-quantitative analysis		
Source parameter	Mode	Electrospray (ESI)	
	Polarity	Negative	
	In-source CID (eV)	0	
	Sheath gas flow rate	35	
	Aux gas flow rate	8	
	Sweep gas flow rate	1	
	Spray voltage (V)	3000	

LC–MS/MS system	Thermo Scientific Dionex UltiMate 3000	
	Capillary temp.(°C)	320
	S-Lens RF level	50
	Heater temp. (°C)	350
Acquisition mode	Full MS / ddMS2 (TopN)	
Full MS	Resolution	70,000
	AGC target	3e6
	Scan range (m/z)	77 to 1155
dd-MS^2	Resolution	17,500
	AGC target	1e5
	Loop count	20
	MSX count	1
	Top N	20
	Isolation window (m/z)	0.7
	(N)CE / stepped (N)CE	nce: 15, 60
	Dynamic exclusion	10.0 s
Mass Calibration[1]	Acetic acid (CH_3COO^-)	59.01385
	Sodium dodecyl sulfate ($C_{12}H_{25}SO_4^-$)	265.14790
	Taurocholic acid ($C_{26}H_{44}NO_7S^-$)	514.28440

[1] Mass calibration was performed before every analysis. Acetic acid was included in the calibration to improve the mass accuracy of low mass calibration

3.4.3. Workflow of Nontarget Analysis

Data analysis- The data analysis workflows for nontarget analysis of PFAS are illustrated in **Figure 10**. Thermo Scientific Compound Discoverer (CD) 3.3 software was used for compound detection and identification. The approach for nontarget analysis from Compound Discoverer 3.3 was illustrated in **Figure 11**. The initial processing nodes, such as Input Files and Select Spectra, are depicted. Unknown peak identification is conducted using the Detect Compounds node. Integration of information from multiple raw data files is accomplished through the Group Compounds node. Various nodes for annotating unknown compounds in both MS1 and MS2 spectral data are employed. including the 'Search ChemSpider node' (MS1), the 'Search Neutral Losses node' (MS2), the 'Compound Class Scoring node ' (MS2), the 'Search mzCloud node' (MS2) node, the 'Assign Compound Annotations node', and the 'Predict Compositions node' (MS1 and MS2). Specifically, the 'Search for ChemSpider node' was used to screen various databases based on formulas within a 5 ppm mass tolerance (MS1). The databases included Alfa Chemistry, ECHA, EPA DSSTox, EPA ToxCast, KEGG, PubMed, Sigma-Aldrich, Toxin, and Toxin-Target Database. The 'Compound Class Scoring node' (MS2) and the 'Search Neutral Losses node' (MS2) were used for fragment and neutral loss searching, respectively. Detailed specifications of workflow nodes are provided in **Table 10.**

CLs were adapted from the upgraded classification of Charbonnet et al.,[56] which clarify and contextualize Schymanski's guideline[55] for communicating confidence in the identification of small organic molecules by HRMS. The detailed identification criteria[56] are provided in

doi:10.6342/NTU202402180

Table 11. PFAS compounds identified through nontarget analysis, subsequently verified with authentic standards to attain CL1a/CL1b, were classified as 'CL-1 identified PFAS'. Quantification of these CL-1 identified PFAS was carried out using the 1/x weighted least squares linear regression method with external standards, as detailed in Section 3.4.4. PFAS compounds identified through nontarget analysis, which lacked authentic standards and remained within CL2-CL3, were classified as tentatively identified PFAS. The semi-quantification of these tentatively identified PFAS was performed using ‘selective reference compounds’ with similar structures, comparable RTs, or identical fluoroalkyl chains. The average response factor ($\overline{RF_R}$) derived from at least five different concentrations of the selective reference standard was then used for semi-quantification, and detailed procedures are provided in Section 3.4.5.

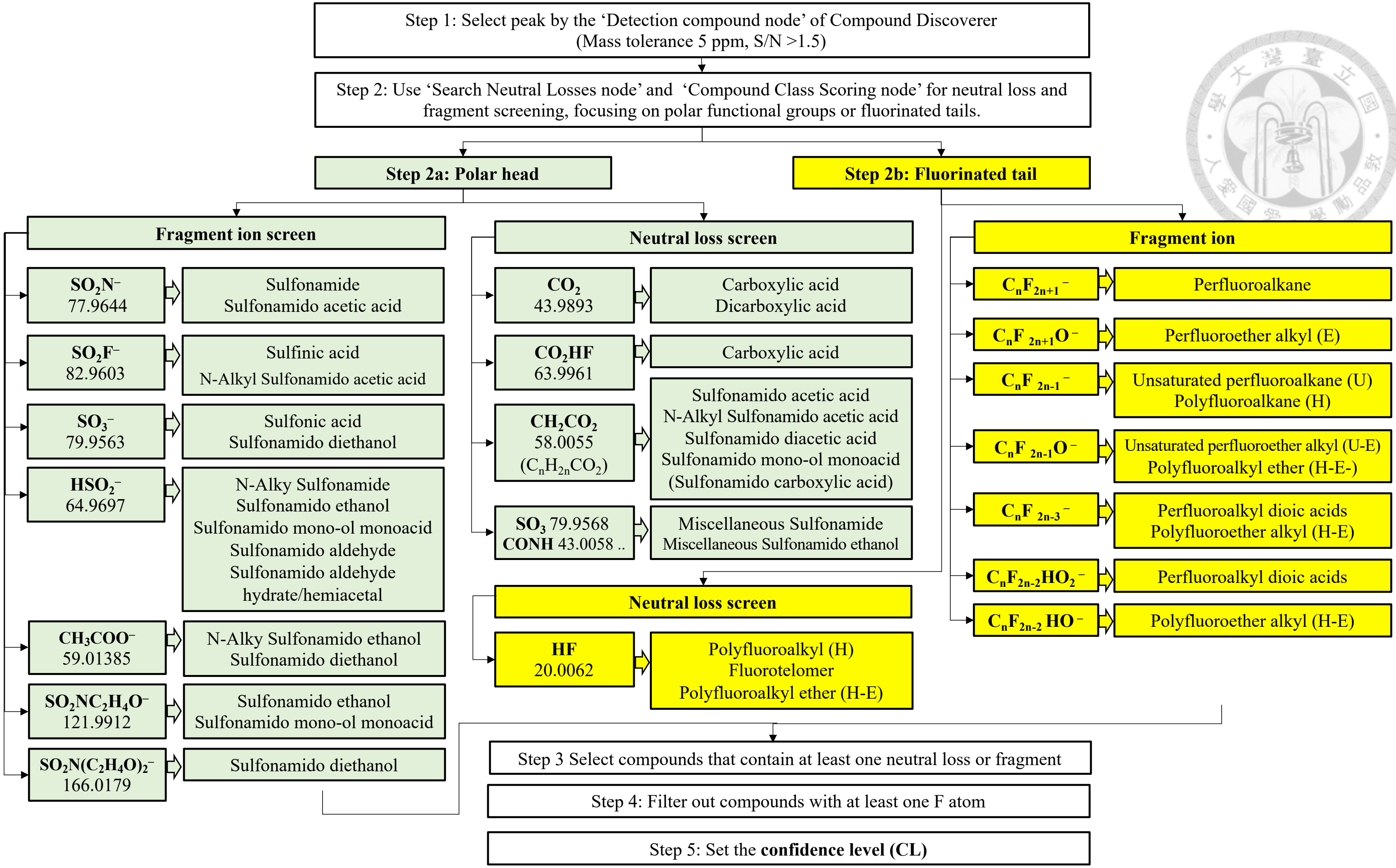

Figure 10 The workflow of nontarget analysis

doi:10.6342/NTU202402180

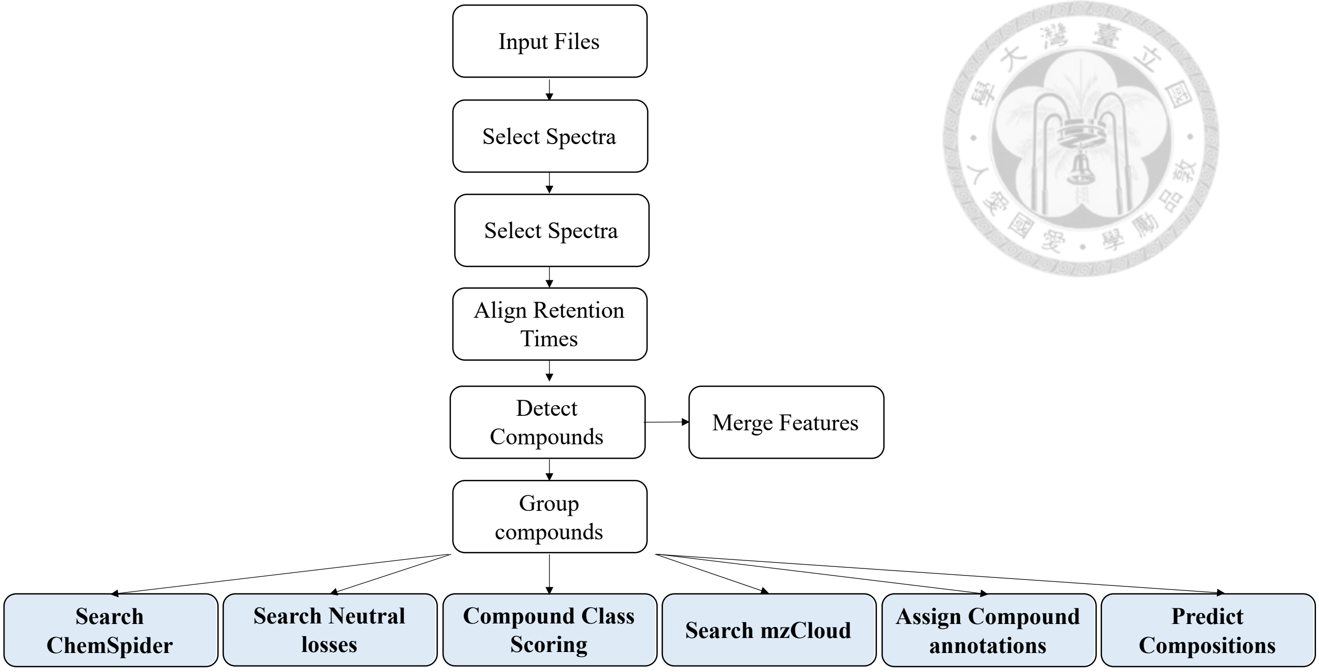

- Databases: Alfa Chemistry, ECHA, EPA DSSTox, EPA Toxcast, KEGG, PubMed, Sigma-Aldrich, Toxin, Toxin-Target Database
- Scan mode: by formula or mass
- Mass tolerance: 5 ppm

- Neutral loss searching
- NL: C_2H_4O, CH_2CO_2, CH_3OH, CO_2, CO_2HF, $CO_2(HF)_4$, HF

- Fragment searching
- For fluoroalkyl tail: CF_3^-, CF_3O^-, $C_2F_3^-$, $C_2F_5^-$, $C_2F_5O^-$, $C_3F_5^-$, $C_3F_7^-$, $C_4F_7O^-$, $C_4F_7^-$, $C_4F_9^-$, $C_5F_9^-$, $C_5F_{11}^-$, $C_6F_{11}^-$, $C_6F_{13}^-$, $C_8F_{17}^-$, CO_2F^-
- For polar head: SO_2^- , SO_2H^-, SO_2F^-, SO_3^-, SO_3F^- , $O_2SNCH_2^-$, O_2SN^- , $O_2SNC_2H_4O^-$, $O_2SNC_3H_6O^-$, $O_2SNC_4H_8O_2^-$

- Autoprocessed; Reference
- Activation energy Tolerance: 20

- Mass tolerance: 5ppm
- Data sources:
  mzCloud Search
  mzVault Search
  Predicted Compositions
  MassList Search
  ChemSpider Search

- Max. element counts C90 H190 Br5 Cl4 F30 N10 O38 P5 S10
- Mass tolerance: 5 ppm
- Fragment matching within mass tolerance 10 ppm

Figure 11 The nontarget analysis workflow from Compound Discoverer 3.3 software, showing select data processing nodes and the associated workflow connections for nontarget analysis.

Table 10 Specifications for the nontarget workflow nodes from Compound Discoverer 3.3 Software

Node	Setting	Description	Criteria/Specification
Search ChemSpider	Search Setting	Database(s)	Alfa Chemistry; ECHA; EPA DSSTox; EPA Toxcast; KEGG; PubMed; Sigma-Aldrich; Toxin, Toxin-Target Database
		Mass Tolerance	5 ppm
		Search Mode	By Formula or Mass
Search mzCloud	General Setting	Library	Autoprocessed; Reference
	DDA Search	Identify Search	HighChem HighRes
		Match Activation Energy	Match with Tolerance
		Activation Energy Tolerance	20
		Similarity Search	None
Search Neutral losses	General Setting	Neutral Losses	C_2H_4O (44.03); CH_2CO_2 (58.01); CH_3OH (32.03); CO_2 (43.99); CO_2HF (64.00); $CO_2(HF)_4$ (124.01); HF (20.01)
		High Acc. Mass Tolerance	2.5 mmu
		Low Acc. Mass Tolerance	0.5 Da
Predict Compositions	Prediction Settings	Mass Tolerance	5 ppm
		Max. Element Counts	C90 H190 Br5 Cl4 F30 N10 O38 P5 S10
	Pattern Matching	S/N Threshold	3
	Fragment Matching	Mass Tolerance	10 ppm
Compound Class Scoring	General Setting	Compound Class	CF_3^-, CF_3O^-, $C_2F_3^-$, $C_2F_5^-$, $C_2F_5O^-$, $C_3F_5^-$, $C_3F_7^-$, $C_4F_7O^-$, $C_4F_7^-$, $C_4F_9^-$, $C_5F_9^-$, $C_5F_{11}^-$, $C_6F_{13}^-$, $C_8F_{17}^-$, CO_2F^-, SO_2^-, SO_2H^-, SO_2F^-, SO_3^-, SO_3F^-, SO_3H^-. NSO_2^-, $O_2SNCH_2^-$, $O_2SNC_2H_4O^-$, $O_2SNC_3H_6O^-$, $O_2SNC_4H_8O_2^-$
		S/N Threshold	50
		High Acc. Mass Tolerance	20 ppm
		Low Acc. Mass Tolerance	20 ppm
Assign Compound	General	Mass Tolerance	5 ppm

Node	Setting	Description	Criteria/Specification
annotations	Setting		
	Data Sources	Data Source#1	mzCloud Search
		Data Source#2	mzVault Search
		Data Source#3	Predicted Compositions
		Data Source#4	MassList Search
		Data Source#5	ChemSpider Search

doi:10.6342/NTU202402180

Table 11 Requirements for identification for the target and nontarget analysis and confidence levels (CLs) of proposed nontarget PFAS structures according to Charbonnet et al. scale[56]

Analysis	**Acquisition**		Requirements for identification
Target analysis	Multiple reaction monitoring (MRM) transitions		ion ratio from sample extracts should be within ±30% (relative) of average of calibration standards
Analysis	**CL**[56]	Identification confidence[56]	Requirements for identification[56]
Nontarget analysis (NTA)	Level 1a	Confirmed by reference standard	accurate mass, mass defect, isotopic pattern match, consistent RT, library MS^2, reference standard
	Level 1b	Indistinguishable from reference standard	accurate mass, mass defect, isotopic pattern match, consistent RT, library MS^2, reference standard
	Level 2a	Probable by library spec. match	accurate mass, mass defect, isotopic pattern match, consistent RT, library MS^2
	Level 2b	Probable by diagnostic fragmentation evidence	accurate mass, mass defect, isotopic pattern match, consistent RT (optional), homologue ≥1 & ≥CL3 (optional), diagnostic MS2 fragment ≥3
	Level 2c	Probable by diagnostic homologue evidence	accurate mass, mass defect, isotopic pattern match, consistent RT, homologue ≥2 & ≥CL2a, diagnostic MS2 fragment≥2
	Level 3a	Positional isomer candidates	accurate mass, mass defect, isotopic pattern match, consistent RT (optional), homologue ≥1 & ≥CL3 (optional), subclass-aligned MS2 fragment ≥1
	Level 3b	Fragmentation-based candidate	accurate mass, mass defect, isotopic pattern match, consistent RT (optional), homologue ≥1 & ≥CL3 (optional), subclass-aligned MS2 fragment ≥1
	Level 3c	Circumstantial candidate with fragmentation evidence	accurate mass, mass defect, isotopic pattern match, consistent RT (optional), homologue ≥1 & ≥CL3 (optional), subclass-aligned (in silico) MS2 fragment ≥1
	Level 3d	Circumstantial candidate with homologue evidence	accurate mass, mass defect, isotopic pattern match, consistent RT, homologue ≥2 & ≥CL2a
	Level 4	Unequivocal molecular formula	accurate mass, mass defect, isotopic pattern match
	Level 5a	PFAS suspect screening exact mass match	accurate mass (suspect list match)

Analysis	**Acquisition**		Requirements for identification
	Level 5b	Nontarget PFAS exact mass of interest	accurate mass, mass defect (optional), homologue ≥3(optional), subclass-aligned (in silico) MS2 fragment ≥2(optional)

3.4.4. Quantification of CL-1 identified PFAS

PFAS compounds identified through nontarget analysis, subsequently verified with authentic standards to attain CL1a/CL1b, were classified as 'CL-1 identified PFAS'. In quantifying seven CL1-identified PFAS using the LC–QE, a linear regression analysis with a minimum of five concentration levels weighted by 1/x was conducted. The calibration curve was created using an external standard and precursor ions as the quantification ion for each CL-1 identified PFAS, as outlined in **Table 12**. The quantification formula is as follows:

$$y=a*x+b$$

(Eq 1)

where y equals the response of the precursor ion of CL1-identified PFAS (A_T) and x equals the concentration of the PFAS (C_T).

Table 12 The calibration of 7 CL1-identified PFAS on the LC–QE

Acronym	Range of linearity (µg/L)	Standard type	Adduct ion	Precursor ion	Theoretical m/z of precursor ion[2]
TFA	0.5-75	External	$[M\text{-}H]^-$	$C_2F_3O_2^-$	112.98559
PFPrA	0.5-75	External	$[M\text{-}H]^-$	$C_3F_5O_2^-$	162.98239
TFMS	0.5-75	External	$[M\text{-}H]^-$	$CF_3O_3S^-$	148.95257
PFBSi	0.5-75	External	$[M\text{-}H]^-$	$C_4F_9O_2S^-$	282.94807
FBSA	0.5-75	External	$[M\text{-}H]^-$	$C_4HF_9NO_2S^-$	297.95897
FBSE	0.5-50	External	$[M\text{-}H]^-$	$C_6H_5F_9NO_3S^-$	341.98519
FBSEE diol	0.5-50	External	$[M+CH_3COO]^-$	$C_9H_{13}F_9NO_6S^-$	446.03253

[1] The limit of quantification (LOQ) was determined as the lowest linear calibration point with the presence of a MS2 fragment.

[2] Precursor ion was used as a quantitative ion with 5 ppm mass accuracy of the theoretical m/z.

3.4.5. Semi-quantification of tentatively identified PFAS

PFAS compounds identified through nontarget analysis, which lacked authentic standards and remained within CL2-CL3, were classified as tentatively identified PFAS. The semi-quantification of these tentatively identified PFAS was performed using ‘selective reference compounds’ with similar structures, comparable RTs, or identical fluoroalkyl chains. The average response factor ($\overline{RF_R}$) derived from at least five different concentrations of the selective reference standard was then used for semi-quantification, and detailed procedures are provided in **Table 13.**

doi:10.6342/NTU202402180

Table 13 Semi-quantitative analysis of 13 tentatively identified PFAS on the LC–QE

Acronym	Selective reference standard	Calibration type	Precursor ion	Formula of precursor ion	Theoretical m/z of precursor ion[1]
PFdiCA(C3)	PFBA	y=$\overline{RF}_{PFBA}$*x	$[M\text{-}H]^-$	$C_3HF_2O_4^-$	138.9848
PFdiCA(C4)	PFBA	y=$\overline{RF}_{PFBA}$*x	$[M\text{-}H]^-$	$C_4HF_4O_4^-$	188.9816
PFdiCA(C5)	PFBA	y=$\overline{RF}_{PFBA}$*x	$[M\text{-}H]^-$	$C_5HF_6O_4^-$	238.9785
PFdiCA(C6)	PFBA	y=$\overline{RF}_{PFBA}$*x	$[M\text{-}H]^-$	$C_6HF_8O_4^-$	288.9753
PFdiCA(C7)	PFBA	y=$\overline{RF}_{PFBA}$*x	$[M\text{-}H]^-$	$C_7HF_{10}O_4^-$	338.9721
PFdiCA(C8)	PFBA	y=$\overline{RF}_{PFBA}$*x	$[M\text{-}H]^-$	$C_8HF_{10}O_4^-$	388.9689
MeFBSA	FBSA	y=$\overline{RF}_{FBsA}$*x	$[M\text{-}H]^-$	$C_5H_3F_9NO_2S^-$	311.9746
FTSE	FBSE	y=$\overline{RF}_{FBsE}$*x	$[M\text{-}H]^-$	$C_4H_5F_5NO_3S^-$	241.9916
FPrSE	FBSE	y=$\overline{RF}_{FBsE}$*x	$[M\text{-}H]^-$	$C_5H_5F_7NO_3S^-$	291.9884
FBSAA	PFBS	y=$\overline{RF}_{PFBs}$*x	$[M\text{-}H]^-$	$C_6H_3F_9NO_4S^-$	355.9645
MeFBSAA	PFBS	y=$\overline{RF}_{PFBs}$*x	$[M\text{-}H]^-$	$C_7H_5F_9NO_4S^-$	369.9812
FBSAA diacid	PFBS	y=$\overline{RF}_{PFBs}$*x	$[M\text{-}H]^-$	$C_8H_5F_9NO_6S^-$	413.9699
FBSEE mono-ol monoacid	PFBS	y=$\overline{RF}_{PFBs}$*x	$[M\text{-}H]^-$	$C_8H_7F_9NO_5S^-$	399.9907

[1] Precursor ion was used as a quantitative ion with 5 ppm mass accuracy of the theoretical m/z

3.4.6. QA/QC of Nontarget Analysis

3.4.6.1. Verification of Solid Phase Extraction

To verify the recovery of SPE, QC samples were prepared in 200 mL of DI water with 0.1 μg/L of 25 PFAS (no ISs spiked) and subjected to SPE. The theoretical analytical concentration of the QC samples was 12 μg/L. The calibration of 25 PFAS on LC-QE were conducted for the calculation of the recovery of SPE. The method calibrates 25 PFAS analytes using external standards using LC–QE. Quantification was performed using precursor ions for the 25 PFAS analytes, as detailed in **Table 14**. Each PFAS analyte was quantified with precursor ions and product ions for confirmation. A weighted linear regression analysis (1/x) of the calibration curve with a minimum of five concentration levels (0.5-75 μg/L) was carried out for the quantitation of 25 target PFAS.

The quantification formula is as follows:

$$y=a*x+b \qquad \text{(Eq 1)}$$

where y equals the response of the precursor ion of PFAS (A_T) and x equals the concentration of the PFAS (C_T).

doi:10.6342/NTU202402180

Table 14 Calibration of 25 PFAS on the LC–QE for verification of pretreatment processing

Acronym	Adduct ion	Precursor ion	Theoretical m/z of precursor ion[1]
PFBA	$[M-H]^-$	$C_4F_7O_2^-$	212.97920
PFPeA	$[M-H]^-$	$C_5F_9O_2^-$	262.97600
PFHxA	$[M-H]^-$	$C_6F_{11}O_2^-$	312.97281
PFHpA	$[M-H]^-$	$C_7F_{13}O_2^-$	362.96962
PFOA	$[M-H]^-$	$C_8F_{15}O_2^-$	412.96642
PFNA	$[M-H]^-$	$C_9F_{17}O_2^-$	462.96323
PFDA	$[M-H]^-$	$C_{10}F_{19}O_2^-$	512.96003
PFUdA	$[M-H]^-$	$C_{11}F_{21}O_2^-$	562.95684
PFDoA	$[M-H]^-$	$C_{12}F_{23}O_2^-$	612.95365
PFTrDA	$[M-H]^-$	$C_{13}F_{25}O_2^-$	662.95045
PFTeDA	$[M-H]^-$	$C_{14}F_{27}O_2^-$	712.94726
PFBS	$[M-H]^-$	$C_4F_9O_3S^-$	298.94299
PFPeS	$[M-H]^-$	$C_5F_{11}O_3S^-$	348.93979
PFHxS	$[M-H]^-$	$C_6F_{13}O_3S^-$	398.93660
PFHpS	$[M-H]^-$	$C_7F_{15}O_3S^-$	448.93341
PFOS	$[M-H]^-$	$C_8F_{17}O_3S^-$	498.93021
PFNS	$[M-H]^-$	$C_9F_{19}O_3S^-$	548.92702
PFDS	$[M-H]^-$	$C_{10}F_{21}O_3S^-$	598.92382
4:2 FTSA	$[M-H]^-$	$C_6H_4F_9O_3S^-$	326.97429
6:2 FTSA	$[M-H]^-$	$C_8H_4F_{13}O_3S^-$	426.96790
8:2 FTSA	$[M-H]^-$	$C_{10}H_4F_{17}O_3S^-$	526.96151
6:2 Cl-PFESA (9Cl-PF3ON)	$[M-H]^-$	$C_8ClF_{16}O_4S^-$	530.89558
FOSA	$[M-H]^-$	$C_8HF_{17}NO_2S^-$	497.94620
MeFOSAA	$[M-H]^-$	$C_{11}H_4F_{17}NO_4S^-$	569.96733
EtFOSAA	$[M-H]^-$	$C_{12}H_6F_{17}NO_4S^-$	583.98298

[1] Precursor ion was used as quantitative ion with 5 ppm mass accuracy of the theoretical m/z

3.4.6.2.Verification of Nylon Filtration

To assess potential filtration losses from nylon filter during the pretreatment, a 2 mL solution containing 20 μg/L of 25 target PFAS in methanol was prepared to assess losses associated with nylon filter filtration. One milliliter of the solution was subjected to nylon filter filtration, followed by dilution to reach a final mixture of 30:70 (vol:vol) methanol/water. Concurrently, another 1 mL of the solution was left unfiltered and diluted to the same final mixture of 30:70 (vol:vol) methanol/water. Four duplicate samples were prepared.

3.4.6.3.Verification of Workflow of Nontarget Analysis

To verify the efficiency of the nontarget analysis processing in **Figure 10**, a PFAS standard mixture containing 39 compounds from 11 PFAS categories listed in Table 15 were prepared as a QC sample to evaluate the detection rate. The prepared concentrations of standard mix are as follow: PFCAs & PFSAs & n:2 FTSAs & FASA & N-alkyl FASAAs :30 μg/L ; n:3 FTCAs & n:2 FTUCAs & Ether-PFCAs &Cl-Ether-PFSAs & N-alkyl FASAs & N-alkyl FASEs: 60 μg/L.

doi:10.6342/NTU202402180

Table 15 List of compounds included in the native PFAS standards obtained from Wellington Laboratories, Canada, used to establish the patterns rules of fragmentation and neutral loss for various types of PFAS

Category	Name	Abbreviation	Prepared conc. (μg/L)
PFCAs	Perfluoro-n-butanoic acid	PFBA	30
	Perfluoro-n-pentanoic acid	PFPeA	30
	Perfluoro-n-hexanoic acid	PFHxA	30
	Perfluoro-n-heptanoic acid	PFHpA	30
	Perfluoro-n-octanoic acid	PFOA	30
	Perfluoro-n-nonanoic acid	PFNA	30
	Perfluoro-n-decanoic acid	PFDA	30
	Perfluoro-n-undecanoic acid	PFUdA	30
	Perfluoro-n-dodecanoic acid	PFDoA	30
	Perfluoro-n-tridecanoic acid	PFTrDA	30
	Perfluoro-n-tetradecanoic acid	PFTeDA	30
n:3 FTCAs	3:3 Fluorotelomer carboxylic acid	3:3 FTCA	60
	5:3 Fluorotelomer carboxylic acid	5:3 FTCA	60
	7:3 Fluorotelomer carboxylic acid	7:3 FTCA	60
n:2 FTUCAs	6:2 fluorotelomer unsaturated carboxylic acid	6:2 FTUCA	60
	8:2 fluorotelomer unsaturated carboxylic acid	8:2 FTUCA	60
	10:2 fluorotelomer unsaturated carboxylic acid	10:2 FTUCA	60
Ether-PFCAs	Hexafluoropropylene oxide-dimer acid	HFPO-DA (GenX)	60
	2,2,3-Trifluoro-3-(1,1,2,2,3,3-hexafluoro-3-trifluoromethoxy-propoxy)-propionic acid	DONA	60
PFSAs	Perfluoropropanesulfonic acid	PFPrS	30
	Potassium perfluoro-1-butanesulfonate	PFBS	30
	Sodium perfluoro-1-pentanesulfonate	PFPeS	30
	Potassium perfluorohexanesulfonate	Linear and branched isomers of PFHxS	30

doi:10.6342/NTU202402180

Category	Name	Abbreviation	Prepared conc. (μg/L)
	Sodium perfluoro-1-heptanesulfonate	PFHpS	30
	Potassium perfluorooctanesulfonate	Linear and branched isomers of PFOS	30
	Sodium perfluoro-1-nonanesulfonate	PFNS	30
	Sodium perfluoro-1-decanesulfonate	PFDS	30
n:2 FTSAs	Sodium 1H,1H,2H,2H-perfluoro-1-hexanesulfonate (4:2 Fluorinated telomer sulfonate)	4:2 FTSA	30
	Sodium 1H,1H,2H,2H-perfluoro-1-octanesulfonate (6:2 Fluorinated telomer sulfonate)	6:2 FTSA	30
	Sodium 1H,1H,2H,2H-perfluoro-1-decanesulfonate (8:2 Fluorinated telomer sulfonate)	8:2 FTSA	30
Cl-Ether-PFSAs	Potassium 9-chlorohexadecafluoro-3-oxanonane-1-sulfonate	9Cl-PF3ONS	60
	Potassium 11-chloroeicosafluoro-3-oxaundecane-1-sulfonate	11Cl-PF3OUdS	60
FASA	Perfluoro-1-octanesulfonamide	FOSA	30
N-alkyl FASAs	N-Methylperfluorooctanesulfonamide	MeFOSA	60
	N-Ethylperfluorooctanesulfonamide	EtFOSA	60
N-alkyl FASEs	2-(N-Methylperfluorooctanesulfonamido)ethanol	MeFOSE	60
	2-(N-Ethylperfluorooctanesulfonamido)ethanol	EtFOSE	60
N-alkyl FASAAs	N-methylperfluoro-1-octanesulfonamidoacetic acid	MeFOSAA	30
	N-ethylperfluoro-1-octanesulfonamidoacetic acid	EtFOSAA	30

doi:10.6342/NTU202402180

3.5. Degradation Experiment of FBSEE Diol in Activated Sludge and Its Pretreatment

The cleaned sludges for the degradation experiment were obtained by transferring 25 mL of the sludge solution into eight separate 50 mL PP centrifuge tubes, followed by centrifugation at 6000 rpm for 15 min. After each centrifugation, we removed the solution from the centrifuge tubes, added 50 mL of DI water, vortexed it for 5 min, centrifuged it again at 6000 rpm for 15 min, and subsequently removed the solution from the centrifuge tube. This process was repeated three times, and each cleaned sludge sample was then combined with 50 mL of DI water and placed in a 200 mL PP bottle with perforated caps. Subsequently, four cleaned sludge solutions were designated as the control samples (symbol S, n = 4), while four cleaned sludge solutions with FBSEE diol at a spiked concentration of 800 μg/L (2067 nM) formed the test samples (symbol SC, n = 4). Another group of four samples, labeled the DI control group (symbol DI, n = 4), was created by introducing FBSEE diol into 50 mL of DI water (fortified concentration of 2067 nM) within 200 mL PP bottles equipped with perforated caps. These 12 samples were then simultaneously shaken at 250 rpm on a horizontal shaker at room temperature for time intervals of 5 min, 2 days, 3 days, and

doi:10.6342/NTU202402180

4 days, denoted by symbols 1, 2, 3, and 4, respectively. SC4 corresponds to the test samples of FBSEE diol undergoing a four day degradation process within the sludge. At the end of each designed time interval, approximately 0.5 mL was withdrawn and subsequently centrifuged. After centrifugation, the clear supernatant was reconstituted in a methanol/water ratio of 3:7 (v/v) mixture for further analysis in LC-QE, and the estimated fortified concentration of FBSEE diol was 560 μg/L (1447 nM).

4. Results and discussion

4.1. Target Analysis

4.1.1 The Calibration

A linear regression analysis weighted by 1/x of the calibration curve for the quantitation of 25 target PFAS on LC–QqQ were shown in **Table 16**. All the correlation coefficients (R) were larger than 0.995.

Table 16 Calibration of 25 target PFAS on the LC–QqQ

Acronym	Internal standard	Range of linearity (ng/L)	LOQ (ng/L)[1]	R
PFBA	M4PFBA	10-2000	10	0.9983
PFPeA	M5PFPeA	10-2000	10	0.9980
PFHxA	M5PFHxA	10-2000	10	0.9979
PFHpA	M4PFHpA	10-2000	10	0.9966
PFOA	M8PFOA	10-2000	10	0.9990
PFNA	M9PFNA	10-2000	10	0.9979
PFDA	M9PFNA	10-1000	10	0.9966
PFUdA	M7PFUdA	10-1000	10	0.9956
PFDoA	MPFDoA	10-1000	10	0.9985
PFTrDA	M2PFTeDA	10-1000	10	0.9991
PFTeDA	M2PFTeDA	10-1000	10	0.9989
PFBS	M3PFBS	10-2000	10	0.9984
PFPeS	M3PFBS	10-2000	10	0.9969
PFHxS	M3PFHxS	10-1000	10	0.9995
PFHpS	M3PFHxS	10-2000	10	0.9970

Acronym	Internal standard	Range of linearity (ng/L)	LOQ (ng/L)[1]	R
PFOS	M8PFOS	10-100	10	0.9957
PFNS	M8PFOS	10-1000	10	0.9955
PFDS	MPFDoA	10-1000	10	0.9964
4:2 FTSA	M2-4:2FTSA	10-2000	10	0.9984
6:2 FTSA	M2-6:2FTSA	10-2000	10	0.9987
8:2 FTSA	M2-8:2FTSA	10-2000	10	0.9984
6:2 Cl-PFESA (9Cl-PF3ON)	M8PFOS	10-2000	10	0.9977
FOSA	M8FOSA	10-2000	10	0.9962
MeFOSAA	d_3-N-MeOFSAA	10-2000	10	0.9968
EtFOSAA	d_3-N-MeOFSAA	20-1000	20	0.9964

[1] The limit of quantification (LOQ) was determined as the lowest linear calibration point with the presence of MRM2 transition.

4.1.2 Quantitative Determination

Table 17 provide a summary of 25 target PFAS concentrations in each sample from the plant/WWTP, along with their respective method detection limits (MDLs). **Table 18** and **Figure 12** provide a summary of 25 target PFAS concentrations in each plant and WWTP, after combined the concentration of multiple sewage samples from single semiconductor plants (plant A with four sewage samples, and plant C with three sewage samples). Given the scarce research on PFAS in the semiconductor industry, we conducted a comparative sewage analysis with Jacob et al.'s study on upstream wastewater from three U.S. fabs.[26] Both studies identified perfluorobutane sulfonate

(PFBS) as the predominant compound, serving as a photoacid generator (PAG) to a potential substitution for PFOS, with our observed concentrations (0.127 to 6.71 μg/L) similar to Jacob et al.'s findings (0.505 to 8.04 μg/L). Comparable concentrations of PFOS, PFOA, PFCAs (C5-C14), and 6:2 FTSA were observed in both studies. PFOS was detected at extremely low concentrations in both studies, with our results ranging from N.D. to <LOQ (0.01μg/L) and Jacob et al.'s from N.D. to 0.008 μg/L. PFOA was present with our concentrations ranging from 0.011 to 0.037 μg/L, and Jacob et al. reporting levels between 0.013 and 0.069 μg/L. Our study detected other PFCAs (C5-C14) at lower concentrations, ranging from N.D. to 0.285 μg/L, while Jacob et al. reported concentrations ranging from N.D. to 0.194 μg/L. 6:2 FTSA was detected at a minimal concentration of only 0.022 μg/L in the effluent of WWTP4 in our study, while Jacob et al. reported it in the range of N.D. to 0.006 μg/L in wastewater. Notably, our study showed significantly higher and broader PFBA concentrations (0.572 to 4.84 μg/L) compared to Jacob et al.'s findings (N.D. to 0.206 μg/L). This discrepancy may be associated with its patented use in photo-imaging sensor materials[7] manufactured in the studied semiconductor plants. Figures 10(a) and 10(b) summarize the concentrations of 25 target PFAS in 5 semiconductor plants and 3 WWTP effluents, with a total of 34.7 μg/L across all samples. PFBS and PFBA, both C4 series PFAS, constituted 93% of the total PFAS concentration.

Table 17 Quantitative concentrations (µg/L) of 25 target PFAS in each sewage sample and effluent sample on the LC–QqQ

Class	Subclass	Acronym	MDL^1 (µg/L)	Sewage from semiconductor plants										Effluent from WWTP		
				Plant A				Plant B	Plant C			Plant D	Plant E	WWTP 3 (A, B)	WWTP 4 (C, D)	WWTP 5 (E)
				No.184	No.185	No.186	No.187	No.190	No.194	No.195	No.196	No.197	No.191			
Perfluoroalkyl acids (PFAAs)	Perfluoroalkyl carboxylic acids (PFCAs)	PFBA	0.0005	**0.680**	**0.772**	**0.835**	**0.862**	**2.25**	**3.66**	**1.77**	**1.98**	**4.84**	**0.572**	**1.24**	**1.69**	**0.49**
		PFPeA	0.0002	**0.219**	**0.223**	**0.367**	**0.356**	**0.062**	**0.134**	**0.205**	**0.204**	**0.141**	**0.197**	**0.125**	**0.101**	**0.161**
		PFHxA	0.0001	**0.091**	**0.095**	**0.157**	**0.176**	**0.031**	**0.057**	**0.086**	**0.084**	**0.049**	**0.086**	**0.070**	**0.037**	**0.068**
		PFHpA	0.0002	**0.039**	**0.040**	**0.081**	**0.081**	**0.016**	**0.019**	**0.022**	**0.023**	**0.019**	**0.043**	**0.032**	**0.018**	**0.031**
		PFOA	0.0008	**0.027**	**0.025**	**0.055**	**0.049**	**0.011**	**0.012**	**0.011**	**0.011**	**0.012**	**0.033**	**0.021**	**0.014**	**0.022**
		PFNA	0.0002	**0.019**	**0.018**	**0.033**	**0.032**	<MDL	**0.013**	**0.010**	**0.012**	**0.011**	**0.039**	**0.017**	**0.012**	**0.015**
		PFDA	0.0003	**0.013**	**0.014**	**0.018**	**0.024**	<MDL	**0.012**	<MDL	**0.011**	**0.010**	**0.032**	**0.010**	<MDL	<MDL
		PFUdA	0.0004	<MDL	<MDL	**0.021**	**0.028**	<MDL	**0.020**	<MDL	<MDL	<MDL	**0.027**	<MDL	<MDL	<MDL
		PFDoA	0.0004	<MDL	**0.010**	**0.011**	**0.012**	<MDL	**0.012**	**0.010**	<MDL	<MDL	<MDL	<MDL	<MDL	<MDL
		PFTrDA	0.0007	<MDL	<MDL	<MDL	<MDL	<MDL	<MDL	<MDL	<MDL	<MDL	<MDL	<MDL	<MDL	<MDL
		PFTeDA	0.0006	<MDL	<MDL	<MDL	<MDL	<MDL	<MDL	<MDL	<MDL	<MDL	<MDL	<MDL	<MDL	<MDL
	Perfluoroalkyl sulfonic acids (PFSAs)	PFBS	0.0001	**2.23**	**1.74**	**0.523**	**0.557**	**2.12**	**3.08**	**2.78**	**2.78**	**6.71**	**0.127**	**1.68**	**2.61**	**0.121**
		PFPeS	0.0001	<MDL	<MDL	<MDL	<MDL	<MDL	<MDL	<MDL	<MDL	<MDL	<MDL	<MDL	<MDL	<MDL
		PFHxS	0.0002	<MDL	<MDL	<MDL	<MDL	<MDL	<MDL	<MDL	<MDL	<MDL	<MDL	<LOQ	<MDL	<MDL
		PFHpS	0.0001	<MDL	<MDL	<MDL	<MDL	<MDL	<MDL	<MDL	<MDL	<MDL	<MDL	<MDL	<MDL	<MDL
		PFOS	0.0005	<MDL	<MDL	<LOQ	<LOQ	<MDL	<MDL	<MDL	<MDL	<MDL	<LOQ	<LOQ	<LOQ	<MDL
		PFNS	0.0002	<MDL	<MDL	<MDL	<MDL	<MDL	<MDL	<MDL	<MDL	<MDL	<MDL	<MDL	<MDL	<MDL

Class	Subclass	Acronym	MDL[1] (μg/L)	Sewage from semiconductor plants										Effluent from WWTP		
				Plant A				Plant B	Plant C			Plant D	Plant E	WWTP 3 (A, B)	WWTP 4 (C, D)	WWTP 5 (E)
				No.184	No.185	No.186	No.187	No.190	No.194	No.195	No.196	No.197	No.191			
		PFDS	0.0002	<MDL	<MDL	<MDL	<MDL	<MDL	<MDL	<MDL	<MDL	<MDL	<MDL	<MDL	<MDL	<MDL
	Fluorotelomer sulfonic acid	4:2 FTSA	0.0001	<MDL	<MDL	<MDL	<MDL	<MDL	<MDL	<MDL	<MDL	<MDL	<MDL	<MDL	<MDL	<MDL
		6:2 FTSA	0.0002	<MDL	<MDL	<MDL	<MDL	<MDL	<MDL	<MDL	<MDL	<MDL	<MDL	<MDL	**0.022**	<MDL
		8:2 FTSA	0.0004	<MDL	<MDL	<MDL	<MDL	<MDL	<MDL	<MDL	<MDL	<MDL	<MDL	<MDL	<MDL	<MDL
	Chlorinated polyfluorinated ether sulfonates (Cl-PFESAs)	6:2 Cl-PFESA (9Cl-PF3ON)	0.0001	<MDL	<MDL	<MDL	<MDL	<MDL	<MDL	<MDL	<MDL	<MDL	<MDL	<MDL	<MDL	<MDL
Perfluoroalkane sulfonamides (FASAs)	Perfluoroalkane sulfonamides (FASAs)	FOSA	0.0004	<MDL	<MDL	<MDL	<MDL	<MDL	<MDL	<MDL	<MDL	<MDL	<MDL	<MDL	<MDL	<MDL
Perfluoroalkane sulfonamido substances	N-alkyl perfluoroalkane sulfonamido acetic acids	MeFOSAA	0.0002	<MDL	<MDL	<MDL	<MDL	<MDL	<MDL	<MDL	<MDL	<MDL	<MDL	<MDL	<MDL	<MDL
		EtFOSAA	0.0004	<MDL	<MDL	<MDL	<MDL	<MDL	<MDL	<MDL	<MDL	<MDL	<MDL	<MDL	<MDL	<MDL

[1] MDL: method detection limit, which was evaluated with seven spiked samples based on the guideline from Appendix B to 40 CFR Part 136, definition and procedure for the determination of the method detection limit, revision 2.

[2] QDLs of each PFAS are provided in Table 16.

Table 18 Concentrations (µg/L) of 25 target PFAS in sewage from semiconductor plants and effluents from industrial WWTPs

Subclass	Semiconductor plant A[4]	Semiconductor plant B	Semiconductor plant C[4]	Semiconductor plant D	Semiconductor plant E	WWTP 3 (A,B)	WWTP 4 (C,D)	WWTP 5 (E)	ΣAll
PFBA	0.782	2.25	2.78	4.84	0.572	1.24	1.69	0.493	14.6
PFPeA	0.285	0.062	0.169	0.141	0.192	0.125	0.101	0.161	1.24
PFHxA	0.126	<MDL	0.071	0.049	0.086	0.070	0.037	0.068	0.539
PFHpA	0.058	<MDL	<MDL	<MDL	0.043	0.032	0.018	0.031	0.239
PFOA	0.037	0.011	0.011	0.012	0.033	0.021	0.014	0.022	0.161
PFNA	0.025	<MDL	0.012	0.011	0.039	<MDL	<MDL	0.015	0.131
PFDA	0.017	<MDL	0.009	0.010	0.032	0.010	<MDL	<MDL	0.078
PFUdA	0.011	<MDL	0.010	<MDL	0.027	<MDL	<MDL	<MDL	0.048
PFDoA	0.008	<MDL	0.009	<MDL	<MDL	<MDL	<MDL	<MDL	0.017
PFTrDA	<MDL	<MDL	<MDL	<MDL	<MDL	<MDL	<MDL	<MDL	<MDL
PFTeDA	<MDL	<MDL	<MDL	<MDL	<MDL	<MDL	<MDL	<MDL	<MDL
PFBS	1.33	2.12	2.93	6.71	0.127	1.68	2.61	0.121	17.6
PFPeS	<MDL	<MDL	<MDL	<MDL	<MDL	<MDL	<MDL	<MDL	<MDL
PFHxS	<MDL	<MDL	<MDL	<MDL	<MDL	<MDL	<LOQ	<MDL	<MDL
PFHpS	<MDL	<MDL	<MDL	<MDL	<MDL	<MDL	<MDL	<MDL	<MDL
PFOS	<LOQ	<MDL	<MDL	<MDL	<LOQ	<LOQ	<LOQ	<MDL	<MDL
PFNS	<MDL	<MDL	<MDL	<MDL	<MDL	<MDL	<MDL	<MDL	<MDL
PFDS	<MDL	<MDL	<MDL	<MDL	<MDL	<MDL	<MDL	<MDL	<MDL
4:2 FTSA	<MDL	<MDL	<MDL	<MDL	<MDL	<MDL	<MDL	<MDL	<MDL
6:2 FTSA	<MDL	<MDL	<MDL	<MDL	<MDL	<MDL	0.022	<MDL	0.022

Subclass	Semiconductor plant A[4]	Semiconductor plant B	Semiconductor plant C[4]	Semiconductor plant D	Semiconductor plant E	WWTP 3 (A,B)	WWTP 4 (C,D)	WWTP 5 (E)	ΣAll
8:2 FTSA	<MDL	<MDL	<MDL	<MDL	<MDL	<MDL	<MDL	<MDL	<MDL
9Cl-PF3ONS	<MDL	<MDL	<MDL	<MDL	<MDL	<MDL	<MDL	<MDL	<MDL
FOSA	<MDL	<MDL	<MDL	<MDL	<MDL	<MDL	<MDL	<MDL	<MDL
MeFOSAA	<MDL	<MDL	<MDL	<MDL	<MDL	<MDL	<MDL	<MDL	<MDL
EtFOSAA	<MDL	<MDL	<MDL	<MDL	<MDL	<MDL	<MDL	<MDL	<MDL
ΣAll	**2.68**	**4.44**	**6.00**	**11.8**	**1.15**	**3.18**	**4.49**	**0.911**	**34.7**

[1] n.d : no peak was observed.

[2] <LOQ=Concentration was less than the limit of quantification.

[3] <MDL=Concentration was less than the method detection limit.

[4] The concentration calculation procedure for plant A and plant C with multiple sewage sources is outlined in Table 3.

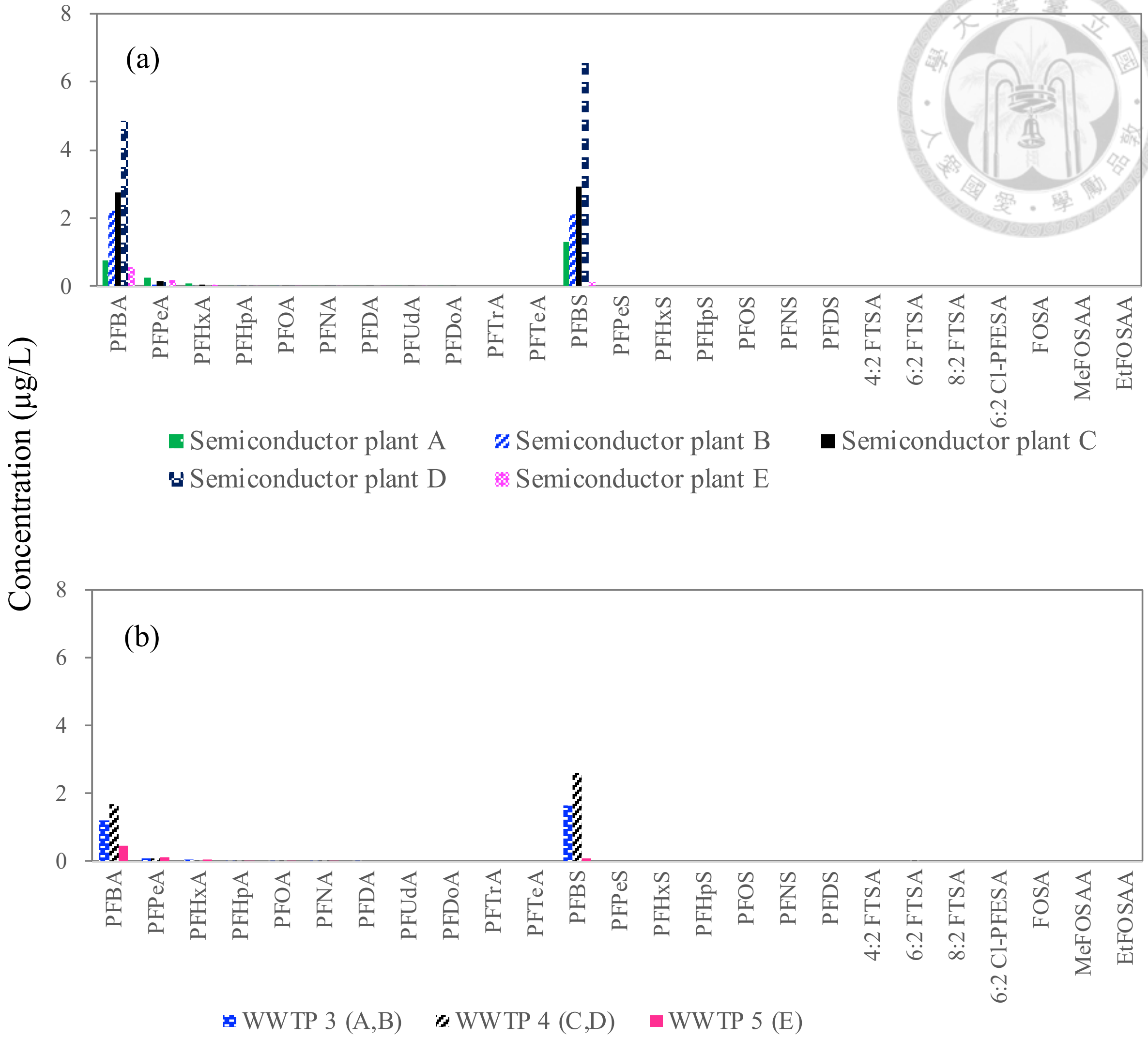

Figure 12. Concentrations of 25 target PFAS in (a) sewage from semiconductor plants A-E and (b) effluents from WWTP 3-5.

doi:10.6342/NTU202402180

4.1.3 QA/QC of Target Analysis

Direct injection analysis serves as a tool for quickly assessing the PFAS distribution in wastewater. For the QA/QC measurement, **Table 19** displays recoveries for QC samples and spiked samples (45% to 132%) and RPD between duplicate samples (0.0% to 24.3%). Specifically, the ranges of recoveries for the spiked samples analyzed were 45-132% for PFCAs, 59-112% for PFSAs, 88-121% for n:2 FTSAs, 78-81% for 6:2 Cl-PFESA, 110-123% for FOSA, and 99-128% for N-alkyl FOSAAs. Regarding the verification of centrifugation-induced losses in hydrophobic PFAS, sewage and effluent samples from the same sampling points were recollected in August 2023 to verify the impact of centrifugation pretreatment for target analysis. The result showed that centrifugation before adding internal standards in the pretreatment process minimally impacted short-chain PFAS but led to significant loss for long-chain PFAS, particularly over 90% loss of M2PFTeDA (**Table 20**). While most detected PFAS are short-chain and minimally affected, it is crucial to consider potential loss in long-chain PFAS during pretreatment.

doi:10.6342/NTU202402180

Table 19 Accuracy and precision of QC samples for 25 target PFAS on the LC–QqQ

Acronym	Recovery (%) of QC sample		Recovery (%) of matrix spike sample		RPD[1] of duplicate sample (%)	
	QC1	QC2	No. 190	No. 191	No.194	WWTP3
PFBA	93.0	82.2	69.2	72.3	0.0	10.3
PFPeA	100.4	97.2	106.7	116.8	1.2	8.7
PFHxA	98.6	91.0	99.4	110.6	4.5	15.4
PFHpA	98.1	89.9	85.1	100.7	7.0	15.3
PFOA	106.1	94.2	91.2	106.0	3.2	14.1
PFNA	93.3	92.1	98.4	113.7	7.4	6.7
PFDA	104.5	90.1	83.6	93.9	15.0	5.8
PFUdA	100.2	99.1	108.8	132.0	7.0	--
PFDoA	113.2	95.6	96.3	129.5	7.2	--
PFTrDA	117.5	112.1	41.1	44.7	--	--
PFTeDA	96.8	92.8	88.2	123.6	--	--
PFBS	96.0	90.6	61.3	111.9	5.8	24.3
PFPeS	92.0	86.7	74.2	88.4	--	--
PFHxS	103.0	96.6	99.6	96.5	--	--
PFHpS	96.0	87.1	105.4	86.4	--	--
PFOS	101.8	91.6	101.2	105.9	--	--
PFNS	112.6	109.7	68.3	66.1	--	--
PFDS	101.7	89.5	58.5	82.0	--	--
4:2 FTSA	96.2	89.6	87.7	90.1	--	--
6:2 FTSA	107.6	94.6	102.8	109.9	--	--
8:2 FTSA	112.4	97.7	102.5	121.1	--	--
6:2 Cl-PFESA (9Cl-PF3ON)	91.5	85.3	81.0	78.3	--	--
FOSA	110.6	93.8	109.8	123.2	--	--
MeFOSAA	102.6	96.1	98.7	119.7	--	--
EtFOSAA	111.8	105.3	109.0	128.1	--	--

[1] RPD: relative percent difference; RPD = absolute value (primary sample measurement - duplicate sample measurement)/[(primary sample measurement + duplicate sample measurement) / 2)] × 100%

doi:10.6342/NTU202402180

Table 20 Verification of centrifugation-induced losses in hydrophobic PFAS on the LC–QqQ

Internal standard	Recovery (%)[1] (n=11)[2]	
	Average	SD
M4PFBA	94.4	10.6
M5PFPeA	105.5	12.9
M5PFHxA	102.2	12.8
M4PFHpA	98.9	10.8
M8PFOA	94.9	7.8
M9PFNA	81.0	6.1
M6PFDA	51.8	9.0
M7PFUdA	26.8	9.7
MPFDoA	10.4	5.0
M2PFTeDA	7.8	4.3
M3PFBS	99.7	10.5
M3PFHxS	93.2	6.6
M8PFOS	60.5	6.3
M2-4:2FTSA	81.2	21.2
M2-6:2FTSA	78.6	9.1
M2-8:2FTSA	45.0	13.4
M8FOSA	53.4	8.2
d_3-N-MeOFSAA	40.0	13.7
d_5-N-EtOFSAA	20.1	8.7

[1] Recovery = [area of IS where IS were added before centrifugation/area of IS where IS were added after centrifugation] *100%; Average = mean of recovery; SD = standard deviation of recovery.

[2] Eight sewage samples and three effluent samples were fortified with internal standards (ISs) both before and after centrifugation. The concentration of ISs in the samples was 5 ng/L.

4.2. Nontarget analysis

4.2.1. Novel approach

Screening functional polar heads is essential for identifying non-targeted PFAS that lack obvious fluorocarbon fragments and for discovering the various reaction products formed in the polar functional groups during semiconductor manufacturing. Identifying non-target substances can be complex and time-consuming. To simplify the process, we have streamlined our approach by summarizing the identified surfactant PFAS search through the screening of polar functional groups based on fragments and neutral loss for the 12 classes with distinct polar functional groups. This summary, as presented in **Table 21**, serves as a valuable reference for the non-target analysis of PFAS. For a detailed overview of fragments and neutral loss features, **Table 22** presents information on sulfonamido substances, while **Table 23** focuses on fluoroalkyl acids.

By searching for $[NSO_2]^-$ fragment searching and excluding substances lacking fluorine based on isotopic formulas, we identified the predominant perfluoroalkane sulfonamides (FASAs) and various FASA series chemicals, resulting in the detection of 9 subclasses (1a-1i) in **Table 24**. Notably, in the presence of substances with N-alkyl substitutions, SO_2^- (63.9625) and SO_2H^- (64.9697) became dominant fragments and the weak fragment SO_2F^- (82.9603) was observed. N-Methyl perfluorobutane sulfonamide

doi:10.6342/NTU202402180

(MeFBSA) was identified in the effluents of WWTP. To the best of our knowledge, 9 identified FASAs (including 2 E-FBSA isomers) of these subclasses have been reported for the first time, as shown in **Table 24**.

doi:10.6342/NTU202402180

Table 21 Summary of fragment and neutral loss (NL) screening from the fluorinated tail and polar head, respectively, in the study. Normal font subclasses recognized from both tail and head, bold subclasses only from headgroup, italicized subclass from tail.

By tail / By head	$[C_nF_{2n+1}]^-$	$[C_nF_{2n+1}O]^-$	$[C_nF_{2n-1}]^-$	$[C_nF_{2n-1}O]^-$	$[C_nF_{2n-3}]^-$	HF[a]	No prior fragments or NL from fluorinated tail
$[SO_2N]^-$	FASAAs	E-FASA E-FASAA	H-FASAAs				**FASAs** **H-FASAs**
$[SO_2F]^-$	PFSAi N-Alkyl FASAAs						
$[SO_3]^-$	FASEEs			H_2-E-PFSA	H_2-E-PFSA	H-PFSAs n:2 FTSA H_2-E-PFSA	**PFSAs**
$[HSO_2]^-$	N-Alkyl FASA FASEE mono-ol monoacid	E-FASE	U-FASE	E-H-FASE U-E-FASE			**FASE** **H-FASE** **Miscellaneous FASE** **FASAcAL** **FASAcAL hydrate/ hemiacetal**
$[SO_2NC_2H_4O]^-$	FASEE mono-ol monoacid	E-FASE	U-FASE	H-E-FASE U-E-FASE			**FASE** **H-FASE** **Miscellaneous FASE**
$[SO_2N(C_2H_4O)_2]^-$	FASEE						**H-FASEE**

By tail By head	$[C_nF_{2n+1}]^-$	$[C_nF_{2n+1}O]^-$	$[C_nF_{2n-1}]^-$	$[C_nF_{2n-1}O]^-$	$[C_nF_{2n-3}]^-$ HF[a]	No prior fragments or NL from fluorinated tail
CO_2	PFCA U-E-PFCA PFdiCA		U-PFCA U-E-PFCA PFdiCA	U-E-PFCA	PFdiCA	
CO_2HF[a]	H-E-PFCA H_2-E-PFCA	H-E-PFCA	H-PFCA	H-E-PFCA		
$C_nH_{2n}CO_2$[a,b]	FASAA FASPrA N-Alkyl FASAA FASEE diacid FASEE mono-ol monoacid	E-FASAA	H-FASAA			
X=SO_3, CONH, etc [a]						**Miscellaneous FASAs** **Miscellaneous FASEs**
No prior fragments and NL from headgroup		*E-PFCA*				

a: neutral losses from MS2 spectra

b: the neutral loss from sulfonamido carboxylic acid is "$C_nH_{2n}CO$"$_2$, exemplified by sulfonamido acetic acid (CH_2CO_2 58.0055) and sulfonamido propanoic acid ($C_2H_4CO_2$ 72.02113).

Table 22 Proposed strategies of fragmentation and neutral loss of sulfonamides and sulfonamido substances identified in this study

Class	Hydrophilic group	Subclass	Fragment 1 (m/z)	Fragment 2 (m/z)	Neutral loss (m/z)
Sulfonamides	$SO_2N(X)H$	Per-and polyfluoroalkyl sulfonamides[1] (X=H) and miscellaneous FASAs (X=SO_3H, $CONH_2$, CH_2NO_2, etc.)	SO_2N^- (77.9644)		X-H
	$SO_2N(R')H$	N-Alkyl FASAs	SO_2H^- (64.9697)	SO_2F^- (82.9603)	
Sulfonamido ethanols	$SO_2N(X)CH_2CH_2OH$	Per- and polyfluoroalky sulfonamido ethanol (FASEs (X=H) and miscellaneous FASEs (X=SO_3H, $CONH_2$)	SO_2H^- (64.9697)	$SO_2NC_2H_4O^-$ (121.9912) $SO_2NCH_2^-$ (91.9806)	X-H
	$SO_2N(R')CH_2CH_2OH$	N-Alkyl FASEs	$CH_3CO_2^-$ (59.0139)		
Sulfonamido diethanols	$SO_2N(CH_2CH_2OH)_2$	N,N-bis(2-hydroxyethyl) per- and polyfluoroalkane sulfonamide (FASEE diol)	SO_3^- (79.9563)	$SO_2N(C_2H_4O)_2^-$ (166.0179) $SO_2N(C_2H_4)CH_2^-$ (136.00739) $SO_2NC_2H_4O^-$ (121.9912)	
Sulfonamido carboxylic acids	$SO_2N(H)C_nH_{2n}CO_2H$[2]	Per- and polyfluoroalkane[3] carboxylic acid (FASCAs)	SO_2N^- (77.9644)	SO_2F^- (82.9603)	$C_nH_{2n}CO_2$[2,3]
	$SO_2N(R')CH_2COOH$	N-Alkyl FASAAs	SO_2F^- (82.9603)		CH_2CO_2 (58.0055)

Class	Hydrophilic group	Subclass	Fragment 1 (m/z)	Fragment 2 (m/z)	Neutral loss (m/z)
Sulfonamido diacetic acids	$SO_2N(CH_2COOH)_1$	Per- and polyfluoroalkyl sulfonamido diacetic acid (FASEE diacid)	SO_2F^- (82.9603)		CH_2CO_2 (58.0055)
N-ethylhydroxyl sulfonamido acetic acids	$SO_2N(CH_2CH_2OH)$ CH_2COOH	N-(2-hydroxyethyl) perfluoroalkane sulfonamido acetic acid (FASEE mono-ol monoacid)	SO_2F^- (82.9603) SO_2H^- (64.9697)	$SO_2NC_2H_4O^-$ (121.9912) $SO_2NCH_2^-$ (91.9806)	CH_2CO_2 (58.0055)
Sulfonamido acetaldehyde	SO_2NHCH_2COH	Per- and polyfluoroalkyl sulfonamido acetaldehyde (FASAceAL)	SO_2H^- (64.9697)	SO_2^- (63.96245)	
Sulfonamido acetaldehyde hydrate/hemiacetal	$SO_2NHCH_2CH(OH)(OX)$ ($X=H$ (hydrate); $X=CH_3$ (hemiacetal))	Per- and polyfluoroalkyl sulfonamido acetaldehyde (FASAceAL hyrate/ hemiacetal)	SO_2H^- (64.9697)	SO_2^- (63.96245)	H_2O (18.0106) MeOH (32.0262)

1: The neutral loss of sulfonamido carboxylic acid is $C_nH_{2n}CO_2$, exemplified by sulfonamido acetic acid (58.0055) and sulfonamido propanoic acid (72.02113).

Table 23 Proposed strategies of fragmentation and neutral loss of per- and polyfluoroalkyl acids (PFAAs) identified in this study

Class	Hydrophilic group	Subclass	Fragment 1 (m/z)	Fragment 2 (m/z)	Neutral loss (m/z)
Carboxylic acids	-COOH	Perfluoroalkyl carboxylic acids (PFCAs); Unsaturated PFCAs (U-PFCAs); Unsaturated perfluoroalkyl ether carboxylic acids (U-E-PFCAs)			CO_2 (43.9893)
		Hydro substituted PFCAs (H-PFCAs);			CO_2HF (63.9961)
		Hydro substituted E-PFCAs (H_n-E-PFCAs)			CO_2 (43.9893)
		Perfluoroalkyl ether carboxylic acids (E-PFCAs)			Not detected
Dicarboxylic acid	$-(COOH)_2$	Perfluoroalkyl dicarboxylic acids (PFdiCAs)			CO_2 (43.9893)
Sulfonic acid	$-SO_3H$	Perfluoroalkane sulfonic acids (PFSAs)	SO_3^- (79.9563)	SO_3F^- (98.9547)	
		Hydro substituted PFSAs (H-PFSAs)	SO_3^- (79.9563)		HF (20.0062)
		Hydro substituted and ether PFSAs (H_n-E-PFSAs)	SO_3H^- (80.96519)	SO_3^- (79.9563)	HF (20.0062)
Sulfinic acid	$-SO_2H$	Perfluoroalkyl sulfinic acid	SO_2F^- (82.9603)		

doi:10.6342/NTU202402180

The Compound Class Scoring node (MS2) identified precursor ions with hydrophilic fragments $[SO_2NC_2H_4O]^-$ (121.9917) and $[SO_2NCH_2]^-$ (91.9812)[53] for FASE subclasses with sulfonamido ethanol segments, as shown in **Figure 13**(**a**). Additionally, fluoroalkyl fragments from the hydrophobic tail were used to identify fluorocarbon surfactants. By conducting $[SO_2NC_2H_4O]^-$ and $[SO_2NCH_2]^-$ fragment searching and subsequently excluding substances lacking fluorine based on isotopic formulas, we identified the predominant perfluoroalkane sulfonamido ethanol (FASEs) and miscellaneous FASE series, resulting in the detection of 8 subclasses (2a-2h). To the best of our knowledge, 9 identified structure of FASEs of these subclasses have been reported for the first time, as shown in Table 24. It is noted that the fluoroalkyl fragment as $C_4F_9^-$ was not obvious in the MS2 spectrum of FBSE; thus, identification via the specific fragment of $O_2SNC_2H_4O^-$ rather than fluoroalkyl fragment is highly feasible. Using this approach, class 3 with segment of sulfonamido diethanols and class 6 with N-(2-hydroxyethyl) sulfonamido acetic acid were identified as well.

The Searching Neutral Losses node (MS2) was used for identification of the precursor ion with the neutral loss of 58.0055 for the subclass of FASAAs for the subclass of FASAAs. Therefore, incorporating a neutral loss of CH_2CO_2 in the nontarget approach enables effective identification of substances with sulfonamido acetic acids, indicating their characteristics during collision in the CAD cell. The neutral loss of CH_2CO_2 served as an indicator for identifying subclasses of PFAS with sulfonamido acetic acid segments are first presented in our study, as shown in **Figure 13**(**b**). Based on this approach, class 4 of sulfonamido carboxylic acids, class 5 of sulfonamido diacetic acids and class 6 of N-ethylhydroxyl sulfonamido acetic acids have been identified, and 5 of 9 PFAS belonging these classes with CH_2CO_2 have been first recognized.

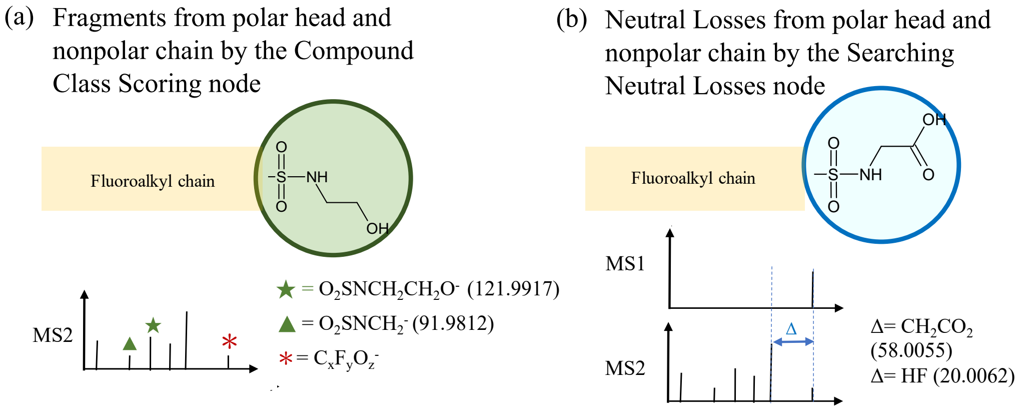

Figure 13 Identification workflow for nontarget analysis based on the hydrophilic functionality and hydrophobic fluoroalkyl chain of surfactant PFAS were conducted by the (a) Compound Class Scoring node (MS2) and the (b)Searching Neutral Losses node (MS2), respectively.

For miscellaneous FASAs and FASEs (subclass 1d-1i and subclass 2g-2h of **Table 24**), the prominent signals at 297.9590, representing $[C_4F_9SO_2N]^-$, and 341.9852, representing $[C_4F_9SO_2NC_2H_4OH]^-$, suggest that these ions likely retain the original structures of FBSA and FBSE during fragmentation. Hence, the neutral loss between $[M\text{-}H]^-$ and their associated fragment ($[C_4F_9SO_2NH]^-$ for FBSA and $[C_4F_9SO_2NC_2H_4OH]^-$ for FBSE), would be practical to identify these series of headgroups, despite potential variations at the fluorinated tail end. This approach uniquely emphasizes the neutral loss of segments such as SO_3, CONH, CH_3OH, and H_2O for miscellaneous FASAs and FASEs, underscoring its novelty in identifying reaction products reported for the first time. The initial proposed structure belonging to miscellaneous FASAs and miscellaneous are provided in **Figure 14**. In addition, our study leads the way in developing neutral loss screens for CO_2, $HFCO_2$, $C_nH_{2n}CO_2$, etc., serving as indicators to distinguish classes such as carboxylic acid, dicarboxylic acid, and sulfonamido carboxylic acid, each characterized by terminal carboxylate structures.

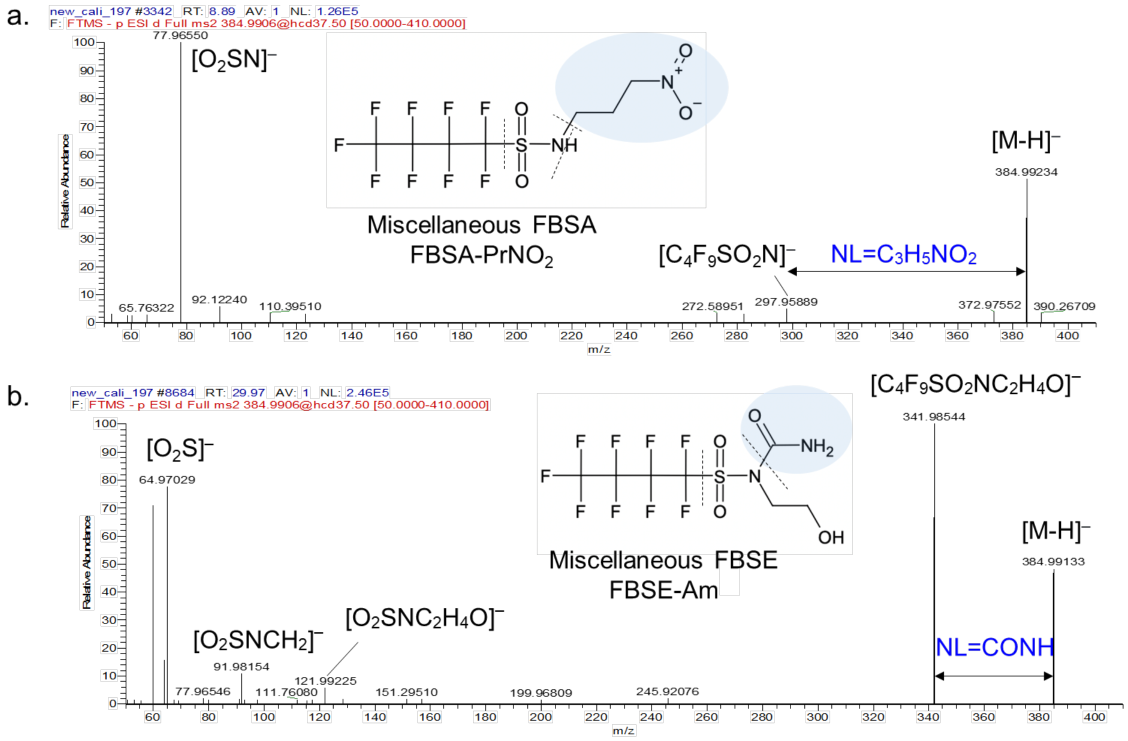

Figure 14 FBSA-$PrNO_2$ and FBSE-Am are polar-head isomers, presenting the subclass of sulfonamide and sulfonamido ethanol respectively

4.2.2. Terminology

Table 24 summarizes 83 identified PFAS from 12 subclasses of 3 classes with their identified CLs, 30 of which were first reported in sewage from industry and effluents from the associated WWTPs. The predominant identified PFAS compounds were perfluorobutane sulfonamido substances, perfluorobutane sulfonamide and ultrashort and short-chain PFAAs. Through the matching of RTs and MS2 fragments with the available authentic standards, the 21 identified PFAS were categorized as CL1a/CL1b, denoted as 'CL1-identified PFAS'. (**Figure 15**) The other 62 compounds without the acquisition of authentic standards for further confirmation were categorized as CL2b to CL3c, denoted as 'tentatively identified PFAS'. Notably, although FBSE and FBSA were confirmed with the standards, the CL remained 1b due to insufficient data for isomer-specific assignment. The following is a discussion of the identified results for the 12 classes with distinct polar functional groups.

doi:10.6342/NTU202402180

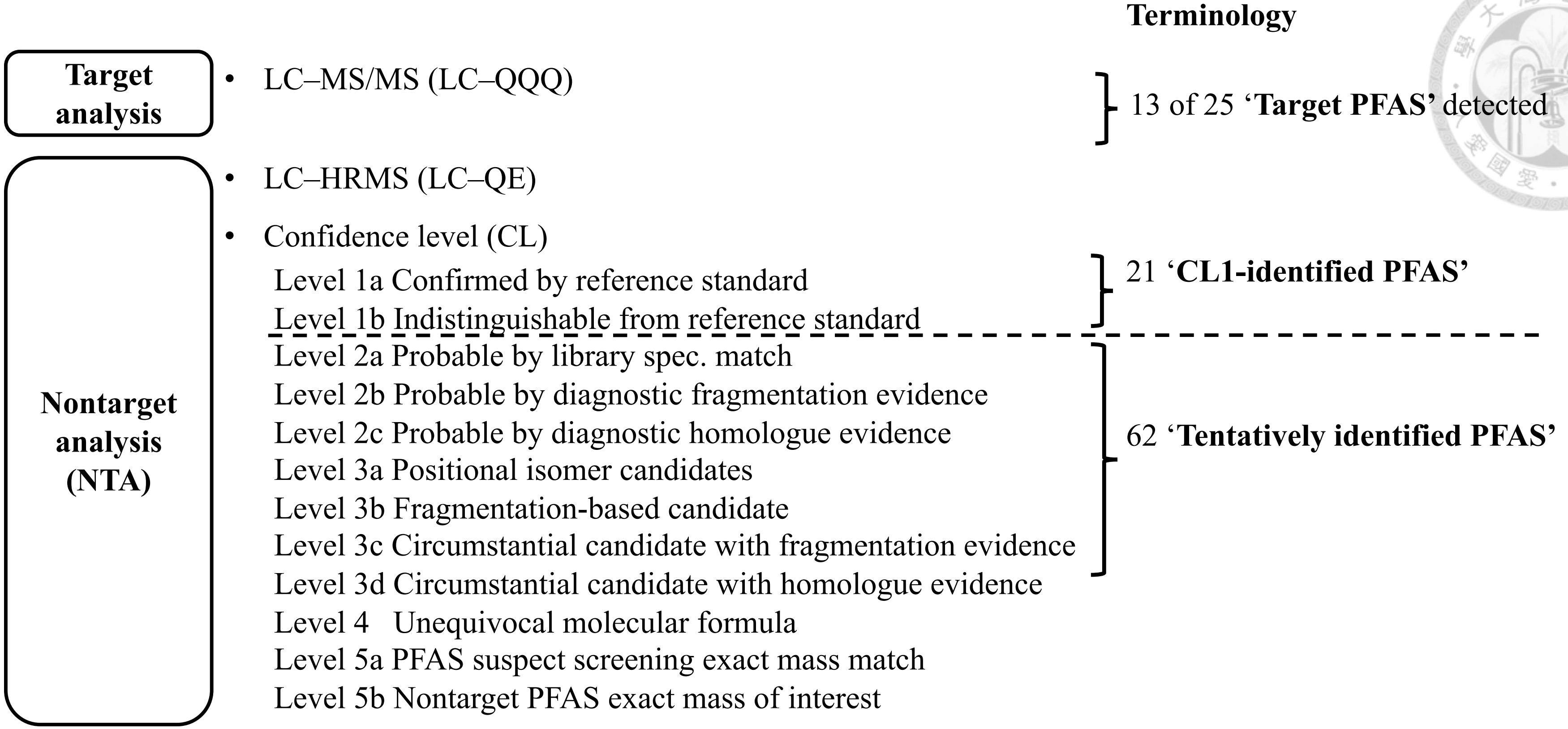

Figure 15 Target analysis and nontarget analysis categorized by the CLs scope[56] for proposed structure

Table 24 Identified PFAS categorized by polar head class, subclass, compound number theoretical precursor ion, retention time (RT), confidence level (CL), and first report.

Class	Subclass		Aberration	Number [a]	RT (min)	Theoretical precursor ion $[M-H]^-$	CL	Q/SQ/NQ/QQ [d]	First report [f]
Sulfonamides $–SO_2NH_2$	1a	Perfluoroalkane sulfonamides (FASAs)	FBSA	1a-1	21.97	297.95897	1a	Q	
	1b	Hydro-substituted perfluoroalkyl sulfonamides (H-FASAs)	H-FBSA	1b-1	10.69	279.96840	3a	NQ	V
	1c	Perfluoroalkyl ether sulfonamides (E-FASAs)	E-FBSA(1)	1c-1	25.91	313.95389 [b]	2b	NQ	V
			E-FBSA(2)	1c-2	27.37	313.95389 [b]	2b	NQ	V
Miscellaneous sulfonamides $–SO_2N(X)H$	1d	X:SO_3H	FBSA-SO_3H	1d-1	3.58	377.91579	2b	NQ	V
	1e	X:$CONH_2$	FBSA-Am	1e-1	8.72	340.96479	2b	NQ	V
	1f	X:CH_2CONH_2	FBSA-MeAm	1f-1	10.72	354.98044	3a	NQ	V
	1g	X:CH_2NO_2	FBSA-$MeNO_2$	1g-1	7.28	356.95970	3a	NQ	V
	1h	X:$C_3H_6NO_2$	FBSA-$PrNO_2$	1h-1	8.81	384.99100 [c]	3a	NQ	V
	1i	X:CH_2N_2H	FBSA-diazene	1i-1	22.28	339.98077	3a	NQ	V
N-alkyl sulfonamides $–SO_2N(R')H$	1j	N-methyl perfluoroalkane sulfonamides (MeFASAs) R=CH_3	MeFBSA	1j-1	36.77	311.97462	1a	SQ	
Sulfonamido ethanols $–SO_2N(H)CH_2CH_2OH$	2a	Perfluoroalkane sulfonamido ethanols (FASEs)	FEtSE	2a-1	9.46	241.99158	2b	SQ	
			FPrSE	2a-2	18.47	291.98838	2b	SQ	
			FBSE	2a-3	30.00	341.98519	1b	Q	
	2b	Hydro substituted perfluoroalkane sulfonamido ethanols (H-FASEs)	H-FBSE(1)	2b-1	15.84	323.99461 [b]	3a	NQ	V
			H-FBSE(2)	2b-2	19.05	323.99461 [b]	3a	NQ	V
	2c	Perfluoroalkyl ether sulfonamido ethanols (E-FASEs)	E-FBSE(1)	2c-1	33.94	357.98010 [b]	2b	NQ	V
			E-FBSE(2)	2c-2	34.28	357.98010 [b]	2b	NQ	V
			E-FBSE(3)	2c-3	35.10	357.98010 [b]	2b	NQ	V
	2d	Hydrogen substituted perfluoroalkyl ether sulfonamido ethanols (E-H-FASEs)	H-E-FBSE	2d-1	21.41	339.98952	3a	NQ	V
	2e	Unsaturated perfluoroalkane sulfonamido ethanols (U-FASEs)	U-FBSE	2e-1	16.76	303.98838	3a	NQ	V
	2f	unsaturated perfluoroalkyl ether sulfonamido ethanols (U-E-FASEs)	U-E-FBSE	2f-1	23.78	319.98330	3a	NQ	V
Miscellaneous sulfonamido ethanols $–SO_2N(X)CH_2CH_2OH$	2g	X:SO_3H	FBSE-SO_3H	2g-1	17.79	421.94200	2b	NQ	V
	2h	X:$CONH_2$	FBSE-Am	2h-1	29.97	384.99100 [c]	2b	NQ	V
N-alkyl sulfonamido ethanols $–SO_2N(R')CH_2CH_2OH$	2i	N-methyl perfluoroalkane sulfonamido ethanols (MeFASEs) R=CH_3	MeFBSE	2i-1	35.21	416.02197 [e]	3a	NQ	
Sulfonamido diethanols $–SO_2N(CH_2$	3a	N,N-bis(2-hydroxyethyl) perfluoroalkane sulfonamides (FASEE	FBSEE (diol)	3a-1	31.52	446.03253 [e]	1a	Q	

Class	Subclass		Aberration	Number[a]	RT (min)	Theoretical precursor ion $[M-H]^-$	CL	Q/SQ/NQ/QQQ[d]	First report[f]
$CH_2OH)_2$		diols)							
	3b	Hydro-substituted FASEE diol (H-FASEE diols)	H-FBSEE	3b-1	16.96	428.04195 ^{e}	2b	NQ	V
Sulfonamido carboxylic acids $-SO_2NH(CH_2)_n COOH$	4a	perfluoroalkane sulfonamido acetic acids (FASAAs)	FBSAA	4a-1	15.50	355.96445 ^{c}	1b	SQ	
			Headgroup isomer of FBSAA	4a-2	9.93	355.96445 ^{c}	3a	NQ	V
	4b	Hydro-substituted FASAAs (H-FASAAs)	H-FBSAA	4b-1	7.29	337.97387	3a	NQ	V
	4c	Perfluoroalky ether sulfonamido acetic acids (E-FASAAs)	E-FBSAA(1)	4c-1	18.73	371.95937 ^{b}	3a	NQ	V
			E-FBSAA(2)	4c-2	19.73	371.95937 ^{b}	3a	NQ	V
	4d	N-methyl FASAAs (N-MeFASAAs)	MeFBSAA	4d-1	20.38	369.98120 ^{c}	1a	SQ	
	4e	Perfluoroalkane sulfonamido propanoic acids (FASPrAs)	FBSPrA	4e-1	19.06	369.98120 ^{c}	2b	NQ	V
Sulfonamido diacetic acids $-SO_2N(CH_2COOH)_2$	5a	perfluoroalkane sulfonamido diacetic acids (FASEE diacids)	FBSEE diacid	5a-1	5.83	413.96993	2b	SQ	
N-ethylhydroxyl sulfonamido acetic acids $-SO_2N(CH_2CH_2OH)(CH_2COOH)$	6a	N-(2-hydroxyethyl) perfluoroalkane sulfonamido acetic acids (FASEE mono-ol monoacid)	FBSEE mono-ol monoacid	6a-1	17.10	399.99067	2b	SQ	V
Sulfonamido acetaldehyde $-SO_2N(H)CH_2COH$	7	Perfluoroalkane sulfonamido acetaldehyde (FASALs, keto and enol form)	FBSAcAL(1)	7a-1	13.03	339.96954 ^{c}	3a	NQ	V
			FBSAcAL(2)	7a-2	30.03	339.96954 ^{c}	3a	NQ	V
Sulfonamido acealdehyde hydrate/hemiacetal $-SO_2N(H)CH_2C(OH)(OR)H$	8a	Perfluoroalkane sulfonamido acetaldehyde hydrate (R=H)	FBSAcAL hydrate	8a-1	30.01-32.63	357.98010	2b	NQ	V
	8b	Perfluoroalkane sulfonamido acetaldehyde hemiacetal (R=CH_3)	FBSAcAL hemiacetal	8b-1	33.16	371.99575	2b	NQ	V
Carboxylic acid $-COOH$	9a	Perfluoroalkyl carboxylic acids (PFCAs)	TFA	9a-1	1.38	112.98559	1a	Q	
			PFPrA	9a-2	2.65	162.98239	1a	Q	
			PFBA	9a-3	4.43	212.97920	1a	QQQ	
			PFPeA	9a-4	8.15	262.97600	1a	QQQ	
			PFHxA	9a-5	15.87	312.97281	1a	QQQ	
			PFHpA	9a-6	25.52	362.96962	1a	QQQ	
			PFOA	9a-7	35.28	412.96642	1a	QQQ	
			PFNA	9a-8	45.98	462.96323	1a	QQQ	
			PFDA	9a-9	54.82	512.96003	1a	QQQ	
U-E-PFPeA(1) U-E-PFPeA(2)			PFUdA	9a-10	63.08	562.95684	1a	QQQ	
	9b	Unsaturated PFCAs (U-PFCAs)	U-PFHxA	9b-1	10.53	274.97600	3a	NQ	
U-E-PFHxA(1)	9c	Unsaturated-E-PFCAs (U-E-PFCAs)	U-E-PFBA	9c-1	3.20	190.97731	3a	NQ	
			U-E-PFPeA(1)	9c-2	3.29	240.97411 ^{b}	3a	NQ	

Class	Subclass		Aberration	Number[a]	RT (min)	Theoretical precursor ion $[M-H]^-$	CL	Q/SQ/NQ/QQQ[d]	First report[f]
			U-E-PFPeA(2)	9c-3	6.36	240.97411 [b]	3a	NQ	
			U-E-PFHxA(1)	9c-4	3.66	290.97092 [b]	3a	NQ	
			U-E-PFHxA(2)	9c-5	5.80	290.97092 [b]	3a	NQ	
			U-E-PFHxA(3)	9c-6	11.07	290.97092 [b]	3a	NQ	
	9d	Hydro-substituted PFCAs (H-PFCAs)	H-PFBA	9d-1	3.23	194.98862	3a	NQ	
			H-PFPeA	9d-2	4.74	244.98543	3a	NQ	
			H-PFHxA	9d-3	9.35	294.98223	3a	NQ	
	9e	Hydro-substituted E-PFCAs (H-E-PFCAs)	H-E-PFPrA	9e-1	1.9	160.98673	3a	NQ	
			H-E-PFBA(1)	9e-2	3.13	210.98353 [b]	3a	NQ	
			H-E-PFBA(2)	9e-3	3.77	210.98353 [b]	3a	NQ	
			H-E-PFBA(3)	9e-4	9.83	210.98353 [b]	3a	NQ	
		Multihydro-substituted E-PFCAs (H_n-E-PFCAs)	H_2-E-PFBA	9e-5	1.77	192.99296	3a	NQ	
	9f	Per- and polyfluoroalkyl ether carboxylic acids (E-PFCAs)	E- PFPrA	9f-1	3.36	178.97731	3a	NQ	
			E- PFBA	9f-2	5.82	228.97411	3a	NQ	
			E- PFPeA	9f-3	10.14	278.97092	3a	NQ	
Dicarboxylic acid $-(COOH)_2$	10a	Perfluoroalkyl dicarboxylic acids (PFdiCAs)	PFdiCA(C3)	10a-1	1.01	138.98484	3c	SQ	
			PFdiCA(C4)	10a-2	1.13	188.98164	2c	SQ	
			PFdiCA(C5)	10a-3	1.18	238.97845	2c	SQ	
			PFdiCA(C6)	10a-4	1.25	288.97525	2b	SQ	
			PFdiCA(C7)	10a-5	2.54	338.97206	3c	SQ	
			PFdiCA(C8)	10a-6	3.57	388.96887	2c	SQ	
Sulfonic acid $-SO_3H$	11a	Perfluoroalkane sulfonic acids (PFSAs)	TFMS	11a-1	1.77	148.95257	1a	Q	
			PFBS	11a-2	9.83	298.94299	1a	QQQ	
	11b	Hydro substituted PFSAs (H-PFSAs)	H-PFEtS	11b-1	1.91	180.95880	3a	NQ	
			H-PFPrS	11b-2	3.57	230.95560	3a	NQ	
			H-PFBS	11b-3	5.18	280.95241	3a	NQ	
	11c	Hydro substituted perfluoroalkyl ether sulfonic acids (H_n-E-PFSAs)	H_2-E-PFTS	11c-1	1.31	178.96313	3a	NQ	
			H_2-E-PFPrS	11c-2	2.57	228.95994	3a	NQ	
	11d	Fluorotelomer sulfonic acid	6:2FTSA	11d-1	33.95	426.96790	1a	QQQ	
Sulfinic acids $-SO_2H$	12a	Perfluoroalkyl sulfinic acids (PFSiA)	PFBSi	12a-1	11.39	282.94807	1a	Q	

a: Compound number is made up of the subclass and serial number. For each chemical structure, please refer to Appendix.

b: The presence of structural isomers varied in the fluorinated chain.

c: The presence of structural isomers varied in the polar functional head.

d: Q: Quantitation using a Q-Exactive mass spectrometry (QE) instrument.

SQ: Semi-quantitation with a QE instrument.

NQ: Qualification only; no quantitation.

QQQ: Quantitation using a triple quadrupole instrument, only qualification with QE.

e: The precursor ion was an acetate adduct $[M+CH_3COO]^-$

f: The structures of these compounds have been firstly identified in current study

Class I Perfluoroalkane sulfonamides

Subclass 1a-1c Per and polyfluoroalkane sulfonamides (FASAs) FASAs are distinguishable by their unique fragment $[NSO_2]^-$ 77.9655.[53] This distinctive characteristic serves as a unique identifier for subclass 1a-1c, and subsequently for subclass 1d-1i. Our study identified perfluorobutane sulfonamide (FBSA) of subclass 1a in sewage and effluent from semiconductor manufacturing (**Figure 16**). Even though the authentic standard confirmation included RT matching and MS2 spectrum matching (**Figure 17**), there is still insufficient data to differentiate between branched and linear isomers, so the confidence level (CL) remained at 1b (detailed criteria for CL were shown in Table). FBSA was detected at high concentrations of 1.71-141 μg/L in sewage from semiconductor plants A, B, C, and D and 33.0 to 40.3 μg/L in effluent from WWTP3 and WWTP4. FBSA was not detected in the sewage of semiconductor plant E or the effluent from WWTP5. FBSA has been patented as a photoresist quencher, an etching solution for silicon dioxide coatings and a cleaning solvent in the process of manufacturing semiconductor devices.[7,59,60] FBSA has been reported in Great Lakes fish from Canada with concentrations ranging from <0.01 to 8.73 ng/g w.w.,[61] surface water,[57] soil at firefighting training grounds,[53] and landfill leachate at a concentration of 530 ± 170 ng/L.[62] A 3M plant reportedly discharged FBSA into the Tennessee River of Alabama in 2019[63] and into the Schelde River of Belgium In 2021.[64] Bioaccumulation factors for FASAs were significantly higher, ranging from 10 to 1000 times greater than those observed for their terminal

doi:10.6342/NTU202402180

perfluoroalkyl sulfonates.[65] This is the first time that FBSA has been identified as being widely used in semiconductor manufacturing.

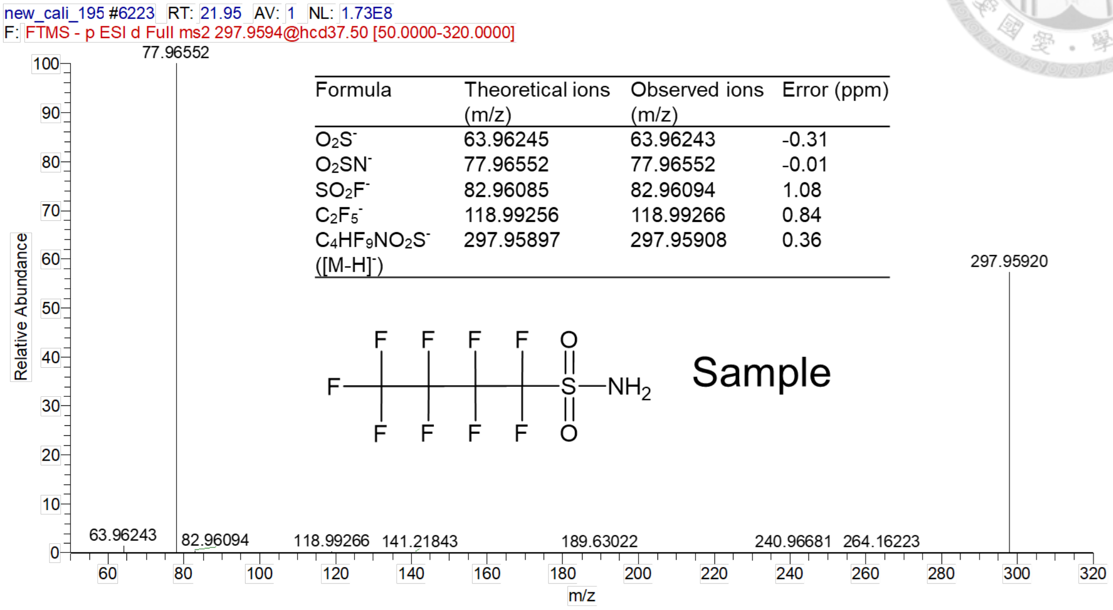

Formula	Theoretical ions (m/z)	Observed ions (m/z)	Error (ppm)
O_2S^-	63.96245	63.96243	-0.31
O_2SN^-	77.96552	77.96552	-0.01
SO_2F^-	82.96085	82.96094	1.08
$C_2F_5^-$	118.99256	118.99266	0.84
$C_4HF_9NO_2S^-$ ($[M-H]^-$)	297.95897	297.95908	0.36

Figure 16 MS2 spectrum of FBSA from sample no. 195

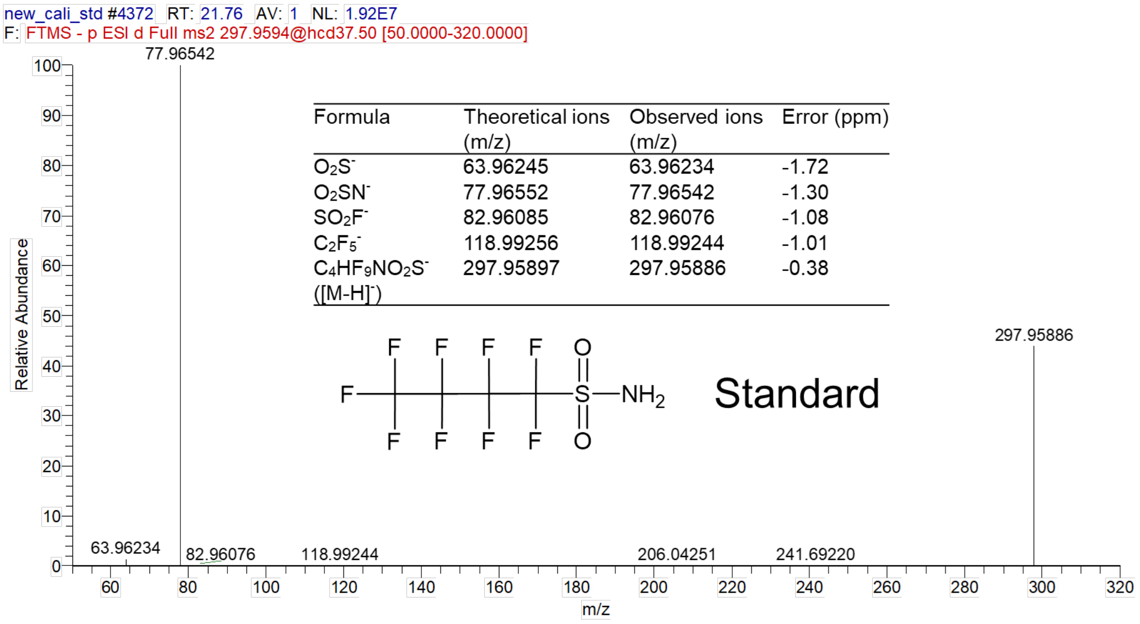

Formula	Theoretical ions (m/z)	Observed ions (m/z)	Error (ppm)
O_2S^-	63.96245	63.96234	-1.72
O_2SN^-	77.96552	77.96542	-1.30
SO_2F^-	82.96085	82.96076	-1.08
$C_2F_5^-$	118.99256	118.99244	-1.01
$C_4HF_9NO_2S^-$ ($[M-H]^-$)	297.95897	297.95886	-0.38

Figure 17 MS2 spectrum of FBSA from authentic standard

By searching for $[NSO_2]^-$ fragment searching and excluding substances lacking fluorine based on isotopic formulas, we further discovered hydro-substituted FBSA (H-FBSA), and ether FBSA (E-FBSA) in subclasses 1b and 1c. Notably, no obvious fluoroalkyl fragmentations $[C_xF_yO_z]^-$ were detected during screening, suggesting that $[NSO_2]^-$ is a feasible screening tool for identifying these subclasses. In **Figure 18**, the CL for H-FBSA remained at 3a, reflecting uncertainty about the position of the hydrogen. In our study, hydrogen-substituted FBSA, H-FBSA has been detected, however, no other multiple hydrogens substituted FBSA, such fluorotelomer sulfonamides, has been observed. Previous researchers have identified fluorotelomer sulfonamides in AFFF, characterized by the $[H_2NSO_2]^-$ fragment,[66, 67] distinguishing them from perfluoroalkane sulfonamides (FASAs) in our study, which exhibit the characteristic $[NSO_2]^-$ fragment. The introduction of the $[H_2NSO_2]^-$ fragment is attributed to the substantial presence of hydrogens in the fluorotelomer. Furthermore, E-FBSA, which has two isomers, was recognized by its specific ether fragments $[CF_3O]^-$(84.99067) and $[C_2F_5O]^-$(134.98748) with an isotope pattern matching of $C_4F_9H_2O_3SN$ (**Figure 19** and **20**) and the CL was set to 2b.

doi:10.6342/NTU202402180

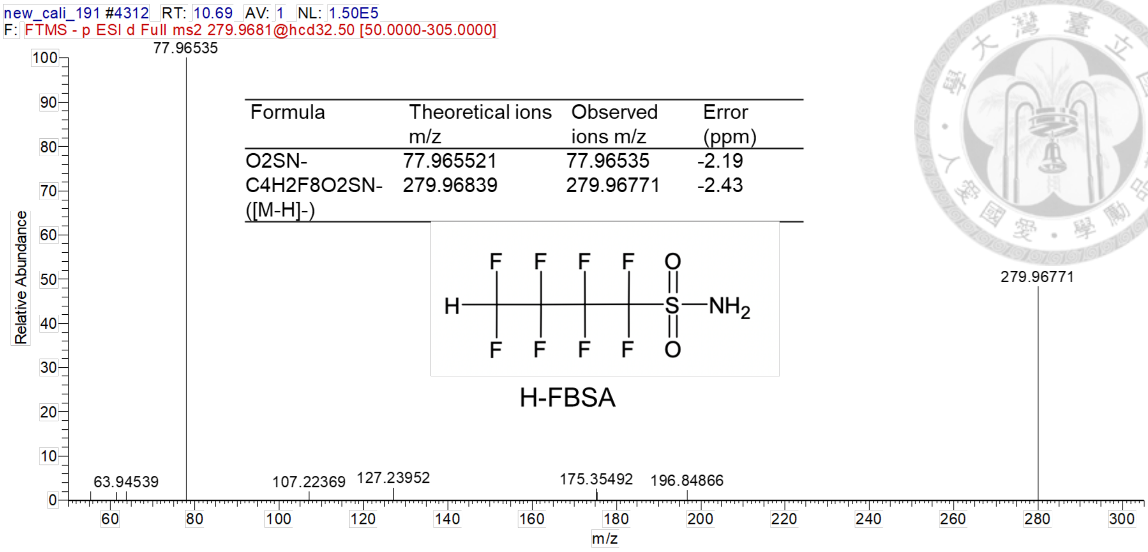

Formula	Theoretical ions m/z	Observed ions m/z	Error (ppm)
O2SN-	77.965521	77.96535	-2.19
C4H2F8O2SN- ([M-H]-)	279.96839	279.96771	-2.43

Figure 18 MS2 spectrum of H-FBSA.

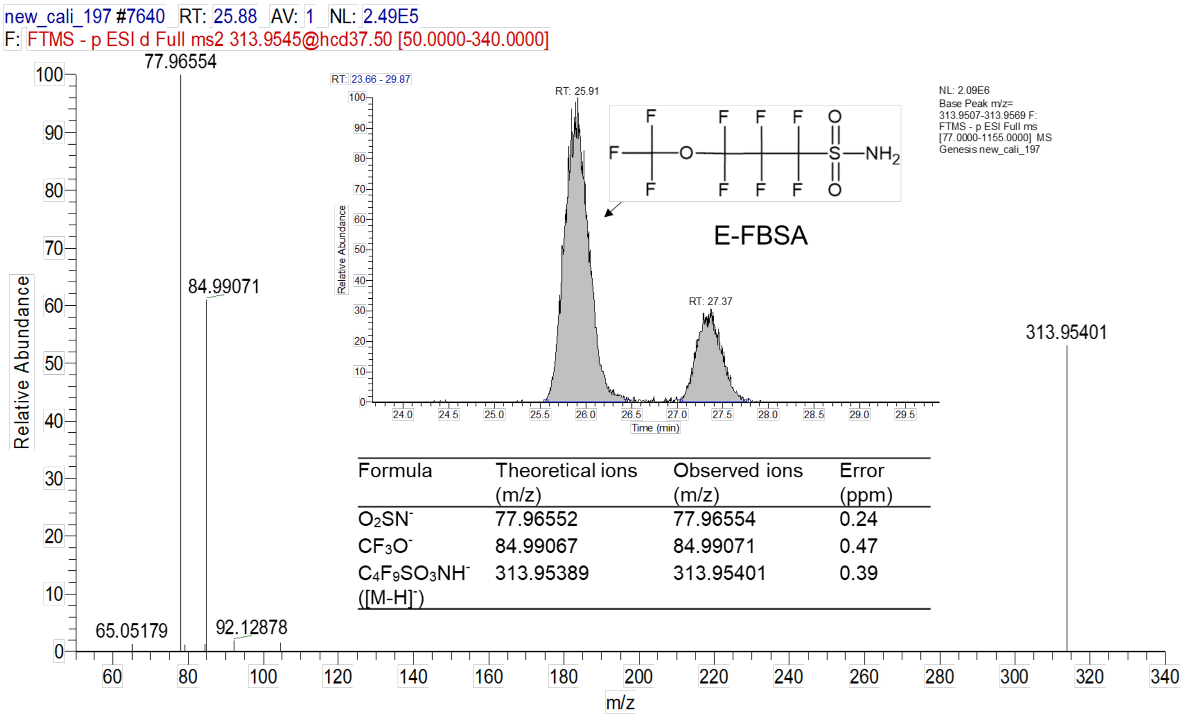

Formula	Theoretical ions (m/z)	Observed ions (m/z)	Error (ppm)
O_2SN^-	77.96552	77.96554	0.24
CF_3O^-	84.99067	84.99071	0.47
$C_4F_9SO_3NH^-$ ($[M-H]^-$)	313.95389	313.95401	0.39

Figure 19 MS2 spectrum of one of the structural isomers of E-FBSA(1). The unique fragmentation of CF_3O^- was identified and led to the proposal of the structures of isomers at confidence level 2b.

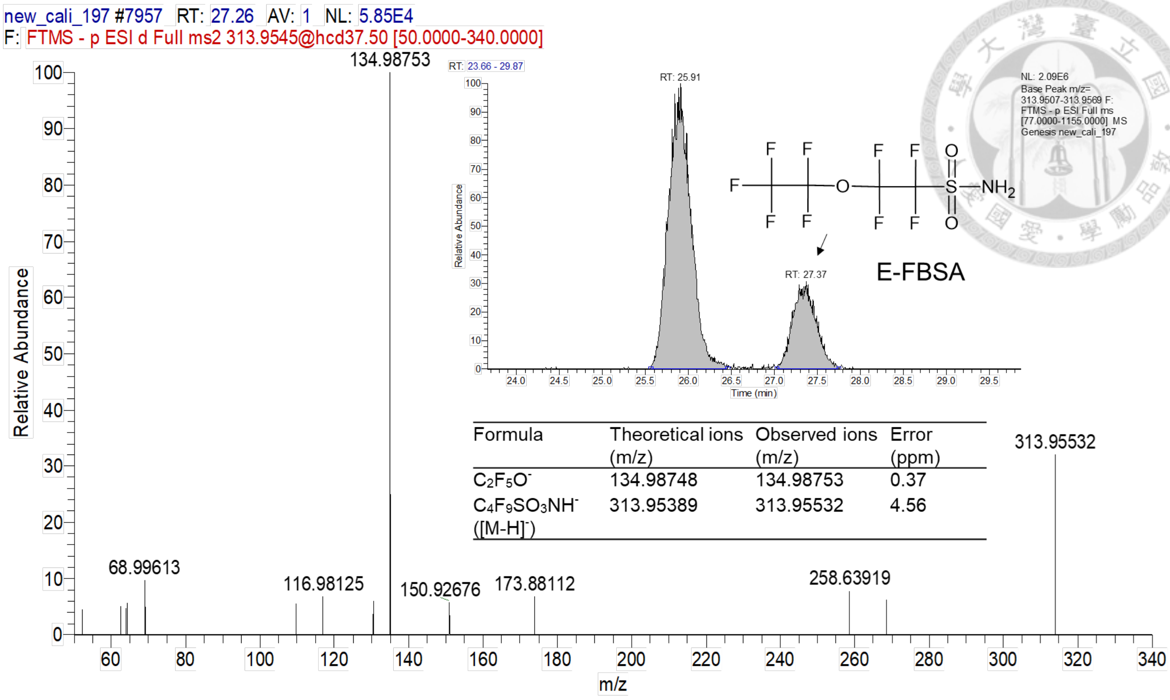

Formula	Theoretical ions (m/z)	Observed ions (m/z)	Error (ppm)
$C_2F_5O^-$	134.98748	134.98753	0.37
$C_4F_9SO_3NH^-$ ($[M-H]^-$)	313.95389	313.95532	4.56

Figure 20 MS2 spectrum of the structural isomer of E-FBSA(2). The unique fragmentation of $C_2F_5O^-$ was identified and led to the proposal of the structures of isomers at confidence level 2b. The greater RT (27.37 min) of E-FBSA was indicative of the increased symmetry of the alkyl structure, which matched the proposed structure.

Subclass 1d-1i Miscellaneous FASAs These 6 identified subclasses (1d-1i) each exhibit variations in the functional group as $-SO_2N(X)H$ with the structure $C_4F_9SO_2N(H)XH$ (X= SO_3; CONH; CH_2CONH; $CHNO_2$; $C_3H_5NO_2$; CH_2N_2 as subclass 1d-1i). Despite these versatile polar headgroups from miscellaneous FASAs, all these compounds contain the $[SO_2N]^-$ (77.9644) fragment. Furthermore, the miscellaneous FASAs were identified, with additional indications of these subclasses observed through neutral loss of X. For instance, subclass 1h showed a neutral loss of $C_3H_5NO_2$, as demonstrated in **Figure 21**. This introduces a new screening approach for miscellaneous FASAs from neutral loss of X and is reported for the first time.

doi:10.6342/NTU202402180

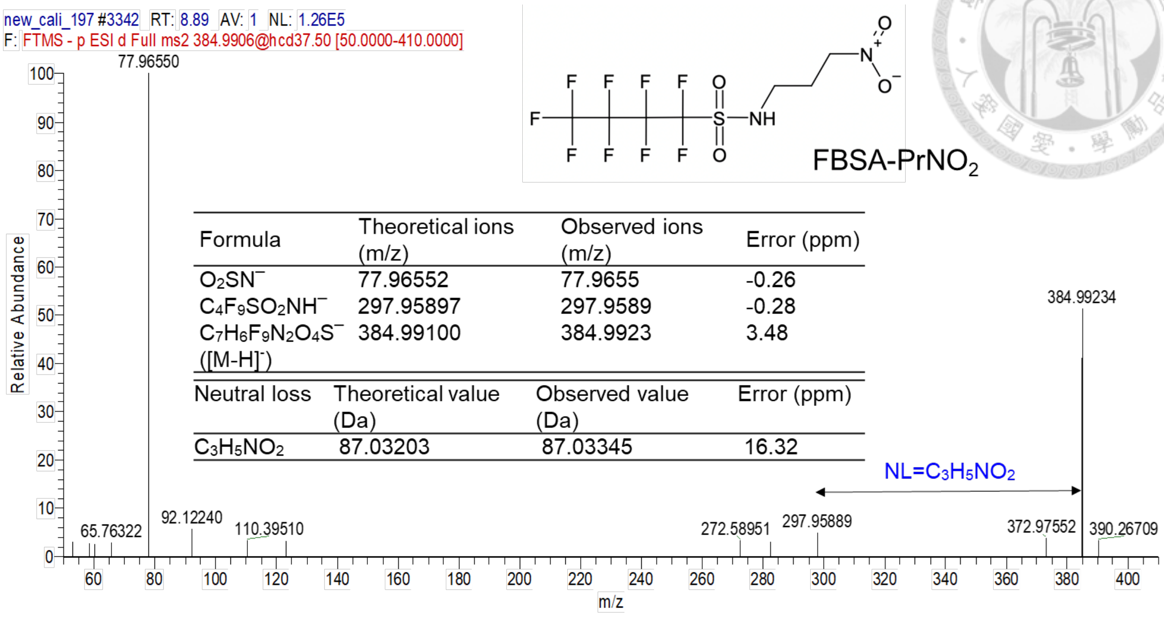

Formula	Theoretical ions (m/z)	Observed ions (m/z)	Error (ppm)
O_2SN^-	77.96552	77.9655	-0.26
$C_4F_9SO_2NH^-$	297.95897	297.9589	-0.28
$C_7H_6F_9N_2O_4S^-$ ([M-H]$^-$)	384.99100	384.9923	3.48

Neutral loss	Theoretical value (Da)	Observed value (Da)	Error (ppm)
$C_3H_5NO_2$	87.03203	87.03345	16.32

Figure 21 MS2 spectrum of the structural isomer of FBSA-PrNO$_2$. The unique fragment of SO_2N^- and neutral loss of $C_3H_5NO_2$ was identified and led to the proposal of the structures of isomers at confidence level 3a.

Subclass 1j N-alkyl perfluoroalkane sulfonamides (N-alkyl FASAs) In the presence of substances featuring N-alkyl substitutions of FASAs, the feature of $[SO_2N]^-$ from FASAs was no longer detected. The primary fragments shifted to $[SO_2]^-$ (63.9625) and $[SO_2H]^-$ (64.9697), with the additional observation of the weak fragment $[SO_2F]^-$ (82.9603). Fragments $[C_4F_9]^-$ and $[SO_2F]^-$ were detected in the MS2 spectrum (**Figure 22**) and further confirmed as MeFBSA through RT and MS2 spectrum matching (**Figure 23**), resulting in setting the CL to 1. MeFBSA has been detected in landfill leachate at a semiquantitation of 100 ng/L.[62] The 3M company in Belgium discharged MeFBSA into the Schelde River in 2021.[68] Although MeFBSA and N-ethyl FBSA (EtFBSA) have been patented as cleaning solutions in semiconductor

doi:10.6342/NTU202402180

manufacturing,[7,60] MeFBSA and EtFBSA were examined but not detected in all sewage. MeFBSA was slightly detected in the effluents of WWTP3 and WWTP4 at concentrations of 0.038 μg/L and 0.161 μg/L, respectively, as shown in **Table 27**.

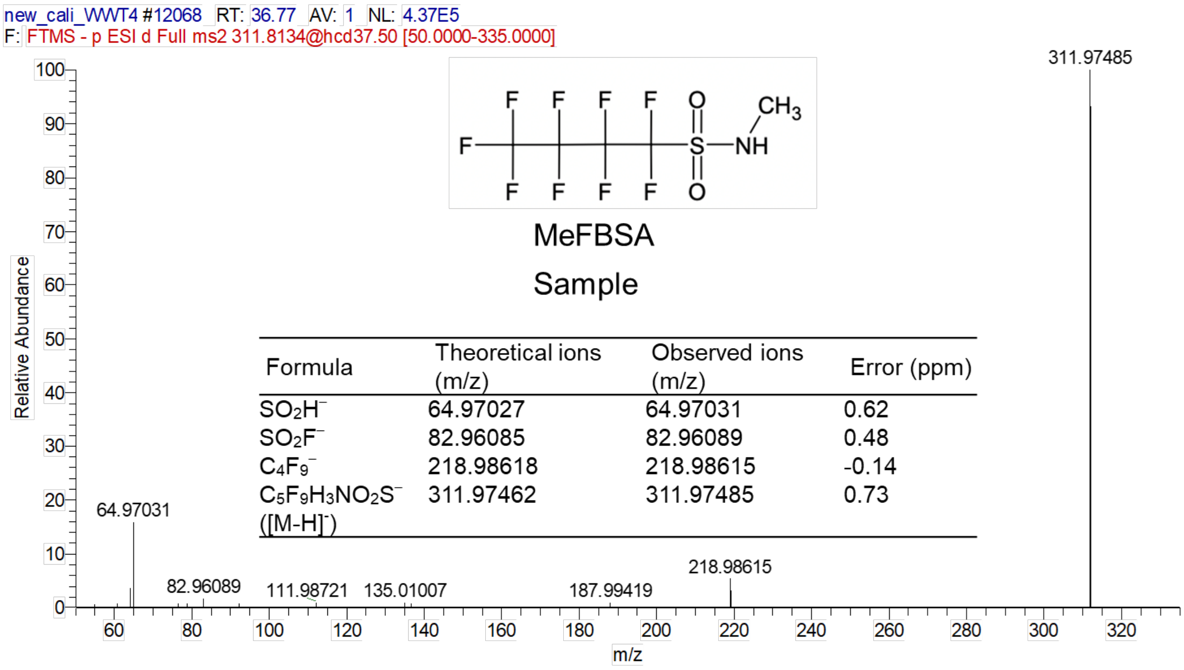

Formula	Theoretical ions (m/z)	Observed ions (m/z)	Error (ppm)
SO_2H^-	64.97027	64.97031	0.62
SO_2F^-	82.96085	82.96089	0.48
$C_4F_9^-$	218.98618	218.98615	-0.14
$C_5F_9H_3NO_2S^-$ ($[M-H]^-$)	311.97462	311.97485	0.73

Figure 22 MS2 spectrum of MeFBSA from sample WWTP4

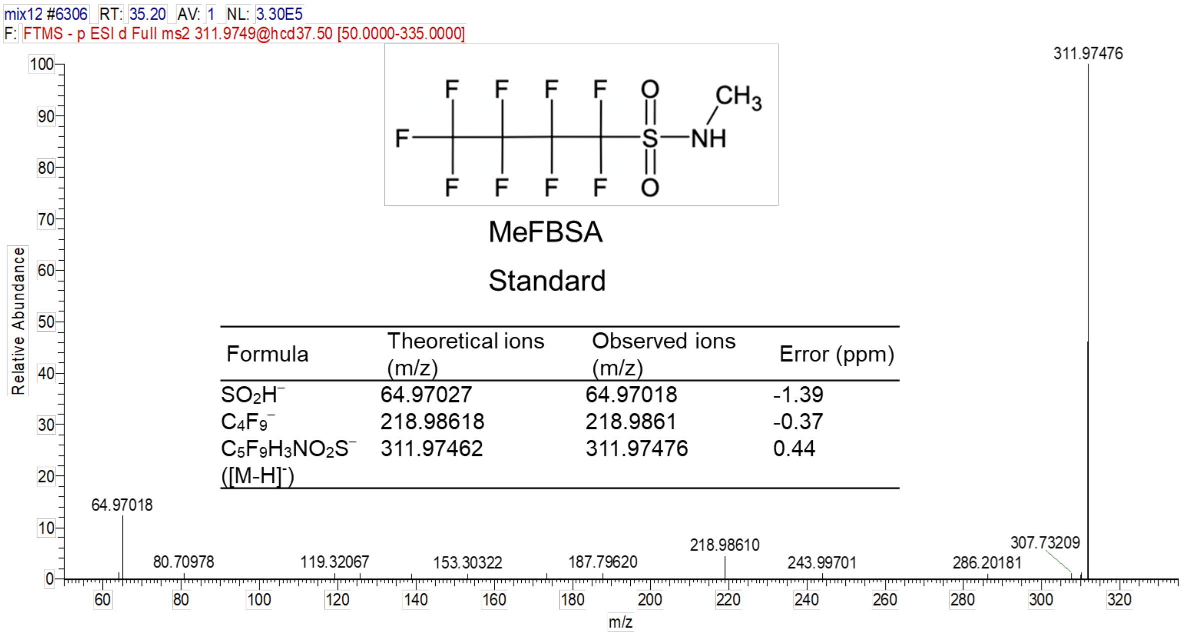

Formula	Theoretical ions (m/z)	Observed ions (m/z)	Error (ppm)
SO_2H^-	64.97027	64.97018	-1.39
$C_4F_9^-$	218.98618	218.9861	-0.37
$C_5F_9H_3NO_2S^-$ ($[M-H]^-$)	311.97462	311.97476	0.44

Figure 23 MS2 spectrum of MeFBSA from authentic standard.

Class II Perfluoroalkane sulfonamido substances

Subclass 2a-2f Per and polyfluoroalkane sulfonamido ethanols (FASEs) The nontarget approach introduces novel fragment-based indicators $[O_2SNC_2H_4O]^-$ and $[O_2SNCH_2]^-$[53] for identifying subclasses with specific sulfonamido ethanol segments, as shown in **Figure 13**(a). By conducting $[O_2SNC_2H_4O]^-$ and $[O_2SNCH_2]^-$ fragment searching, we identified the predominant perfluoroalkane sulfonamido ehtaol (FASEs) and miscellaneous FASE series, resulting in the detection of 8 subclasses (2a-2h). Among them, 6 subclasses (2a-2f) displaying variations in the fluoroalkyl chain were effectively identified, including perfluorobutane sulfonamido ethanol (FBSE), hydro-substituted perfluorobutane sulfonamido ethanol (H-FBSE), perfluorobutyl ether sulfonamido ehtanol (E-FBSE), hydro-substituted perfluorobutyl ether sulfonamido ehtanol (H-E-FBSE), unsaturated perfluorobutane sulfonamido ehtanol (U-FBSE), and unsaturated perfluorobutyl ether sulfonamido ehtanol (U-FBSE). Among the largest peaks in the samples was a feature at 341.98519 m/z and was identified as perfluorobutane sulfonamido ethanol (FBSE). It is noted that the fluoroalkyl fragment as $[C_4F_9]^-$ was not obvious in the MS2 spectrum of FBSE (**Figure 24**); thus, identification via the specific fragment of $[O_2SNC_2H_4O]^-$ is highly feasible.[53] FBSE was separated into several peaks for branched and linear FBSE isomers (**Figure 24**). The CL increased after confirmation with the reference standard through RT matching and MS2 spectrum matching. However, due to insufficient data for isomer-specific assignment, the CL remained 1b. (**Figure 25**)

doi:10.6342/NTU202402180

FBSE was the most abundant substance in the sewage of semiconductor plants A, B, C, and D at concentrations up to 34.0 to 482 µg/L and decreased to 1.72 to 21.4 µg/L in the effluent of WWTP3 and WWTP4. FBSE, patented for silicon wafer etching and cleaning,[7,59,60] and its notable presence in semiconductor plant sewage might be associated with 3M's Electronic Surfactant 4200—an anionic fluorochemical surfactant in a 25% aqueous solution to enhance wetting in BHF.[22] Identified as 1,1,2,2,3,3,4,4,4-nonafluoro-N-(2-hydroxyethyl)-ammonium salt in 3M's safety data sheet (SDS), this surfactant clarifies FBSE's notable presence in semiconductor sewage. PFOS, previously used as the surfactant in BHF formulations,[5] has been supplanted by FBSE in Novec 4200 formulations. This transition marks a pioneering discovery in our study, demonstrating FBSE as a predominant alternative surfactant extensively utilized in semiconductor fabrication. Notably, there was 0.007 µg/L FBSE in the method blank sample (**Table 27**), and this concentration was one-twentieth of the lowest concentration (0.143 µg/L) in the effluent from WWTP5. Thus, we attributed the extremely low level to the residuals in the LC–MS/MS system.

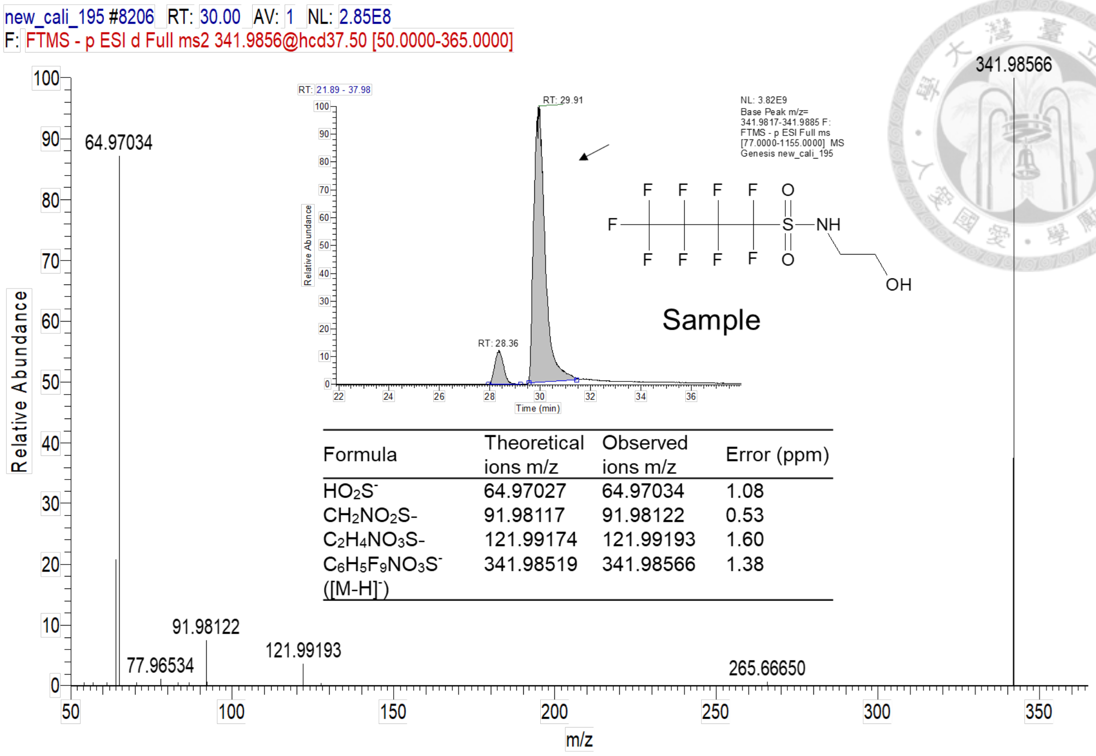

Formula	Theoretical ions m/z	Observed ions m/z	Error (ppm)
HO_2S^-	64.97027	64.97034	1.08
CH_2NO_2S-	91.98117	91.98122	0.53
$C_2H_4NO_3S$-	121.99174	121.99193	1.60
$C_6H_5F_9NO_3S^-$ ($[M-H]^-$)	341.98519	341.98566	1.38

Figure 24 MS2 spectrum of FBSE from sample no. 195

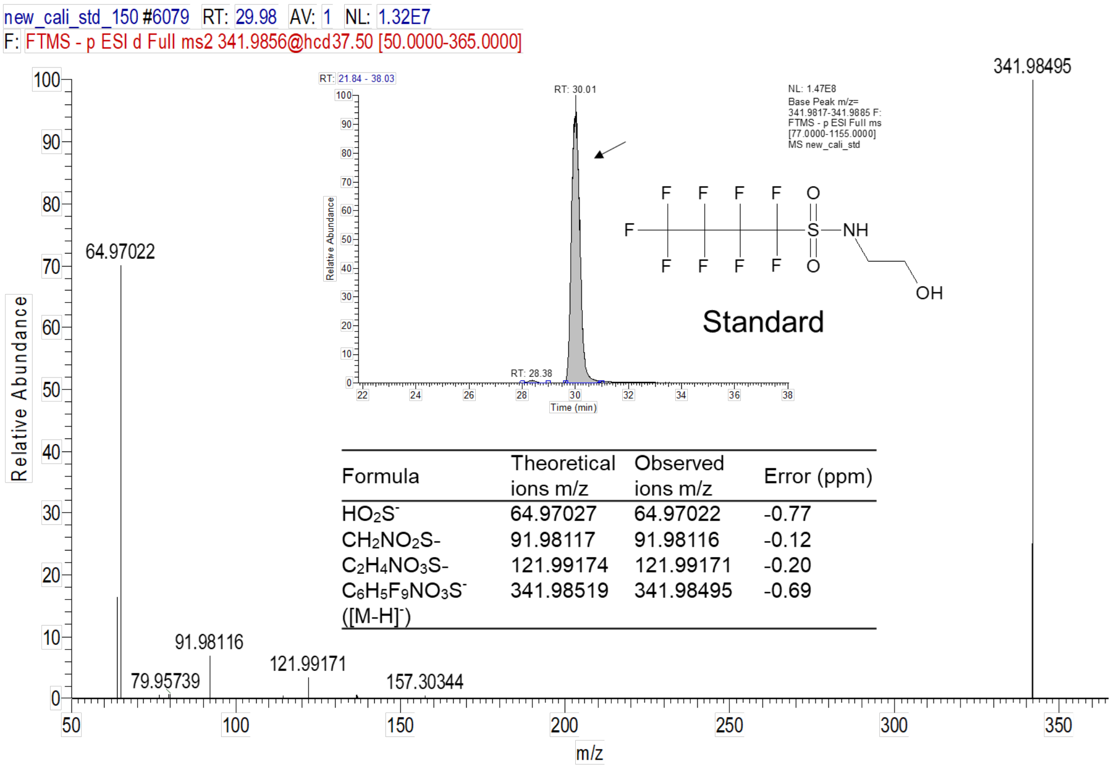

Formula	Theoretical ions m/z	Observed ions m/z	Error (ppm)
HO_2S^-	64.97027	64.97022	-0.77
CH_2NO_2S-	91.98117	91.98116	-0.12
$C_2H_4NO_3S$-	121.99174	121.99171	-0.20
$C_6H_5F_9NO_3S^-$ ($[M-H]^-$)	341.98519	341.98495	-0.69

Figure 25 MS2 spectrum of FBSE from authentic standard

doi:10.6342/NTU202402180

Figure 26 displays the MS2 spectrum and proposed structure of hydro-substituted perfluorobutane sulfonamido ethanol (H-FBSE). The confidence level for H-FBSE remains at 3a due to uncertainties in identifying the position of hydrogen. Next, three isomers of perfluorobutyl ether sulfonamide ethanol (E-FBSE) were identified and three characteristic peaks from fragments $[CF_3O]^-$, $[C_3F_7O]^-$, and $[C_2F_5O]^-$ were observed by chromatography, and their structures were proposed (**Figure 27**, **28**, and **29**) with a confidence level of 2b. The greater RT (35.13 min) of the E-FBSE isomer was indicative of the increased symmetry of the alkyl structure matching the proposed structure. The presence of hydrogen-substituted perfluorobutyl ether sulfonamido ethanols (H-E-FBSEs) with the specific fluoroalkyl ether fragment $[C_2F_3O]^-$ (96.9907, 0.72 ppm) was indicative of the loss of HF from $[C_2F_4HO]^-$ (116.9971, 1.54 ppm). U-FBSE with the fragment $[C_4F_7]^-$ (180.9896, 0.99 ppm) was detected. We proposed a confidence level of 3a due to the lack of further information to determine the position of the double bond. Unsaturated perfluoroalkyl ether sulfonamido ethanols (U-E-FASEs) with the specific fragments $[C_3F_5]^-$(130.9928, 1.91 ppm) and $[C_4F_7O]^-$(196.98503, 3.79 ppm) were detected, which suggested the position of the oxygen atom (**Figure 30**). However, the position of the unsaturated bond remained uncertain, so the confidence level was set to 3a. To the best of our knowledge, 5 subclasses (subclasses 2b-2f) of FASEs with various fluoroalkyl chains have been reported for the first time (**Table 24**).

doi:10.6342/NTU202402180

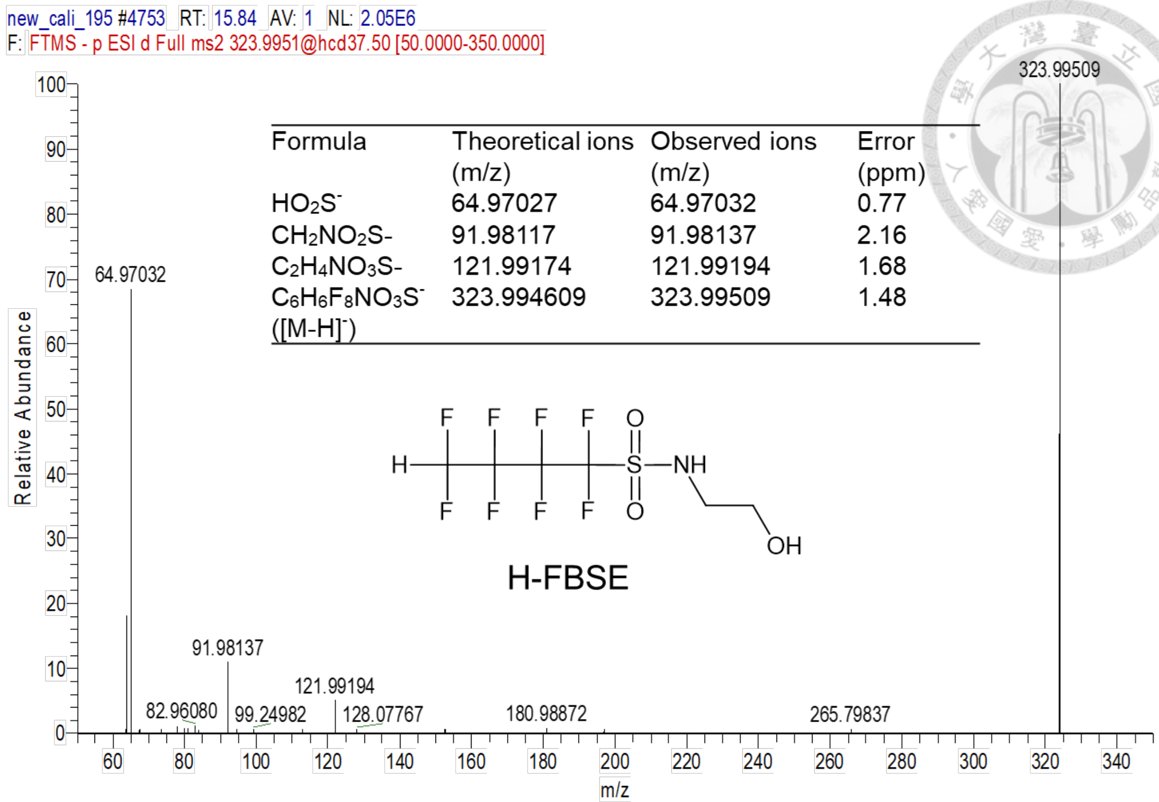

Formula	Theoretical ions (m/z)	Observed ions (m/z)	Error (ppm)
HO_2S^-	64.97027	64.97032	0.77
CH_2NO_2S-	91.98117	91.98137	2.16
$C_2H_4NO_3S$-	121.99174	121.99194	1.68
$C_6H_6F_8NO_3S^-$ ($[M-H]^-$)	323.994609	323.99509	1.48

Figure 26 MS2 spectrum of H-FBSE. Due to the uncertainty of the position of hydrogen, the CL was set to 3a.

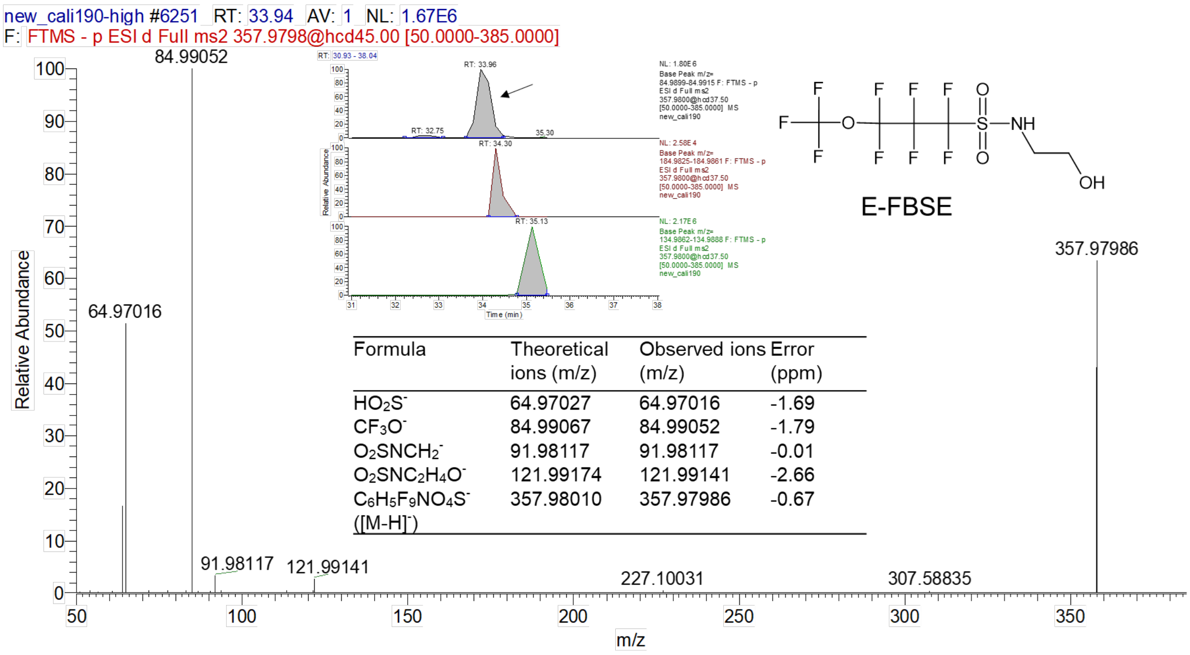

Formula	Theoretical ions (m/z)	Observed ions (m/z)	Error (ppm)
HO_2S^-	64.97027	64.97016	-1.69
CF_3O^-	84.99067	84.99052	-1.79
$O_2SNCH_2^-$	91.98117	91.98117	-0.01
$O_2SNC_2H_4O^-$	121.99174	121.99141	-2.66
$C_6H_5F_9NO_4S^-$ ($[M-H]^-$)	357.98010	357.97986	-0.67

Figure 27 MS2 spectrum from one of structural isomers of E-FBSE(1).

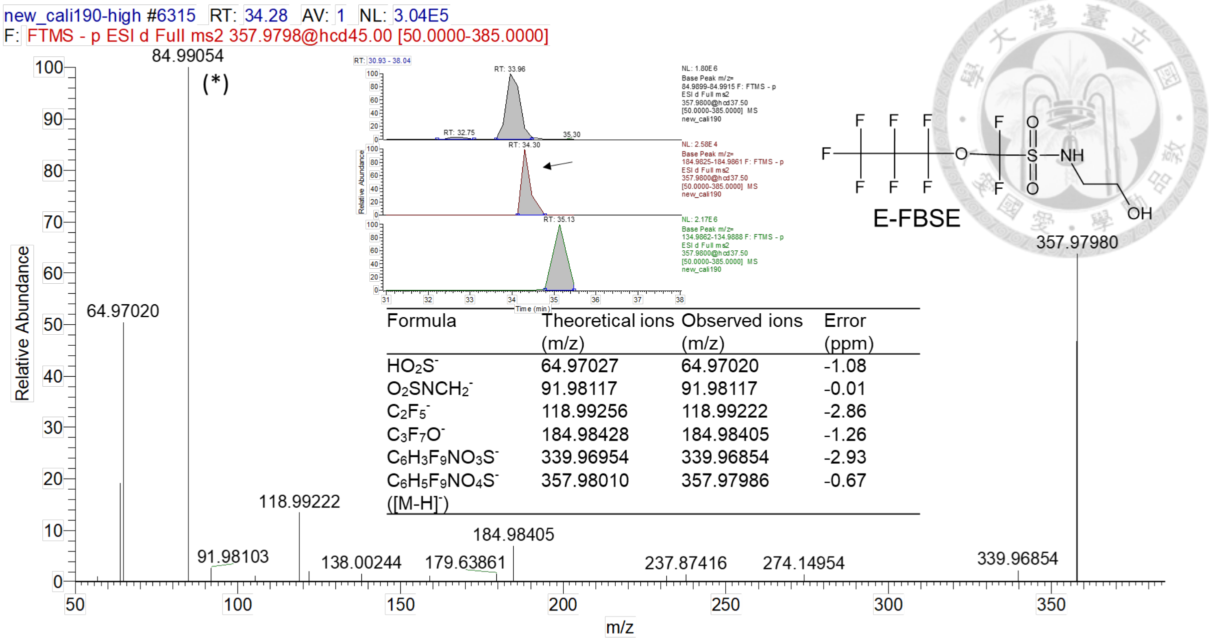

Formula	Theoretical ions (m/z)	Observed ions (m/z)	Error (ppm)
HO_2S^-	64.97027	64.97020	-1.08
$O_2SNCH_2^-$	91.98117	91.98117	-0.01
$C_2F_5^-$	118.99256	118.99222	-2.86
$C_3F_7O^-$	184.98428	184.98405	-1.26
$C_6H_3F_9NO_3S^-$	339.96954	339.96854	-2.93
$C_6H_5F_9NO_4S^-$ ($[M-H]^-$)	357.98010	357.97986	-0.67

*the fragment CF_3O^- from of 1,1,2,2,3,3-hexafluoro-N-(2-hydroxyethyl)- 3-(trifluoromethoxy)propane-1-sulfonamide at RT 33.94

Figure 28 MS2 spectrum of one of structural isomers of E-FBSE(2).

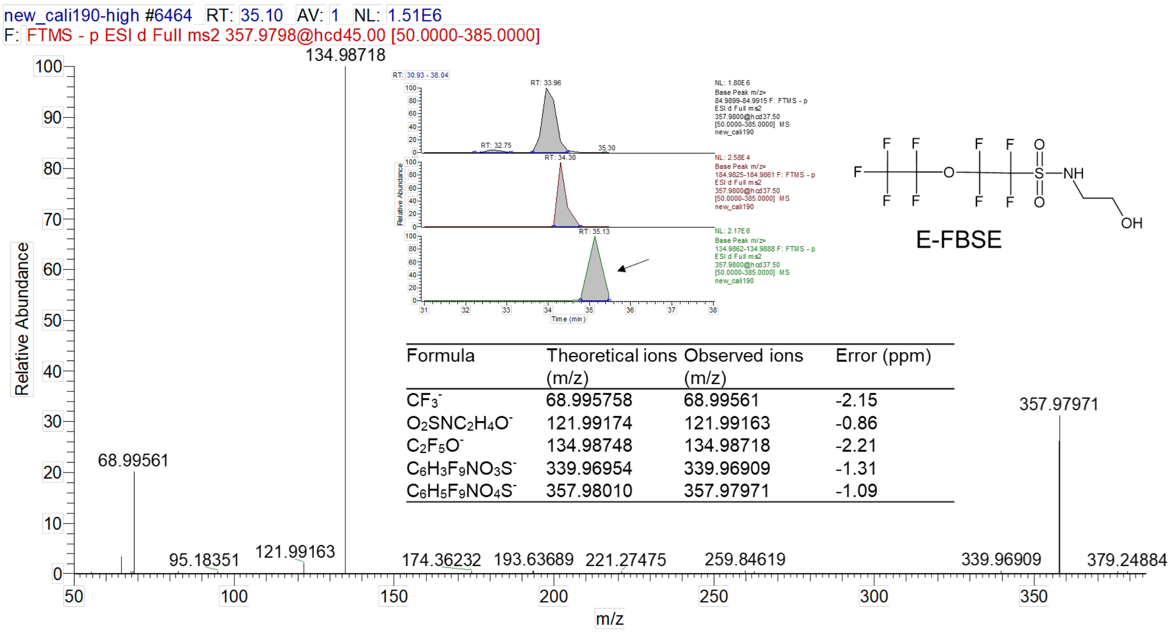

Formula	Theoretical ions (m/z)	Observed ions (m/z)	Error (ppm)
CF_3^-	68.995758	68.99561	-2.15
$O_2SNC_2H_4O^-$	121.99174	121.99163	-0.86
$C_2F_5O^-$	134.98748	134.98718	-2.21
$C_6H_3F_9NO_3S^-$	339.96954	339.96909	-1.31
$C_6H_5F_9NO_4S^-$	357.98010	357.97971	-1.09

Figure 29 MS2 spectrum of one of structural isomers of E-FBSE(3).

doi:10.6342/NTU202402180

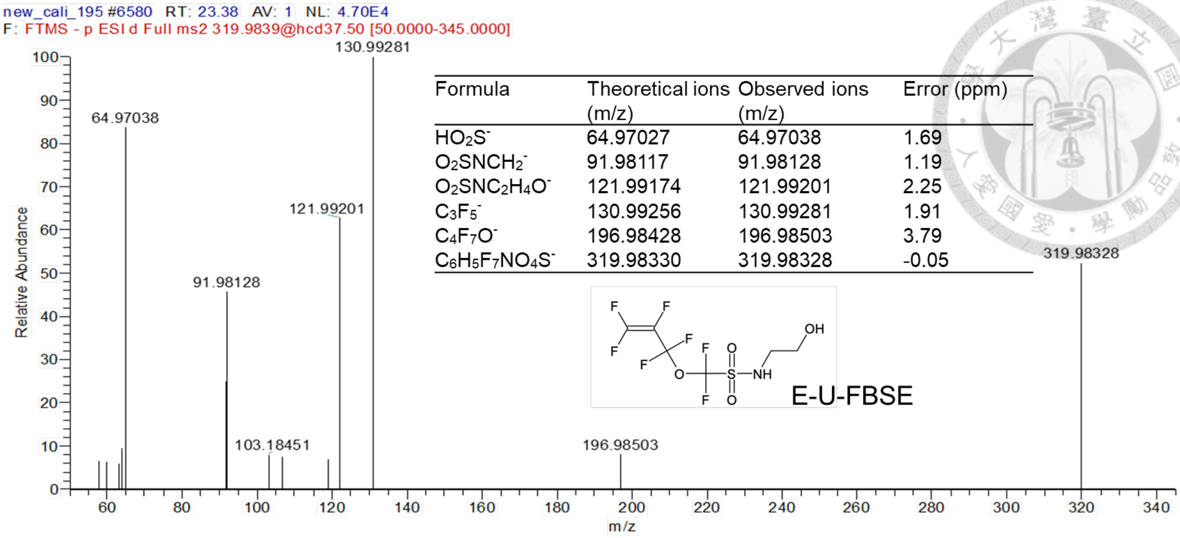

Formula	Theoretical ions (m/z)	Observed ions (m/z)	Error (ppm)
HO_2S^-	64.97027	64.97038	1.69
$O_2SNCH_2^-$	91.98117	91.98128	1.19
$O_2SNC_2H_4O^-$	121.99174	121.99201	2.25
$C_3F_5^-$	130.99256	130.99281	1.91
$C_4F_7O^-$	196.98428	196.98503	3.79
$C_6H_5F_7NO_4S^-$	319.98330	319.98328	-0.05

Figure 30 MS2 spectrum of E-U-FBSE

Subclass 2g-2h Miscellaneous FBSEs The subclass with the structure $C_4F_9SO_2N(C_2H_4OH)$ XH (X:SO_3; X: CONH) were detected in subclasses 2g and 2h, identified through characteristic fragment $[SO_2NC_2H_4O]^-$ (121.9912) screening. Notably, subclasses 2g and 2h could be detected through neutral loss screening of SO_3 and CONH. (**Figure 31**)

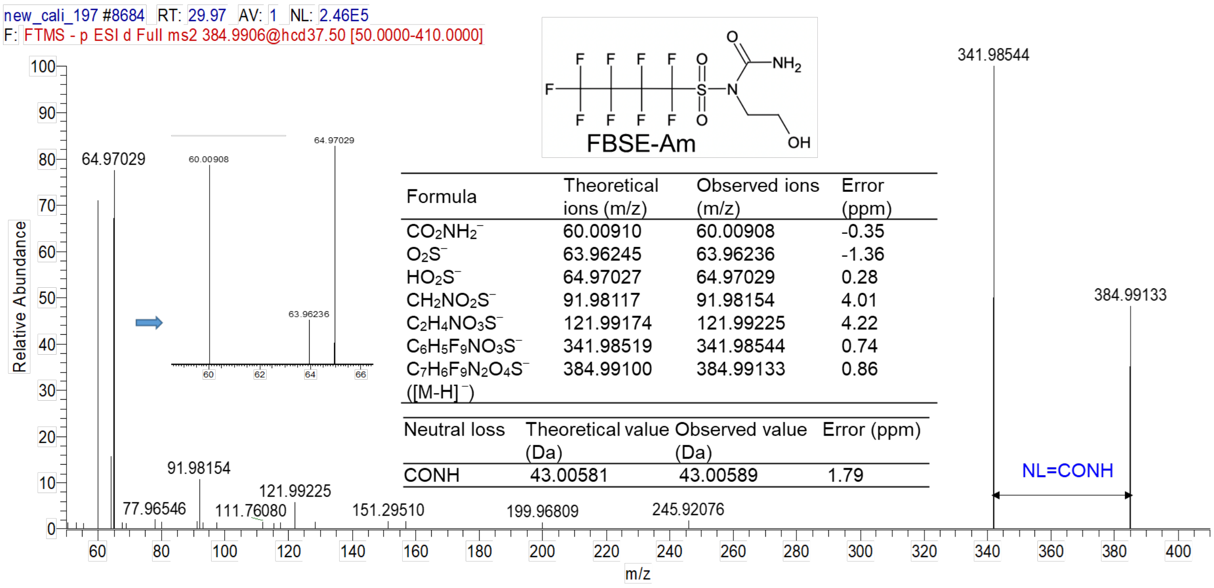

Formula	Theoretical ions (m/z)	Observed ions (m/z)	Error (ppm)
$CO_2NH_2^-$	60.00910	60.00908	-0.35
O_2S^-	63.96245	63.96236	-1.36
HO_2S^-	64.97027	64.97029	0.28
$CH_2NO_2S^-$	91.98117	91.98154	4.01
$C_2H_4NO_3S^-$	121.99174	121.99225	4.22
$C_6H_5F_9NO_3S^-$	341.98519	341.98544	0.74
$C_7H_6F_9N_2O_4S^-$ ($[M-H]^-$)	384.99100	384.99133	0.86

Neutral loss	Theoretical value (Da)	Observed value (Da)	Error (ppm)
CONH	43.00581	43.00589	1.79

Figure 31 MS2 spectrum of FBSE-Am

Subclass 2i N-alkyl perfluoroalkane sulfonamido ethanol To explore the subclass of N-alkyl perfluoroalkane sulfonamido ethanol, we examined the authentic standards of MeFOSE and EtFOSE, revealing characteristic MS2 spectrum of this subclass. Both MeFOSE and EtFOSE displayed an acetate adduct $[M+CH_3COO]^-$. In alkyl-substituted sulfonamido ethanol, no $[SO_2NC_2H_4O]^-$ (121.9912) and $[SO_2NCH_2]^-$ (91.9806) fragments were observed; only $[CH_3COO]^-$ (59.01385) appeared. Screening of the acetate adduct of MeFBSE (416.02197) in sample no. 190 revealed fragments of $[SO_2NC_2H_4O]^-$ (121.99250) and $[SO_2H]^-$ (64.97031) at RT 35.82 (**Figure 32**). The MeFBSE in Sample no. 190, presumed to be branched, contained fragments of $[SO_2NC_2H_4O]^-$ (121.99250) and $[SO_2H]^-$ (64.97031), possibly distinct from the linear form of authentic standard (**Figure 33**). Owing to the lack of additional fragments, we assigned CL for MeFBSE as 1b due to insufficient isomeric data. Notably, previous researchers identified fluorotelomer sulfonamido ethanol, like 6:2 FTSAm-EtOH, which contains the $[SO_2NC_2H_4O]^-$ (121.9912) fragment.[67] This fragment, unaffected by the functional fluoroalkyl chain, remains consistent across fluorotelomer compounds, serving as a unique indicator of sulfonamido ethanol.

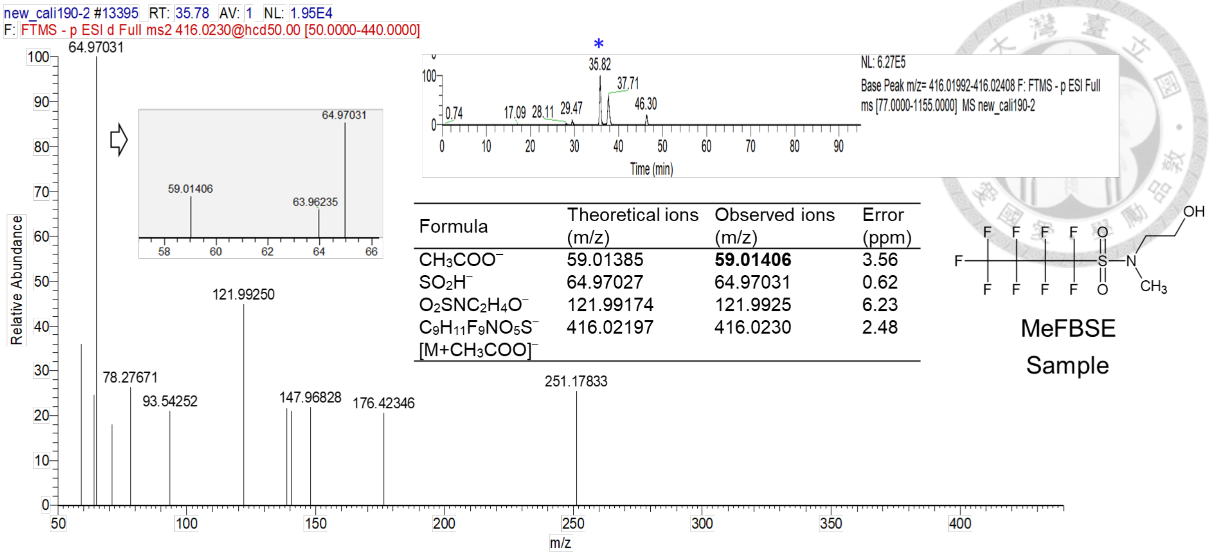

Formula	Theoretical ions (m/z)	Observed ions (m/z)	Error (ppm)
CH_3COO^-	59.01385	**59.01406**	3.56
SO_2H^-	64.97027	64.97031	0.62
$O_2SNC_2H_4O^-$	121.99174	121.9925	6.23
$C_9H_{11}F_9NO_5S^-$ $[M+CH_3COO]^-$	416.02197	416.0230	2.48

Figure 32 MS2 spectrum of MeFBSE from sample no.190

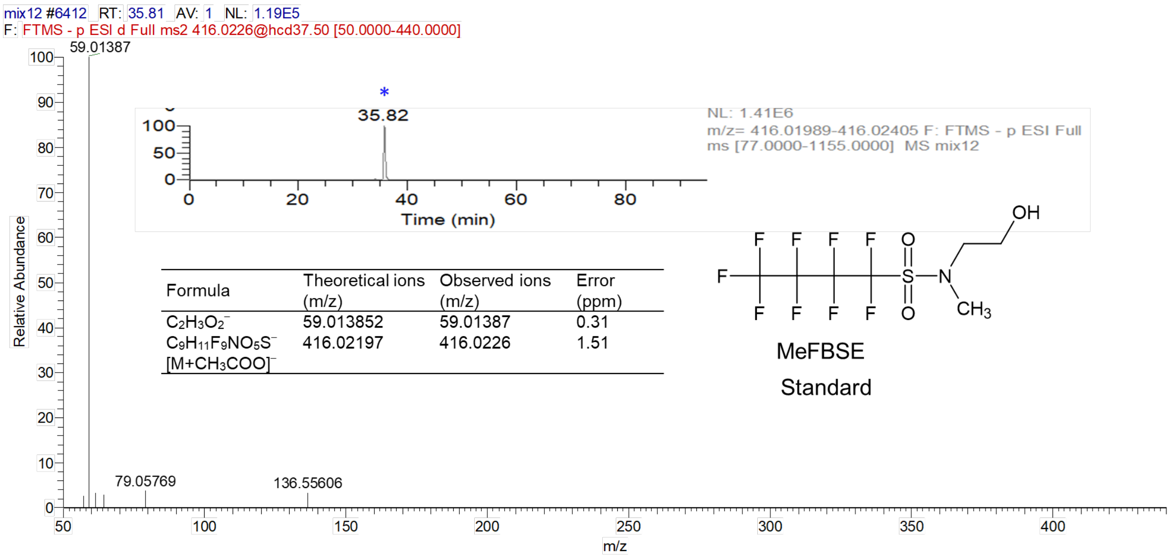

Formula	Theoretical ions (m/z)	Observed ions (m/z)	Error (ppm)
$C_2H_3O_2^-$	59.013852	59.01387	0.31
$C_9H_{11}F_9NO_5S^-$ $[M+CH_3COO]^-$	416.02197	416.0226	1.51

Figure 33 MS2 spectrum of MeFBSE from authentic standard

Subclass 3a-3b Sulfonamido diethanol N,N-bis(2-hydroxyethyl)perfluorobutane sulfonamide (FBSEE diol) was identified in the form of an acetate adduct $[M+CH_3COO]^-$, $[M\text{-}H]^-$, a formate adduct $[M+HCOO]^-$, and a dimer ion $[2M\text{-}H]^-$, in the order of their observed intensities (**Figure 34**). This structure displayed characteristic fragments, such as

doi:10.6342/NTU202402180

$[SO_2N(C_2H_4O)_2]^-$, $[SO_2N(C_2H_4O)CH_2]^-$, and $[SO_2NC_2H_4O]^-$ in **Figure 35** and **Figure 36**, suggesting the presence of an N,N-2-bishydroxyethyl sulfonamide group. Additionally, the high-intensity $[SO_3]^-$ fragment served as a confirming indicator. The observation underscores the effectiveness of the screening method based on its polar functional group of FBSEE diol. This has been confirmed using the authentic standard with a confidence level (CL) set to 1a, as depicted in **Figure 37**. The concentrations of FBSEE diol in the sewage ranged from n.d. to 83.5 μg/L, and those in the effluent ranged from n.d. to 3.96 μg/L in **Table 27**. No literature or patents claim that FBSEE diol is used in semiconductor manufacturing, and this is the first time that FBSEE diol has been observed to be deployed in semiconductor manufacturing. A 3M plant admitted that FBSEE diol had been illegally released to the Tennessee River in Alabama.[63] The investigation of the Morgan County Sanitary Landfill by the 3M Environmental Laboratory showed that FBSEE diol was detected in air and water samples.[69] Notably, FBSA, FBSE, and FBSEE diol were observed at high detection rates of 85%, 100%, and 69%, respectively. Moreover, hydrogen-substituted FBSEE diol (H-FBSEE diol) was detected with an acetate adduct and the unique fragment $[O_2SN(C_2H_4O)_2]^-$ (166.0174, -2.16 ppm) for the first time. The confidence level was set to 3a due to insufficient data to determine the position of hydrogen

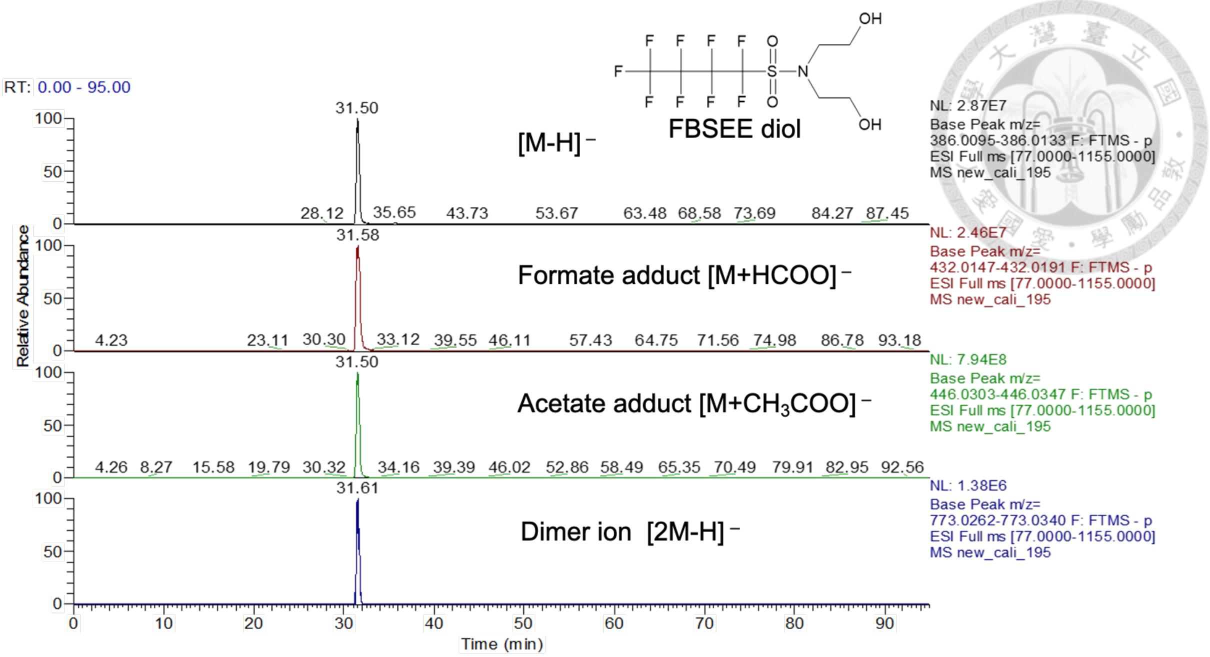

Figure 34 The observations of four adduct ion of FBSEE diol in sample no. 195.

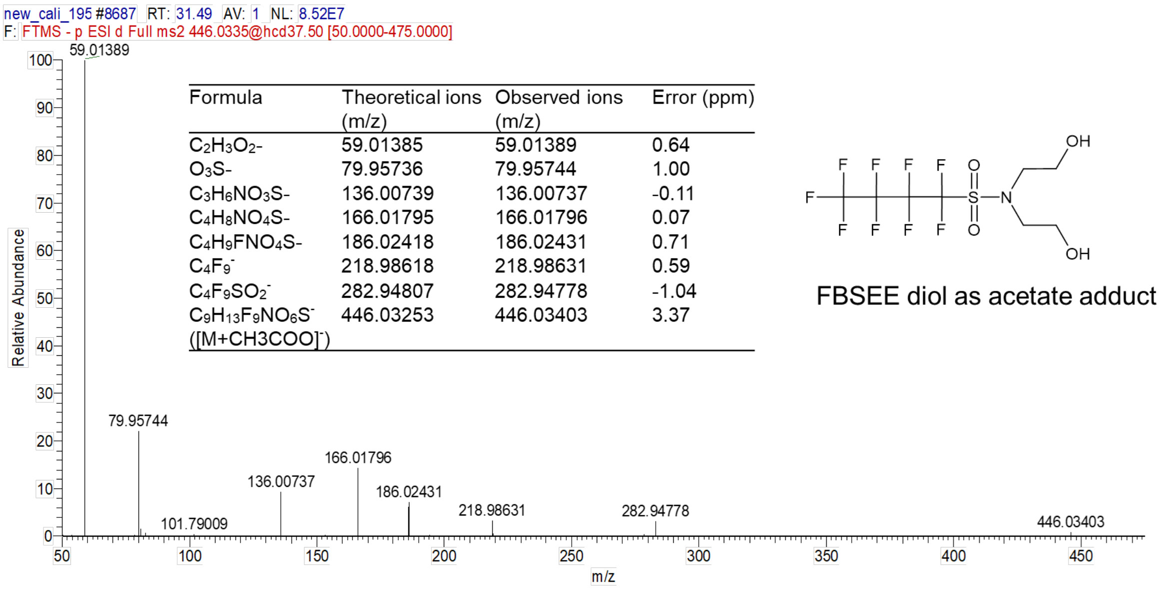

Formula	Theoretical ions (m/z)	Observed ions (m/z)	Error (ppm)
$C_2H_3O_2^-$	59.01385	59.01389	0.64
O_3S^-	79.95736	79.95744	1.00
$C_3H_6NO_3S^-$	136.00739	136.00737	-0.11
$C_4H_8NO_4S^-$	166.01795	166.01796	0.07
$C_4H_9FNO_4S^-$	186.02418	186.02431	0.71
$C_4F_9^-$	218.98618	218.98631	0.59
$C_4F_9SO_2^-$	282.94807	282.94778	-1.04
$C_9H_{13}F_9NO_6S^-$ ([M+CH3COO]⁻)	446.03253	446.03403	3.37

Figure 35 MS2 spectrum of FBSEE diol as acetate adduct in sample no.195.

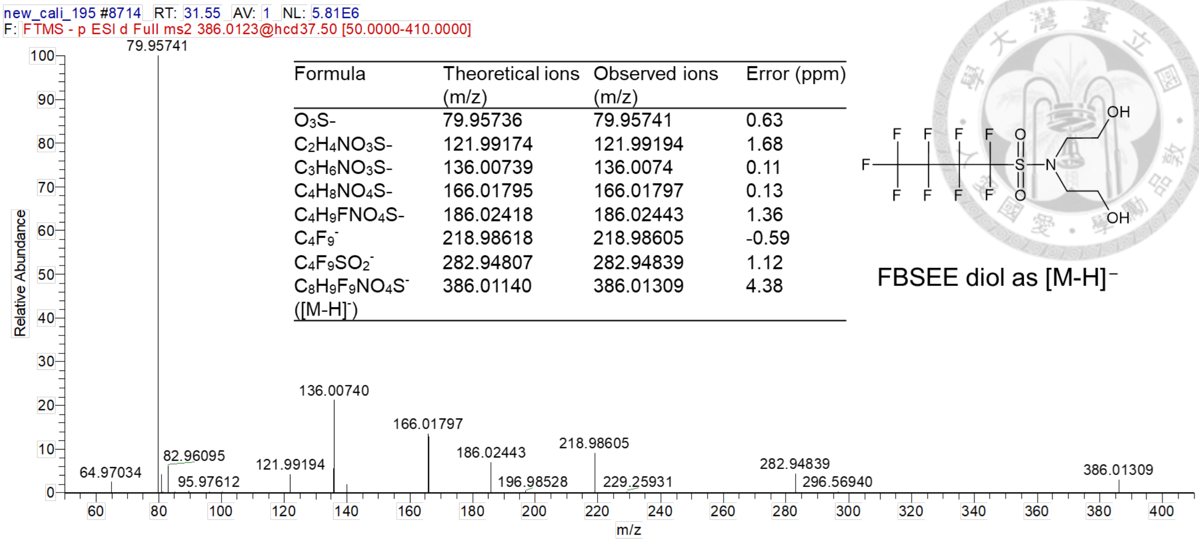

Formula	Theoretical ions (m/z)	Observed ions (m/z)	Error (ppm)
O_3S-	79.95736	79.95741	0.63
$C_2H_4NO_3S$-	121.99174	121.99194	1.68
$C_3H_6NO_3S$-	136.00739	136.0074	0.11
$C_4H_8NO_4S$-	166.01795	166.01797	0.13
$C_4H_9FNO_4S$-	186.02418	186.02443	1.36
$C_4F_9^-$	218.98618	218.98605	-0.59
$C_4F_9SO_2^-$	282.94807	282.94839	1.12
$C_8H_9F_9NO_4S^-$ ($[M-H]^-$)	386.01140	386.01309	4.38

Figure 36 MS2 spectrum of FBSEE diol was observed as $[M-H]^-$ in sample no.195.

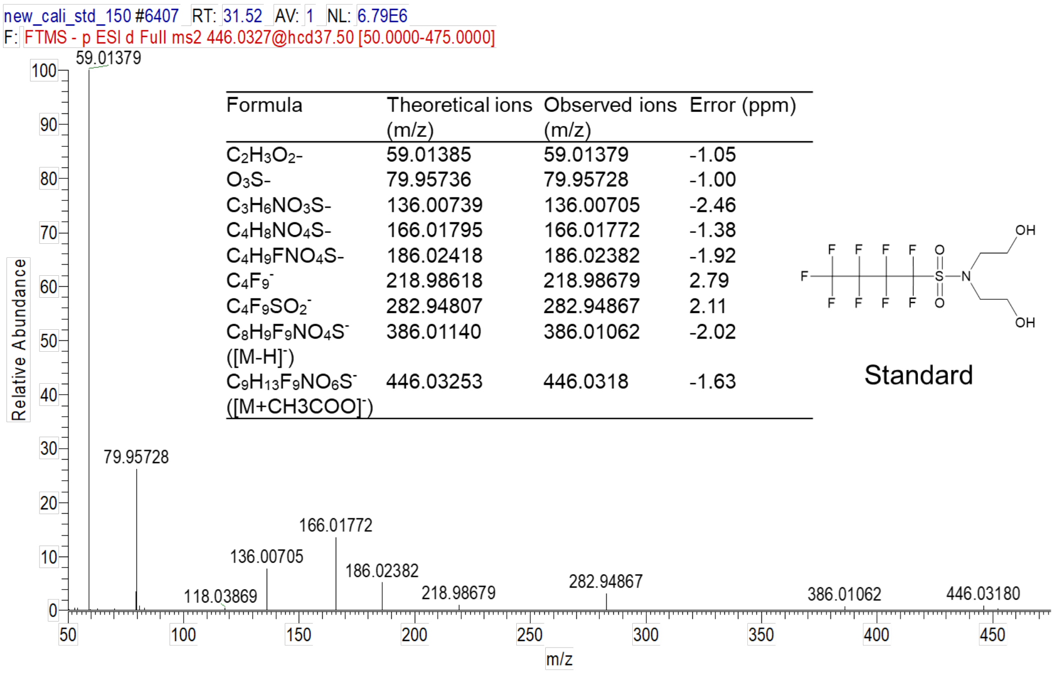

Formula	Theoretical ions (m/z)	Observed ions (m/z)	Error (ppm)
$C_2H_3O_2$-	59.01385	59.01379	-1.05
O_3S-	79.95736	79.95728	-1.00
$C_3H_6NO_3S$-	136.00739	136.00705	-2.46
$C_4H_8NO_4S$-	166.01795	166.01772	-1.38
$C_4H_9FNO_4S$-	186.02418	186.02382	-1.92
$C_4F_9^-$	218.98618	218.98679	2.79
$C_4F_9SO_2^-$	282.94807	282.94867	2.11
$C_8H_9F_9NO_4S^-$ ($[M-H]^-$)	386.01140	386.01062	-2.02
$C_9H_{13}F_9NO_6S^-$ ($[M+CH3COO]^-$)	446.03253	446.0318	-1.63

Figure 37 MS2 spectrum of FBSEE diol from authentic standard

Subclass 4 Sulfonamido carboxylic acid This subclass features a structure with sulfonamido linked to a carboxylic acid group, releasing the carboxylic acid group ($C_nH_{2n}CO_2$) during

doi:10.6342/NTU202402180

collision. A precursor ion at 355.96460, with a neutral loss of CH_2CO_2 (-1.86 ppm), was identified as perfluorobutane sulfonamido acetic acid (FBSAA) (**Figure 38**) and confirmed by its authentic standard at CL1a (**Figure 39**). FBSAA has been identified downstream of manufacturing facilities in Alabama,[57] in Chinese municipal WWTPs,[36] and in landfill leachate at a semiquantified level of 55 ng/L.[62]

In this study, FBSAA was detected semiquantitatively at concentrations from n.d. to 11.0 μg/L in sewage and at extremely high concentrations of 0.780 to 227 μg/L in effluent (**Table 27**). FBSAA has been patented as an etching solution in the semiconductor process.[7,59] However, it is difficult to distinguish whether FBSAA was directly used in the process or was formed by the oxidation of FBSE. After wastewater treatment, the concentration of FBSAA dramatically increased and we attributed this to the oxidation of FBSE to form FBSAA during biotreatment processes, and further discussion follows.

doi:10.6342/NTU202402180

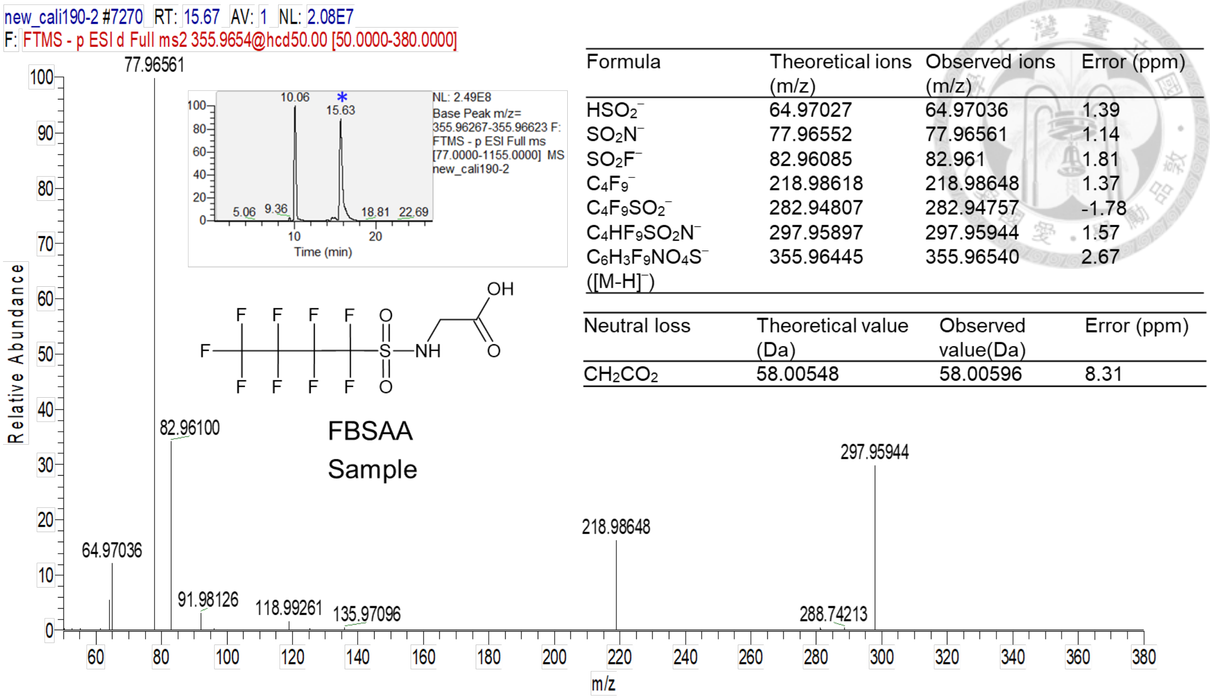

Formula	Theoretical ions (m/z)	Observed ions (m/z)	Error (ppm)
HSO_2^-	64.97027	64.97036	1.39
SO_2N^-	77.96552	77.96561	1.14
SO_2F^-	82.96085	82.961	1.81
$C_4F_9^-$	218.98618	218.98648	1.37
$C_4F_9SO_2^-$	282.94807	282.94757	-1.78
$C_4HF_9SO_2N^-$	297.95897	297.95944	1.57
$C_6H_3F_9NO_4S^-$ ([M-H]$^-$)	355.96445	355.96540	2.67

Neutral loss	Theoretical value (Da)	Observed value(Da)	Error (ppm)
CH_2CO_2	58.00548	58.00596	8.31

Figure 38 MS2 spectrum of FBSAA from sample no. WWTP4

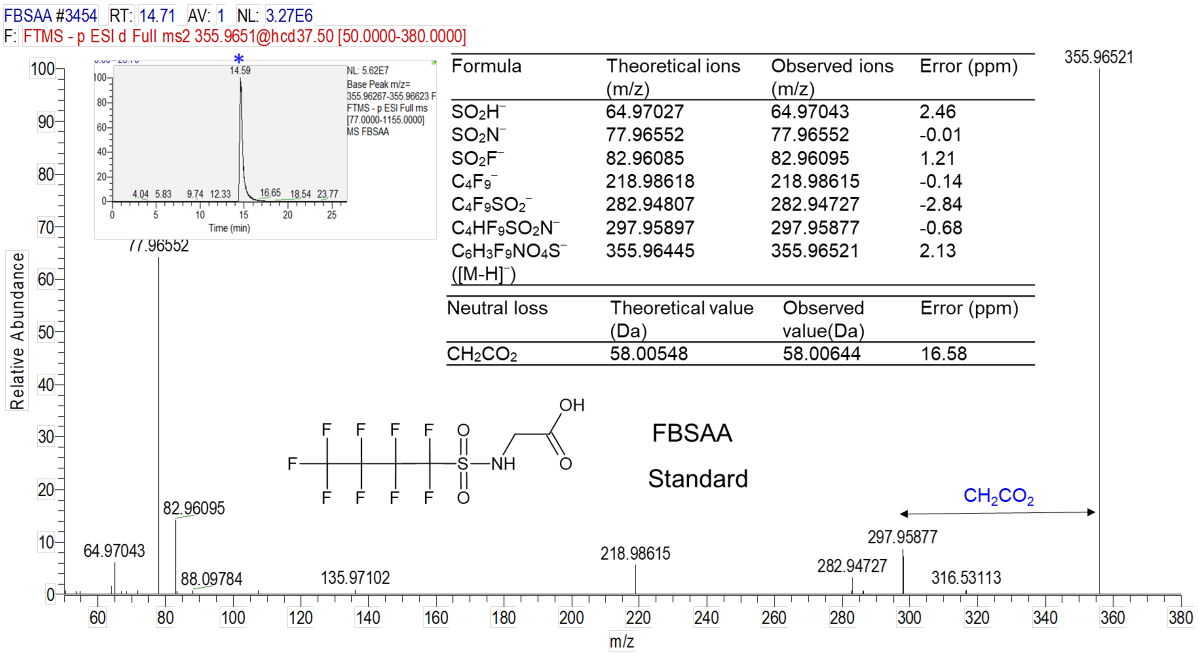

Formula	Theoretical ions (m/z)	Observed ions (m/z)	Error (ppm)
SO_2H^-	64.97027	64.97043	2.46
SO_2N^-	77.96552	77.96552	-0.01
SO_2F^-	82.96085	82.96095	1.21
$C_4F_9^-$	218.98618	218.98615	-0.14
$C_4F_9SO_2^-$	282.94807	282.94727	-2.84
$C_4HF_9SO_2N^-$	297.95897	297.95877	-0.68
$C_6H_3F_9NO_4S^-$ ([M-H]$^-$)	355.96445	355.96521	2.13

Neutral loss	Theoretical value (Da)	Observed value(Da)	Error (ppm)
CH_2CO_2	58.00548	58.00644	16.58

Figure 39 MS2 spectrum of FBSAA from authentic standard.

Through RT alignment and consistent MS2 spectrum, we verified the presence of FBSAA at 15.5 minutes with CL1a (**Figure 39**). Notably, an isomer of FBSAA with higher polarity presented at RT 9.93 minutes, showcasing distinct MS2 spectrum (**Figure 40**) that suggest structural differences. Considering the potential isomerization between acid and diol forms [70], fragment analysis led to the proposal of a diol structure for the isomer.

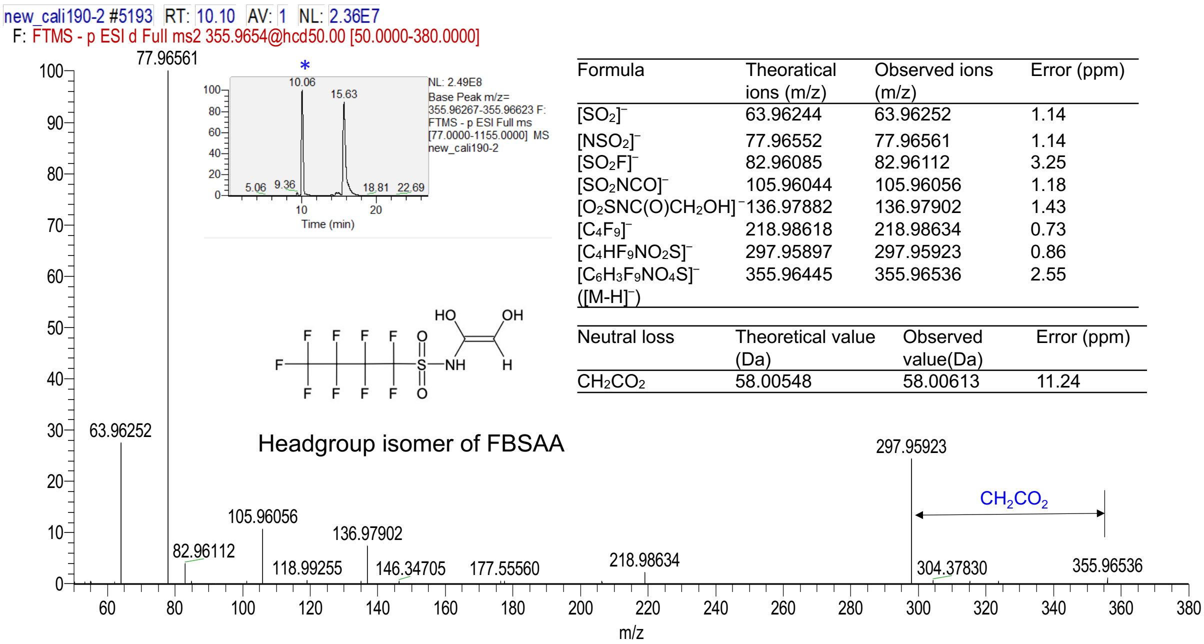

Formula	Theoratical ions (m/z)	Observed ions (m/z)	Error (ppm)
$[SO_2]^-$	63.96244	63.96252	1.14
$[NSO_2]^-$	77.96552	77.96561	1.14
$[SO_2F]^-$	82.96085	82.96112	3.25
$[SO_2NCO]^-$	105.96044	105.96056	1.18
$[O_2SNC(O)CH_2OH]^-$	136.97882	136.97902	1.43
$[C_4F_9]^-$	218.98618	218.98634	0.73
$[C_4HF_9NO_2S]^-$	297.95897	297.95923	0.86
$[C_6H_3F_9NO_4S]^-$ ($[M-H]^-$)	355.96445	355.96536	2.55

Neutral loss	Theoretical value (Da)	Observed value(Da)	Error (ppm)
CH_2CO_2	58.00548	58.00613	11.24

Figure 40 MS2 spectrum of an isomer of FBSAA at RT 10.10 min

A series of compounds consistently displayed a neutral loss of CH_2CO_2 (58.00548 Da), allowing for the further identification of hydrogen-substituted FBSAA (**Figure 41**), E-FBSAA, and N-methyl FBSAA (MeFBSAA) (**Figure 42**). Initially, a molecular ion at 337.97387 with fragments $[C_4F_7]^-$, $[SO_2N]^-$, $[SO_2F]^-$, and $[C_4H_2F_8O_2SN]^-$, and the formula inferred through isotopic pattern matching as $C_6H_5F_8O_4SN$ (mass tolerance 1.26 ppm, within 5 ppm), were

doi:10.6342/NTU202402180

further suggested to represent hydrogen-substituted FBSAA (**Figure 41**). However, the position of the hydrogen remained undetermined, leading to the assignment of a level 3 confidence for the structure. H-FBSAA is being reported for the first time. Furthermore, features as 371.95937 are proposed as perfluorobutyl ether sulfonamido acetic acid (E-FBSAA), which has two structural isomers, was separated with the column at RTs of 18.73 min and 19.73 min. Fragments of fluoroether $[CF_3O]^-$ and $[C_2F_5O]^-$ were observed and providing the position of oxygen for the CL at 2b. Furthermore, MeFBSAA with isotope matching to $C_7H_6F_9NO_4S$ (369.9790, -2.98 ppm) (**Figure 42**) was subsequently confirmed by the matching RT and MS2 spectrum of the authentic standards (**Figure 43**). MeFBSAA was identified downstream of manufacturing facilities in Alabama[57] and in landfill leachate at levels of 41-8000 ng/L.[35,71]. N-Alkyl perfluorobutane sulfonamidoacetate (N-alkyl FBSAA) has been patented as a cleaning component for silicon wafers;[60] however, this subclass was examined but not detected in wastewater. Extremely low concentrations of MeFBSAA were detected in effluents from WWTP3 and WWTP4, with low concentrations of 0.029 and 0.018 μg/L, respectively, as shown in **Table 27**. Thus, we concluded that N-alkyl FBSAA was not the main chemical used in the studied semiconductor plants.

doi:10.6342/NTU202402180

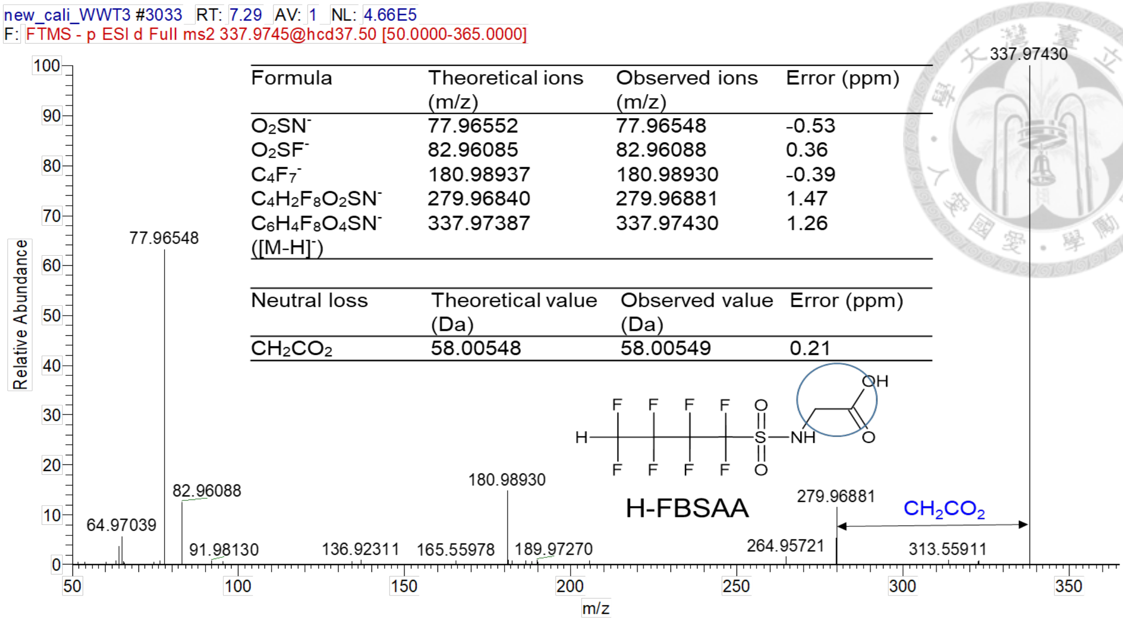

Formula	Theoretical ions (m/z)	Observed ions (m/z)	Error (ppm)
O_2SN^-	77.96552	77.96548	-0.53
O_2SF^-	82.96085	82.96088	0.36
$C_4F_7^-$	180.98937	180.98930	-0.39
$C_4H_2F_8O_2SN^-$	279.96840	279.96881	1.47
$C_6H_4F_8O_4SN^-$ ([M-H]$^-$)	337.97387	337.97430	1.26

Neutral loss	Theoretical value (Da)	Observed value (Da)	Error (ppm)
CH_2CO_2	58.00548	58.00549	0.21

Figure 41 MS2 spectrum of H-FBSAA from sample no. WWTP3.

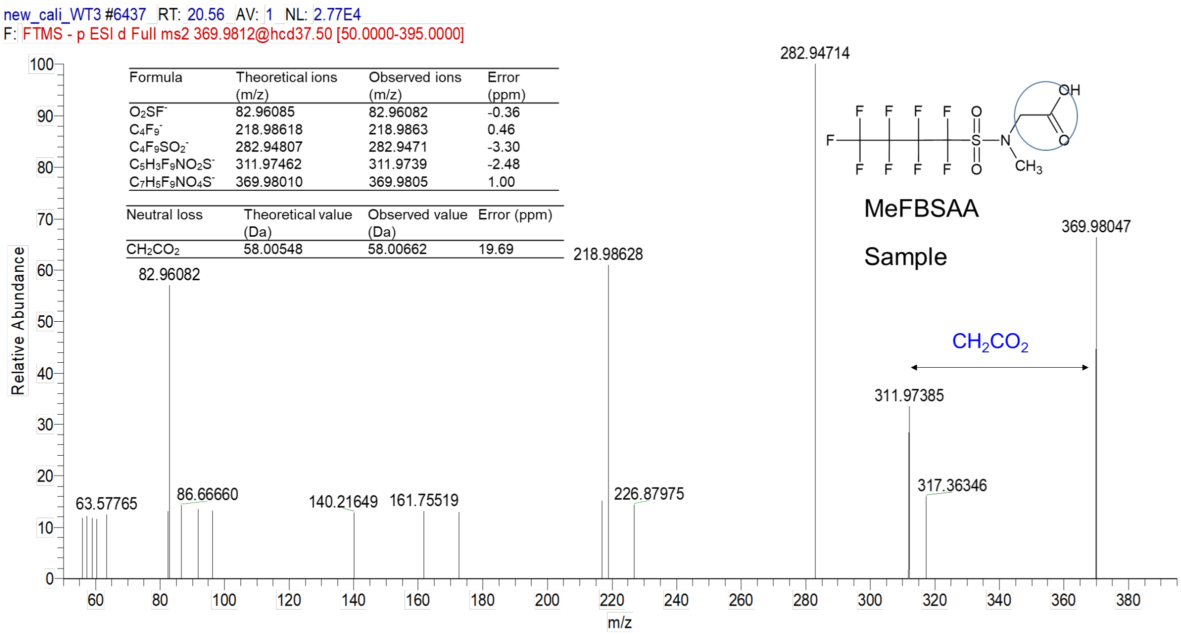

Formula	Theoretical ions (m/z)	Observed ions (m/z)	Error (ppm)
O_2SF^-	82.96085	82.96082	-0.36
$C_4F_9^-$	218.98618	218.9863	0.46
$C_4F_9SO_2^-$	282.94807	282.9471	-3.30
$C_5H_3F_9NO_2S^-$	311.97462	311.9739	-2.48
$C_7H_5F_9NO_4S^-$	369.98010	369.9805	1.00

Neutral loss	Theoretical value (Da)	Observed value (Da)	Error (ppm)
CH_2CO_2	58.00548	58.00662	19.69

Figure 42 MS2 spectrum of MeFBSAA from sample no. WWTP3.

doi:10.6342/NTU202402180

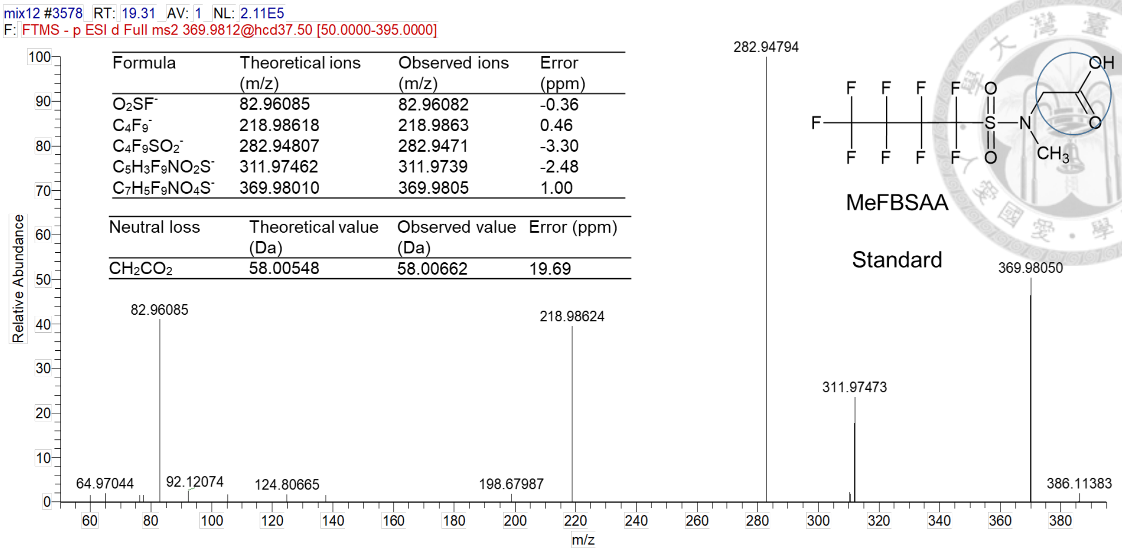

Formula	Theoretical ions (m/z)	Observed ions (m/z)	Error (ppm)
O_2SF^-	82.96085	82.96082	-0.36
$C_4F_9^-$	218.98618	218.9863	0.46
$C_4F_9SO_2^-$	282.94807	282.9471	-3.30
$C_5H_3F_9NO_2S^-$	311.97462	311.9739	-2.48
$C_7H_5F_9NO_4S^-$	369.98010	369.9805	1.00

Neutral loss	Theoretical value (Da)	Observed value (Da)	Error (ppm)
CH_2CO_2	58.00548	58.00662	19.69

Figure 43 MS2 spectrum of MeFBSAA from authentic standard.

A ‘structural isomer’ of MeFBSAA, $C_7H_6F_9NO_4S$ (369.9702, -2.38 ppm), was identified for the first time as perfluorobutane sulfonamido propanoic acid (FBSPrA) (**Figure 44**). The neutral loss of $C_2H_4CO_2$ released from collision indicates propanoic acid. The presence of only $[SO_2F]^-$ (82.9603) fragments, not $[SO_2N]^-$ (77.9644), serves as a distinguishing rule between FASAA and N-alkyl FASAA. Notably, the distinct neutral loss of CH_2CO_2 might be affected by the significant presence of hydrogens in the fluorotelomer, resulting in the neutral loss of HF instead [67]. However, the fluorotelomer series was not detected in this study; additional information for exclusion purposes is provided.

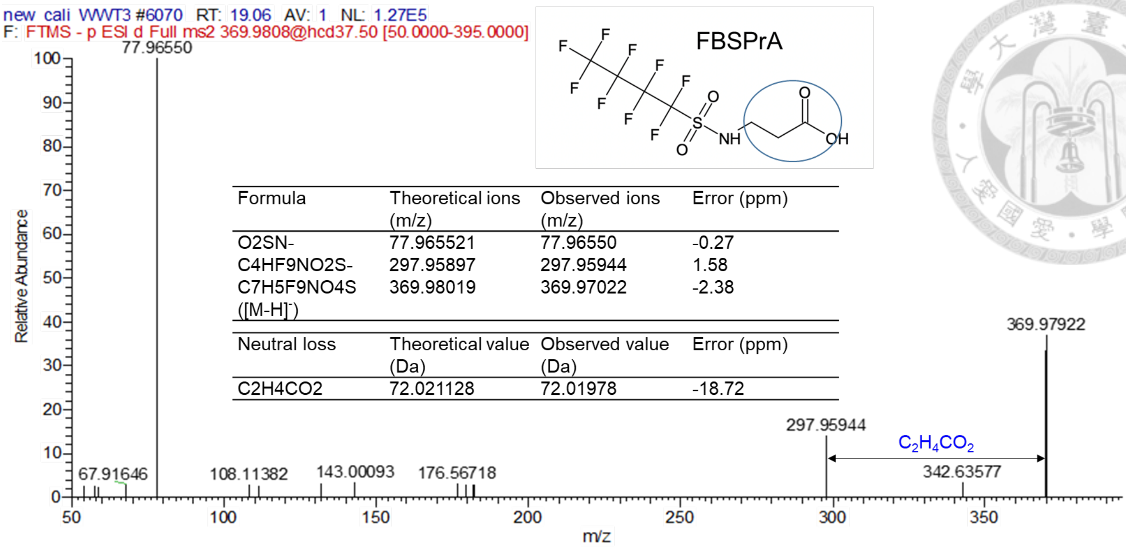

Formula	Theoretical ions (m/z)	Observed ions (m/z)	Error (ppm)
O2SN-	77.965521	77.96550	-0.27
C4HF9NO2S-	297.95897	297.95944	1.58
C7H5F9NO4S ($[M-H]^-$)	369.98019	369.97022	-2.38

Neutral loss	Theoretical value (Da)	Observed value (Da)	Error (ppm)
C2H4CO2	72.021128	72.01978	-18.72

Figure 44 MS2 spectrum of FBSPrA from sample no. WWTP3.

Subclass 5 sulfonamido diacetic acid Perfluorobutane sulfonamido diacetic acid (FBSEE diacid) with precursor ion m/z 413.97073 was found with a neutral loss scan of CH_2CO_2 and was also identified by ChemSpider matching at CL4. The MS2 spectrum of sulfonamido diacetic acid shows two pairs of neutral losses of CH_2O_2, indicating that diacetic acid was linked to the sulfonamido group. The main characteristic fragment was SO_2F^- (82.9603), while the intensity of SO_2N^- (77.9644) was notably weak (**Figure 45**). A substance with the same precursor ion and similar MS2 spectrum was previously proposed as the anhydride form.[32] Considering the observation of two neutral losses of CH_2COOH as a feature of dicarboxylic acid, the ChemSpider match of FBSEE diacid, and the possible presence of the degradation product of FBSEE diol, we proposed the structure of FBSEE diacid with CL2b.

The semiquantified concentrations of FBSEE diacid in sewage ranged from n.d. to 0.029

μg/L and increased up to n.d. to 12.5 μg/L in effluents (**Table 27**). There is no literature or patents indicating that FBSEE diacid is used in the semiconductor manufacturing process. The concentrations of FBSEE diacid in sewage were relatively low, and they dramatically increased by approximately 900 times after treatment. We attributed the presence of FBSEE diacid to the final oxidation of FBSEE diol through microbial biotransformation during the procedures of WWTPs. FBSEE diol was reported to be rapidly transformed to a diacid,[72] which corresponded to our de tection of FBSEE diacid in both sewage and effluents from the semiconductor industry.

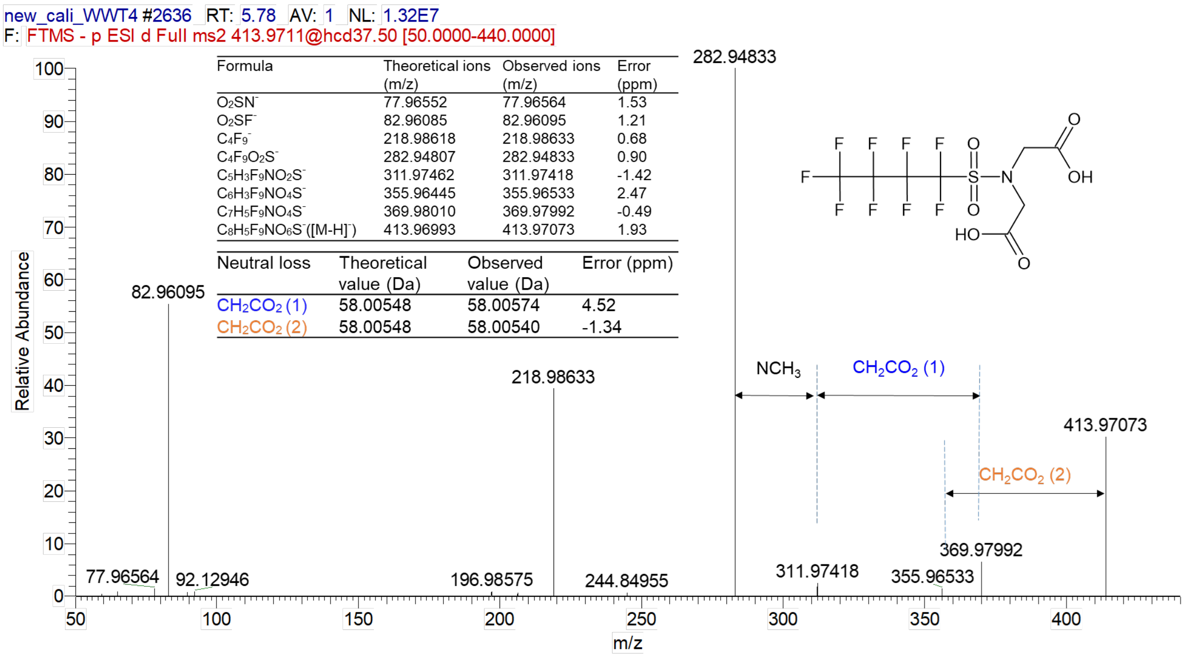

Formula	Theoretical ions (m/z)	Observed ions (m/z)	Error (ppm)
O_2SN^-	77.96552	77.96564	1.53
O_2SF^-	82.96085	82.96095	1.21
$C_4F_9^-$	218.98618	218.98633	0.68
$C_4F_9O_2S^-$	282.94807	282.94833	0.90
$C_5H_3F_9NO_2S^-$	311.97462	311.97418	-1.42
$C_6H_3F_9NO_4S^-$	355.96445	355.96533	2.47
$C_7H_5F_9NO_4S^-$	369.98010	369.97992	-0.49
$C_8H_5F_9NO_6S^-$([M-H]$^-$)	413.96993	413.97073	1.93

Neutral loss	Theoretical value (Da)	Observed value (Da)	Error (ppm)
CH_2CO_2 (1)	58.00548	58.00574	4.52
CH_2CO_2 (2)	58.00548	58.00540	-1.34

Figure 45 MS2 spectrum of FBSEE diacid

Subclass 6 N-hydroxyethyl sulfonamido acetic acid The substance with the precursor ion 399.9903 was identified by the specific fragment of $[O_2SNC_2H_4O]^-$ (121.9912). The An obvious fragment 341.9852 was referred to as the FBSE fragment. The difference between 341.9852 and 399.9903 represents the neutral loss of CH_2CO_2 (**Figure 46**). Consequently, we referred to this substance as N-(2-hydroxyethyl) perfluorobutane sulfonamido acetic acid (FBSEE mono-ol monoacid) at confidence level 2b.[73] The concentrations of FBSEE mono-ol monoacid were determined semiquantitatively to range from n.d. to 0.372 µg/L and n.d. to 0.312 µg/L in sewage and effluent, respectively (**Table 27**). No literature or patents have claimed that FASEE mono-ol monoacid has been used in the semiconductor process. We presumed that the occurrence of FASEE mono-ol monoacid in wastewater was due to the one-side chain oxidation of FBSEE diol, and it is further oxidized to the final oxidation product as FBSEE diacid. FASEE mono-ol monoacid, as an intermediate metabolite of FBSEE diol, was identified for the first time.

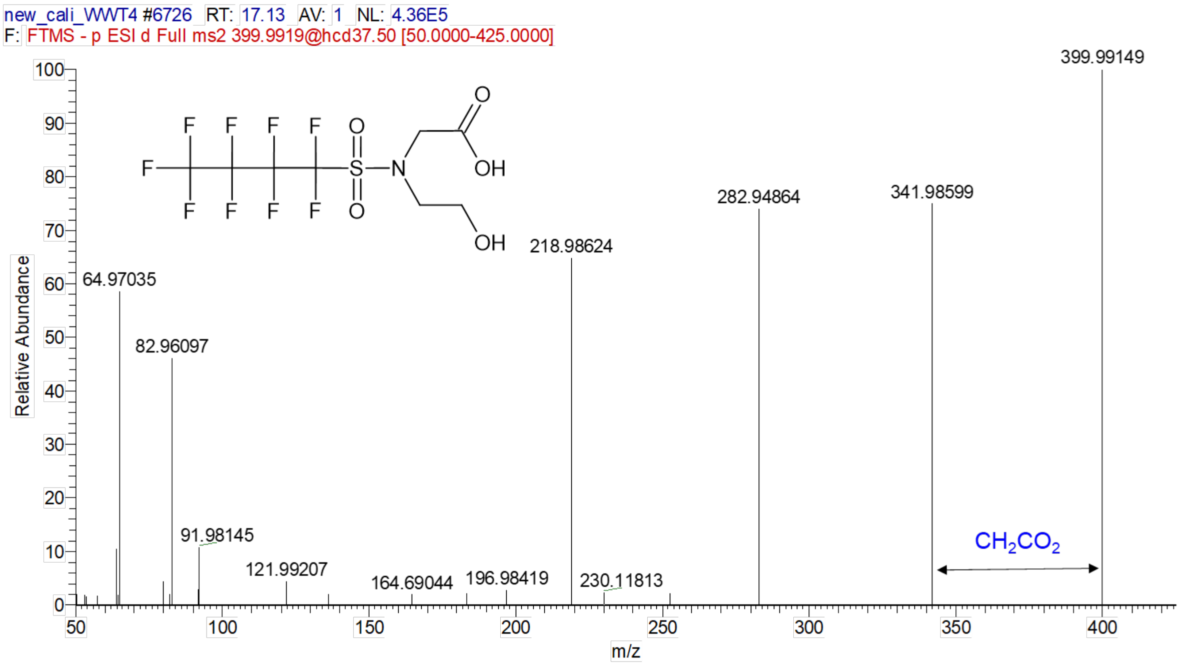

Formula	Theoretical ions (m/z)	Observed ions (m/z)	Error (ppm)
HO_2S^-	64.97027	64.97035	1.23
O_2SF^-	82.96085	82.96097	1.45
$O_2SNCH_2^-$	91.98117	91.98145	3.03
$O_2SNC_2H_4O^-$	121.99174	121.99207	2.75
$C_4F_9^-$	218.98618	218.98624	0.27
$C_4F_9SO_2^-$	282.94807	282.94864	2.00
$C_6H_5F_9NO_3S^-$	341.98519	341.98599	2.35
$C_8H_7F_9NO_5S^-$ ($[M-H]^-$)	399.99067	399.99149	2.06

Neutral loss	Theoretical value (Da)	Observed value (Da)	Error (ppm)
CH_2CO_2	58.00548	58.00550	0.38

Figure 46 MS2 spectrum of FBSEE mono-ol monoacid

Subclass 7 Sulfonamido acealdehyde The class with the structure where sulfonamido linked to acetaldehyde. $C_6H_3F_9NO_3S^-$(339.9703, 2.09 ppm) was observed with the fragments $[O_2S]^-$ (63.9625, 0.67 ppm) and $[HO_2S]^-$(64.9703, 0.58 ppm), along with the RT of ~31 min, which was detected for the first time as perfluorobutane sulfonamido acetaldehyde (**Figure 47**). A structure isomer was observed with higher polarity (RT 13 min) and was identified as perfluorobutane sulfonamido acetaldehyde (enol form) at CL3a (**Figure 48**).

doi:10.6342/NTU202402180

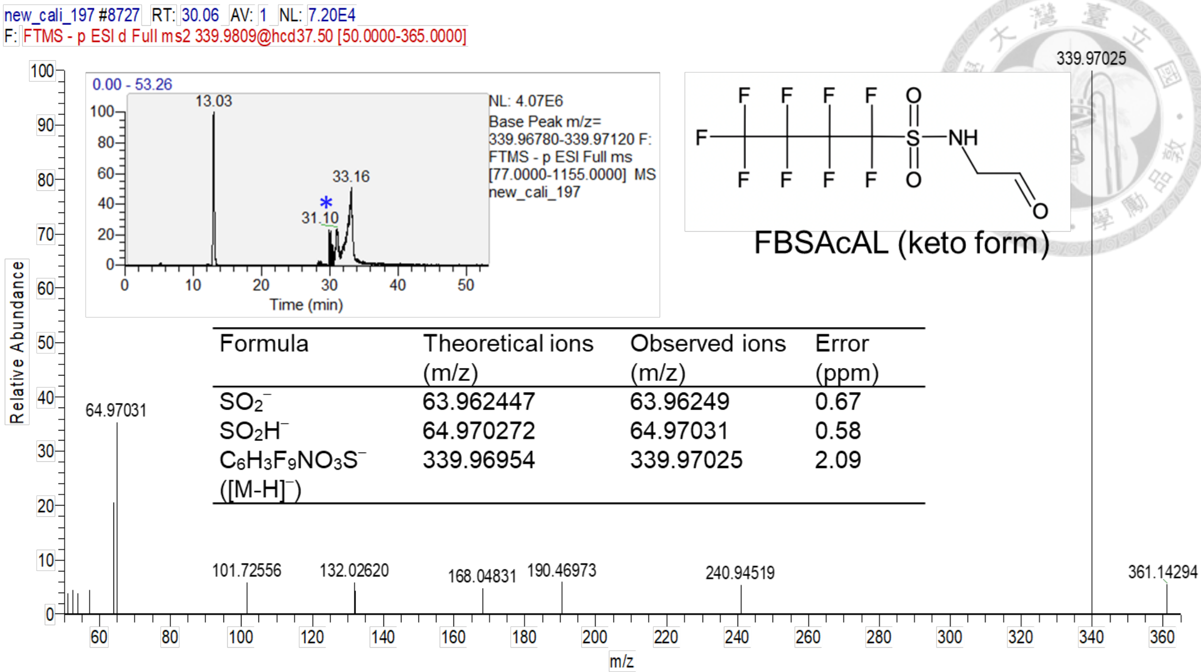

Formula	Theoretical ions (m/z)	Observed ions (m/z)	Error (ppm)
SO_2^-	63.962447	63.96249	0.67
SO_2H^-	64.970272	64.97031	0.58
$C_6H_3F_9NO_3S^-$ ($[M-H]^-$)	339.96954	339.97025	2.09

Figure 47 MS2 spectrum of FBSAcAL (keto form) from sample no. 197.

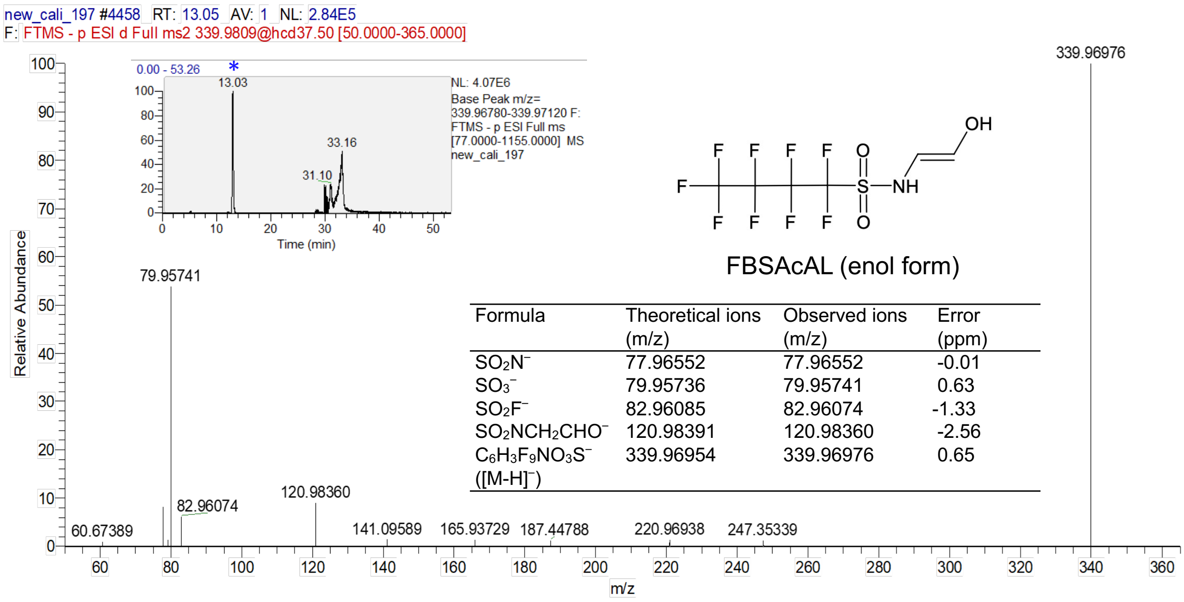

Formula	Theoretical ions (m/z)	Observed ions (m/z)	Error (ppm)
SO_2N^-	77.96552	77.96552	-0.01
SO_3^-	79.95736	79.95741	0.63
SO_2F^-	82.96085	82.96074	-1.33
$SO_2NCH_2CHO^-$	120.98391	120.98360	-2.56
$C_6H_3F_9NO_3S^-$ ($[M-H]^-$)	339.96954	339.96976	0.65

Figure 48 MS2 spectrum of FBSAcAL (enol form) from sample no. 197.

doi:10.6342/NTU202402180

Subclass 8 Sulfonamido acealdehyde hydrate/hemiacetal $[C_6H_5F_9NO_4S]^-$ (357.9812, 2.99 ppm) was observed with a neutral loss of H_2O which was identified as perfluoroalkane sulfonamido acetaldehyde hydrate, as water adds to the carbonyl function of acetaldehydes (**Figure 49**). Moreover, $[C_7H_7F_9NO_4S]^-$ (371.9954, -0.89 ppm) was detected with a neutral loss of CH_3OH, which indicated the production of additional reaction of methanol to acetaldehyde. Hydrates and hemiacetals are the products of addition reactions of oxygen-based nucleophiles, such as water and methanol, to aldehydes, which have been reported for the first time.

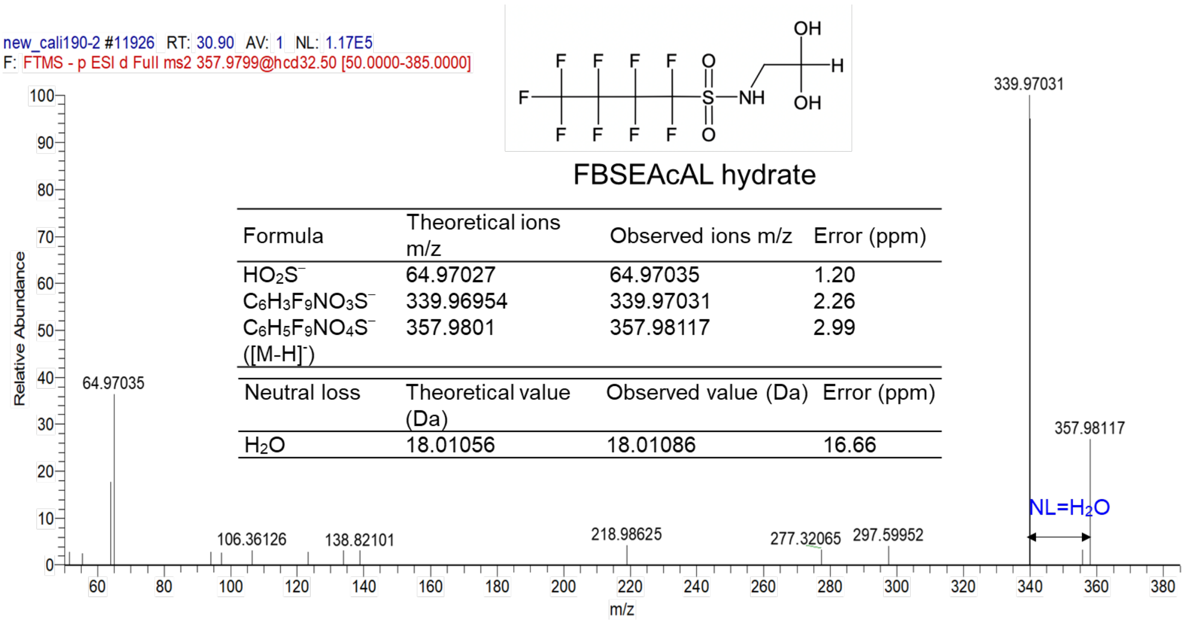

Formula	Theoretical ions m/z	Observed ions m/z	Error (ppm)
HO_2S^-	64.97027	64.97035	1.20
$C_6H_3F_9NO_3S^-$	339.96954	339.97031	2.26
$C_6H_5F_9NO_4S^-$ ($[M-H]^-$)	357.9801	357.98117	2.99

Neutral loss	Theoretical value (Da)	Observed value (Da)	Error (ppm)
H_2O	18.01056	18.01086	16.66

Figure 49 MS2 spectrum of FBSAcAL hydrate from sample no. 190

Class III Perfluoroalkyl acids (PFAAs)

Subclass 9 carboxylic acid Integrating CO_2 neutral loss into the nontarget approach improves the identification of carboxylic acid-containing compounds, revealing their collision

doi:10.6342/NTU202402180

characteristics in the CAD cell, including subclasses 9a-9e, encompassing perfluoroalkyl carboxylic acids (PFCAs), unsaturated PFCAs (U-PFCAs), Unsaturated-E-PFCAs (U-E-PFCAs), hydro-substituted PFCAs (H-PFCAs), and hydro-substituted E-PFCAs (H-E-PFCAs). Trifluoroacetic acid (TFA, C2) and perfluoropropionic acid (PFPrA, C3) were identified with fragments from $[CF_3]^-$ and $[C_2F_5]^-$, respectively, and produced neutral loss of CO_2 as well. TFA and PFPrA were subsequently confirmed and elevated to CL1a based on the matching of RTs (1.4 min for TFA, 2.7 min for PFPrA) and MS2 spectrum of the authentic standard. TFA and PFPrA were detected with an average of approximately 1 μg/L and 0.01 μg/L, respectively, in 46 samples from 13 drinking water suppliers in Germany.[74] PFPrA has been reported in influent (1.1–41 ng/L) and effluent (<0.1–38 ng/L) from municipal WWTPs.[75] TFA and PFPrA were detected in all samples with concentrations of 2.65-19.9 μg/L in sewage and 3.00-20.1 μg/L in effluents. In comparison with a previous study, TFA and PFPrA were reported in wastewater from three electronic fabrication facilities at concentrations of 1.57-15.3 μg/L and 0.237-4.18 μg/L, respectively.[27] Trifluoroacetic anhydride has been claimed to passivate the compound semiconductor surface by terminating the surface;[76] thus, the occurrence of ultrashort-chain TFA and PFPrA in sewage seems to be equal and comparable with a previous study.[27]

The MS2 spectrum of U-E-PFCA(C6) is shown in **Figure 50**. The detection of CO_2 alongside other fluorinated fragments ($[C_3F_5]^-$, $[C_4F_7]^-$, $[C_5F_9O]^-$, $[C_6F_9O_3]^-$) and confirmation through isotope pattern matching with a formula of $C_6F_9O_3H$ allowed us to propose the structure of U-E-PFCA (C6) as CL 3a due to uncertainties regarding the position of the unsaturated bond.

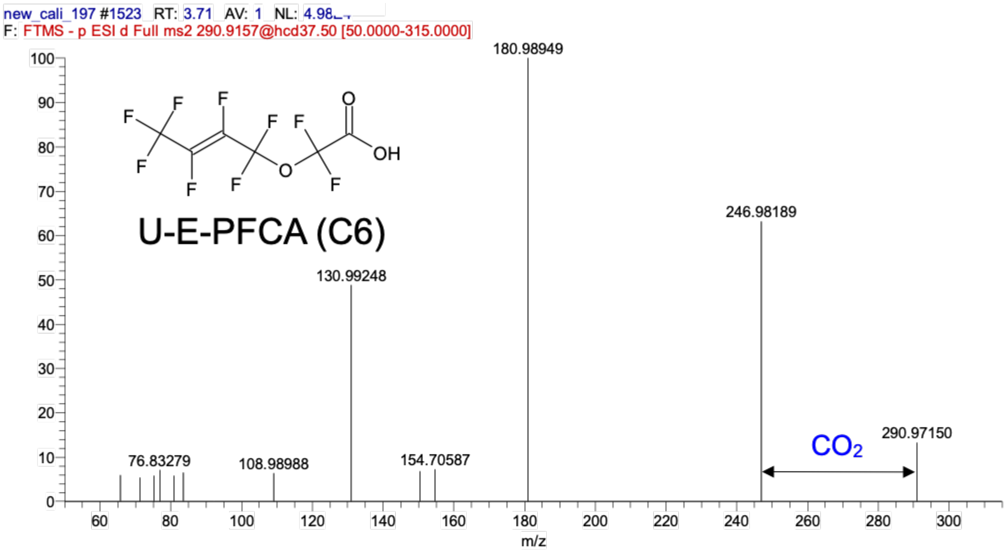

Formula	Theoretical ions (m/z)	Observed ions (m/z)	Error (ppm)
$C_3F_5^-$	130.99256	130.99248	-0.61
$C_4F_7^-$	180.98937	180.98949	0.66
$C_5F_9O^-$	246.98109	246.98189	3.24
$C_6F_9O_3^-$ ($[M-H]^-$)	290.97092	290.97150	2.00

Neutral loss	Theoretical value (Da)	Observed value (Da)	Error (ppm)
CO_2	43.98983	43.98961	-4.96

Figure 50 MS2 spectrum of U-E-PFCA(C6)

In addition, hydro-substituted PFCAs (H-PFCAs), hydro-substituted E-PFCAs (H-E-PFCAs) and H_n-E-PFCAs (subclasses 9d and 9e) produced neutral loss of CO_2HF, which was derived through the combination of CO_2 and HF, with HF originating from the hydrogen-substituted fluoroalkyl chain, as their MS2 spectrum are shown in **Figure 51** and **Figure 52** for

H-PFCA(C4) and H_2-E-PFCA(C4) respectively. Contrarily, achieving a neutral loss of CO_2 in the PFCA series typically requires the presence of $[M\text{-}H]^-$ as a precursor ion and $[M\text{-}H\text{-}CO_2]^-$ as a product ion. However, due to E-PFCA's inherent susceptibility to in-source collision-induced dissociation (CID),[32, 77] CO_2 can be lost, resulting in the formation of $[M\text{-}H\text{-}CO_2]^-$ as the precursor ion. Subsequently, within the collision chamber, C–O cleavage generates $[C_xF_yO_z]^-$ fragments. Thus, there is no neutral loss of CO_2 between the precursor ion and the production ion. This occurrence was observed during our QC sample testing with HFPO-DA (GenX), where the precursor ion was identified as $[M\text{-}H\text{-}CO_2]^-$ (284.9779) in **Table 33** and the product ion as $[C_3F_7O]^-$ (184.9842) in Table 34, precluding a neutral loss of 44. Therefore, E-PFAC detection relies on $C_nF_{2n+1}O^-$ fragments and isotope pattern matching rather than CO_2 screening. This aspect is also outlined in **Table 21**, highlighting the importance of simultaneously scanning the fluorinated tail and polar head to enhance the effectiveness of fragment-based nontarget analysis.

doi:10.6342/NTU202402180

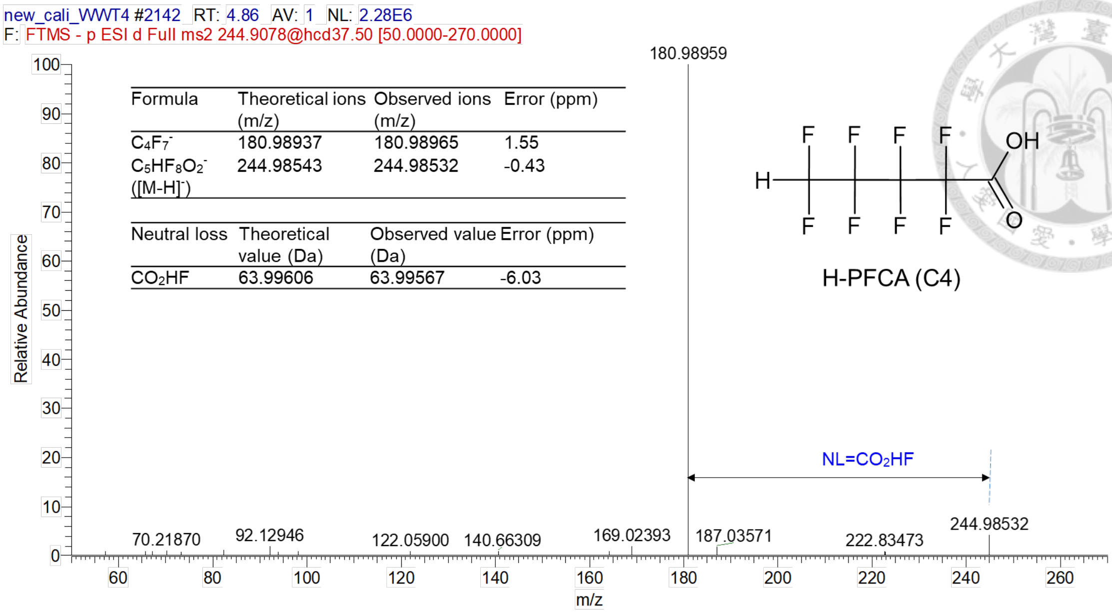

Formula	Theoretical ions (m/z)	Observed ions (m/z)	Error (ppm)
$C_4F_7^-$	180.98937	180.98965	1.55
$C_5HF_8O_2^-$ ($[M-H]^-$)	244.98543	244.98532	-0.43

Neutral loss	Theoretical value (Da)	Observed value (Da)	Error (ppm)
CO_2HF	63.99606	63.99567	-6.03

Figure 51 MS2 spectrum of H-PFCA(C4). The confident level remained at 3a due to the uncertainty of H position.

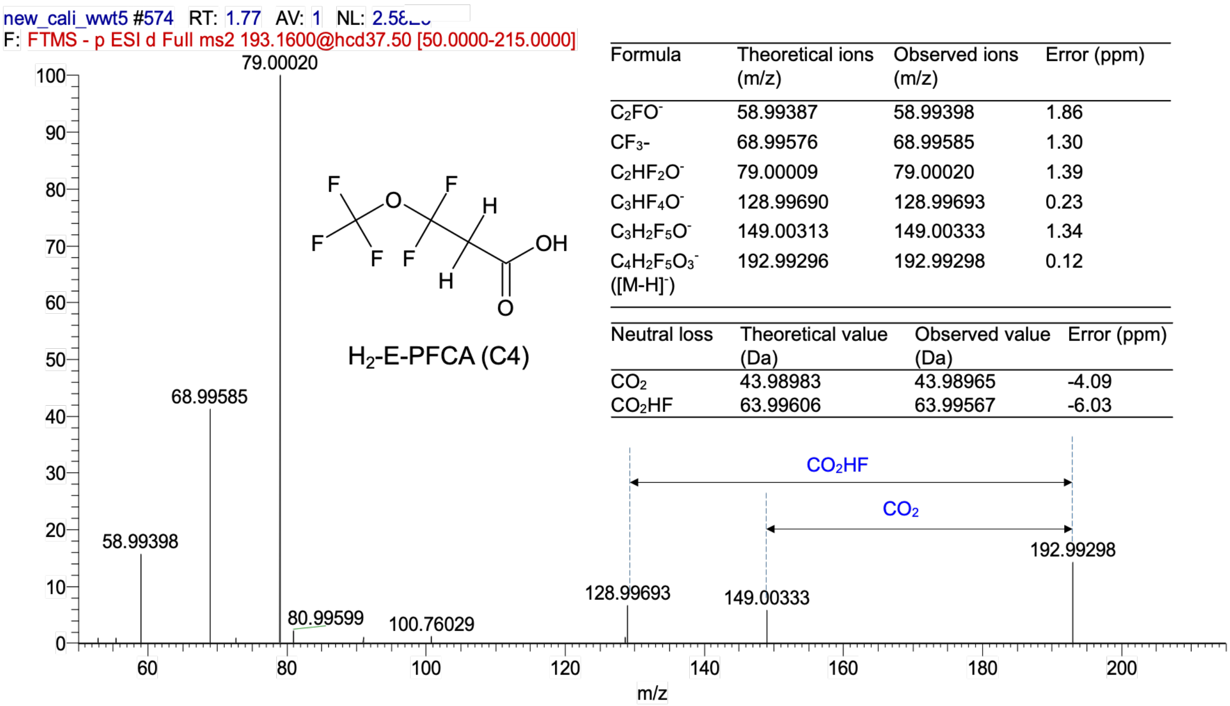

Formula	Theoretical ions (m/z)	Observed ions (m/z)	Error (ppm)
C_2FO^-	58.99387	58.99398	1.86
CF_3-	68.99576	68.99585	1.30
$C_2HF_2O^-$	79.00009	79.00020	1.39
$C_3HF_4O^-$	128.99690	128.99693	0.23
$C_3H_2F_5O^-$	149.00313	149.00333	1.34
$C_4H_2F_5O_3^-$ ($[M-H]^-$)	192.99296	192.99298	0.12

Neutral loss	Theoretical value (Da)	Observed value (Da)	Error (ppm)
CO_2	43.98983	43.98965	-4.09
CO_2HF	63.99606	63.99567	-6.03

Figure 52 MS2 spectrum of H_2-E-PFCA(C4)

Subclass 10 dicarboxylic acid Perfluoroalkyl dioic acids (PFdiCA) are comprised of the functional group of dicarboxylic acid. PFdiCA (C3-C5) were detected with a neutral loss of CO_2; PFdiCA (C6-C8) lacked the detection of neutral loss of CO_2, presumably due to their low abundance in the samples. The fragment-based fluoroalkyl chain such as $[C_xF_y]^-$ and the isotopic pattern of fluorine could be alternatives to identify this subclass. Enormous perfluoroalkyl fragments $[C_2F_3]^-$, $[C_3F_5]^-$, $[C_4F_7]^-$, $[C_5F_9]^-$, and $[C_6F_{11}]^-$ were set as indicators, and PFdiCAs (C4-C7) were recognized (**Figure 53** and **Figure 54**). The fragments $[C_2HF_2O_2]^-$, $[C_3HF_4O_2]^-$ and $[C_4HF_6O_2]^-$ were detected with neutral loss of CO_2 from PFdiCAs (C3-C5) as $[M-H-CO_2]^-$. Perfluorobutyl dicarboxylic acid (PFdiCA, C4) has been patented as a quencher in a photoresist,[7,78] and perfluorohexyl dicarboxylic acid (PFdiCA, C6) has been patented as an antireflective coating.[7,79] The presence of PFdiCAs (C3-C8) in semiconductor manufacturing is reported for the first time. The semi-quantitative levels of PFdiCAs (C3-C8) were n.d. to 0.431 μg/L in sewage and n.d. to 0.390 μg/L in effluents.

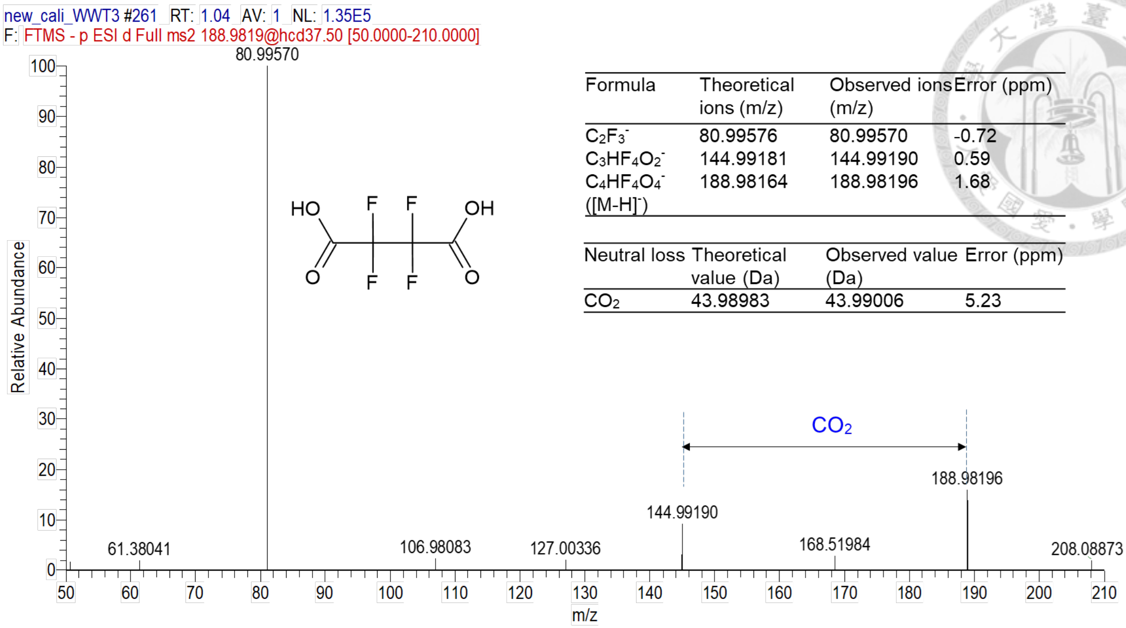

Formula	Theoretical ions (m/z)	Observed ions (m/z)	Error (ppm)
$C_2F_3^-$	80.99576	80.99570	-0.72
$C_3HF_4O_2^-$	144.99181	144.99190	0.59
$C_4HF_4O_4^-$ ($[M-H]^-$)	188.98164	188.98196	1.68

Neutral loss	Theoretical value (Da)	Observed value (Da)	Error (ppm)
CO_2	43.98983	43.99006	5.23

Figure 53 MS2 spectrum of PFdiCA(C4) from the sample (WWTP3)

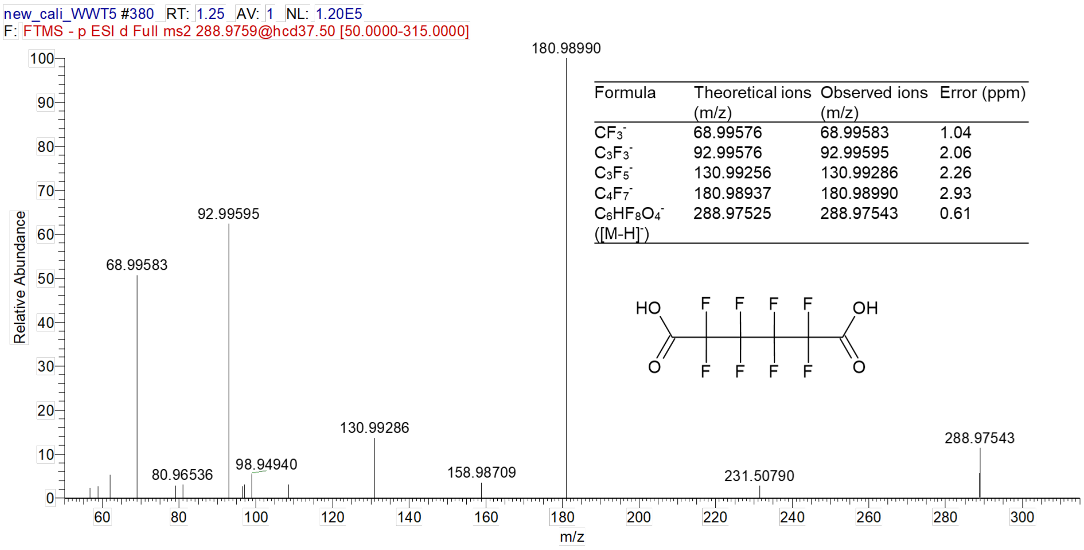

Formula	Theoretical ions (m/z)	Observed ions (m/z)	Error (ppm)
CF_3^-	68.99576	68.99583	1.04
$C_3F_3^-$	92.99576	92.99595	2.06
$C_3F_5^-$	130.99256	130.99286	2.26
$C_4F_7^-$	180.98937	180.98990	2.93
$C_6HF_8O_4^-$ ($[M-H]^-$)	288.97525	288.97543	0.61

Figure 54 MS2 spectrum of PFdiCA(C6) from the sample (WWTP5)

Subclass 11 sulfonic acid Perfluoroalkyl sulfonic acids (PFSAs, subclass 11a, C1 and C4) and hydrogen-substituted PFSA (H-PFSA, subclass 11b, C2-C4) were distinguished by the presence of $[SO_3]^-$ and $[SO_3F]^-$. Trifluoromethanesulfonic acid (TFMS) was identified based on the quick peak at RT 1.8 min in chromatography with the specific fragments $[CF_3]^-$, $[SO_3]^-$, $[FO_2S]^-$, and $[FO_3S]^-$ (**Figure 55**) and further reached CL1 after confirmation with an authentic standard (**Figure 56**). In the case of multi-hydrogen-substituted perfluoroalkyl ether sulfonic acids (H_2-E-PFSA, C4), the dominant fragments of polar head shifted from $[SO_3]^-$ to $[HSO_3]^-$. Additionally, for the subclasses with hydrogen-substituted PFSAs, such as H-PFSA(C2, C3) and H_2-E-PFSA (C4), a neutral loss of HF was observed (**Figure 57**). TFMS has been recently reported in environmental water samples at concentrations up to 1 μg/L from three European countries.[80] Moreover, TFMS were detected with an average of approximately 0.1 μg/L in 46 samples from 13 drinking water suppliers in Germany.[74] TFMS were reported in three wastewater effluents from electronic fabrication facilities at concentration of 0.121-0.175 μg/L.[27] TFMS is used in the manufacture of chemicals and optic, electric and electronic equipment[81,82] and as a photo-acid generator in photolithography.[20, 83]

The quantitative levels of TFMS were 0.004-0.489 μg/L in sewage and 0.342-1.42 μg/L in effluents (**Table 27**), possibly elevated in effluents due to contributions from other industrial wastewater. TFMS concentrations (0.121-0.175 μg/L) in past studies on electronic fabrication wastewater effluents[27] similar to our findings, likely linked to its use as a PAG to replace PFOS in photolithography photoresist.[20, 83]

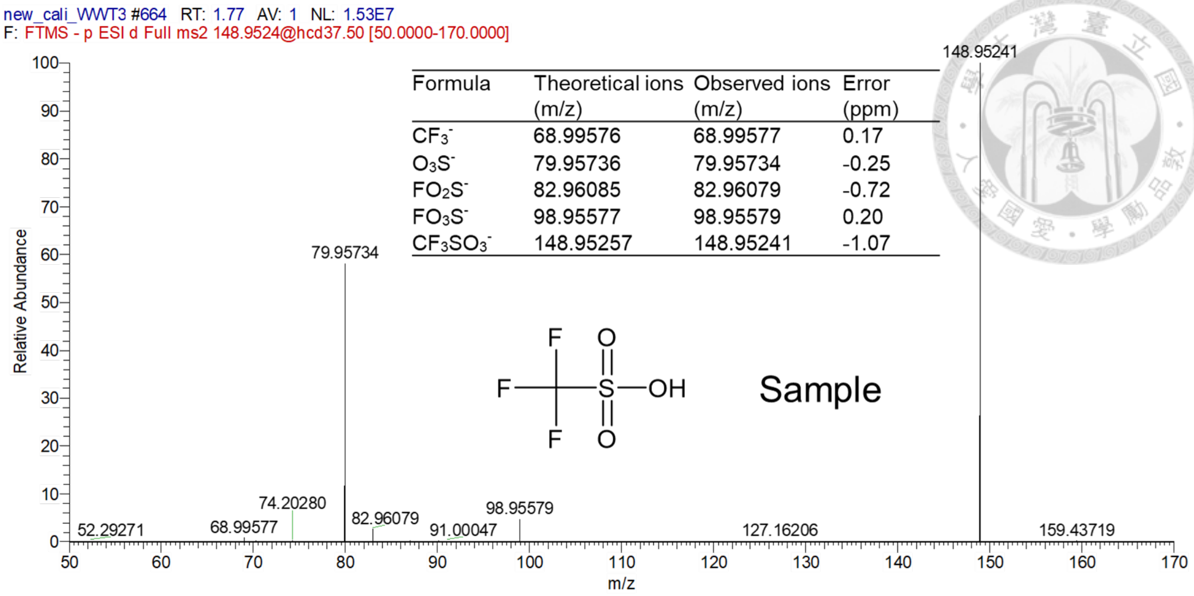

Formula	Theoretical ions (m/z)	Observed ions (m/z)	Error (ppm)
CF_3^-	68.99576	68.99577	0.17
O_3S^-	79.95736	79.95734	-0.25
FO_2S^-	82.96085	82.96079	-0.72
FO_3S^-	98.95577	98.95579	0.20
$CF_3SO_3^-$	148.95257	148.95241	-1.07

Figure 55 MS2 spectrum of TFMS from the sample (WWTP3)

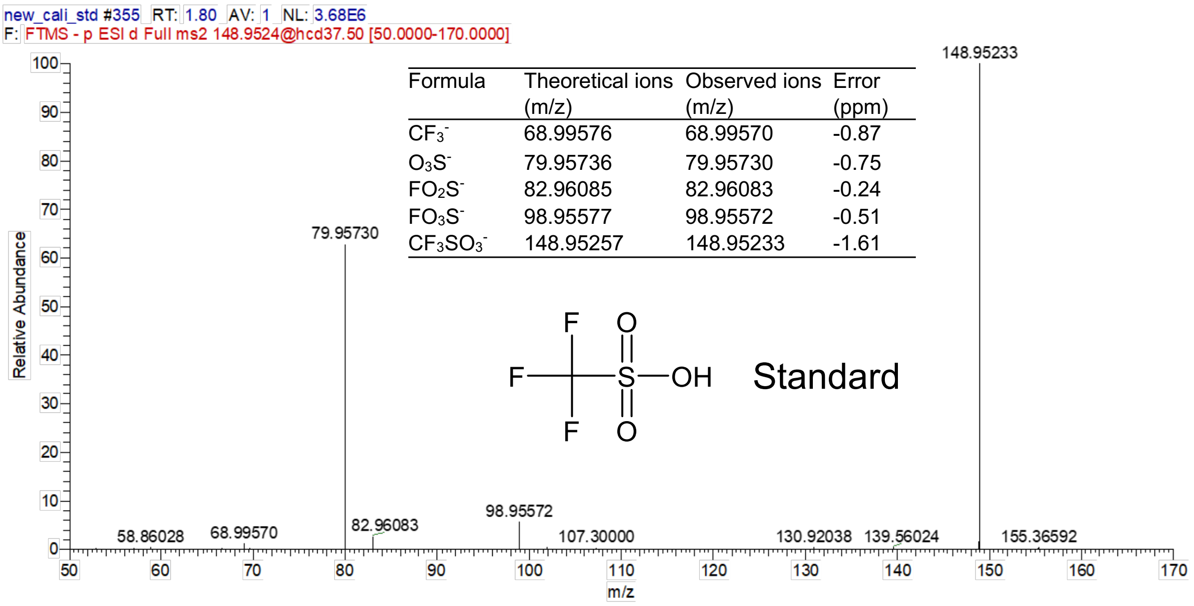

Formula	Theoretical ions (m/z)	Observed ions (m/z)	Error (ppm)
CF_3^-	68.99576	68.99570	-0.87
O_3S^-	79.95736	79.95730	-0.75
FO_2S^-	82.96085	82.96083	-0.24
FO_3S^-	98.95577	98.95572	-0.51
$CF_3SO_3^-$	148.95257	148.95233	-1.61

Figure 56 MS2 spectrum of TFMS from the authentic standard

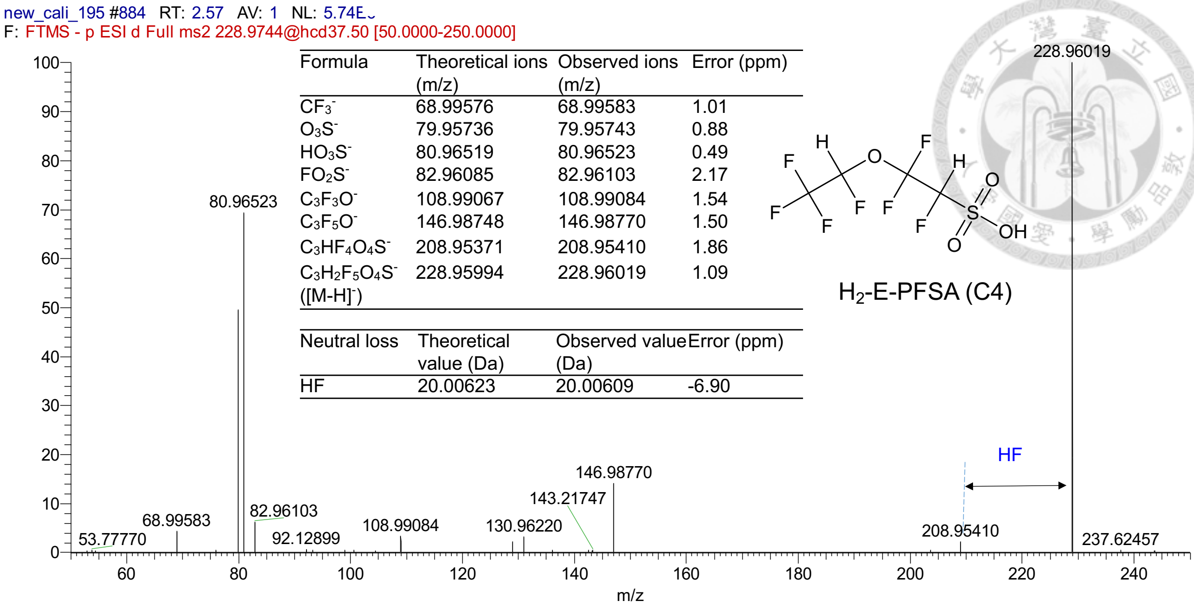

Formula	Theoretical ions (m/z)	Observed ions (m/z)	Error (ppm)
CF_3^-	68.99576	68.99583	1.01
O_3S^-	79.95736	79.95743	0.88
HO_3S^-	80.96519	80.96523	0.49
FO_2S^-	82.96085	82.96103	2.17
$C_3F_3O^-$	108.99067	108.99084	1.54
$C_3F_5O^-$	146.98748	146.98770	1.50
$C_3HF_4O_4S^-$	208.95371	208.95410	1.86
$C_3H_2F_5O_4S^-$ ($[M-H]^-$)	228.95994	228.96019	1.09

Neutral loss	Theoretical value (Da)	Observed value (Da)	Error (ppm)
HF	20.00623	20.00609	-6.90

Figure 57 MS2 spectrum of E-H_2-PFSA(C4) with fragments $[SO_3H]^-$, $[SO_3]^-$, $[SO_2F]^-$, $[CF_3]^-$, $[C_3F_3O]^-$, $[C_3F_5O]^-$ were detected. The substitution of F by hydrogen produces the neutral loss of HF. Due to the uncertainty of the position of H atom, it was set to level 3a

Subclass 12 Sulfinic acid Subclass 4 perfluorobutyl sulfinate (PFBSi) was identified with clear fragments of $[SO_2F]^-$ as the specific feature of sulfinic acid (**Figure 60**). It was further confirmed with an authentic standard based on the RT and the MS2 spectrum (**Figure 61**). Recently, PFBSi has been reported in a river from manufacturing facilities in Alabama,[57] surface water,[32] landfill leachate and groundwater,[35] and PFBSi was reported as a biodegradation product from MeFBSE.[84] Perfluoroalkane sulfinic acids, arising from the degradation of commercial precursor compounds containing the $C_nF_{2n+1}SO_2N$ moiety, may act as degradation by-products of fluorosurfactants in 3M foam.[2, 73]

PFBSi was detected at concentrations of 0.152-4.24 μg/L in sewage from semiconductor plants A, B, C, and D and at concentrations of 1.83 and 1.99 μg/L in effluents from their

doi:10.6342/NTU202402180

WWTPs (**Table 27**). In contrast, PFBSi was not detected in the sewage of semiconductor plant E or in the effluent of WWTP5. In most studies, PFBSi was identified through nontarget screening with no further quantitation[35,32,57], and this is the first study to identify PFBSi with quantitative analysis in the environment. The presence of PFBSi was related to the presence of perfluorobutane sulfonamido substances, and further discussion follows.

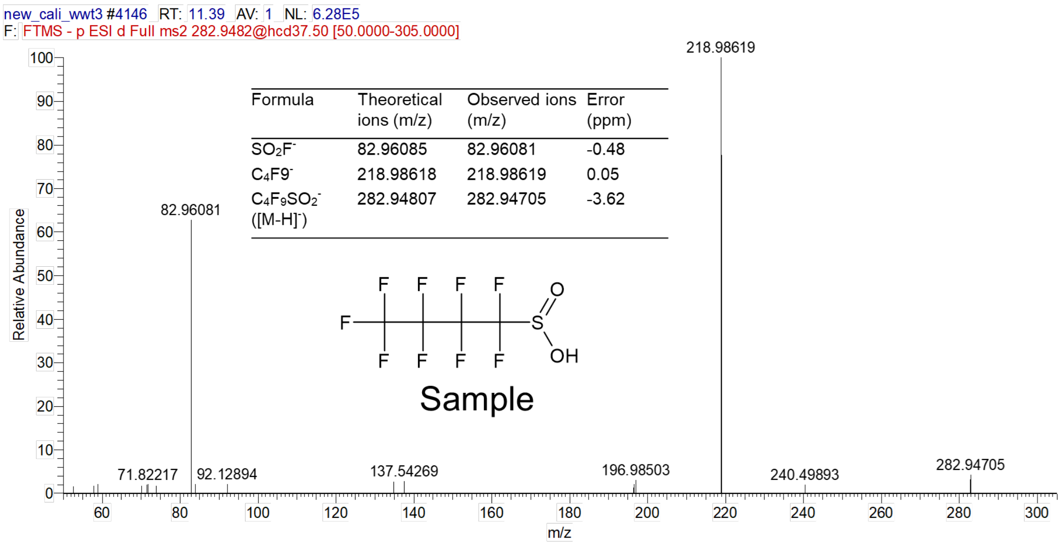

Formula	Theoretical ions (m/z)	Observed ions (m/z)	Error (ppm)
SO_2F^-	82.96085	82.96081	-0.48
$C_4F_9^-$	218.98618	218.98619	0.05
$C_4F_9SO_2^-$ ([M-H]$^-$)	282.94807	282.94705	-3.62

Figure 58 MS2 spectrum of PFBSi from sample WWTP3.

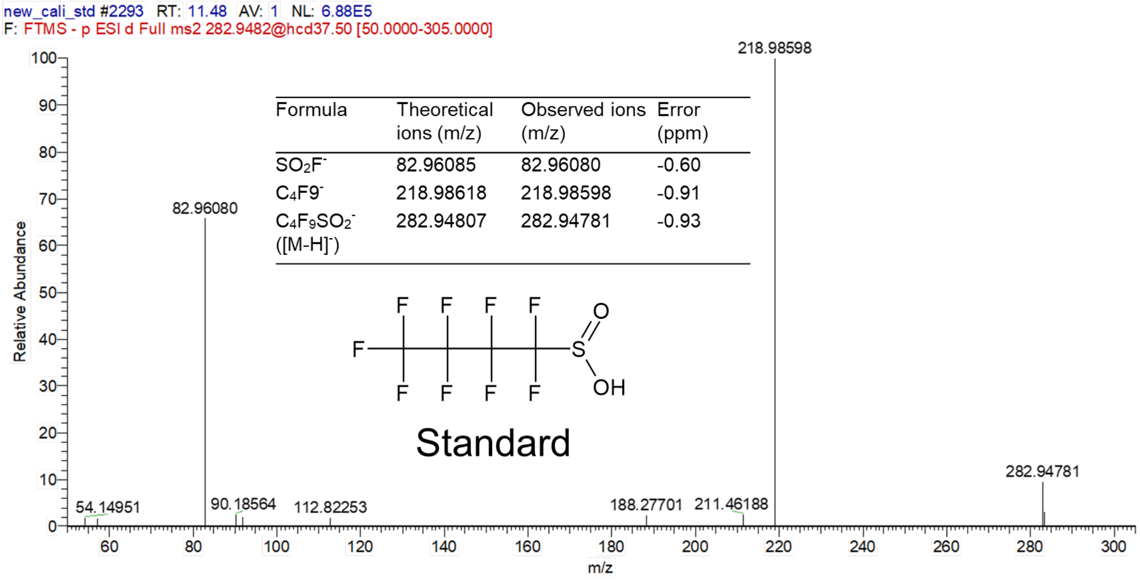

Formula	Theoretical ions (m/z)	Observed ions (m/z)	Error (ppm)
SO_2F^-	82.96085	82.96080	-0.60
$C_4F_9^-$	218.98618	218.98598	-0.91
$C_4F_9SO_2^-$ ([M-H]$^-$)	282.94807	282.94781	-0.93

Figure 59 MS2 spectrum of PFBSi from authentic standard

4.2.3. Concentrations of Nontarget PFAS

4.2.3.1. Calibration of CL1-identified PFAS

Quantification of 7 CL-1 identified PFAS was carried out using the 1/x weighted least squares linear regression method with external standards. The quantification of 7 CL1-identified PFAS on the LC–QE resulted in correlation coefficients (R^2) exceeding 0.995, and the calibration curve was established based on an external standard as shown in **Table 25**. The quantification formula is as follows:

$$y=a*x+b \qquad \text{(Eq 1)}$$

where y equals the response of the precursor ion of CL1-identified PFAS (A_T) (**Table 25**) and x equals the concentration of the PFAS (C_T).

Table 25 The calibration of 7 CL1-identified PFAS on the LC–QE

Acronym	Linearity (μg/L)	LOQ[1] (μg/L)	R^2	Standard type	Adduct ion	Precursor ion	Theoretical m/z of precursor ion[2]
TFA	0.5-75	0.5	0.9965	External	$[M-H]^-$	$C_2F_3O_2^-$	112.98559
PFPrA	0.5-75	0.5	0.9957	External	$[M-H]^-$	$C_3F_5O_2^-$	162.98239
TFMS	0.5-75	0.5	0.9962	External	$[M-H]^-$	$CF_3O_3S^-$	148.95257
PFBSi	0.5-75	0.5	0.9975	External	$[M-H]^-$	$C_4F_9O_2S^-$	282.94807
FBSA	0.5-75	0.5	0.9959	External	$[M-H]^-$	$C_4HF_9NO_2S^-$	297.95897
FBSE	0.5-50	0.5	0.9983	External	$[M-H]^-$	$C_6H_5F_9NO_3S^-$	341.98519
FBSEE diol	0.5-50	0.5	0.9986	External	$[M+CH_3COO]^-$	$C_9H_{13}F_9NO_6S^-$	446.03253

[1] The limit of quantification (LOQ) was determined as the lowest linear calibration point with the presence of a MS2 fragment.

[2] Precursor ion was used as a quantitative ion with 5 ppm mass accuracy of the theoretical m/z

4.2.3.2.Semi-quantitative Process

Semiquantitative analysis was performed on tentatively identified PFAS through nontarget analysis, as no authentic standards were available for further qualitative and quantitative analysis. Therefore, the semi-quantification of these PFAS relied on calibration using ‘selective reference compounds’ with similar structures, comparable RTs, or identical fluoroalkyl chain. The average response factor ($\overline{RF_R}$) from at least five different concentrations of the selective reference standard was calculated and applied for semiquantification (**Table 26**). For example, in cases where no authentic standard was available for PFdiCA, we used PFBA, which has a similar structure, as the selective reference standard. The $\overline{RF_R}$ of PFBA was determined by measuring the responses from at least five different concentrations of PFBA. The quantification formula is as follows:

$$y=\overline{RF_R}*x \qquad \text{(Eq 3)}$$

where y represents the response of the precursor ion (**Table 26**) of the tentatively identified PFAS (A), and x represents the concentration of the identified PFAS (C), which could be calculated once 'y' was determined.

doi:10.6342/NTU202402180

Table 26 Semi-quantitative analysis of 13 tentatively identified PFAS on the LC–QE

Acronym	Selective reference standard	Calibration type	Standard type	Precursor ion	Formula of precursor ion	Theoretical m/z of precursor ion[1]
PFdiCA(C3)	PFBA	$y=\overline{RF}_{PFBA}*x$	External	$[M-H]^-$	$C_3HF_2O_4^-$	138.98484
PFdiCA(C4)	PFBA	$y=\overline{RF}_{PFBA}*x$	External	$[M-H]^-$	$C_4HF_4O_4^-$	188.98164
PFdiCA(C5)	PFBA	$y=\overline{RF}_{PFBA}*x$	External	$[M-H]^-$	$C_5HF_6O_4^-$	238.97845
PFdiCA(C6)	PFBA	$y=\overline{RF}_{PFBA}*x$	External	$[M-H]^-$	$C_6HF_8O_4^-$	288.97525
PFdiCA(C7)	PFBA	$y=\overline{RF}_{PFBA}*x$	External	$[M-H]^-$	$C_7HF_{10}O_4^-$	338.97206
PFdiCA(C8)	PFBA	$y=\overline{RF}_{PFBA}*x$	External	$[M-H]^-$	$C_8HF_{10}O_4^-$	388.96887
MeFBSA	FBSA	$y=\overline{RF}_{FBsA}*x$	External	$[M-H]^-$	$C_5H_3F_9NO_2S^-$	311.97462
FTSE	FBSE	$y=\overline{RF}_{FBsE}*x$	External	$[M-H]^-$	$C_4H_5F_5NO_3S^-$	241.99158
FPrSE	FBSE	$y=\overline{RF}_{FBsE}*x$	External	$[M-H]^-$	$C_5H_5F_7NO_3S^-$	291.98838
FBSAA	PFBS	$y=\overline{RF}_{PFBs}*x$	External	$[M-H]^-$	$C_6H_3F_9NO_4S^-$	355.96445
MeFBSAA	PFBS	$y=\overline{RF}_{PFBs}*x$	External	$[M-H]^-$	$C_7H_5F_9NO_4S^-$	369.98120
FBSAA diacid	PFBS	$y=\overline{RF}_{PFBs}*x$	External	$[M-H]^-$	$C_8H_5F_9NO_6S^-$	413.96993
FBSEE mono-ol monoacid	PFBS	$y=\overline{RF}_{PFBs}*x$	External	$[M-H]^-$	$C_8H_7F_9NO_5S^-$	399.99067

[1] Precursor ion was used as a quantitative ion with 5 ppm mass accuracy of the theoretical m/z

4.2.3.3.Quantitation/ Semi-quantitation

Table 27 provide a summary of 20 identified PFAS concentrations in each sample from the plant/WWTP. **Table 28** provide a summary of 20 identified PFAS concentrations in each sample and in each plant/WWTP, as depicted in Figures 58. In brief, the 20 identified PFAS through nontarget analysis made up a substantial 2104 μg/L (98%) of the total PFAS content (2139 μg/L), as detailed in Table 28, providing insights into our work on nontarget PFAS in the semiconductor industry and their transformation during wastewater treatment. Notably, emerging perfluorobutane sulfonamido derivatives contributed to 1934 μg/L (90%), indicating a shift in surfactant trends within semiconductor manufacturing. Our PFAS analysis focuses on the negative mode, with limitations for certain types, such as cationic PFAS, telomer alcohols, and specific zwitterionic PFAS compounds, which are detectable only in their positively charged state.

doi:10.6342/NTU202402180

Table 27 Quantitative (Q) concentrations of 7 CL1-identified PFAS and semi-quantitative (SQ) concentrations of 13 tentatively identified PFAS in each sample on the LC–QE

Acronym	Quant type	MB	Sewage discharged from semiconductor plants										Effluent from WWTPs		
			Plant A				Plant B	Plant C			Plant D	Plant E	WWTP 3 (A,B)	WWTP 4 (C,D)	WWTP 5 (E)
			184	185	186	187	190	194	195	196	197	191			
TFA	Q	n.d.	22.4	26.2	9.89	19.3	5.39	20.6	13.0	10.9	2.65	19.5	8.39	6.95	20.1
PFPrA	Q	n.d.	8.66	8.38	11.0	20.1	5.82	10.4	7.61	6.16	4.45	9.84	3.09	3.00	6.73
PFdiCA(C3)	SQ	n.d.	0.030	0.033	n.d.	n.d.	n.d.	0.027	n.d.	n.d.	n.d.	0.034	n.d.	n.d.	0.072
PFdiCA(C4)	SQ	n.d.	0.609	0.549	0.069	0.086	0.056	0.315	0.314	0.370	0.080	0.431	0.318	0.208	0.390
PFdiCA(C5)	SQ	n.d.	0.187	0.192	0.124	0.140	0.045	0.217	0.256	0.274	0.107	0.347	0.128	0.130	0.284
PFdiCA(C6)	SQ	n.d.	0.052	0.066	0.019	0.015	n.d.	0.036	0.059	0.092	0.030	0.151	0.068	0.071	0.196
PFdiCA(C7)	SQ	n.d.	n.d.	n.d.	n.d.	n.d.	n.d.	0.030	0.055	0.052	n.d.	0.056	n.d.	n.d.	0.017
PFdiCA(C8)	SQ	n.d.	n.d.	n.d.	n.d.	n.d.	n.d.	n.d.	0.044	0.053	n.d.	0.037	n.d.	n.d.	0.069
TFMS	Q	n.d.	n.d.	n.d.	0.073	0.122	0.025	0.006	0.010	0.010	0.004	0.489	1.420	0.342	0.370
PFBSi	Q	n.d.	0.24	0.32	n.d.	n.d.	4.24	2.37	2.35	3.13	0.27	n.d.	1.83	1.99	n.d.
FBSA	Q	n.d.	3.34	2.45	0.368	0.173	141	34.0	33.0	26.6	57.9	n.d.	33.0	40.3	n.d.
MeFBSA	SQ	n.d.	n.d.	n.d.	n.d.	n.d.	n.d.	n.d.	n.d.	n.d.	n.d.	n.d.	0.038	0.161	n.d.
FTSE	SQ	n.d.	n.d.	n.d.	n.d.	n.d.	0.014	n.d.	n.d.	n.d.	n.d.	n.d.	n.d.	n.d.	n.d.
FPrSE	SQ	n.d.	n.d.	n.d.	n.d.	n.d.	0.022	n.d.	n.d.	n.d.	0.015	n.d.	n.d.	n.d.	n.d.
FBSE	Q	0.007	71.7	52.3	0.405	0.186	482	251	287	255	239	0.883	1.72	21.4	0.143
FBSEE diol	Q	n.d.	13.6	10.8	n.d.	n.d.	83.5	15.4	67.9	61.5	37.4	n.d.	0.77	3.96	n.d.
FBSAA	SQ	n.d.	1.17	6.66	n.d.	n.d.	11.0	8.80	4.73	4.03	1.07	n.d.	227	145	0.780
MeFBSAA	SQ	n.d.	n.d.	n.d.	n.d.	n.d.	n.d.	n.d.	n.d.	n.d.	n.d.	n.d.	0.029	0.018	n.d.
FBSAA diacid	SQ	n.d.	0.002	0.003	n.d.	n.d.	0.029	n.d.	0.012	0.007	0.005	n.d.	12.5	7.07	n.d.
FBSEE mono-ol monoacid	SQ	n.d.	0.013	0.015	n.d.	n.d.	0.372	0.021	0.046	0.035	0.129	n.d.	0.229	0.312	n.d.

[1] n.d : when no peak was observed.

Table 28 Summary of concentrations (μg/L) of 13 subclasses of PFAS in sewage from semiconductor plants and effluents from industrial WWTPs. The PFAS marked with bold font were identified through nontarget analysis.

Subclass	Semiconductor plant A[4]	Semiconductor plant B	Semiconductor plant C[4]	Semiconductor plant D	Semiconductor plant E	WWTP 3 (A,B)	WWTP 4 (C,D)	WWTP 5 (E)	ΣAll
ΣPFCAs	32.9	13.6	28.0	12.2	30.4	13.0	11.8	27.6	170
TFA[5]	***19.9***	***5.39***	***16.3***	***2.65***	***19.5***	***8.39***	***6.95***	***20.1***	***99.2***
PFPrA[5]	***11.7***	***5.82***	***8.65***	***4.45***	***9.84***	***3.09***	***3.00***	***6.73***	***53.3***
PFBA	0.782	2.25	2.78	4.84	0.572	1.24	1.69	0.493	14.6
PFPeA	0.285	0.062	0.169	0.141	0.192	0.125	0.101	0.161	1.24
PFHxA	0.126	<MDL	0.071	0.049	0.086	0.070	0.037	0.068	0.539
PFHpA	0.058	<MDL	<MDL	<MDL	0.043	0.032	0.018	0.031	0.239
PFOA	0.037	0.011	0.011	0.012	0.033	0.021	0.014	0.022	0.161
PFNA	0.025	<MDL	0.012	0.011	0.039	<MDL	<MDL	0.015	0.131
PFDA	0.017	<MDL	0.009	0.010	0.032	0.010	<MDL	<MDL	0.078
PFUdA	0.011	<MDL	0.010	<MDL	0.027	<MDL	<MDL	<MDL	0.048
PFDoA	0.008	<MDL	0.009	<MDL	<MDL	<MDL	<MDL	<MDL	0.017
PFTrDA	<MDL	<MDL	<MDL	<MDL	<MDL	<MDL	<MDL	<MDL	<MDL
PFTeDA	<MDL	<MDL	<MDL	<MDL	<MDL	<MDL	<MDL	<MDL	<MDL
ΣPFdiCAs	0.572	0.101	0.704	0.216	1.06	0.513	0.409	1.03	4.60
PFdiCA (C3)[5]	**0.017**	**n.d.**	**0.014**	**n.d.**	**0.034**	**n.d.**	**n.d.**	**0.072**	**0.137**
PFdiCA (C4)[5]	**0.352**	**0.056**	**0.328**	**0.08**	**0.431**	**0.318**	**0.208**	**0.390**	**2.16**
PFdiCA (C5)[5]	**0.163**	**0.045**	**0.241**	**0.107**	**0.347**	**0.128**	**0.13**	**0.284**	**1.45**
PFdiCA (C6)[5]	**0.04**	**n.d.**	**0.055**	**0.03**	**0.151**	**0.068**	**0.071**	**0.196**	**0.611**

Subclass	Semiconductor plant A[4]	Semiconductor plant B	Semiconductor plant C[4]	Semiconductor plant D	Semiconductor plant E	WWTP 3 (A,B)	WWTP 4 (C,D)	WWTP 5 (E)	ΣAll
PFdiCA (C7) [5]	**n.d.**	**n.d.**	**0.042**	**n.d.**	**0.056**	**n.d.**	**n.d.**	**0.017**	**0.115**
PFdiCA (C8) [5]	**n.d.**	**n.d.**	**0.024**	**n.d.**	**0.037**	**n.d.**	**n.d.**	**0.069**	**0.130**
ΣPFSAs	1.37	2.14	2.94	6.71	0.617	3.10	2.95	0.492	20.3
TFMS [5]	***0.044***	***0.025***	***0.008***	***0.004***	***0.489***	***1.42***	***0.342***	***0.370***	***2.70***
PFBS	1.33	2.12	2.93	6.71	0.127	1.68	2.61	0.121	17.6
PFPeS	<MDL	<MDL	<MDL	<MDL	<MDL	<MDL	<MDL	<MDL	<MDL
PFHxS	<MDL	<MDL	<MDL	<MDL	<MDL	<MDL	<LOQ	<MDL	<MDL
PFHpS	<MDL	<MDL	<MDL	<MDL	<MDL	<MDL	<MDL	<MDL	<MDL
PFOS	<LOQ	<MDL	<MDL	<MDL	<LOQ	<LOQ	<LOQ	<MDL	<MDL
PFNS	<MDL	<MDL	<MDL	<MDL	<MDL	<MDL	<MDL	<MDL	<MDL
PFDS	<MDL	<MDL	<MDL	<MDL	<MDL	<MDL	<MDL	<MDL	<MDL
Σn:2 FTSAs	n.d.	n.d.	n.d.	n.d.	n.d.	n.d.	0.022	n.d.	0.022
4:2 FTSA	<MDL	<MDL	<MDL	<MDL	<MDL	<MDL	<MDL	<MDL	<MDL
6:2 FTSA	<MDL	<MDL	<MDL	<MDL	<MDL	<MDL	0.022	<MDL	0.022
8:2 FTSA	<MDL	<MDL	<MDL	<MDL	<MDL	<MDL	<MDL	<MDL	<MDL
ΣCl-PFESAs	n.d.	n.d.	n.d.	n.d.	n.d.	n.d.	n.d.	n.d.	n.d.
9Cl-PF3ONS	<MDL	<MDL	<MDL	<MDL	<MDL	<MDL	<MDL	<MDL	<MDL
ΣPFSiAs	0.152	4.24	2.55	0.270	n.d.	1.83	1.99	n.d.	11.0
PFBSi [5]	***0.152***	***4.24***	***2.55***	***0.27***	***n.d.***	***1.83***	***1.99***	***n.d.***	***11.0***
ΣFASAs	1.71	141	31.9	57.9	n.d.	33.0	40.3	n.d.	306
FBSA [5]	***1.71***	***141***	***31.9***	***57.9***	***n.d.***	***33.0***	***40.3***	***n.d.***	***306***
FOSA	<MDL	<MDL	<MDL	<MDL	<MDL	<MDL	<MDL	<MDL	<MDL

Subclass	Semiconductor plant A[4]	Semiconductor plant B	Semiconductor plant C[4]	Semiconductor plant D	Semiconductor plant E	WWTP 3 (A,B)	WWTP 4 (C,D)	WWTP 5 (E)	ΣAll
ΣN-alkyl FASAs	n.d.	n.d.	n.d.	n.d.	n.d.	0.038	0.161	n.d.	0.199
MeFBSA[5]	**n.d.**	**n.d.**	**n.d.**	**n.d.**	**n.d.**	**0.038**	**0.161**	**n.d.**	**0.199**
ΣFASEs	34.0	482	261	239	0.883	1.72	21.4	0.143	1040
FTSE[5]	**n.d.**	**0.014**	**n.d.**	**n.d.**	**n.d.**	**n.d.**	**n.d.**	**n.d.**	**0.014**
FPrSE[5]	**n.d.**	**0.022**	**n.d.**	**0.015**	**n.d.**	**n.d.**	**n.d.**	**n.d.**	**0.037**
FBSE [5]	***34.0***	***482***	***261***	***239***	***0.883***	***1.72***	***21.4***	***0.143***	***1040***
ΣFASEE diols	6.68	83.5	39.9	37.4	n.d.	0.766	3.96	n.d.	172
FBSEE diol[5]	***6.68***	***83.5***	***39.9***	***37.4***	***n.d.***	***0.766***	***3.96***	***n.d.***	***172***
ΣFASAAs	2.14	11.0	6.61	1.07	n.d.	227	145	0.78	395
FBSAA[5]	**2.14**	**11.0**	**6.61**	**1.07**	**n.d.**	**227**	**145**	**0.780**	**395**
ΣN-alkyl FASAAs	n.d.	n.d.	n.d.	n.d.	n.d.	0.029	0.018	n.d.	0.048
MeFBSAA[5]	**n.d.**	**n.d.**	**n.d.**	**n.d.**	**n.d.**	**0.029**	**0.018**	**n.d.**	**0.047**
MeFOSAA	<MDL	<MDL	<MDL	<MDL	<MDL	<MDL	<MDL	<MDL	<MDL
EtFOSAA	<MDL	<MDL	<MDL	<MDL	<MDL	<MDL	<MDL	<MDL	<MDL
ΣFASEE diacids	0.001	0.029	0.005	0.005	n.d.	12.5	7.07	n.d.	19.5
FBSEE diacid[5]	**0.001**	**0.029**	**0.005**	**0.005**	**n.d.**	**12.5**	**7.07**	**n.d.**	**19.5**
ΣFASEE mono-ol monoacid	0.008	0.372	0.031	0.129	n.d.	0.229	0.312	n.d.	1.08
FBSEE mono-ol monoacid[5]	**0.008**	**0.372**	**0.031**	**0.129**	**n.d.**	**0.229**	**0.312**	**n.d.**	**1.08**
ΣAll	79.5	738	374	355	33.0	294	236	30.0	2139

[1] n.d : no peak was observed.

[2] <LOQ=Concentration was less than the limit of quantification.

[3] <MDL=Concentration was less than the method detection limit.

[4] The concentration calculation procedure for plant A and plant C with multiple sewage sources is outlined in Table S4.

[5] Identified PFAS quantified in bold and italic; semi-quantified ones marked in bold.

doi:10.6342/NTU202402180

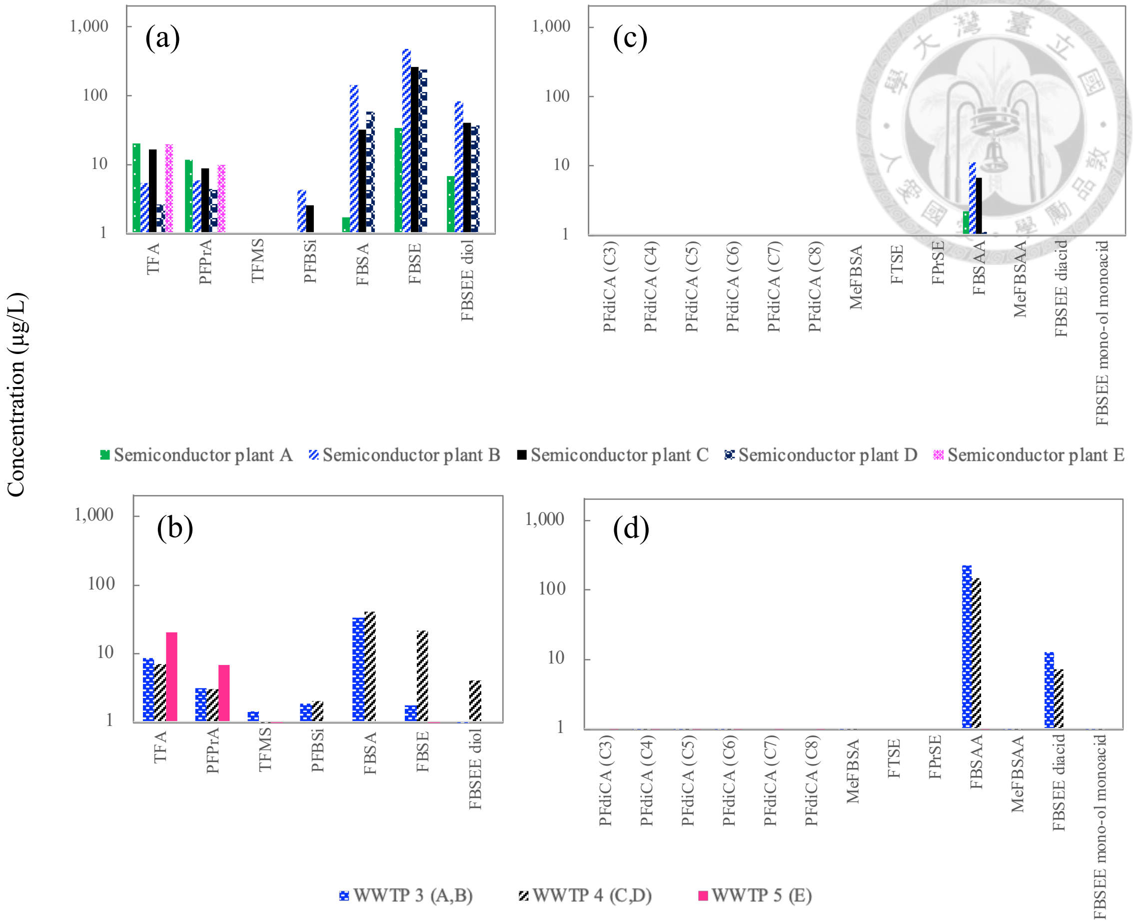

Figure 60 Concentrations of 20 nontarget identified PFAS (a) and (b) Quantification of 7 CL1-identified PFAS in sewage and effluents. (c) and (d) Semi-quantification of 13 tentatively identified PFAS in sewage and effluents.

4.2.4. QA/QC Sample of Nontarget Analysis

4.2.4.1.Verification of Recovery of SPE

To verify the recovery of SPE, QC samples were prepared in 200 mL of DI water with 0.1 μg/L of 25 PFAS (no ISs spiked) and subjected to SPE. The theoretical analytical concentration of the QC samples was 12 μg/L. In quantifying the 25 target PFAS using LC–QE, a linear regression analysis was conducted, with a minimum of five concentration levels weighted by 1/x. The calibration curve, established using an external standard with coefficients (R^2) exceeding 0.995 is provided in **Table 29**. The quantification formula is as follows:

$$y=a*x+b \qquad \text{(Eq 1)}$$

where y equals the response of the precursor ion (**Table 29**) of PFAS (A_T) and x equals the concentration of the PFAS (C_T).

doi:10.6342/NTU202402180

Table 29 Calibration of 25 target PFAS on the LC–QE

Acronym	Linearity (µg/L)	R^2	Calibration type	Standard type	Adduct ion	Precursor ion	Theoretical m/z of precursor ion (m/z) [1]
PFBA	0.5-75	0.9967	y=a*x+b	External	$[M-H]^-$	$C_4F_7O_2^-$	212.97920
PFPeA	0.5-75	0.9972	y=a*x+b	External	$[M-H]^-$	$C_5F_9O_2^-$	262.97600
PFHxA	0.5-75	0.9962	y=a*x+b	External	$[M-H]^-$	$C_6F_{11}O_2^-$	312.97281
PFHpA	0.5-75	0.9970	y=a*x+b	External	$[M-H]^-$	$C_7F_{13}O_2^-$	362.96962
PFOA	0.5-50	0.9978	y=a*x+b	External	$[M-H]^-$	$C_8F_{15}O_2^-$	412.96642
PFNA	0.5-20	0.9981	y=a*x+b	External	$[M-H]^-$	$C_9F_{17}O_2^-$	462.96323
PFDA	0.5-50	0.9978	y=a*x+b	External	$[M-H]^-$	$C_{10}F_{19}O_2^-$	512.96003
PFUdA	0.5-50	0.9977	y=a*x+b	External	$[M-H]^-$	$C_{11}F_{21}O_2^-$	562.95684
PFDoA	0.5-50	0.9975	y=a*x+b	External	$[M-H]^-$	$C_{12}F_{23}O_2^-$	612.95365
PFTrDA	0.5-50	0.9986	y=a*x+b	External	$[M-H]^-$	$C_{13}F_{25}O_2^-$	662.95045
PFTeDA	0.5-75	0.9969	y=a*x+b	External	$[M-H]^-$	$C_{14}F_{27}O_2^-$	712.94726
PFBS	0.5-75	0.9964	y=a*x+b	External	$[M-H]^-$	$C_4F_9O_3S^-$	298.94299
PFPeS	0.5-75	0.9976	y=a*x+b	External	$[M-H]^-$	$C_5F_{11}O_3S^-$	348.93979
PFHxS	0.5-75	0.9965	y=a*x+b	External	$[M-H]^-$	$C_6F_{13}O_3S^-$	398.93660
PFHpS	0.5-50	0.9986	y=a*x+b	External	$[M-H]^-$	$C_7F_{15}O_3S^-$	448.93341
PFOS	0.5-50	0.9941	y=a*x+b	External	$[M-H]^-$	$C_8F_{17}O_3S^-$	498.93021
PFNS	0.5-50	0.9960	y=a*x+b	External	$[M-H]^-$	$C_9F_{19}O_3S^-$	548.92702
PFDS	0.5-75	0.9978	y=a*x+b	External	$[M-H]^-$	$C_{10}F_{21}O_3S^-$	598.92382
4:2 FTSA	0.5-75	0.9918	y=a*x+b	External	$[M-H]^-$	$C_6H_4F_9O_3S^-$	326.97429
6:2 FTSA	0.5-75	0.9932	y=a*x+b	External	$[M-H]^-$	$C_8H_4F_{13}O_3S^-$	426.96790
8:2 FTSA	0.5-50	0.9973	y=a*x+b	External	$[M-H]^-$	$C_{10}H_4F_{17}O_3S^-$	526.96151
6:2 Cl-PFESA (9Cl-PF3ON)	0.5-50	0.9950	y=a*x+b	External	$[M-H]^-$	$C_8ClF_{16}O_4S^-$	530.89558
FOSA	0.5-75	0.9988	y=a*x+b	External	$[M-H]^-$	$C_8HF_{17}NO_2S^-$	497.94620
MeFOSAA	0.5-50	0.9986	y=a*x+b	External	$[M-H]^-$	$C_{11}H_4F_{17}NO_4S^-$	569.96733
EtFOSAA	0.5-50	0.9970	y=a*x+b	External	$[M-H]^-$	$C_{12}H_6F_{17}NO_4S^-$	583.98298

[1] Precursor ion was used as quantitative ion with 5 ppm mass accuracy of the theoretical m/z

The QC sample recoveries without internal standard compensation were calculated from four duplicated samples and are presented in **Table 30**. The results of the verification of the SPE pretreatment showed that PFCAs (C4-C14) had recoveries ranging from 45.2±2.6% to 97.5±1.4%, while PFSAs (C4-C10) showed recoveries between 47.3±4.1% and 98.2±8.4%. Cl-PFESAs such as 6:2 Cl-PFESA (9Cl-PF3ON) showed a recovery of 75.2±0.8%, and N-alkyl FASAAs such as Me-FOSAAs and Et-FOSAAs had recoveries of 41.5±2.5% and 49.8±7.1%, respectively. For weakly acidic PFAS, such as 6:2 FTSA, the recovery was 84.2% ± 3.0%, while for neutral PFAS, such as FOSA, the recovery was 52.3% ± 4.9%. Briefly, the recoveries of 25 target PFAS, spanning 6 subclasses of neutral and acidic PFAS, ranged from 41.5% to 98.2%. These results demonstrate acceptable recoveries of acidic and neutral PFAS even without the use of internal standards, and they were further employed in the pretreatment of nontarget analysis.

doi:10.6342/NTU202402180

Table 30 Verification of SPE pretreatment with QC samples on the LC–QE

Compounds	Recovery (%)[1] of QC sample (n=4)[2]	
	Average	SD
PFBA	97.5	1.4
PFPeA	96.5	1.9
PFHxA	92.4	4.1
PFHpA	93.6	5.3
PFOA	90.2	4.3
PFNA	85.3	6.8
PFDA	70.0	1.4
PFUdA	57.0	5.8
PFDoA	45.2	2.6
PFTrDA	49.4	5.7
PFTeDA	83.5	13.0
PFBS	98.2	8.4
PFPeS	80.8	10.4
PFHxS	80.9	9.1
PFHpS	82.3	9.9
PFOS	72.2	5.0
PFNS	59.0	5.3
PFDS	47.3	4.1
4:2 FTSA	78.3	4.7
6:2 FTSA	84.2	3.0
8:2 FTSA	67.5	2.8
9Cl-PF3ONS	75.2	0.8
FOSA	52.3	4.9
MeFOSAA	41.5	2.5
EtFOSAA	49.8	7.1

[1] Recovery = [concentration of QC samples/theoretical concentration of QC samples] *100%, Average = mean of recovery; SD = standard deviation of recovery

[2] QC samples were prepared in 200 mL of DI water with 0.1 μg/L of 25 PFAS (no ISs spiked) and subjected to solid-phase extraction. The theoretical analytical concentration of the QC samples was 12 μg/L.

4.2.4.2. Verification of Filtration Loss During SPE

Table 31 summarizes the verification of filtration pretreatment using QC samples on the LC–QE to assess nylon filter filtration losses. Among the 25 target PFAS, only PFTeDA and ETFOSAA exhibited lower recoveries at 77.8±14.4% and 79.3±1.5%, respectively. The remaining 23 PFAS showed higher recoveries ranging from 81.6±2.8% to 97.9±1.5%. These findings demonstrate that pretreatment filtration has minimal impact on the loss of short-chain PFAS and only a minor effect on the loss of long-chain PFAS when PFAS are filtered within organic solvents such as methanol, as used in this study.

doi:10.6342/NTU202402180

Table 31 Verification of filtration pretreatment with QC samples on the LC–QE

Compounds	Recovery (%)[1] (n=4)	
	Average	SD
PFBA	91.3	1.2
PFPeA	91.5	1.3
PFHxA	92.5	2.8
PFHpA	95.1	2.4
PFOA	94.2	2.1
PFNA	90.9	2.1
PFDA	90.8	1.1
PFUdA	84.4	2.5
PFDoA	94.7	6.4
PFTrDA	85.8	9.7
PFTeDA	77.8	14.4
PFBS	97.9	1.5
PFPeS	89.1	1.3
PFHxS	87.7	1.4
PFHpS	89.2	0.7
PFOS	95.7	1.9
PFNS	86.2	2.5
PFDS	80.7	2.3
4:2 FTSA	95.6	2.3
6:2 FTSA	97.4	2.6
8:2 FTSA	92.4	1.9
9Cl-PF3ONS	84.9	9.8
FOSA	94.5	2.9
MeFOSAA	81.6	2.8
EtFOSAA	79.3	1.5

[1] The theoretical preparation concentration was 6 µg/L. Recovery = [concentration of solution with filtration/concentration of solution without filtration] *100%; Average = mean of recovery; SD = standard deviation of recovery.

4.2.4.3. Verification of Nontarget Analysis Efficiency

To verify the efficiency of the nontarget analysis processing in **Figure 10**, a PFAS standard mixture containing 39 compounds from 11 PFAS categories listed in Table 15 were prepared as a QC sample. The prepared concentrations of standard mix are as follow: PFCAs & PFSAs & n:2 FTSA & FASA & N-alkyl FASAA :30 µg/ L, n:3 FTCA & n:2 FTUCA & Ether-PFCA &Cl-Ether-PFSA & N-alkyl FASA & N-alkyl FASE: 60 µg/L. The result showed that 92% (36 out of 39 compounds) were detectable through the processing of fragment-based nontarget analysis as detailed in Table 32. Three PFAS compounds—PFNA, PFTeDA, and MeFOSAA—were not identified using the nontarget analysis process. Upon inspection, we observed that the precursor ion of PFNA were detected with ‘detection node ‘through our nontarget process in Figure. However, the precursor ion of PFNA was recognized as a background ion and listed in the exclusion list (background ions were typically added to the exclusion list to avoid collision and to prevent the collection of their MS2 spectrum), resulting in its exclusion from collision selection. Even though it was not part of the compounds verified through fragment-based nontarget analysis, PFNA was still identified in the MS1 spectrum as $C_9HF_{17}O_2$, aligning with PFNA's formula. Its mass error of 0.45 ppm fell comfortably within the 5 ppm criteria. PFTeDA and MeFOSAA were not detected using the 'detection node,' likely due to a low signal-to-noise ratio, which prevented them from being identified as peaks. The specifics regarding the detection of mass errors, fragments, neutral losses of the 39 compounds are provided in **Table 33** and **Table 34**.

doi:10.6342/NTU202402180

Table 32 The detection results of the QC sample, comprising 39 compounds from 11 PFAS categories, using fragment-based nontarget analysis.

No.	Category (class)	Abbreviation[a]	Number of fragments from tail ($C_xF_yO_z^-$)	Number of fragments from head	Neutral Losses	Detection	Detection rate (%)
1	PFCA	PFBA	1	2	CO_2	Yes	**92**
2		PFPeA	1	0	CO_2	Yes	
3		PFHxA	2	0	CO_2	Yes	
4		PFHpA	3	0	CO_2	Yes	
5		PFOA	4	0	CO_2	Yes	
6		PFNA	0	0		**No**	
7		PFDA	5	0	CO_2	Yes	
8		PFUdA	5	0	CO_2	Yes	
9		PFDoA	6	0	CO_2	Yes	
10		PFTrDA	7	0	CO_2	Yes	
11		PFTeDA	0	0		**No**	
12	n:3 FTCA	3:3 FTCA	0	2	$CO_2(HF)_4$	Yes	
13		5:3 FTCA	0	1	$CO_2(HF)_4$	Yes	
14		7:3 FTCA	1	1	$CO_2(HF)_4$	Yes	
15	n:2 FTUCA	6:2 FTUCA	1	0	CO_2HF	Yes	
16		8:2 FTUCA	3	0	CO_2HF	Yes	
17		10:2 FTUCA	2	0	CO_2HF	Yes	
18	Ether-PFCA	HFPO-DA (GenX)	3	0		Yes	
19		DONA	1	0		Yes	
20	PFSA	PFPrs	3	3	SO_3	Yes	
21		PFBS	0	3		Yes	
22		PFPeS	3	3		Yes	
23		PFHxS	2	3		Yes	
24		PFHpS	2	3		Yes	
25		PFOS	1	3		Yes	
26		PFNS	1	3		Yes	
27		PFDS	1	3		Yes	
28	n:2 FTSA	4:2 FTSA	0	2	HF	Yes	
29		6:2 FTSA	0	2	HF	Yes	
30		8:2 FTSA	0	2	HF	Yes	
31	Cl-Ether-PFSA	9Cl-PF3ONS	1	2		Yes	
32		11Cl-PF3OUdS	1	2		Yes	
33	FASA	FOSA	0	2		Yes	

No.	Category (class)	Abbreviation[a]	Number of fragments from tail ($C_xF_yO_z^-$)	Number of fragments from head	Neutral Losses	Detection	Detection rate (%)
34	N-alkyl	MeFOSA	4	3		Yes	
35	FASA	EtFOSA	4	3		Yes	
36	N-alkyl	MeFOSE	0	1		Yes	
37	FASE	EtFOSE	0	1		Yes	
38	N-alkyl	MeFOSAA	0	0		**No**	
39	FASAA	EtFOSAA	4	3	CH_2CO_2	Yes	

Table 33 Summary of the 39 standard mixture compounds as a QC sample, including precursor ions, mass errors, RTs, peak areas, and neutral losses

No.	Category	Abbreviation	Theoretical formula	Adduct ion of precursor ion	Mass error (ppm)	Precursor ion (m/z)	RT (min)	Area	MS2 spectrum	Neutral losses
1	PFCA	PFBA	C4 H F7 O2	[M-H]-	-0.85	212.9790	4.6	1.22E+08	YES	CO_2
2		PFPeA	C5 H F9 O2	[M-H]-	-0.78	262.9758	8.6	8.34E+07	YES	CO_2
3		PFHxA	C6 H F11 O2	[M-H]-	-0.01	312.9728	16.6	9.82E+07	YES	CO_2
4		PFHpA	C7 H F13 O2	[M-H]-	0.46	362.9698	26.7	1.34E+08	YES	CO_2
5		PFOA	C8 H F15 O2	[M-H]-	0.16	412.9665	37.4	1.58E+08	YES	CO_2
6		PFNA	C9 H F17 O2	[M-H]-	0.45	462.9634	47.8	1.67E+08	No MS2	
7		PFDA	C10 H F19 O2	[M-H]-	-0.51	512.9598	57.3	1.51E+08	YES	CO_2
8		PFUdA	C11 H F21 O2	[M-H]-	0.98	562.9574	65.7	1.28E+08	YES	CO_2
9		PFDoA	C12 H F23 O2	[M-H]-	1.93	612.9548	73.1	1.05E+08	YES	CO_2
10		PFTrDA	C13 H F25 O2	[M-H]-	2.55	662.9522	79.6	8.40E+07	YES	CO_2
11		PFTeDA	C14 H F27 O2	No detectable feature					No MS2	
12	n:3 FTCA	3:3 FTCA	C6 H5 F7 O2	[M-H]-	-0.64	241.0104	8.9	1.06E+08	YES	$CO_2(HF)_4$
13		5:3 FTCA	C8 H5 F11 O2	[M-H]-	-0.16	341.0041	28.9	1.51E+08	YES	$CO_2(HF)_4$
14		7:3 FTCA	C10 H5 F15 O2	[M-H]-	0.04	440.9977	51.3	1.51E+08	YES	$CO_2(HF)_4$
15	n:2 FTUCA	6:2 FTUCA	C8 H2 F12 O2	[M-H]-	0.07	356.9791	28.4	1.09E+08	YES	CO_2HF
16		8:2 FTUCA	C10 H2 F16 O2	[M-H]-	0.14	456.9727	50.1	1.87E+08	YES	CO_2HF
17		10:2 FTUCA	C12 H2 F20 O2	[M-H]-	1.39	556.9670	68.1	1.49E+08	YES	CO_2HF
18	Ether-PFCA	HFPO-DA (GenX)	C6 H F11 O3	[M-CO_2-H]-	0.13	284.9779	19.5	2.26E+07	YES	
19		DONA	C7 H2 F12 O4	[M-H]-	-0.4	376.9687	28.1	4.45E+08	YES	
20	PFSA	PFPrs	C3 H F7 O3 S	[M-H]-	-1.36	248.9459	5.5	1.06E+09	YES	SO_3
21		PFBS	C4 H F9 O3 S	[M-H]-	-0.91	298.9427	10.3	7.00E+08	YES	
22		PFPeS	C5 H F11 O3 S	[M-H]-	-0.11	348.9398	18.8	5.77E+08	YES	
23		n-PFHxS	C6 H F13 O3 S	[M-H]-	-0.13	398.9366	28.5	4.78E+08	YES	
23		br-PFHxS	C6 H F13 O3 S	[M-H]-	0.03	398.9366	25.9	2.71E+07	YES	
23		br-PFHxS	C6 H F13 O3 S	[M-H]-	0.03	398.9366	26.4	5.45E+07	YES	

No.	Category	Abbreviation	Theoretical formula	Adduct ion of precursor ion	Mass error (ppm)	Precursor ion (m/z)	RT (min)	Area	MS2 spectrum	Neutral losses
23		br-PFHxS	C6 H F13 O3 S	[M-H]-	0.79	398.9369	27.0	8.80E+06	YES	
24		PFHpS	C7 H F15 O3 S	[M-H]-	0.14	448.9335	38.8	5.44E+08	YES	
25		n-PFOS	C8 H F17 O3 S	[M-H]-	0.28	498.9304	48.7	3.95E+08	YES	
25		br-PFOS	C8 H F17 O3 S	[M-H]-	0.61	498.9305	45.0	2.80E+07	YES	
25		br-PFOS	C8 H F17 O3 S	[M-H]-	0.77	498.9306	46.0	6.05E+07	YES	
26		PFNS	C9 H F19 O3 S	[M-H]-	-0.04	548.9270	57.8	3.91E+08	YES	
27		PFDS	C10 H F21 O3 S	[M-H]-	0.81	598.9243	65.9	2.95E+08	YES	
28	n:2 FTSA	4:2 FTSA	C6 H5 F9 O3 S	[M-H]-	-0.15	326.9742	15.6	1.37E+08	YES	HF
29		6:2 FTSA	C8 H5 F13 O3 S	[M-H]-	-0.16	426.9678	36.4	1.12E+08	YES	HF
30		8:2 FTSA	C10 H5 F17 O3 S	[M-H]-	0.15	526.9616	56.6	8.43E+07	YES	HF
31	Cl-Ether-PFSA	9Cl-PF3ONS	C8 H Cl F16 O4 S	[M-H]-	-0.14	530.8955	54.9	6.40E+08	YES	
32		11Cl-PF3OUdS	C10 H Cl F20 O4 S	[M-H]-	1.49	630.8901	70.7	4.03E+08	YES	
33	FASA	FOSA	C8 H2 F17 N O2 S	[M-H]-	0.6	497.9465	66.7	2.63E+08	YES	
34	N-alkyl FASA	MeFOSA	C9 H4 F17 N O2 S	[M-H]-	0.84	511.9623	78.7	2.20E+08	YES	
35		EtFOSA	C10 H6 F17 N O2 S	[M-H]-	1	525.9780	83.8	2.81E+08	YES	
36	N-alkyl FASE	MeFOSE	C11 H8 F17 N O3 S	[M+CH_3COO]-	0.32	616.0107	78.7	1.19E+08	YES	
37		EtFOSE	C12 H10 F17 N O3 S	[M+CH_3COO]-	-0.02	630.0261	83.5	1.56E+08	YES	
38	N-alkyl FASAA	MeFOSAA	C11 H6 F17 N O4 S	No detectable feature					No MS2	
39		EtFOSAA	C12 H8 F17 N O4 S	[M-H]-	1.34	583.9838	65.9	1.03E+08	YES	CH_2CO_2

Table 34 Summary of the 39 standard mixture compounds as a QC sample, including their fragment ions from the fluorinated tail ($C_xF_yO_z^-$) and polar head groups

No.	Category	Abbreviation	CF_3-	C_2F_5-	C_3F_7-	C_4F_9-	C_5F_{11}-	C_6F_{13}-	C_7F_{15}-	C_8F_{17}-	CF_3O-	C_2F_5O-	C_3F_7O-	SO2N-	SO_3-	SO_3F-	SO_2F-	SO_2-	SO_2H-	SO_3H-	CO_2F-	CH_3COO-
1	PFCA	PFBA	0	0	1	0	0	0	0	0	0	0	0	0	0	0	0	1	1	0	0	0
2	PFCA	PFPeA	0	0	0	1	0	0	0	0	0	0	0	0	0	0	0	0	0	0	0	0
3	PFCA	PFHxA	0	1	0	0	1	0	0	0	0	0	0	0	0	0	0	0	0	0	0	0
4	PFCA	PFHpA	0	1	1	0	0	1	0	0	0	0	0	0	0	0	0	0	0	0	0	0
5	PFCA	PFOA	0	1	1	1	0	0	1	0	0	0	0	0	0	0	0	0	0	0	0	0
6	PFCA	PFNA	No MS2 spectrum																			
7	PFCA	PFDA	0	1	1	1	1	1	0	0	0	0	0	0	0	0	0	0	0	0	0	0
8	PFCA	PFUdA	0	1	1	1	1	1	0	0	0	0	0	0	0	0	0	0	0	0	0	0
9	PFCA	PFDoA	0	1	1	1	1	1	1	0	0	0	0	0	0	0	0	0	0	0	0	0
10	PFCA	PFTrDA	0	1	1	1	1	1	1	1	0	0	0	0	0	0	0	0	0	0	0	0
11	PFCA	PFTeDA	No MS2 spectrum																			
12	n:3 FTCA	3:3 FTCA	0	0	0	0	0	0	0	0	0	0	0	0	0	0	0	0	0	0	1	1
13	n:3 FTCA	5:3 FTCA	0	0	0	0	0	0	0	0	0	0	0	0	0	0	0	0	0	0	1	0
14	n:3 FTCA	7:3 FTCA	1	0	0	0	0	0	0	0	0	0	0	0	0	0	0	0	0	0	1	0
15	n:2 FTUCA	6:2 FTUCA	1	0	0	0	0	0	0	0	0	0	0	0	0	0	0	0	0	0	0	0

No.	Category	Abbreviation	CF_3-	C_2F_5-	C_3F_7-	C_4F_9-	C_5F_{11}-	C_6F_{13}-	C_7F_{15}-	C_8F_{17}-	CF_3O-	C_2F_5O-	C_3F_7O-	SO2N-	SO_3-	SO_3F-	SO_2F-	SO_2-	SO_2H-	SO_3H-	CO_2F-	CH_3COO-
16	n:2 FTUCA	8:2 FTUCA	1	1	1	0	0	0	0	0	0	0	0	0	0	0	0	0	0	0	0	0
17	n:2 FTUCA	10:2 FTUCA	1	1	0	0	0	0	0	0	0	0	0	0	0	0	0	0	0	0	0	0
18	Ether-PFCA	HFPO-DA (GenX)	0	1	1	0	0	0	0	0	0	0	1	0	0	0	0	0	0	0	0	0
19	Ether-PFCA	DONA	0	0	0	0	0	0	0	0	1	0	0	0	0	0	0	0	0	0	0	0
20	PFSA	PFPrs	1	1	1	0	0	0	0	0	0	0	0	0	1	1	1	0	0	0	0	0
21	PFSA	PFBS	0	0	0	0	0	0	0	0	0	0	0	0	1	1	1	0	0	0	0	0
22	PFSA	PFPeS	1	1	0	0	0	0	0	0	1	0	0	0	1	1	1	0	0	0	0	0
23	PFSA	n-PFHxS	0	1	1	0	0	0	0	0	0	0	0	0	1	1	1	0	0	0	0	0
23	PFSA	br-PFHxS	1	0	0	0	0	0	0	0	0	0	0	0	1	1	0	0	0	0	0	0
23	PFSA	br-PFHxS	1	1	1	0	0	0	0	0	0	0	0	0	1	1	1	0	0	0	0	0
23	PFSA	br-PFHxS	0	1	0	0	0	0	0	0	0	0	0	0	1	1	0	0	0	0	0	0
24	PFSA	PFHpS	0	1	0	0	0	0	0	0	1	0	0	0	1	1	1	0	0	0	0	0
25	PFSA	n-PFOS	0	1	0	0	0	0	0	0	0	0	0	0	1	1	1	0	0	0	0	0
25	PFSA	br-PFOS	0	0	0	0	0	0	0	0	0	0	0	0	1	1	0	0	0	0	0	0
25	PFSA	br-PFOS	0	0	1	0	0	0	0	0	0	0	0	0	1	1	1	0	0	0	0	0
26	PFSA	PFNS	0	1	0	0	0	0	0	0	0	0	0	0	1	1	1	0	0	0	0	0

No.	Category	Abbreviation	CF_3-	C_2F_5-	C_3F_7-	C_4F_9-	C_5F_{11}-	C_6F_{13}-	C_7F_{15}-	C_8F_{17}-	CF_3O-	C_2F_5O-	C_3F_7O-	SO2N-	SO_3-	SO_3F-	SO_2F-	SO_2-	SO_2H-	SO_3H-	CO_2F-	CH_3COO-
27	PFSA	PFDS	0	1	0	0	0	0	0	0	0	0	0	0	1	1	1	0	0	0	0	0
28	n:2 FTSA	4:2 FTSA	0	0	0	0	0	0	0	0	0	0	0	0	1	0	0	0	0	1	0	0
29	n:2 FTSA	6:2 FTSA	0	0	0	0	0	0	0	0	0	0	0	0	1	0	0	0	0	1	0	0
30	n:2 FTSA	8:2 FTSA	0	0	0	0	0	0	0	0	0	0	0	0	1	0	0	0	0	1	0	0
31	Cl-Ether-PFSA	9Cl-PF3ONS	0	0	0	0	0	0	0	0	1	0	0	0	0	1	1	0	0	0	0	0
32	Cl-Ether-PFSA	11Cl-PF3OUdS	0	0	0	0	0	0	0	0	1	0	0	0	0	1	1	0	0	0	0	0
33	FASA	FOSA	0	0	0	0	0	0	0	0	0	0	0	1	0	0	0	1	0	0	0	0
34	N-alkyl FASA	MeFOSA	1	1	1	1	0	0	0	0	0	0	0	0	0	0	1	1	1	0	0	0
35	N-alkyl FASA	EtFOSA	0	1	1	1	0	0	0	1	0	0	0	0	0	0	1	1	1	0	0	0
36	N-alkyl FASE	MeFOSE	0	0	0	0	0	0	0	0	0	0	0	0	0	0	0	0	0	0	0	1
37	N-alkyl FASE	EtFOSE	0	0	0	0	0	0	0	0	0	0	0	0	0	0	0	0	0	0	0	1
38	N-alkyl FASAA	MeFOSAA	No MS2 spectrum																			
39	N-alkyl FASAA	EtFOSAA	0	1	1	1	0	0	0	1	0	0	0	1	0	0	1	0	1	0	0	0

doi:10.6342/NTU202402180

4.3. The Composition of PFAS in the Semiconductor Plants and WWTP Effluents

The amounts and percentages of 13 subclasses of PFAS released from different semiconductor plants and their WWTPs are illustrated in **Figure 61**(a) and **Figure 61**(b) and detailed in **Table 28**. The semiconductor industry includes diverse suppliers for logic integrated circuits, dynamic random-access memory devices, solid-state drives, photodiodes, photo-imaging sensors, etc. In general, plants A, B, C, and D mainly supply similar products, and plant E produces another kind of product. The total amounts of PFAS in the sewage of semiconductor plants A, B, C, and D were relatively high, from 79.5 to 738 μg/L, compared to that of the amount of PFAS in the sewage of plant E, which was 33.0 μg/L. Furthermore, for semiconductor plants A, B, C, and D, 10 diverse subclasses of PFAS were detected, including FASEs (34.0-482 μg/L, 43-70%), FASAs (1.71-141 μg/L, 2-19%), FASEE diols (6.68-83.5 μg/L, 8-11%), PFCAs (12.2-32.9 μg/L, 2-41%) and six minor subclasses (FASAAs, PFSAs, PFSiAs, PFdiCAs, FASEE mono-ol monoacids, and FASEE diacids) (n.d. to 11.0 μg/L, <3%). However, the composition of PFAS from plant E was rather simple, including 4 subclasses of PFCAs (30.4 μg/L, 92%), PFdiCA (1.06 μg/L, 3%), FASEs (0.883 μg/L, 3%) and PFSAs (0.617 μg/L, 2%). The disparities in PFAS compositions may be associated with

doi:10.6342/NTU202402180

the manufacturing of distinct semiconductor products or the company's deployment of chemical formulations.

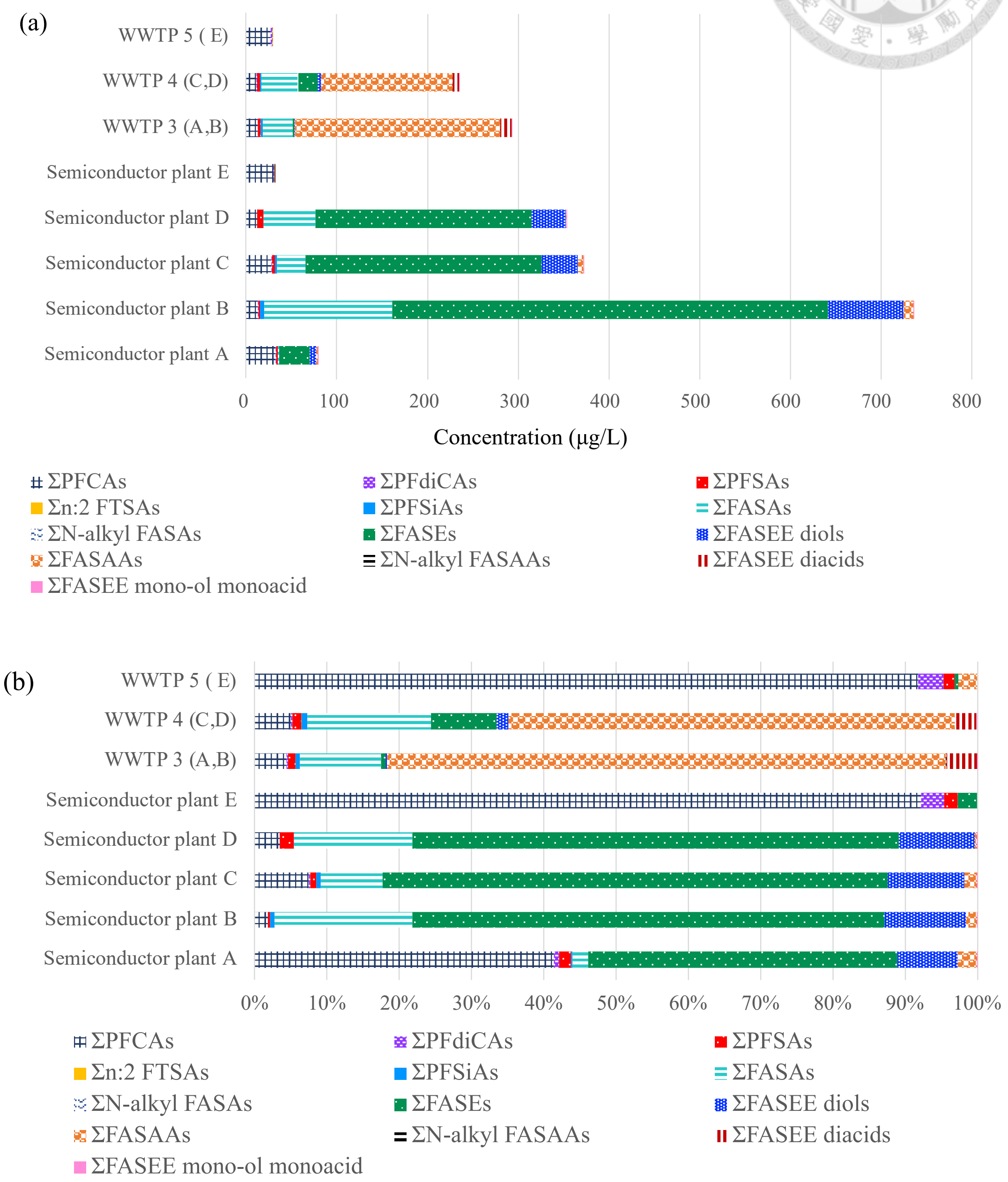

Figure 61 (a) Concentrations (μg/L) of 13 subclasses of PFAS in sewage from 5 semiconductor plants and effluents from 3 WWTPs (b) The composition profile of 13 subclasses of PFAS in sewage from 5 semiconductor plants and effluents from 3 WWTPs

4.4. Byproducts from Chemical Formulation

Two primary methods for PFAS production are the electrochemical fluorination (ECF) process, favored by 3M,[85] and the telomerization process, employed by DuPont.[1] The ECF process generates byproducts, along with both shorter and longer PFAS, with a higher prevalence of branched PFAS, while the telomerization process primarily yields normal PFAS.[86] In our previous study on semiconductor wastewater, FBSE was found at concentrations ranging from 0.883 to 482 μg/L, while perfluoropropane sulfonamido ethanol(FPrSE) and perfluoropropane sulfonamido ethanol (FESE) were detected at semi-concentrations of n.d. to 0.037 μg/L and n.d. to 0.014 μg/L, respectively. [73] FBSE is associated with 3M's electronic surfactant 4200,[22] which is added to buffered hydrofluoric acid (BHF) for etching solutions in semiconductor manufacturing to enhance wetting properties and improving pattern quantity performance. In this study, we reported several FBSE derivatives with varying fluoroalkyl chain in sewage, including those with backbones containing oxygen as ether (E), those with backbones containing unsaturated bonds (U), and those with hydrogen-substituted F as polyfluoroalkyl chains (H). The varied RTs of these substances compared to that of FBSE are as follows: H-FBSE (15.84-19.05 min) < U-FBSE (16.9 min) < H-E-FBSE (21.1min) < U-E-FBSE (23.3 min) < FBSE (29.9 min) < E-FBSE

doi:10.6342/NTU202402180

(33.8-34.9 min). The use of a reversed-phase C18 column for analysis indicates that, in terms of polarity, only E-FBSE was less polar than FBSE, while the others were much more polar, resulting in faster elution. This suggests that in wastewater treatment, using hydrophobic interaction separation methods such as activated carbon adsorption may lead to lower removal efficiency for these polar substances, decreasing susceptibility to adsorption removal.[87] When discharged from wastewater treatment plants, the environmental distribution of these substances may differ significantly due to their distinct properties. Notably, the semiconductor industry encompasses various suppliers, including those for logic integrated circuits, dynamic random-access memory devices, solid-state drives, photodiodes, photo-imaging sensors, and more. Generally, plants A, B, C, and D primarily manufacture similar products, while plant E specializes in a different product line. We discovered that sewage from plants A, B, C, and D contained significant quantities of FBSE, FBSA, and FBSEE, along with various fluoroalkyl sulfonamido derivatives such as E-FBSA, H-FBSE, and U-E-FBSE. In contrast, sewage from plant E, which manufactures different products from plants A, B, C, and D, showed no presence of sulfonamido derivatives. This observation could serve as a distinguishing characteristic for identifying different production lines.

The aforementioned FBSE derivative series, including H-FBSE, U-E-FBSE, U-FBSE, E-FBSE, H-E-FBSE, FBSAA, headgroup isomer of FBSAA, FPrSE, and FEtSE, were confirmed to exist in accordance with the authentic standard of FBSE. Their relative area proportions, shown in **Table 35** in descending order, were as follows: FBSE (99.50%), FPrSE (0.21%), E-FBSE (0.10%), H-FBSE (0.095%), FBSAA (0.036%), U-E-FBSE (0.033%), FEtSE (0.014%), U-FBSE (0.007%), headgroup isomer of FBSAA (0.002%), and H-E-FBSE (0.001%), contributing to a total of approximately 0.5%. In addition, FBSA includes similar byproducts from production, such as H-FBSA (0.01%) and E-FBSA (0.06%), while FBSEE includes comparable byproducts such as H-FBSEE (0.4%). The derivative series of FBSE detected in sewage might originate from the byproducts of chemical formulations, like 3M's electronic surfactant 4200, which contains FBSE as a primary component in semiconductor production. However, these byproducts may arise from transformation processes during manufacturing and among the treatment of wastewater, including the elimination of HF to produce unsaturated PFAS[88,89] and defluorination leading to hydrogen-substituted PFAS under photoelectrochemical processes.[90] Additionally, under biotic metabolism, alcohol oxidation can lead to the formation of carboxylic acids through hydration and oxidation processes,[73,91] with further discussion below.

Table 35 List of impurities in authentic FBSE, FBSA, and FBSEE diol standards

Characteristics	Compound	Compound number	The relative peak area (%)[a]
Standard solution	FBSE	2a-3	99.50
Impurity in standard solution of FBSE	FPrSE	2a-2	0.211
	E-FBSE	2c-1, 2c-2, 2c-3	0.104
	H-FBSE	2b-1, 2b-2	0.095
	FBSAA	4a-1	0.036
	U-E-FBSE	2f-1	0.033
	FEtSE	2a-1	0.014
	U-FBSE	2e-1	0.007
	Headgroup isomer of FBSAA	4a-2	0.002
	H-E-FBSE	2d-1	0.001
Standard solution	FBSA	1a-1	99.93
Impurity in standard solution of FBSA	E-FBSA	1c-1 &1c-2	0.062
	H-FBSA	1b-1	0.012
Standard solution	FBSEE diol	3a-1	99.57
Impurity in standard solution of FBSEE diol	H-FBSEE diol	3b-1	0.403

a: The relative peak area (%) = Peak area of compound / Sum of peak areas of all compounds

doi:10.6342/NTU202402180

4.5. Transformation Products and Reaction Products

4.5.1. Aldehyde and Hydration Products from Oxidation of FBSE

Primary alcohols can undergo oxidation to form either aldehydes or carboxylic acids, depending on the reaction conditions. When carboxylic acids are formed, the alcohol is initially oxidized to an aldehyde, which is further oxidized to the acid. Aldehydes possess a proton attached to the carbonyl carbon, making them susceptible to oxidation into carboxylic acids. The presence of the sulfonamido acetic acid series increased significantly in the effluent, suggesting the transformation of fluorinated alcohols into fluorinated acids through oxidation.

By identifying nontarget PFAS in sewage and effluents, an aldehyde, FBSAcAL (keto form), was identified, likely formed from the oxidation of FBSE. FBSAcAL in both keto and enol forms was detected at 31 minutes and 13 minutes, respectively, showing distinct polarity and MS2 spectra (**Figure 45** and **Figure 46**). Additionally, the hydrated form of FBSAcAL, named FBSAcAL hydrate (RT 30.01-32.63 min), was identified. Moreover, two isomers of FBSAA were detected, with one exhibiting higher polarity at RT 9.93 minutes, indicating structural differences with distinct MS2 spectrum (**Figure 40**). Considering the potential isomerization between acid and diol forms, fragment analysis suggested a diol structure[70] for the isomer. We initially

doi:10.6342/NTU202402180

propose an oxidation pathway, illustrating intermediate transformations of aldehydes (enol and keto forms), aldehyde hydrate, and the isomer of FBSAA in **Figure 62**.

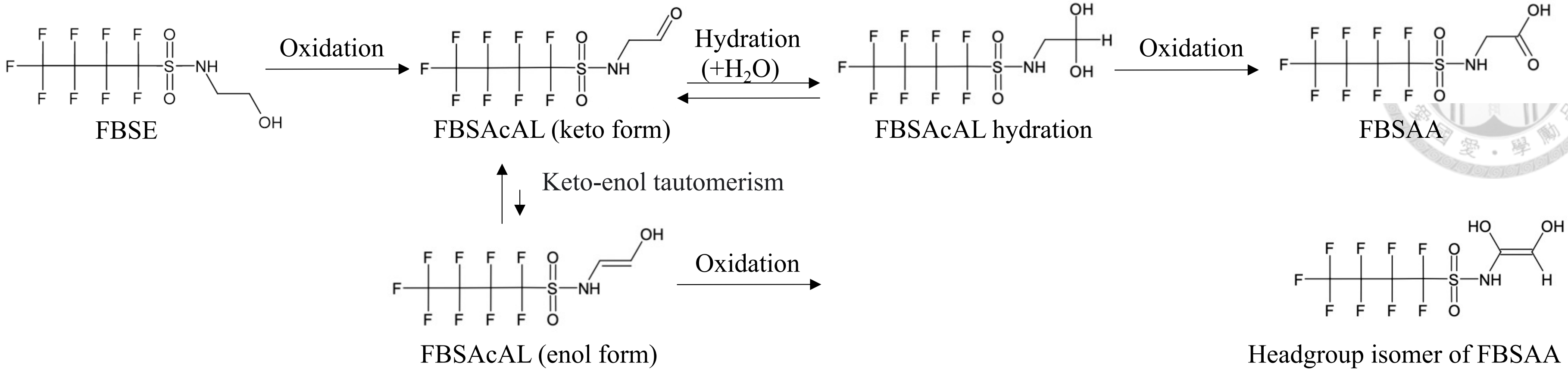

Figure 62 The oxidation pathway of FBSE to FBSAA involves intermediate compounds, including aldehyde and aldehyde hydration. Two isomers of FBSAcAL (keto and enol form) and two isomers of FBSAA were detected.

4.5.2. Aerobic Transformation Pathway of FBSEE diol

The finding that FBSAA and FBSEE diacid make up a substantial portion (65%-82%) of effluents from WWTP3 and WWTP4 in **Figure 61**(b), suggests the potential significance of FBSE and FBSEE diol as PFAS precursors in biotransformation. The predominant metabolite of FBSEE diol in an inherent biodegradability test was held by the European Chemicals Agency (ECHA);[40] however, its metabolic pathway in activated sludge remained unexplored and was established in this study. Our batch experiments constitute three sample groups: cleaned sludge (S), cleaned sludge with FBSEE diol (SC), and FBSEE diol in DI water (DI). These samples were shaken with perforated caps for 5 minutes (S1, SC1, DI1), 2 days (S2, SC2, DI2), 3 days (S3, SC3, DI3), and 4 days (S4, SC4, DI4). First, FBSEE mono-ol monoacid signals appeared within 5 minutes in SC1 (**Figure 63**), revealing swift FBSEE diol oxidation through activated sludge digestion. The signals of FBSEE diacid in SC2 peaked at 493 nM on the second day, confirming it as the primary degradation product. By the fourth day, signals in the batch experiment persisted at 39% of their initial level, aligning with the remaining FBSEE diacid in effluents from WWTP3 and WWTP4 (7.05-12.4%, 3-4%), indicating its expected release into the environment.[69] Additionally, FBSE was oxidized to FBSAA, reaching concentrations from 0.36 nM to 3.87 nM in SC2, emphasizing the

doi:10.6342/NTU202402180

apparent conversion of fluorinated alcohols to fluorinated acids during aerobic treatment. The notable increase in PFBSi (from 33.1 nM to 112 nM) and PFBS (from 0.45 nM to 29.3 nM) from SC1 to SC2 suggests a significant contribution from the degradation of FBSEE diacid to PFBSi and subsequently to PFBS. Meanwhile, the signal for PFBS continued to rise at 52.4 nM in SC4, suggesting that it might represent one of the terminal products and be less prone to biodegradation.[92] The formation of PFBSi through deamination from FBSA was not dominantly observed, despite the similarity in the mechanism to FOSAA converting to FOSA and further to PFOSi and PFOS through deamination.[41,38,39, 93] The in vitro metabolic formation of FBSA did not show concurrent PFBS formation from copolymer surfactants in post-2002 Scotchgard fabric protector products, aligning with our study.[94]

Our study aligns with the majority of transformation products from ECHA. However, due to the absence of a significant increase in the signal of FBSE among SC samples and the detection of FBSE in DI1 implying it as one of the impurities in the FBSEE diol standard, we have denoted our uncertainty about this process with dashed arrows and a question mark (**Figure 64**), suggesting the need for further experiments. Furthermore, our results unveiled additional products, such as FBSEE mono-ol monoacid, FBSAA, and PFBA. The significance lies in the first identification of FBSEE mono-ol monoacid and FBSAA as intermediate transformation products through nontarget screening and further supported by batch experiments. Additionally, PFBA was investigated by ECHA but was not detected. In contrast to ECHA's results, our study revealed delayed PFBA production in SC3 and detected it at very low concentrations (0.29 to 1.07 nM) in SC2-SC4, possibly explaining ECHA's nondetection due to its extremely low concentration. The limitations of this batch experiment, including the incomplete mass balance due to the volatility of FBSEE diol and FBSE,[40] and aldehyde and ketone compounds generated during metabolism, were not monitored in the open system setup. However, this should not affect the proposed pathway and confirmation of FBSE and FBSEE diol as significant PFAS precursors in biotransformation.

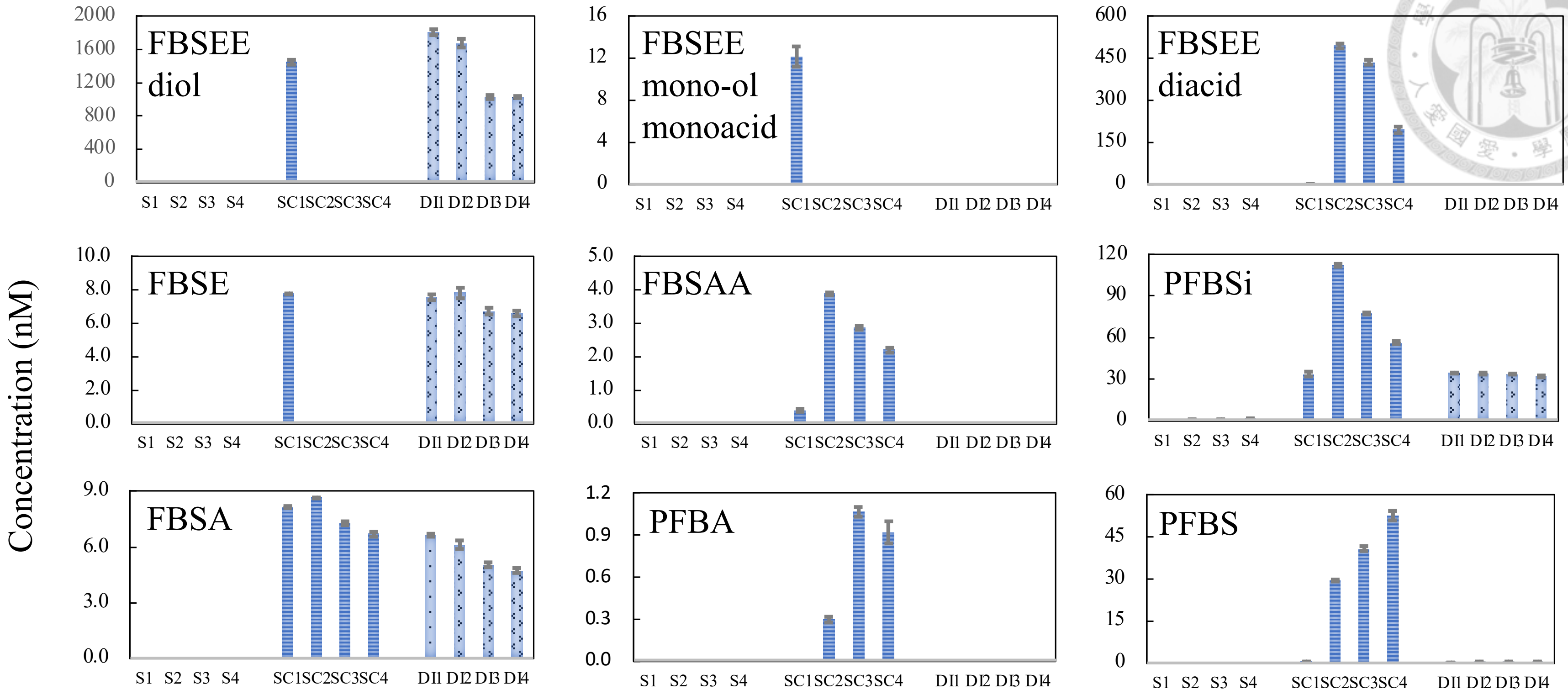

Figure 63. The S, SC, and DI samples represent cleaned sludge solution, cleaned sludge solution spiked FBSEE diol, and FBSEE diol in DI water without sludge, respectively. Each set comprised four replicate samples. Samples were subjected to agitation at designed times of 5 minutes, 2 days, 3 days, and 4 days, corresponding to numbers 1, 2, 3, and 4.

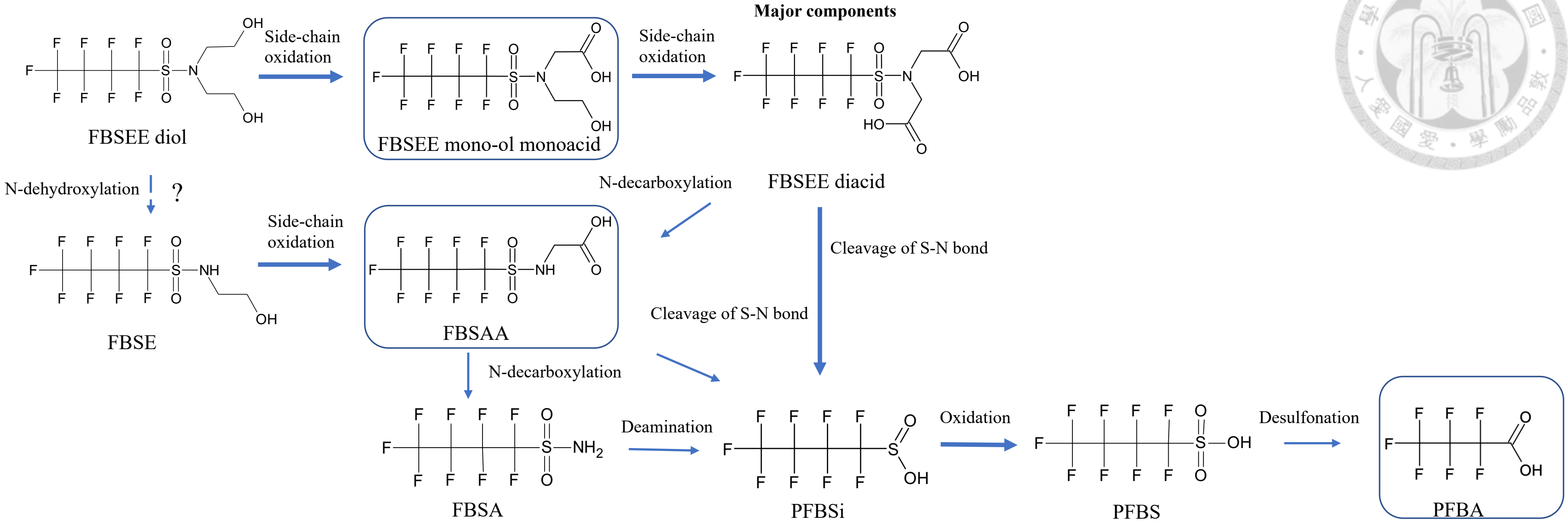

Figure 64 Proposed metabolic pathway of FBSEE diol in the wastewater treatment procedure. The compounds marked with bounding are substances not detected by the ECHA.

4.5.3. Reaction products

Due to the intricate nature of semiconductor processes, among the 12 prominent semiconductor industries in South Korea, 11 utilize 135 chemical constituents.[95] These include sulfuric acid, chromic acid, tetramethyl ammonium hydroxide, ethylene oxide, potassium dichromate, isopropanol, and formaldehyde, 33% (range: 16-56%) of the chemical compositions remain undisclosed due to commercial confidentiality. Notably, the undisclosed ingredients are predominantly employed in the photolithography process. The complex chemical condition involved in these semiconductor processes include strong acids, alkalis, and potent oxidants, and UV light is used in the photolithography process. Among the intricate blends of industrial chemicals in sewage, various reactions may take place, including hydration, oxidation, sulfonation, amide formation, and nitration. Additionally, during the biological treatment in wastewater treatment plants, reactions such as oxidation, deamination, desulfonation, and dicarboxylation occur. Due to the exceptional stability of the fluoroalkyl chain, reactions in the polar functional section led to distinct mass defect values for each transformation. This renders the use of homologous patterns for screening impractical. Our fragment-based approach overcomes the limitations of conventional homologous series. In total, we have identified 83 PFAS from 43 subclasses, with 29 substances reported for the first time. (Table 24)

FBSA-PrNO$_2$ and FBSE-Am are isomers with distinct polar head groups—sulfonamide and sulfonamido ethanol, respectively. (**Figure 14**) FBSA-PrNO$_2$ exhibit $[SO_2N]^-$ fragment along with an additional signal for the neutral loss of $C_3H_5NO_2$, categorizing it as miscellaneous FASAs (Subclass 1h). In contrast, FBSE-Am demonstrates a specific signal at 121.9917, confirming its classification as FASEs, and its neutral loss of CONH categorizes it within the miscellaneous FASEs (Subclass 2h). The RT of FBSA-PrNO$_2$ was 8.81 minutes, while that of FBSE-Am was 29.97 minutes, indicating significant differences in polarity. Thus, the headgroup isomers exhibit unique reactivity and physicochemical properties, may impact the variations in sludge metabolism during wastewater treatment in WWTPs[87]. Furthermore, E-FBSEs and FBSAcAL hydrate (Subclass 8a) are differentiated by their respective polar head groups: sulfonamido ethanol and sulfonamido acetaldehyde hydrate. (**Figure 65**) Specifically, fragment 121.9917 is unique to sulfonamido ethanol, while the hydrate can be identified by the neutral loss of H_2O. Finally, MeFBSAA and FBSPrA, which are polar head isomers, exhibit differences in the number of carbons in the sulfonamido carboxylic acid. (**Figure 66**) This clearly results in distinct neutral losses—one for acetic acid (CH_2CO_2) and the other for propanoic acid ($C_2H_4CO_2$). Additionally, MeFASAA showed no $[NSO_2]^-$ fragment signal, indicating solely the presence of only the $[SO_2F]^-$

doi:10.6342/NTU202402180

fragment signal due to N-methyl substitution. Conversely, FBSPrA exhibited a distinct $[SO_2N]^-$ fragment, signifying the lack of additional N-substitution. The specific fragmentation patterns have been classified in **Table 21**. This investigation unveiled 23 isomeric PFAS, including isomers with different headgroups and functional tail groups. These results emphasize the significance of understanding varied reactions and the overall composition of PFAS emissions in semiconductor wastewater, highlighting its complexity and posing challenges for subsequent wastewater treatment.

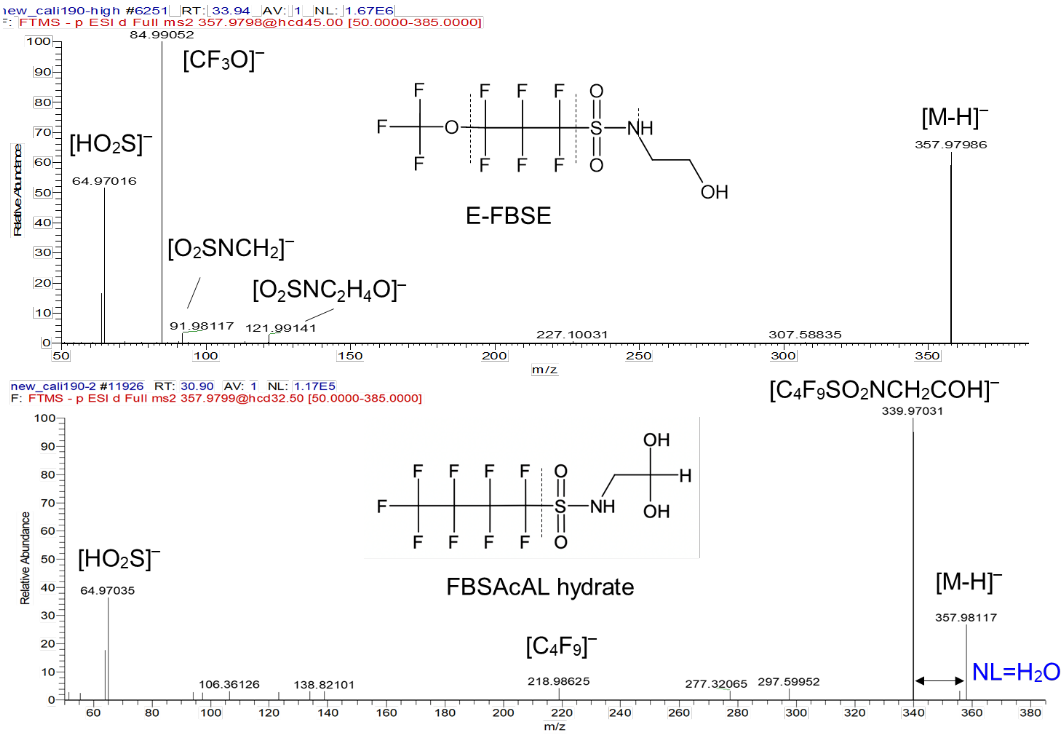

Figure 65 MS2 spectra of E-FBSE and FBSAcAL hydrate as polarhead isomers

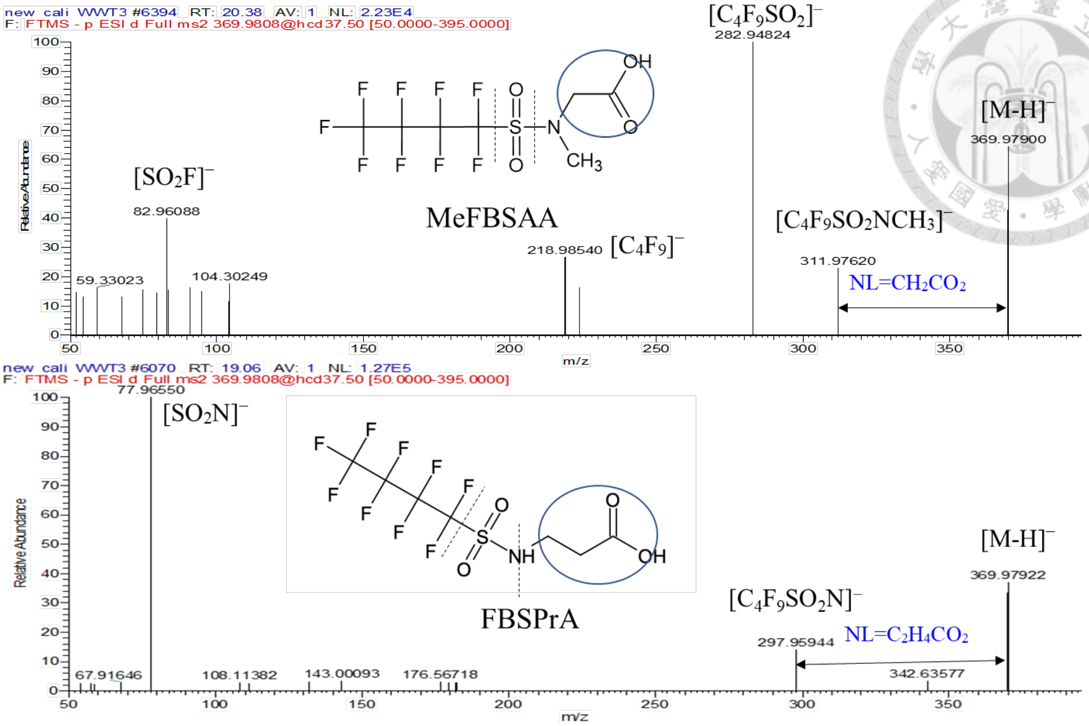

Figure 66 MS2 spectra of MeFBSAA and FBSPrA as polarhead isomers

5. Conclusions, Experimental Implication, and Suggestions

5.1. Conclusions

Semiconductor manufacturing employs per- and polyfluoroalkyl substances (PFAS) as fluoroasurfactants to enhance the quality of photolithography lines. For the nontarget PFAS approach, mass defect and homologous patterns are potent tools for uncovering PFAS within a series of homologous substances. However, industrial chemicals exhibit diverse and unique functional groups, making homologues less likely to occur in industrial manufacturing. Our research, employing a fragment-based approach to investigate nontarget PFAS, overcomes conventional homologous series limitations. In a mixture of PFAS standards used as a quality control (QC) sample, 92% (36 out of 39 compounds spanning 11 compound classes) were detectable through the fragment-based nontarget procedure. This indicates the effectiveness of this approach in identifying the hydrophobic and hydrophilic characteristics of various fluorosurfactants. Notably, 83 PFAS were detected in wastewater and effluent samples from semiconductor industry, including 29 newly discovered compounds, categorized into three groups. The dominant identified PFAS compounds were C4 sulfonamido derivatives, including perfluorobutane sulfonamido ethanol (FBSE), perfluorobutane sulfonamide (FBSA), and perfluorobutane sulfonamido diethanol (FBSEE diol), with

doi:10.6342/NTU202402180

maximum concentrations of 482 μg/L, 141 μg/L, and 83.5 μg/L in sewage, respectively. Subsequently, three ultrashort chain perfluoroalkyl acids (PFAAs) were identified in all samples, ranging from 0.004 μg/L to 19.9 μg/L. Three effluent samples from the associated industrial wastewater treatment plants (WWTPs) were further analyzed. This finding, that the C4 sulfonamido acetic acid series constitutes a significant portion (65%-82%) of effluents from WWTP3 and WWTP4, emphasizes the conversion of fluorinated alcohols to fluorinated acids during aerobic treatment. The identification of the intermediate metabolites of FBSEE diol, further supported by our laboratory batch studies, prompts the proposal of a novel metabolic pathway for FBSEE diol. The total amount of perfluorobutane sulfonamido derivatives reached 1934 μg/L (90%), while that of PFAAs, which have typically received attention, was only 205 μg/L (10%). This suggests that perfluorobutane sulfonamido derivatives are emerging as a new trend in fluorosurfactants used in the semiconductor industry, serving as PFAS precursors and contributing to the release of their metabolites into the environment. In addition, this study revealed 25 isomeric PFAS, encompassing headgroup isomers and functional tail group isomers. These findings underscore the importance of comprehending diverse reactions and the overall emission compositions of PFAS in semiconductor wastewater, highlighting its complexity and presenting challenges for subsequent wastewater treatment.

doi:10.6342/NTU202402180

5.2. Environmental implications

To investigate the potential source of PFAS in the semiconductor industry, we employed a distinctive nontarget approach, utilizing fragment and neutral loss strategies to screen both the hydrophilic head and hydrophobic chain of fluorosurfactants, enabling the identification of neutral and acidic PFAS compounds outside homologous series. Specifically, the predominant identified PFAS compounds are C4 sulfonamido derivatives, including FBSE, FBSA, and FBSEE diol, with maximum concentrations of 482 μg/L, 141 μg/L, and 83.5 μg/L in sewage. The study offers the first evidence of their dominant deployment in semiconductor manufacturing through nontarget analysis. Notably, their metabolites, including FBSAA, FBSEE diacid, FBSEE mono-ol monoacid, PFBSi, and PFBS, were identified. This finding, further supported by our degradation experiment, clearly suggests that WWTPs effectively converted fluorinated alcohols into fluorinated acids through aerobic treatment. This study reveals the crucial role of perfluorobutane sulfonamido substances and perfluorobutane sulfonamide as PFAS precursors in the semiconductor industry, contributing to the release of their degradation products from WWTPs into the environment.

Perfluorobutane sulfonamido derivatives, which accounted for 90% (1934 μg/L) of the total (2139 μg/L), far exceeded the concentration of PFAAs (205 μg/L), the

doi:10.6342/NTU202402180

compounds typically receiving more attention. Our research findings align with the emerging reports of perfluorobutane sulfonamido derivatives in the global environment, such as the presence of FBSA in Great Lakes fish[61] and the detection of FBSA, FBSEE diol, and FBSAA downstream of fluorochemical manufacturing facilities in the United States and Belgium.[57,64] These reports, mirroring our study, highlight the growing importance of perfluorobutane sulfonamido derivatives in terms of their use and distribution, possibly linked to supplier formulation changes.[22]

5.3. Suggestions

1. A fragment-based approach has been developed to identify unique industrial chemicals, proving its effectiveness in understanding the diverse reaction and biotransformation products that constitute the actual emissions of PFAS in semiconductor wastewater. It is suggested to further investigate environmental matrices—such as surface water, groundwater, soil, and air—to fully comprehend the fate and transportation of perfluorobutane sulfonamido derivatives from industrial use and discharge.
2. The toxicity of these emerging PFAS has not yet been conclusively determined internationally. Therefore, it is essential to continue gathering more information and closely monitoring international toxicity assessment data to understand their potential hazards.
3. According to the technical report from the semiconductor industry, which highlights the longstanding challenge of eliminating PFAS usage in semiconductor processes.[5,6] There is an ongoing need for research to identify emerging PFAS compounds and assess their degradation during wastewater treatment.
4. Regulating PFAS precursors under the Stockholm Convention presents challenges due to the absence of standards and standardized identification methods for the

diverse range of PFAS precursors. These precursors undergo degradation, forming terminal PFAS through amendments to polar functional groups. This complexity makes it difficult to recognize and quantify precursor levels, complicating market surveillance without authentic standards. Although our streamlined fragment-based approach offers a strategic solution for identifying PFAS precursors, our PFAS analysis primarily targets the negative mode. However, certain types like cationic PFAS, telomer alcohols, and specific zwitterionic PFAS compounds, which are detectable only in their positively charged state, were not within the scope of this study. We suggest further investigation into these compounds in future studies.

doi:10.6342/NTU202402180

6. References

(1) Kissa, E. *Fluorinated surfactants and repellents*; CRC Press, 2001.

(2) Buck, R. C.; Franklin, J.; Berger, U.; Conder, J. M.; Cousins, I. T.; de Voogt, P.; Jensen, A. A.; Kannan, K.; Mabury, S. A.; van Leeuwen, S. P. Perfluoroalkyl and polyfluoroalkyl substances in the environment: terminology, classification, and origins. *Integr Environ Assess Manag* **2011**, *7* (4), 513-541. DOI: 10.1002/ieam.258 From NLM.

(3) Olsen, G. W.; Mair, D. C.; Lange, C. C.; Harrington, L. M.; Church, T. R.; Goldberg, C. L.; Herron, R. M.; Hanna, H.; Nobiletti, J. B.; Rios, J. A.; et al. Per- and polyfluoroalkyl substances (PFAS) in American Red Cross adult blood donors, 2000–2015. *Environmental Research* **2017**, *157*, 87-95. DOI: https://doi.org/10.1016/j.envres.2017.05.013.

(4) OECD. Reconciling Terminology of the Universe of Per-and Polyfluoroalkyl Substances: Recommendations and Practical Guidance, OECD Series on Risk Management, No. 61. OECD Publishing Paris: 2021. Wang, Z.; Buser, A. M.; Cousins, I. T.; Demattio, S.; Drost, W.; Johansson, O.; Ohno, K.; Patlewicz, G.; Richard, A. M.; Walker, G. W.; et al. A New OECD Definition for Per- and Polyfluoroalkyl Substances. *Environmental Science & Technology* **2021**, *55* (23), 15575-15578. DOI: 10.1021/acs.est.1c06896.

(5) PFOS and PFOA Conversion to Short-Chain PFAS-Containing Materials Used in Semiconductor Manufacturing, Semiconductor PFAS Consortium Photolithography Working Group. **2023**.

(6) Semiconductor Industry Association, S. *PFAS-Containing Surfactants Used in Semiconductor Manufacturing. Semiconductor PFAS consortium photolithography working group,* ; 2023.

(7) Glüge, J.; Scheringer, M.; Cousins, I. T.; DeWitt, J. C.; Goldenman, G.; Herzke, D.; Lohmann, R.; Ng, C. A.; Trier, X.; Wang, Z. An overview of the uses of per- and polyfluoroalkyl substances (PFAS). *Environ Sci Process Impacts* **2020**, *22* (12), 2345-2373. DOI: 10.1039/d0em00291g From NLM.

(8) Norden. SPIN – Substances in preparations in Nordic countries, http://www.spin2000.net/spinmyphp/,. **published 2020, accessed April 8, 2020.**

(9) Butenhoff, J. L.; Olsen, G. W.; Pfahles-Hutchens, A. The applicability of biomonitoring data for perfluorooctanesulfonate to the environmental public health continuum. *Environ Health Perspect* **2006**, *114* (11), 1776-1782. DOI: 10.1289/ehp.9060 From NLM.

(10) PFOA Stewardship Program Baseline Year Summary Report. U.S. EPA.

(11) US EPA. TSCA Section 8(a)(7) Reporting and Recordkeeping Requirements for Perfluoroalkyl and Polyfluoroalkyl Substances https://reurl.cc/A44b03, 2023.

(12) Nielsen, C. J. Potential PFBS and PFHxS Precursors - literature study and theoretical assessment of abiotic degradation pathways leading to PFBS and PFHxS. University of Oslo, 2017.

(13) Lin, A. Y.; Panchangam, S. C.; Lo, C. C. The impact of semiconductor, electronics and optoelectronic industries on downstream perfluorinated chemical contamination in Taiwanese rivers. *Environ Pollut* **2009**, *157* (4), 1365-1372. DOI: 10.1016/j.envpol.2008.11.033 From NLM.

(14) Lin, A. Y.; Panchangam, S. C.; Tsai, Y. T.; Yu, T. H. Occurrence of perfluorinated compounds in the aquatic environment as found in science park effluent, river water, rainwater, sediments, and biotissues. *Environ Monit Assess* **2014**, *186* (5), 3265-3275. DOI: 10.1007/s10661-014-3617-9 From NLM.

(15) Wang, Z.; Cousins, I. T.; Scheringer, M.; Hungerbühler, K. Fluorinated alternatives to long-chain perfluoroalkyl carboxylic acids (PFCAs), perfluoroalkane sulfonic acids (PFSAs) and their potential precursors. *Environ Int* **2013**, *60*, 242-248. DOI: 10.1016/j.envint.2013.08.021 From NLM.

(16) Wang, Z.; Cousins, I. T.; Scheringer, M.; Hungerbuehler, K. Hazard assessment of fluorinated alternatives to long-chain perfluoroalkyl acids (PFAAs) and their precursors: status quo, ongoing challenges and possible solutions. *Environ Int* **2015**, *75*, 172-179. DOI: 10.1016/j.envint.2014.11.013 From NLM.

(17) Krulikowski, L. J. a. S. Taiwan—The Silicon Island. Commission, U. S. I. T., Ed.; February 2024.

(18) TSIA 2022 年第四季暨 2022 全年台灣 IC 產業營運成果出爐. Taiwan Semiconductor Industry Association: February, 2023. .

(19) Background on Semiconductor Manufacturing and PFAS, Semiconductor PFAS Consortium. **2023**.

(20) PFAS-Containing Photo-Acid Generators Used in Semiconductor Manufacturing, Semiconductor PFAS consortium photolithography working group, the Semiconductor Industry Association (SIA). **2023**.

(21) PFAS-Containing Materials Used in Semiconductor Manufacturing Assembly Test Packaging and Substrate Processes, Semiconductor PFAS Consortium Assembly, Test, Packaging and Substrates Working Group. **2023**.

(22) Semiconductor Industry Association, S. PFAS-Containing Wet Chemistries Used in Semiconductor Manufacturing, Semiconductor PFAS Consortium Wet Chemicals Working Group. 2023.

(23) POPRC. *Report on the assessment of alternatives to perfluorooctane sulfonic acid*

(PFOS), its salts and perfluorooctane sulfonyl fluoride (PFOSF); UNEP/POPS/POPRC.14/INF/13; 2019.

(24) “Joint Statement of the 21st Meeting of World Semiconductor Council." World Semiconductor Council 21st Meeting. Kyoto. **2017**.

(25) Mueller, R.; Yingling, V. History and use of per-and polyfluoroalkyl substances (PFAS). *Interstate Technology & Regulatory Council* **2017**.

(26) Jacob, P.; Barzen-Hanson, K. A.; Helbling, D. E. Target and Nontarget Analysis of Per- and Polyfluoralkyl Substances in Wastewater from Electronics Fabrication Facilities. *Environmental Science & Technology* **2021**, *55* (4), 2346-2356. DOI: 10.1021/acs.est.0c06690.

(27) Jacob, P.; Helbling, D. E. Rapid and Simultaneous Quantification of Short- and Ultrashort-Chain Perfluoroalkyl Substances in Water and Wastewater. *ACS ES&T Water* **2023**, *3* (1), 118-128. DOI: 10.1021/acsestwater.2c00446.

(28) (OECD), O. f. E. C.-O. a. D. OECD Environment, Health and Safety Publications Series on Emission Scenario Documents No. 9: Emission Scenario Document on Photoresist Use in Semiconductor Manufacturing. https://one.oecd.org/document/env/jm/mono(2004)14/rev1/en/pdf. . **2010.** .

(29) Nason, S. L.; Koelmel, J.; Zuverza-Mena, N.; Stanley, C.; Tamez, C.; Bowden, J. A.; Godri Pollitt, K. J. Software Comparison for Nontargeted Analysis of PFAS in AFFF-Contaminated Soil. *J Am Soc Mass Spectrom* **2021**, *32* (4), 840-846. DOI: 10.1021/jasms.0c00261 From NLM.

(30) Jeong, Y.; Da Silva, K. M.; Iturrospe, E.; Fuiji, Y.; Boogaerts, T.; van Nuijs, A. L. N.; Koelmel, J.; Covaci, A. Occurrence and contamination profile of legacy and emerging per- and polyfluoroalkyl substances (PFAS) in Belgian wastewater using target, suspect and non-target screening approaches. *Journal of Hazardous Materials* **2022**, *437*, 129378. DOI: https://doi.org/10.1016/j.jhazmat.2022.129378.

(31) Liu, Y.; Pereira, A. D. S.; Martin, J. W. Discovery of C5–C17 Poly- and Perfluoroalkyl Substances in Water by In-Line SPE-HPLC-Orbitrap with In-Source Fragmentation Flagging. *Analytical Chemistry* **2015**, *87* (8), 4260-4268. DOI: 10.1021/acs.analchem.5b00039.

(32) Hensema, T. J.; Berendsen, B. J. A.; van Leeuwen, S. P. J. Non-targeted identification of per- and polyfluoroalkyl substances at trace level in surface water using fragment ion flagging. *Chemosphere* **2021**, *265*, 128599. DOI: 10.1016/j.chemosphere.2020.128599 From NLM.

(33) Zweigle, J.; Bugsel, B.; Zwiener, C. FindPFΔS: Non-Target Screening for PFAS─Comprehensive Data Mining for MS(2) Fragment Mass Differences. *Anal Chem* **2022**, *94* (30), 10788-10796. DOI: 10.1021/acs.analchem.2c01521 From NLM.

(34) Wang, Y.; Yu, N.; Zhu, X.; Guo, H.; Jiang, J.; Wang, X.; Shi, W.; Wu, J.; Yu, H.;

Wei, S. Suspect and Nontarget Screening of Per- and Polyfluoroalkyl Substances in Wastewater from a Fluorochemical Manufacturing Park. *Environ Sci Technol* **2018**, *52* (19), 11007-11016. DOI: 10.1021/acs.est.8b03030 From NLM.

(35) Liu, T.; Hu, L. X.; Han, Y.; Dong, L. L.; Wang, Y. Q.; Zhao, J. H.; Liu, Y. S.; Zhao, J. L.; Ying, G. G. Non-target and target screening of per- and polyfluoroalkyl substances in landfill leachate and impact on groundwater in Guangzhou, China. *Sci Total Environ* **2022**, *844*, 157021. DOI: 10.1016/j.scitotenv.2022.157021 From NLM.

(36) Wang, X.; Yu, N.; Qian, Y.; Shi, W.; Zhang, X.; Geng, J.; Yu, H.; Wei, S. Non-target and suspect screening of per- and polyfluoroalkyl substances in Chinese municipal wastewater treatment plants. *Water Res* **2020**, *183*, 115989. DOI: 10.1016/j.watres.2020.115989 From NLM.

(37) Munoz, G.; Michaud, A. M.; Liu, M.; Vo Duy, S.; Montenach, D.; Resseguier, C.; Watteau, F.; Sappin-Didier, V.; Feder, F.; Morvan, T.; et al. Target and Nontarget Screening of PFAS in Biosolids, Composts, and Other Organic Waste Products for Land Application in France. *Environ Sci Technol* **2022**, *56* (10), 6056-6068. DOI: 10.1021/acs.est.1c03697 From NLM.

(38) Zhang, W.; Pang, S.; Lin, Z.; Mishra, S.; Bhatt, P.; Chen, S. Biotransformation of perfluoroalkyl acid precursors from various environmental systems: advances and perspectives. *Environmental Pollution* **2021**, *272*, 115908. DOI: https://doi.org/10.1016/j.envpol.2020.115908.

(39) Zhang, L.; Lee, L. S.; Niu, J.; Liu, J. Kinetic analysis of aerobic biotransformation pathways of a perfluorooctane sulfonate (PFOS) precursor in distinctly different soils. *Environ Pollut* **2017**, *229*, 159-167. DOI: 10.1016/j.envpol.2017.05.074 From NLM.

(40) ECHA 27023/5/1. https://echa.europa.eu/registration-dossier/-/registered-dossier/27023/5/1.

(41) Mejia Avendaño, S.; Liu, J. Production of PFOS from aerobic soil biotransformation of two perfluoroalkyl sulfonamide derivatives. *Chemosphere* **2015**, *119*, 1084-1090. DOI: https://doi.org/10.1016/j.chemosphere.2014.09.059.

(42) UNEP, D. SC-9/12. Listing of Perfluorooctanoic Acid (PFOA), its Salts and PFOA-Related Compounds. 2019; UNEP-POPS-COP.9-SC-9-12
Conference of the Parties to the Stockholm Convention on Persistent Organic Pollutants, Geneva, Switzerland (2019).

(43) Posner, S.; Roos, S.; Poulsen, P. B.; Jörundsdottir, H. Ó.; Gunnlaugsdóttir, H.; Trier, D. X.; Jensen, A. A.; Katsogiannis, A. A.; Herzke, D.; Bonefeld-Jörgensen, E. C.; et al. *Per and polyfluorinated substances in the Nordic Countries: Use, occurence and toxicology*; Nordic Council of Ministers, 2013.

(44) Cheremisinoff, N. P. *Perfluorinated chemicals (PFCs): contaminants of concern*; John Wiley & Sons, 2016.

(45) Guidance on best available techniques and best environmental practices for the use of perfluorooctane sulfonic acid (PFOS) and related chemicals listed under the Stockholm Convention. UNEP: March 2017.

(46) Renner, R. The long and the short of perfluorinated replacements. *Environ Sci Technol* **2006**, *40* (1), 12-13. DOI: 10.1021/es062612a From NLM.

(47) EPA and 3M ANNOUNCE PHASE OUT OF PFOS. May, 2000.

(48) Loi, E. I. H.; Yeung, L. W. Y.; Mabury, S. A.; Lam, P. K. S. Detections of Commercial Fluorosurfactants in Hong Kong Marine Environment and Human Blood: A Pilot Study. *Environmental Science & Technology* **2013**, *47* (9), 4677-4685. DOI: 10.1021/es303805k.

(49) Poulsen, P. B.; Gram, L. K.; Jensen, A. A.; Rasmussen, A. A.; Ravn, C.; Møller, P.; Jørgensen, C.; Løkkegaard, K. *Substitution of PFOS for use in non-decorative hard chrome plating*; Environmental Protection Agency Washington, 2011.

(50) REACH - Registration, Evaluation, Authorisation and Restriction of Chemicals Regulation. 2013.

(51) Lucci, P.; Pacetti, D.; Núñez, O.; Frega, N. G. Current trends in sample treatment techniques for environmental and food analysis. *Chromatography: The Most Versatile Method of Chemical Analysis. InTech* **2012**, 127-164.

(52) Arsenault, J. C. *Beginner's Guide to SPE: Solid-Phase Extraction*; Waters Corporation, 2012.

(53) Baduel, C.; Mueller, J. F.; Rotander, A.; Corfield, J.; Gomez-Ramos, M. J. Discovery of novel per- and polyfluoroalkyl substances (PFASs) at a fire fighting training ground and preliminary investigation of their fate and mobility. *Chemosphere* **2017**, *185*, 1030-1038. DOI: 10.1016/j.chemosphere.2017.06.096 From NLM.

(54) Schymanski, E. L.; Singer, H. P.; Slobodnik, J.; Ipolyi, I. M.; Oswald, P.; Krauss, M.; Schulze, T.; Haglund, P.; Letzel, T.; Grosse, S.; et al. Non-target screening with high-resolution mass spectrometry: critical review using a collaborative trial on water analysis. *Anal Bioanal Chem* **2015**, *407* (21), 6237-6255. DOI: 10.1007/s00216-015-8681-7 From NLM.

(55) Schymanski, E. L.; Jeon, J.; Gulde, R.; Fenner, K.; Ruff, M.; Singer, H. P.; Hollender, J. Identifying small molecules via high resolution mass spectrometry: communicating confidence. *Environ Sci Technol* **2014**, *48* (4), 2097-2098. DOI: 10.1021/es5002105 From NLM.

(56) Charbonnet, J. A.; McDonough, C. A.; Xiao, F.; Schwichtenberg, T.; Cao, D.; Kaserzon, S.; Thomas, K. V.; Dewapriya, P.; Place, B. J.; Schymanski, E. L.; et al. Communicating Confidence of Per- and Polyfluoroalkyl Substance Identification via High-Resolution Mass Spectrometry. *Environ Sci Technol Lett* **2022**, *9* (6), 473-481. DOI: 10.1021/acs.estlett.2c00206 From NLM.

doi:10.6342/NTU202402180

(57) Newton, S.; McMahen, R.; Stoeckel, J. A.; Chislock, M.; Lindstrom, A.; Strynar, M. Novel Polyfluorinated Compounds Identified Using High Resolution Mass Spectrometry Downstream of Manufacturing Facilities near Decatur, Alabama. *Environ Sci Technol* **2017**, *51* (3), 1544-1552. DOI: 10.1021/acs.est.6b05330 From NLM.

(58) McCord, J.; Strynar, M. Identification of Per- and Polyfluoroalkyl Substances in the Cape Fear River by High Resolution Mass Spectrometry and Nontargeted Screening. *Environ Sci Technol* **2019**, *53* (9), 4717-4727. DOI: 10.1021/acs.est.8b06017 From NLM.

(59) Parent, M.; Savu, P.; Flynn, R. Fluorinated surfactants for buffered acid etch solutions. US20040089840, 2004.

(60) Savu, P.; Lamanna, W.; Parent, M. Fluorinated sulfonamide surfactants for aqueous cleaning solutions. US20050197273, 2005.

(61) Chu, S.; Letcher, R. J.; McGoldrick, D. J.; Backus, S. M. A New Fluorinated Surfactant Contaminant in Biota: Perfluorobutane Sulfonamide in Several Fish Species. *Environ Sci Technol* **2016**, *50* (2), 669-675. DOI: 10.1021/acs.est.5b05058 From NLM.

(62) Maldonado, V. Y.; Schwichtenberg, T.; Schmokel, C.; Witt, S. E.; Field, J. A. Electrochemical Transformations of Perfluoroalkyl Acid (PFAA) Precursors and PFAAs in Landfill Leachates. *ACS ES&T Water* **2022**, *2* (4), 624-634. DOI: 10.1021/acsestwater.1c00479.

(63) Hogue, C. 3M admits to unlawful release of PFAS. *C&EN Global Enterprise* **2019**, *97* (26), 16-16. DOI: 10.1021/cen-09726-polcon1.

(64) Barrett, A. New 3M FBSA Scandal in Belgium. Bioplastics News, 2021.

(65) Pickard, H. M.; Haque, F.; Sunderland, E. M. Bioaccumulation of Perfluoroalkyl Sulfonamides (FASA). *Environmental Science & Technology Letters* **2024**. DOI: 10.1021/acs.estlett.4c00143.

(66) Zhao, M.; Yao, Y.; Dong, X.; Baqar, M.; Fang, B.; Chen, H.; Sun, H. Nontarget Identification of Novel Per- and Polyfluoroalkyl Substances (PFAS) in Soils from an Oil Refinery in Southwestern China: A Combined Approach with TOP Assay. *Environmental Science & Technology* **2023**, *57* (48), 20194-20205. DOI: 10.1021/acs.est.3c05859.

(67) Fang, B.; Zhang, Y.; Chen, H.; Qiao, B.; Yu, H.; Zhao, M.; Gao, M.; Li, X.; Yao, Y.; Zhu, L.; et al. Stability and Biotransformation of 6:2 Fluorotelomer Sulfonic Acid, Sulfonamide Amine Oxide, and Sulfonamide Alkylbetaine in Aerobic Sludge. *Environmental Science & Technology* **2024**. DOI: 10.1021/acs.est.3c05506.

(68) Barrett, A. 3M Dumping me-FBSA and me-FBSE in Belgian Rivers. Bioplastics News, 2021.

(69) Tennessee Riverkeeper Inc v. 3M Company (5:16-cv-01029). District Court, N.D.

doi:10.6342/NTU202402180

Alabama: 2021; Vol. Retrived Oct.2, 2023 from https://fingfx.thomsonreuters.com/gfx/legaldocs/lbvgnowzwpq/Riverkeeper%20Settlement%20Agreement%2010-19-21%20(002)-compressed.pdf?utm_source=Sailthru&utm_medium=email&utm_campaign=Outgoing%20Paul%20Hastings%20chair%20says%20top-down%20law%20firm%20culture%20waning&utm_term=DailyDocket-MailingList%20v2.

(70) Rogers, C. O.; Lockwood, K. S.; Nguyen, Q. L.; Labbe, N. J. Diol isomer revealed as a source of methyl ketene from propionic acid unimolecular decomposition. *International Journal of Chemical Kinetics* **2021**, *53* (12), 1272-1284.

(71) Allred, B. M.; Lang, J. R.; Barlaz, M. A.; Field, J. A. Orthogonal zirconium diol/C18 liquid chromatography–tandem mass spectrometry analysis of poly and perfluoroalkyl substances in landfill leachate. *Journal of Chromatography A* **2014**, *1359*, 202-211. DOI: https://doi.org/10.1016/j.chroma.2014.07.056.

(72) ECHA 27023/6/2/1. https://echa.europa.eu/registration-dossier/-/registered-dossier/27023/6/2/1.

(73) Chen, Y.-J.; Wang, R.-D.; Shih, Y.-L.; Chin, H.-Y.; Lin, A. Y.-C. Emerging Perfluorobutane Sulfonamido Derivatives as a New Trend of Surfactants Used in the Semiconductor Industry. *Environmental Science & Technology* **2024**, *58* (3), 1648-1658. DOI: 10.1021/acs.est.3c04435.

(74) Neuwald, I. J.; Hübner, D.; Wiegand, H. L.; Valkov, V.; Borchers, U.; Nödler, K.; Scheurer, M.; Hale, S. E.; Arp, H. P. H.; Zahn, D. Ultra-Short-Chain PFASs in the Sources of German Drinking Water: Prevalent, Overlooked, Difficult to Remove, and Unregulated. *Environmental Science & Technology* **2022**, *56* (10), 6380-6390. DOI: 10.1021/acs.est.1c07949.

(75) Zhang, W.; Zhang, Y.; Taniyasu, S.; Yeung, L. W.; Lam, P. K.; Wang, J.; Li, X.; Yamashita, N.; Dai, J. Distribution and fate of perfluoroalkyl substances in municipal wastewater treatment plants in economically developed areas of China. *Environ Pollut* **2013**, *176*, 10-17. DOI: 10.1016/j.envpol.2012.12.019 From NLM.

(76) Blackwell, J. M.; Rachmady, W.; Kearns, G. J.; Morrison, D. J. High K dielectric growth on metal triflate or trifluoroacetate terminated III-V semiconductor surfaces. US7763317B2, 2010.

(77) Mulin, L.; Katz, D.; Riddell, N.; Plumb, R.; Burgess, J.; Jogsten, I. Reduction of LC/MS In-Source Fragmentation of HFPO-DA (GenX) Through Mobile Phase Additive Selection: Experiments to Increase [MH]-Formation. In *DioXin 2018: 38th International Symposium on Halogenated Persistent Organic Pollutants*, 2018; Society of Environmental Toxicology and Chemistry Krakow, Poland. Zweigle, J.; Bugsel, B.; Zwiener, C. FindPFΔS: Non-Target Screening for PFAS─Comprehensive Data Mining

for MS2 Fragment Mass Differences. *Analytical Chemistry* **2022**, *94* (30), 10788-10796. DOI: 10.1021/acs.analchem.2c01521.

(78) Hatakeyama, J.; Ohashi, M. Resist Composition and Patterning Process. US20200073237, 2020.

(79) Akiyama, Y.; Noya, G.; Kuramoto, K.; Takano, Y. Surface antireflection film forming composition and pattern forming method using the same. JP2009145658A, 2009.

(80) Schulze, S.; Zahn, D.; Montes, R.; Rodil, R.; Quintana, J. B.; Knepper, T. P.; Reemtsma, T.; Berger, U. Occurrence of emerging persistent and mobile organic contaminants in European water samples. *Water Research* **2019**, *153*, 80-90. DOI: https://doi.org/10.1016/j.watres.2019.01.008.

(81) Brunn, H.; Arnold, G.; Körner, W.; Rippen, G.; Steinhäuser, K. G.; Valentin, I. PFAS: forever chemicals—persistent, bioaccumulative and mobile. Reviewing the status and the need for their phase out and remediation of contaminated sites. *Environmental Sciences Europe* **2023**, *35* (1), 20. DOI: 10.1186/s12302-023-00721-8.

(82) ECHA: substance info card—trifluoromethanesulphonic acid. https://echa.europa.eu/de/substance-information/-/substanceinfo/100.014.625.

(83) Lee, C.-T. *Development and advanced characterization of novel chemically amplified resists for next generation lithography*; Georgia Institute of Technology, 2008. Christopher, K. O.; Florian, K.; Jingyuan, D. Review of essential use of fluorochemicals in lithographic patterning and semiconductor processing. *Journal of Micro/Nanopatterning, Materials, and Metrology* **2022**, *21* (1), 010901. DOI: 10.1117/1.JMM.21.1.010901.

(84) Lange, C. C. Anaerobic biotransformation of N-methyl perfluorobutanesulfonamido ethanol and N-ethyl perfluorooctanesulfonamido ethanol. *Environmental Toxicology and Chemistry* **2018**, *37* (3), 768-779. DOI: https://doi.org/10.1002/etc.4014.

(85) Paul, A. G.; Jones, K. C.; Sweetman, A. J. A first global production, emission, and environmental inventory for perfluorooctane sulfonate. *Environmental science & technology* **2009**, *43* (2), 386-392.

(86) Benskin, J. P.; De Silva, A. O.; Martin, J. W. Isomer profiling of perfluorinated substances as a tool for source tracking: a review of early findings and future applications. *Reviews of Environmental Contamination and Toxicology Volume 208: Perfluorinated alkylated substances* **2010**, 111-160.

(87) Londhe, K.; Lee, C.-S.; McDonough, C. A.; Venkatesan, A. K. The Need for Testing Isomer Profiles of Perfluoroalkyl Substances to Evaluate Treatment Processes. *Environmental Science & Technology* **2022**, *56* (22), 15207-15219. DOI: 10.1021/acs.est.2c05518.

doi:10.6342/NTU202402180

(88) Loewen, M.; Halldorson, T.; Wang, F.; Tomy, G. Fluorotelomer Carboxylic Acids and PFOS in Rainwater from an Urban Center in Canada. *Environmental Science & Technology* **2005**, *39* (9), 2944-2951. DOI: 10.1021/es048635b.

(89) Jin, B.; Liu, H.; Che, S.; Gao, J.; Yu, Y.; Liu, J.; Men, Y. Substantial defluorination of polychlorofluorocarboxylic acids triggered by anaerobic microbial hydrolytic dechlorination. *Nat Water* **2023**, *1* (5), 451-461. DOI: 10.1038/s44221-023-00077-6 From NLM.

(90) Yang, J.-S.; Lai, W. W.-P.; Lin, A. Y.-C. New insight into PFOS transformation pathways and the associated competitive inhibition with other perfluoroalkyl acids via photoelectrochemical processes using GOTiO2 film photoelectrodes. *Water Research* **2021**, *207*, 117805. DOI: https://doi.org/10.1016/j.watres.2021.117805.

(91) Jin, B.; Zhu, Y.; Zhao, W.; Liu, Z.; Che, S.; Chen, K.; Lin, Y.-H.; Liu, J.; Men, Y. Aerobic Biotransformation and Defluorination of Fluoroalkylether Substances (ether PFAS): Substrate Specificity, Pathways, and Applications. *Environmental Science & Technology Letters* **2023**, *10* (9), 755-761. DOI: 10.1021/acs.estlett.3c00411.

(92) Arvaniti, O. S.; Stasinakis, A. S. Review on the occurrence, fate and removal of perfluorinated compounds during wastewater treatment. *Sci Total Environ* **2015**, *524-525*, 81-92. DOI: 10.1016/j.scitotenv.2015.04.023 From NLM.

(93) Zhao, S.; Ma, X.; Fang, S.; Zhu, L. Behaviors of N-ethyl perfluorooctane sulfonamide ethanol (N-EtFOSE) in a soil-earthworm system: Transformation and bioaccumulation. *Science of The Total Environment* **2016**, *554-555*, 186-191. DOI: https://doi.org/10.1016/j.scitotenv.2016.02.180.

(94) Chu, S.; Letcher, R. J. In vitro metabolic formation of perfluoroalkyl sulfonamides from copolymer surfactants of pre- and post-2002 scotchgard fabric protector products. *Environ Sci Technol* **2014**, *48* (11), 6184-6191. DOI: 10.1021/es500169x From NLM.

(95) Yoon, C.; Kim, S.; Park, D.; Choi, Y.; Jo, J.; Lee, K. Chemical Use and Associated Health Concerns in the Semiconductor Manufacturing Industry. *Safety and Health at Work* **2020**, *11* (4), 500-508. DOI: https://doi.org/10.1016/j.shaw.2020.04.005.

7. Appendix

The list of identified PFAS, along with their abbreviation, molecular formulas and chemical structures, in this study.

Number	Chemical name	Abbreviation	Molecular formula (M)	Precursor ion	Structure
1a-1	1,1,2,2,3,3,4,4,4-nonafluorobutane-1-sulfonamide	FBSA	$C_4H_2F_9NO_2S$	$[M-H]^-$	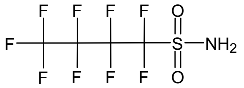
1b-1	1,1,2,2,3,3,4,4-octafluorobutane-1-sulfonamide	H-FBSA	$C_4H_3F_8NO_2S$	$[M-H]^-$	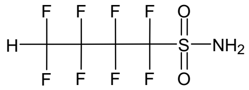
1c-1 1c-2	1,1,2,2,3,3-hexafluoro-3-(trifluoromethoxy)propane-1-sulfonamide 1,1,2,2-tetrafluoro-2-(pentafluoroethoxy)ethane-1-sulfonamide	E-FBSA	$C_4H_2F_9NO_3S$	$[M-H]^-$	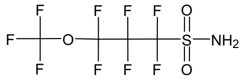 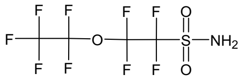
1d-1	(1,1,2,2,3,3,4,4,4-nonafluorobutane-1-sulfonyl)sulfamic acid	FBSA-SO$_3$H	$C_4HF_9S_2O_5N$	$[M-H]^-$	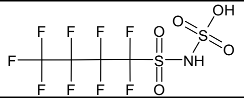
1e-1	N-carbamoyl-1,1,2,2,3,3,4,4,4-nonafluorobutane-1-sulfonamide	FBSA-Am	$C_5H_3F_9N_2O_3S$	$[M-H]^-$	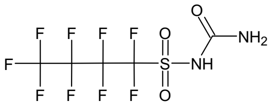
1f-1	2-(1,1,2,2,3,3,4,4,4-nonafluorobutane-1-sulfonamido)acetamide	FBSA-MeAm	$C_6H_5F_9N_2O_3S$	$[M-H]^-$	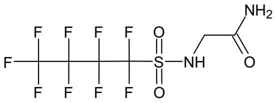
1g-1	1,1,2,2,3,3,4,4,4-nonafluoro-N-(nitromethyl)butane-1-sulfonamide	FBSA-MeNO$_2$	$C_5H_3F_9N_2O_4S$	$[M-H]^-$	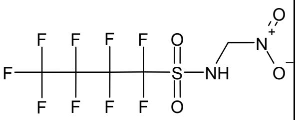
1h-1	1,1,2,2,3,3,4,4,4-nonafluoro-*N*-(3-nitropropyl)butane-1-sulfonamide	FBSA-PrNO$_2$	$C_7H_7F_9N_2O_4S$	$[M-H]^-$	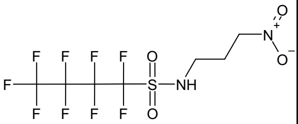
1i-1	N-(diazenylmethyl)-1,1,2,2,3,3,4,4,4-nonafluorobutane-1-sulfonamide	FBSA-diazene	$C_5H_4F_9N_3O_2S$	$[M-H]^-$	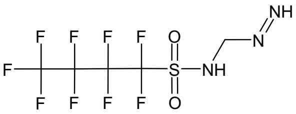
1j-1	1,1,2,2,3,3,4,4,4-nonafluoro-*N*-methylbutane-1-sulfonamide	MeFBSA	$C_5H_4F_9NO_2S$	$[M-H]^-$	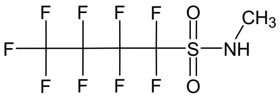
2a-1	1,1,2,2,2-pentafluoro-N-(2-hydroxyethyl)ethane-1-sulfonamide	FEtSE	$C_4H_6F_5NO_3S$	$[M-H]^-$	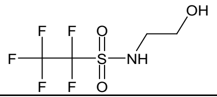
2a-2	1,1,2,2,3,3,3-heptafluoro-N-(2-	FPrSE	$C_5H_6F_7NO_3S$	$[M-H]^-$	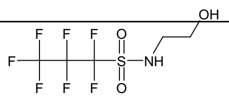

Number	Chemical name	Abbreviation	Molecular formula (M)	Precursor ion	Structure
	hydroxyethyl)propane-1-sulfonamide				
2a-3	1,1,2,2,3,3,4,4,4-nonafluoro-N-(2-hydroxyethyl)butane-1-sulfonamide	FBSE	$C_6H_6F_9NO_3S$	$[M-H]^-$	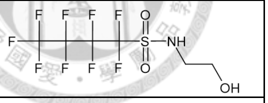
2b-1& 2b-2	1,1,2,2,3,3,4,4-octafluoro-*N*-(2-hydroxyethyl)butane-1-sulfonamide	H-FBSE	$C_6H_7F_8NO_3S$	$[M-H]^-$	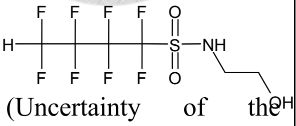 (Uncertainty of the position of H)
2c-1 2c-2 2c-3	1,1,2,2,3,3-hexafluoro-*N*-(2-hydroxyethyl)-3-(trifluoromethoxy)propane-1-sulfonamide 1,1-difluoro-1-(heptafluoropropoxy)-*N*-(2-hydroxyethyl)methanesulfonamide 1,1,2,2-tetrafluoro-*N*-(2-hydroxyethyl)-2-(pentafluoroethoxy)ethane-1-sulfonamide	E-FBSE	$C_6H_6F_9NO_4S$	$[M-H]^-$	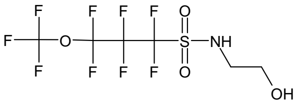 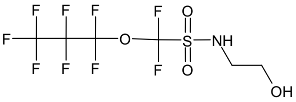 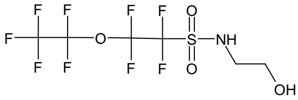
2d-1	1,1,2,2-tetrafluoro-N-(2-hydroxyethyl)-2-(1,1,2,2-tetrafluoroethoxy)ethane-1-sulfonamide	H-E-FBSE	$C_6H_7F_8NO_4S$	$[M-H]^-$	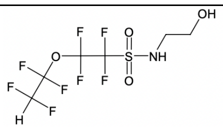
2e-1	1,1,2,2,3,4,4-heptafluoro-N-(2-hydroxyethyl)but-3-ene-1-sulfonamide	U-FBSE	$C_6H_6F_7NO_3S$	$[M-H]^-$	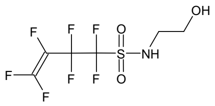
2f-1	1,1-difluoro-N-(2-hydroxyethyl)-1-[(1,1,2,3,3-pentafluoroprop-2-en-1-yl)oxy]methanesulfonamide	U-E-FBSE	$C_6H_6F_7NO_4S$	$[M-H]^-$	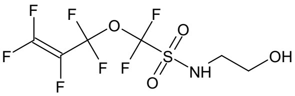
2g-1	(2-hydroxyethyl) (1,1,2,2,3,3,4,4,4-nonafluorobutane-1-sulfonyl)sulfamic acid	FBSE-SO_3H	$C_6H_6F_9NO_6S_2$	$[M-H]^-$	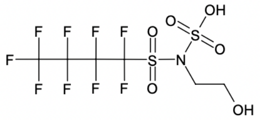
2h-1	*N*-carbamoyl-1,1,2,2,3,3,4,4,4-nonafluoro-*N*-(2-hydroxyethyl)butane-1-sulfonamide	FBSE-Am	$C_7H_7F_9N_2O_4S$	$[M-H]^-$	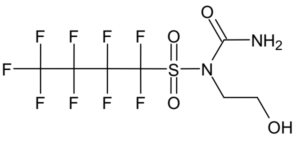
2i-1	1,1,2,2,3,3,4,4,4-nonafluoro-N-(2-hydroxyethyl)-N-methylbutane-1-sulfonamide	MeFBSE	$C_7H_8F_9O_3SN$	$[M+CH_3COO]^-$	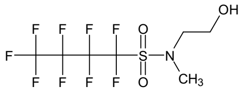
3a-1	1,1,2,2,3,3,4,4,4-nonafluoro-*N*,*N*-bis(2-hydroxyethyl)butane-1-sulfonamide	FBSEE diol	$C_8H_{10}F_9NO_4S_2$	$[M-H]^-$ $[M+CH_3COO]^-$ $[M+HCOO]^-$ $[2M-H]^-$	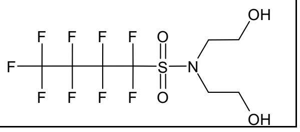

doi:10.6342/NTU202402180

Num ber	Chemical name	Abbreviation	Molecular formula (M)	Precursor ion	Structure
3b-1	1,1,2,2,3,3,4,4-octafluoro-N,N-bis(2-hydroxyethyl)butane-1-sulfonamide	H-FBSEE diol	$C_8H_{11}F_8NO_4S$	$[M+CH_3COO]^-$	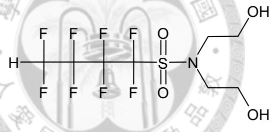
4a-1	(1,1,2,2,3,3,4,4,4-nonafluorobutane-1-sulfonamido)acetic acid	FBSAA	$C_6H_4F_9NO_4S$	$[M-H]^-$	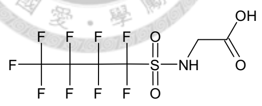
4a-2	N-[(Z)-1,2-dihydroxyethenyl]-1,1,2,2,3,3,4,4,4-nonafluorobutane-1-sulfonamide	Headgroup isomer of FBSAA	$C_6H_4F_9NO_4S$	$[M-H]^-$	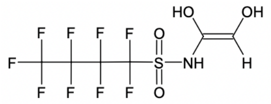
4b-1	[(1,1,2,2,3,3,4,4-octafluorobutane-1-sulfonyl)amino]acetic acid	H-FBSAA	$C_6H_5F_8NO_4S$	$[M-H]^-$	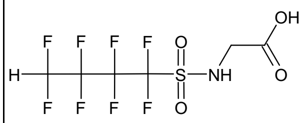
4c-1 4c-2	[1,1,2,2,3,3-hexafluoro-3-(trifluoromethoxy)propane-1-sulfonamido]acetic acid [1,1,2,2-tetrafluoro-2-(pentafluoroethoxy)ethanesulfonamido]acetic acid	E-FBSAA	$C_6H_4F_9NO_5S$	$[M-H]^-$	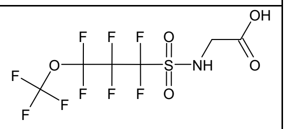 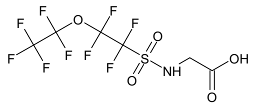
4d-1	[methyl(1,1,2,2,3,3,4,4,4-nonafluorobutane-1-sulfonyl)amino]acetic acid	MeFBSAA	$C_7H_6F_9NO_4S$	$[M-H]^-$	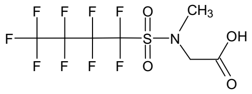
4e-1	3-[(1,1,2,2,3,3,4,4,4-nonafluorobutane-1-sulfonyl)amino]propanoic acid	FBSPrA	$C_7H_6F_9NO_4S$	$[M-H]^-$	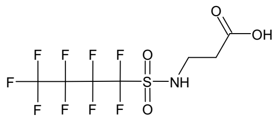
5a-1	2,2'-[(1,1,2,2,3,3,4,4,4-nonafluorobutane-1-sulfonyl)azanediyl]diacetic acid	FBSEE diacid	$C_8H_6F_9NO_6S$	$[M-H]^-$	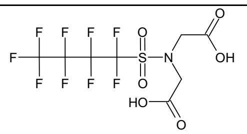
6a-1	[(2-hydroxyethyl)(1,1,2,2,3,3,4,4,4-nonafluorobutane-1-sulfonyl)amino]acetic acid	FBSEE mono-ol monoacid	$C_8H_8F_9NO_5S$	$[M-H]^-$	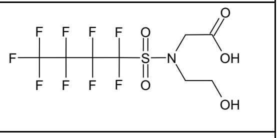
7a-1	1,1,2,2,3,3,4,4,4-nonafluoro-N-[(E)-2-hydroxyethenyl]butane-1-sulfonamide	FBSAcAL (enol form)	$C_6H_4F_9NO_3S$	$[M-H]^-$	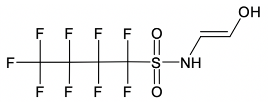
7a-2	1,1,2,2,3,3,4,4,4-nonafluoro-*N*-(2-oxoethyl)butane-1-sulfonamide	FBSAcAL (keto form)	$C_6H_4F_9NO_3S$	$[M-H]^-$	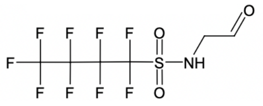
8a-1	*N*-(2,2-dihydroxyethyl)-1,1,2,2,3,3,4,4,4-nonafluorobutane-1-sulfonamide	FBSAcAL hydrate	$C_6H_6F_9NO_4S$	$[M-H]^-$	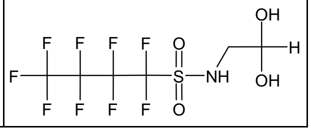

Number	Chemical name	Abbreviation	Molecular formula (M)	Precursor ion	Structure
8b-1	1,1,2,2,3,3,4,4,4-nonafluoro-*N*-(2-hydroxy-2-methoxyethyl)butane-1-sulfonamide	FBSAcAL hemiacetal	$C_7H_8F_9NO_4S$	$[M\text{-}H]^-$	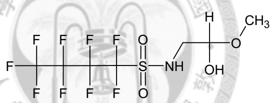
9a-1	trifluoroacetic acid	TFA	$C_2HF_3O_2$	$[M\text{-}H]^-$	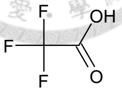
9a-2	pentafluoropropanoic acid	PFPrA	$C_3HF_5O_2$	$[M\text{-}H]^-$	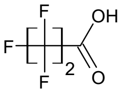
9a-3	heptafluorobutanoic acid	PFBA	$C_4HF_7O_2$	$[M\text{-}H]^-$	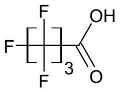
9a-4	nonafluoropentanoic acid	PFPeA	$C_5HF_9O_2$	$[M\text{-}H]^-$	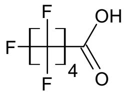
9a-5	undecafluorohexanoic acid	PFHxA	$C_6HF_{11}O_2$	$[M\text{-}H]^-$	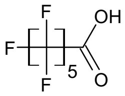
9a-6	tridecafluoroheptanoic acid	PFHpA	$C_7HF_{13}O_2$	$[M\text{-}H]^-$	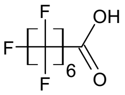
9a-7	pentadecafluorooctanoic acid	PFOA	$C_8HF_{15}O_2$	$[M\text{-}H]^-$	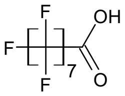
9a-8	heptadecafluorononanoic acid	PFNA	$C_9HF_{17}O_2$	$[M\text{-}H]^-$	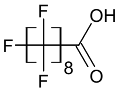
9a-9	nonadecafluorodecanoic acid	PFDA	$C_{10}HF_{19}O_2$	$[M\text{-}H]^-$	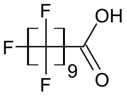
9a-10	henicosafluoroundecanoic acid	PFUdA	$C_{11}HF_{21}O_2$	$[M\text{-}H]^-$	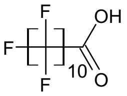
9b-1	(4E)-2,2,3,3,4,5,6,6,6-nonafluorohex-4-enoic acid	U-PFHxA	$C_6HF_9O_2$	$[M\text{-}H]^-$	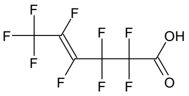
9c-1	difluoro[(1,2,2-trifluoroethen-1-yl)oxy]acetic acid	U-E-PFBA	$C_4HF_5O_3$	$[M\text{-}H]^-$	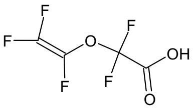
9c-2	difluoro[(1,1,2,3,3-pentafluoroprop-2-en-1-yl)oxy]acetic acid	U-E-PFPeA	$C_5HF_7O_3$	$[M\text{-}H]^-$	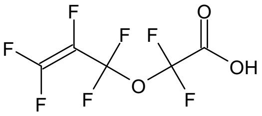

Number	Chemical name	Abbreviation	Molecular formula (M)	Precursor ion	Structure
9c-3	difluoro[[(1*E*)-1,2,3,3,3-pentafluoroprop-1-en-1-yl]oxy]acetic acid	U-E-PFPeA	$C_5HF_7O_3$	$[M-H]^-$	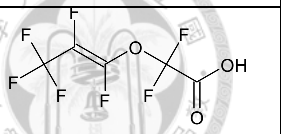
9c-4	difluoro{[(2E)-1,1,2,3,4,4,4-heptafluorobut-2-en-1-yl]oxy}acetic acid	U-E-PFHxA	$C_6HF_9O_3$	$[M-H]^-$	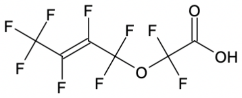
9c-5	(3E)-2,2,3,4-tetrafluoro-4-(pentafluoroethoxy)but-3-enoic acid	U-E-PFHxA	$C_6HF_9O_3$	$[M-H]^-$	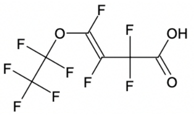
9c-6	2,2,3,3,4,4-hexafluoro-4-[(trifluoroethenyl)oxy]butanoic acid	U-E-PFHxA	$C_6HF_9O_3$	$[M-H]^-$	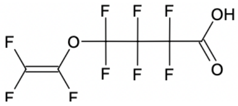
9d-1	2,2,3,3,4,4-hexafluorobutanoic acid	H-PFBA	$C_4H_2F_6O_2$	$[M-H]^-$	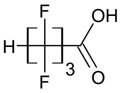
9d-2	2,2,3,3,4,4,5,5-octafluoropentanoic acid	H-PFPeA	$C_5H_2F_8O_2$	$[M-H]^-$	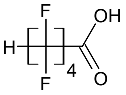
9d-3	2,2,3,3,4,4,5,5,6,6-decafluorohexanoic acid	H-PFHxA	$C_6H_2F_{10}O_2$	$[M-H]^-$	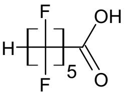
9e-1	(difluoromethoxy)di(fluoro)acetic acid	H-E-PFPrA	$C_3H_2F_4O_3$	$[M-H]^-$	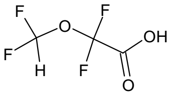
9e-2	difluoro(1,2,2,2-tetrafluoroethoxy)acetic acid	H-E-PFBA	$C_4H_2F_6O_3$	$[M-H]^-$	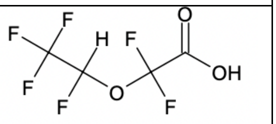
9e-3	2,2,3-trifluoro-3-(trifluoromethoxy)propanoic acid	H-E-PFBA	$C_4H_2F_6O_3$	$[M-H]^-$	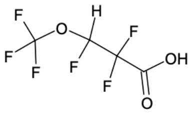
9e-4	difluoro(1,1,2,2-tetrafluoroethoxy)acetic acid	H-E-PFBA	$C_4H_2F_6O_3$	$[M-H]^-$	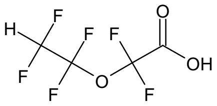
9e-5	3,3-difluoro-3-(trifluoromethoxy)propanoic acid	H_2-E-PFBA	$C_4H_3F_5O_3$	$[M-H]^-$	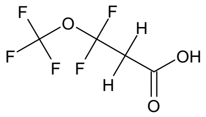
9f-1	difluoro(trifluoromethoxy)acetic acid	E- PFPrA	$C_3HF_5O_3$	$[M-H]^-$	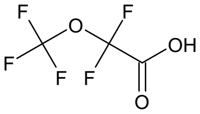

Number	Chemical name	Abbreviation	Molecular formula (M)	Precursor ion	Structure
9f-2	difluoro(pentafluoroethoxy)acetic acid	E- PFBA	$C_4HF_7O_3$	$[M-H]^-$	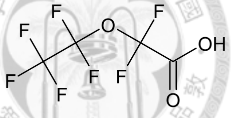
9f-3	2,2,3,3,4,4-hexafluoro-4-(trifluoromethoxy)butanoic acid	E- PFPeA	$C_5HF_9O_3$	$[M-H]^-$	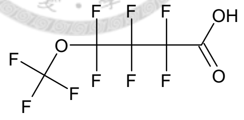
10a-1	difluoropropanedioic acid	PFdiCA(C3)	$C_3H_2F_2O_4$	$[M-H]^-$	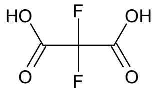
10a-2	tetrafluorobutanedioic acid	PFdiCA(C4)	$C_4H_2F_4O_4$	$[M-H]^-$	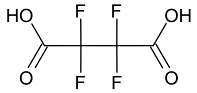
10a-3	hexafluoropentanedioic acid	PFdiCA(C5)	$C_5H_2F_6O_4$	$[M-H]^-$	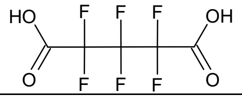
10a-4	octafluorohexanedioic acid	PFdiCA(C6)	$C_6H_2F_8O_4$	$[M-H]^-$	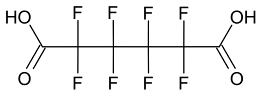
10a-5	decafluoroheptanedioic acid	PFdiCA(C7)	$C_7H_2F_{10}O_4$	$[M-H]^-$	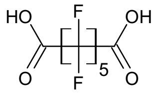
10a-6	dodecafluorooctanedioic acid	PFdiCA(C8)	$C_8H_2F_{10}O_4$	$[M-H]^-$	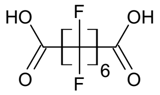
11a-1	trifluoromethanesulfonic acid	TFMS	CHF_3O_3S	$[M-H]^-$	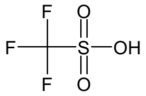
11a-2	nonafluorobutane-1-sulfonic acid	PFBS	$C_4HF_9O_3S$	$[M-H]^-$	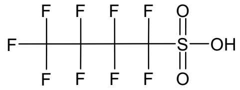
11b-1	1,1,2,2-tetrafluoroethane-1-sulfonic acid	H-PFEtS	$C_2H_2F_4O_3S$	$[M-H]^-$	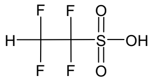
11b-2	1,1,2,2,3,3-hexafluoropropane-1-sulfonic acid	H-PFPrS	$C_3H_2F_6O_3S$	$[M-H]^-$	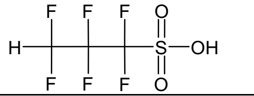
11b-3	1,1,2,2,3,3,4,4-octafluorobutane-1-sulfonic acid	H-PFBS	$C_4H_2F_8O_3S$	$[M-H]^-$	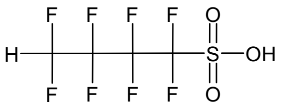
11c-1	1,2,3,3,3-pentafluoropropyl hydrogen sulfate	H_2-E-PFTS	$C_2F_3H_3SO_4$	$[M-H]^-$	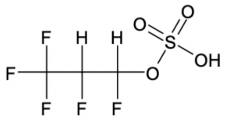
11c-2	1,2,2-trifluoro-2-(1,2,2,2-tetrafluoroethoxy)ethane-1-sulfonic acid	H_2-E-PFPrS	$C_3H_3F_5O_4S$	$[M-H]^-$	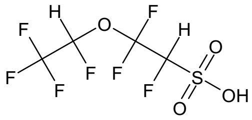

Number	Chemical name	Abbreviation	Molecular formula (M)	Precursor ion	Structure
11d-1	6:2 Fluorotelomer sulfonic acid	6:2 FTSA	$C_8H_5F_{13}O_3S$	$[M\text{-}H]^-$	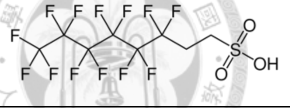
12a-1	nonafluorobutane-1-sulfinic acid	PFBSi	$C_4HF_9O_2S$	$[M\text{-}H]^-$